

**GEOLOGIC CONTROLS ON RESERVOIR  
PROPERTIES OF LOW-PERMEABILITY  
SANDSTONE, FRONTIER FORMATION,  
MOXA ARCH, SOUTHWEST WYOMING**

**TOPICAL REPORT**

(April 1989 - April 1992)

**Bureau of Economic Geology,  
The University of Texas at Austin**

**Prepared in cooperation with  
The Geological Survey of Wyoming**

**Contract No. 5082-211-0708**



**Gas Research Institute**  
8600 West Bryn Mawr Avenue  
Chicago, Illinois 60631

**GEOLOGIC CONTROLS ON RESERVOIR PROPERTIES OF LOW-PERMEABILITY  
SANDSTONE, FRONTIER FORMATION, MOXA ARCH, SOUTHWEST WYOMING**

**TOPICAL REPORT**

(April 1989 - April 1992)

Prepared by

Shirley P. Dutton, H. Scott Hamlin, and Stephen E. Laubach

Bureau of Economic Geology  
W. L. Fisher, Director  
The University of Texas at Austin  
Austin, Texas 78713-7508

Prepared in cooperation with  
The Geological Survey of Wyoming

for

GAS RESEARCH INSTITUTE  
Contract No. 5082-211-0708  
Larry R. Brand, Project Manager

June 1992

## DISCLAIMER

LEGAL NOTICE This report was prepared by the Bureau of Economic Geology as an account of work sponsored by the Gas Research Institute (GRI). Neither GRI, members of GRI, nor any person acting on behalf of either:

- a. Makes any warranty or representation, expressed or implied, with respect to the accuracy, completeness, or usefulness of the information contained in this report, or that the use of any apparatus, method, or process disclosed in this report may not infringe privately owned rights; or
- b. Assumes any liability with respect to the use of, or for damages resulting from the use of, any information, apparatus, method, or process disclosed in this report.

<b>REPORT DOCUMENTATION PAGE</b>	<b>1. REPORT NO.</b> GRI-92/0127	<b>2.</b>	<b>3. Recipient's Accession No.</b>
<b>4. Title and Subtitle</b> Geologic Controls on Reservoir Properties of Low-Permeability Sandstone, Frontier Formation, Moxa Arch, Southwest Wyoming			<b>5. Report Date</b> June 1992
<b>7. Author(s)</b> Shirley P. Dutton, H. Scott Hamlin, and Stephen E. Laubach			<b>6.</b>
<b>9. Performing Organization Name and Address</b> Bureau of Economic Geology The University of Texas at Austin University Station, Box X Austin, TX 78713			<b>8. Performing Organization Rept. No.</b>
<b>12. Sponsoring Organization Name and Address</b> Gas Research Institute 8600 West Bryn Mawr Avenue Chicago, IL 60631			<b>10. Project/Task/Work Unit No.</b>
<b>Project Manager:</b> Larry Brand			<b>11. Contract(C) or Grant(G) No.</b> (C)5082-211-0708 (G)
<b>15. Supplementary Notes</b>			<b>13. Type of Report &amp; Period Covered</b> Topical April 1989 - April 1992
<b>16. Abstract (Limit: 200 words)</b>  This report examines the influence of stratigraphy, diagenesis, natural fractures, and in situ stress on low-permeability, gas-bearing sandstone reservoirs of the Upper Cretaceous Frontier Formation along the Moxa Arch in the Green River Basin, southwestern Wyoming. The main stratigraphic controls on distribution and quality of Frontier reservoirs are sandstone continuity and detrital clay content. The Frontier was deposited in a fluvial-deltaic system, in which most reservoirs lie in marine upper shoreface and fluvial channel-fill sandstone facies. The major causes of porosity loss in Frontier sandstones during burial diagenesis were mechanical and chemical compaction and cementation by calcite, quartz, and authigenic clays. Despite extensive diagenetic modification, reservoir quality is best in facies that had the highest porosity and permeability at the time of deposition. Natural fractures are sparse in Frontier core, but outcrop studies show that fractures commonly are in discrete, irregularly spaced swarms separated by domains having few fractures. Natural fracture swarms are potential high-permeability "sweet spots." Stress-direction indicators give highly scattered estimates of maximum horizontal compression direction ranging from north to east or northeast. The scatter may reflect interference of natural fractures with measurements of stress directions, as well as spatially variable stress directions and low horizontal stress anisotropy.			<b>14.</b>
<b>17. Document Analysis</b>			
<b>a. Descriptors</b> Wyoming, Green River Basin, Frontier Formation, tight gas sandstones, stratigraphy, depositional systems, sandstone diagenesis, reservoir quality, natural fractures, maximum horizontal stress, hydraulic fracture treatment			
<b>b. Identifiers/Open-Ended Terms</b> stratigraphy of Frontier Formation, influence of depositional environment on reservoir development, marine shoreface and fluvial channel-fill sandstone facies, petrography of Frontier Formation, diagenetic history of tight gas sandstones, diagenetic controls on reservoir quality, southwestern Wyoming fracture trends, stress history and fracture of tight gas reservoirs			
<b>c. COSATI Field/Group</b>			
<b>18. Availability Statement</b> Release unlimited		<b>19. Security Class (This Report)</b> Unclassified	<b>21. No. of Pages</b> 217
		<b>20. Security Class (This Page)</b> Unclassified	<b>22. Price</b>

## RESEARCH SUMMARY

- Title** Geologic controls on reservoir properties of low-permeability sandstone, Frontier Formation, Moxa Arch, southwest Wyoming
- Contractor** Bureau of Economic Geology, The University of Texas at Austin, GRI Contract No. 5082-211-0708, entitled "Geologic Analysis of Primary and Secondary Tight Gas Sands Objectives."
- Principal Investigator** S. P. Dutton
- Report Period** April 1989 – April 1992  
Topical Report
- Objectives** To summarize the results of geologic studies of the Frontier Formation on the Moxa Arch in the Green River Basin, southwest Wyoming, and to document the stratigraphic, diagenetic, and structural geologic parameters that influence reservoir behavior in the Frontier.
- Technical Perspective** Since 1982, the Gas Research Institute (GRI) has supported geologic investigations designed to develop knowledge necessary to efficiently produce natural gas from low-permeability sandstone reservoirs. As part of that program, the Bureau of Economic Geology has conducted research on low-permeability sandstones in the Upper Cretaceous Frontier Formation along the Moxa Arch in the Green River Basin, southwest Wyoming. Information gained from three Frontier cooperative wells, combined with geologic characterization of the Frontier throughout the study area, led to the drilling by GRI of a Staged Field Experiment (SFE No. 4) in 1990. The SFE well was drilled and tested for the purpose of research on low-permeability gas reservoirs. This report summarizes the results of geologic studies of the Frontier Formation, and it focuses on the contribution of geology to evaluation and completion of tight gas sandstone wells.
- Results** Geologic characterization of the Frontier Formation focused on four major areas: (1) stratigraphy and depositional systems, (2) diagenesis of reservoir sandstones, (3) distribution of natural fractures, and (4) horizontal stress orientation. Along the Moxa Arch, the Frontier Formation was deposited in fluvial and wave-dominated deltaic systems, in which strike-aligned shoreface sandstone and dip-oriented fluvial channel-fill sandstone form the most important reservoirs. Frontier sandstone reservoirs are enclosed in coastal-plain and nearshore-marine shale and sandy shale.
- The Frontier is divided into several sandstone-bearing intervals. Marine shoreline sandstones in the First (upper) Frontier and the Third and Fourth (lower) Frontier occur only at the north end of the Moxa Arch (La Barge Platform) and are locally productive there. Second Frontier sandstone extends along the length of the Moxa Arch and contains the most prolific gas reservoirs. The Second Frontier is composed of several sandstone benches, of which the First and Second Benches are most widespread. The First Bench comprises laterally discontinuous fluvial channel-fill sandstones, whereas the Second Bench is a single progradational shoreface sandstone having good lateral continuity. The main depositional and stratigraphic controls on distribution and quality of Frontier reservoirs are sandstone continuity and

detrital clay content. On the La Barge Platform, Second Bench upper shoreface sandstone has the lowest detrital clay content and consistently occurs at the top of the laterally continuous shoreface sequence. Most Frontier wells on the La Barge Platform have Second Bench perforations, although variable thickness and diagenetic modification influence the productivity of individual wells. The First Bench contains numerous discontinuous fluvial channel-fill sandstones, each composed internally of a complex arrangement of clay-rich and clay-free zones. Reservoir quality in the First Bench is highly variable, although it improves southward along the Moxa Arch.

According to petrographic examination of 247 thin sections from 13 wells, Frontier sandstones are fine- to medium-grained litharenites and sublitharenites having an average composition of 64 percent quartz, 6 percent feldspar, and 30 percent rock fragments. Clean sandstones contain an average of 1.6 percent primary intergranular porosity and 4.2 percent secondary porosity, which formed because of dissolution of feldspar, chert, and mudstone clasts. Microporosity, estimated as the difference between porosimeter porosity and thin-section porosity, averages 6.5 percent. Calcite, quartz, mixed-layer illite-smectite, and illite are the most abundant cements. Authigenic mixed-layer clays consist of about 80 percent illite layers, suggesting that clays may be only moderately sensitive to fresh water. On the basis of petrographic evidence, the relative order of occurrence of the major events in the diagenetic history of Frontier sandstones was found to be (1) mechanical compaction by grain rearrangement and deformation of ductile grains, (2) formation of illite and mixed-layer illite-smectite rims, (3) precipitation of quartz overgrowths, (4) precipitation of calcite cement, (5) generation of secondary porosity by dissolution of calcite cement and detrital feldspar, chert, and mudstone, (6) precipitation of kaolinite in secondary pores, and (7) chemical compaction by intergranular pressure solution and stylolitization and additional precipitation of quartz cement.

Low permeability in Frontier sandstones is caused by (1) loss of porosity due to compaction, (2) occlusion of pores by cements, particularly calcite and quartz, and (3) lining of primary pores by fibrous illite. Unstressed permeability to air averages 0.19 md in 65 upper-shoreface sandstones (porosity = 14 percent), 0.13 md in 132 fluvial channel-fill sandstones (porosity = 10 percent), and 0.08 md in 271 lower-shoreface sandstones (porosity = 13 percent).

Fractures are sparse in Frontier Formation core, but this does not necessarily mean that natural fractures are not an important reservoir element in these rocks. Fracture networks in outcrops that likely resemble fractures existing at depth have attributes such as wide spacing and great lateral extent that would tend to make them both effective fluid conduits and difficult to intersect and detect with vertical wells. Frontier outcrop studies show that fractures are in networks where fracture connectivity is locally highly variable and anisotropic. The direction of fracture strike can shift by 90 degrees between adjacent beds. Moreover, fractures commonly are in discrete, irregularly spaced swarms separated laterally by domains that have few fractures, rather than in regularly spaced, orthogonal fracture sets. Strikes of some fracture sets can be predicted from regional tectonic extension directions; an optimum direction for drilling in flat-lying rocks can thus be determined. More challenging to predict are fracture orientation in a specific bed, fracture density, and the probability of encountering a dense cluster of fractures by means of hydraulic fractures or horizontal wells.

The Green River Basin is in the cordilleran east-west extension stress province but near the boundary between that province and the east-northeast

compressional mid-plate stress province. The boundaries between stress provinces are vague and may be characterized by transitional or inconsistent stress directions. Features that are consistent with east-west extension are the young north-striking normal faults along the western margin of the basin; they could be interpreted to indicate approximately north-south trending  $S_{Hmax}$ . In contrast, stress-directions from GRI tests in the basin suggest azimuths are widely scattered in the Frontier Formation in the vicinity of the Moxa Arch, with some measured directions more consistent with the east-northeast  $S_{Hmax}$  direction of the nearby mid-plate stress province.

## Technical Approach

Correlation and interpretation of logs from more than 800 wells and cores from 16 wells established the stratigraphic framework of the Frontier at regional and local scales. Cores were used for interpretation and characterization of depositional facies and for lithologic calibration of well logs. The lateral variability in thickness and continuity of individual sandstone bodies were mapped and displayed on cross sections. Frontier production data were compared with sandstone development to better determine the influence of depositional facies on gas productivity.

The composition of Frontier sandstones was determined using core samples from 13 wells on and adjacent to the Moxa Arch. Most cores were from the First and Second Benches of the Second Frontier, but cores of the First and Third Frontier and the Third, Fourth, and Fifth Benches of the Second Frontier also were studied. From each core, representative samples were selected from different facies. Composition of Frontier sandstones and mudstones was determined by standard thin-section petrography, scanning electron microscopy using an energy dispersive X-ray spectrometer, electron microprobe analysis, and X-ray analysis. Analyses of more than 600 core plugs form the data base for porosity and permeability. All porosity and permeability samples were measured under unstressed conditions, and some were also measured under stressed conditions, at calculated in situ overburden pressure.

Fractures in five cores were studied in detail, and six additional cores were surveyed for fracture occurrence. Ninety-two fractures were encountered in ten Frontier wells having more than 1,580 ft (481 m) of core. Oriented core and borehole-imaging geophysical logs provide information on fracture strike. Fracture patterns in Frontier sandstone outcrops were mapped on aerial photographs and topographic base maps. Locations of individual fractures were surveyed using plane table and electronic distance-measuring devices. Fracture descriptions are based on petrographic observations, large-scale outcrop descriptions, scanline measurements, and field maps at scales of 1:50, 1:100, 1:300, and 1:12,000. Fracture attributes in map areas were compared with regional fracture patterns observed during basinwide reconnaissance. The box method was used to estimate fractal dimensions of Frontier fracture networks. This method involves placing grids of square elements of side-length  $r$  successively over a map and counting the number of grid elements ( $N$ ) containing a fracture trace.

Stress-direction indicators used include the orientation of remotely monitored microseismicity from hydraulic fractures, wellbore breakouts, coring-induced fractures, and core-scale phenomena such as core-strain relaxation (ASR), acoustic P-wave velocity anisotropy, and rock-strength anisotropy measured by means of indentation tests. Regional neotectonic deformation, expressed in western Wyoming as earthquakes and young (Quaternary-Recent) fault scarps, also provided an indication of current stress directions.

**Project  
Implications**

This report is one of a series of reports funded by GRI to cover geologic descriptions of tight gas sandstone reservoirs. Other reports were issued on the Travis Peak Formation and Cotton Valley Group. These reports provide a good resource for producers researching the geology of tight gas sandstone reservoirs.

GRI Project Manager  
Larry R. Brand  
Manager, Fracturing Fluids



## CONTENTS

Introduction.....	1
Stratigraphy and Depositional Systems.....	3
Methods.....	5
Regional Geologic Framework.....	9
Structural Setting.....	9
Stratigraphy.....	10
Second Frontier Sandstone on the La Barge Platform.....	18
Sandstone Depositional Patterns.....	18
Clean Sandstone Distribution.....	24
Sandstone Porosity Maps.....	30
Second Bench Production Trends.....	33
GRI Cooperative Wells.....	35
Terra Resources Anderson Canyon No. 3-17.....	35
Wexpro Church Buttes No. 48.....	38
Enron South Hogsback No. 13-8A.....	41
S. A. Holditch & Associates SFE No. 4-24.....	51
Diagenesis of Frontier Sandstones.....	58
Methods.....	59
Frontier Composition.....	60
Grain Size and Sorting.....	60
Framework Grains.....	62
Matrix.....	67
Cements.....	68
Authigenic Clays.....	68
Quartz Overgrowths.....	73
Calcite.....	77

Porosity.....	81
Burial and Thermal History .....	83
Burial-History Curves.....	83
Thermal History.....	86
Interpretation of Diagenetic History.....	89
Early Diagenetic Reactions.....	90
Late Diagenetic Reactions.....	92
Diagenetic Controls on Reservoir Quality .....	99
Porosity.....	99
Permeability .....	104
Depositional Environment .....	106
Geographic Area.....	108
Comparison of Diagenesis in Three Frontier Wells.....	110
Natural Fractures.....	112
Natural Fractures in Core.....	114
Fracture Abundance in Core.....	114
Fracture Dimensions in Core .....	116
Petrography of Fracture-Filling Minerals.....	117
Fracture Orientations in Core.....	119
Natural Fractures in Outcrop .....	122
Setting of Frontier Formation Exposures.....	122
Dominant Fracture Directions .....	123
Style of Fracture Sets.....	128
Fracture Dimensions .....	129
Fracture Spacing.....	132
Fracture Patterns.....	136
Fracture Networks and Connectivity .....	138

Scaling Attributes and Clustering .....	140
Fracture Origins.....	144
Timing and Style of Fracturing.....	144
Predicting Subsurface Fracture Attributes.....	150
Natural Fracture Exploration Targets.....	151
Stress Directions.....	152
Results of Stress-Direction Measurements.....	153
Wellbore Breakouts.....	153
Petal-Centerline Fractures.....	158
Anelastic Strain Recovery.....	159
Acoustic Anisotropy.....	161
Axial Point-Load Tests.....	162
Hydraulic Fracture Microseismic Monitoring.....	166
Interpretation of Stress Data.....	169
Inconsistent Stress Directions.....	169
Low Horizontal Stress Anisotropy.....	170
Stress Provinces.....	172
Summary of Stress-Direction Results.....	174
Conclusions.....	174
Acknowledgments.....	180
References.....	182

### Figures

1. Structure-contour map on the top of the Second Frontier sandstone, showing major structural elements of the western Green River Basin.....	4
2. Map of major Frontier fields associated with the Moxa Arch, western Green River Basin.....	7

3.	Upper Cretaceous stratigraphy in the western Green River Basin.....	11
4.	Regional north-south cross section along the Moxa Arch showing thicknesses and structural attitudes of Upper Cretaceous and Tertiary formations.....	12
5.	Typical gamma-ray/resistivity log, Frontier Formation, north Moxa Arch.....	14
6.	Regional north-south, gamma-ray/resistivity cross section along the Moxa Arch.....	15
7.	Map showing thickness of sandstone in the Second Frontier along the Moxa Arch.....	17
8.	Map showing thickness of sandstone in the Second and Third Benches of the Second Frontier on the La Barge Platform.....	19
9.	Depositional model of a sand-rich strandplain.....	21
10.	Map showing thickness of sandstone in the First Bench of the Second Frontier on the La Barge Platform.....	22
11.	West-east gamma-ray/resistivity stratigraphic cross section of the Second Frontier on the La Barge Platform.....	23
12.	Net clean sandstone map of the Second Bench of the Second Frontier on the La Barge Platform.....	26
13.	Net clean sandstone map of the First Bench of the Second Frontier on the La Barge Platform.....	28
14.	Northwest-southeast schematic cross section showing distribution of shaly sandstone and clean sandstone in the lower Frontier interval, north La Barge Platform.....	29
15.	Map showing net thickness of Second Bench sandstone having at least 15 percent log porosity, northwest part of the La Barge Platform.....	31
16.	Map showing net thickness of Second Bench sandstone having at least 15 percent log porosity, southeast part of the La Barge Platform.....	32
17.	Initial potential map of wells on the La Barge Platform having Second Bench perforations.....	34
18.	Log responses and rock properties in core from the First and Second Benches of the Second Frontier, Terra Anderson Canyon No. 3-17 well, Fontanelle field.....	36
19.	Log responses and core description, Wexpro Church Buttes Unit No. 48 well, Church Buttes field.....	40
20.	Structure-contour map on the top of the Second Frontier, South Hogsback field; location of Enron S. Hogsback No. 13-8A well also shown.....	42
21.	West-east structural cross section in South Hogsback field showing the attitudes of several prominent horizons in the Frontier Formation and the Muddy Sandstone.....	43

22.	West-east stratigraphic cross section showing SP and resistivity logs from the Enron S. Hogsback No. 13-8A well and the nearest offset wells.....	44
23.	Thickness map of high-resistivity sandstone in the Second Bench of the Second Frontier, South Hogsback field.....	45
24.	Thickness map of sandstone in the First Bench of the Second Frontier, South Hogsback field.....	46
25.	Gamma-ray/resistivity log from the Enron S. Hogsback No. 13-8A cooperative well.....	47
26.	Log responses and core description from the Fourth Bench of the Second Frontier, Enron S. Hogsback No. 13-8A well, South Hogsback field.....	49
27.	Log responses and rock properties in core from the First, Second, and Third Benches of the Second Frontier, Enron S. Hogsback No. 13-8A well, South Hogsback field.....	50
28.	Structure-contour map on the top of the Second Frontier, Chimney Butte and Tip Top fields, northeast La Barge Platform.....	53
29.	Gamma-ray/resistivity log from the S. A. Holditch & Associates SFE No. 4 well showing Frontier sandstone zones and cored intervals.....	54
30.	Southwest-northeast stratigraphic cross section showing well logs from SFE No. 4 and offset wells, Chimney Butte and Tip Top fields.....	55
31.	Log responses and rock properties in core from the Second and Third Frontier, SFE No. 4, Chimney Butte field.....	57
32.	Compositional classification of First, Second, and Third Frontier Sandstones.....	63
33.	Compositional classification of Frontier sandstones by depositional environment.....	66
34.	SEM photo of illite tangentially oriented around a secondary pore; quartz crystals project into pore, Terra Anderson Canyon No. 3-17 well.....	71
35.	SEM photo of authigenic fibrous illite lining primary pore, Terra Anderson Canyon No. 3-17 well.....	71
36.	SEM photo of sheets of authigenic illite bridging a pore, Terra Anderson Canyon No. 3-17 well.....	72
37.	SEM photo of cluster of authigenic chlorite flakes, Wexpro Church Buttes No. 48 well.....	72
38.	SEM photo of quartz overgrowth engulfing illite and chlorite cement, Wexpro Church Buttes No. 48 well.....	74
39.	SEM photo of authigenic kaolinite within a secondary pore, Mobil Tip Top No. T71X-6G-28N-113W well.....	74

40.	Kaolinite cement volume in clean sandstones as a function of present burial depth.....	75
41.	Quartz cement volume in clean sandstones as a function of present burial depth.....	76
42.	SEM photo of chert grain showing abundant microporosity, Terra Anderson Canyon No. 3-17 well.....	81
43.	Close-up of surface of chert grain.....	81
44.	Burial history curves for the tops of the Second Frontier, Hilliard, Rock Springs, Ericson-Lance, and undifferentiated Tertiary in wells on the Moxa Arch and in the Green River Basin.....	84
45.	Calcite cement volume in clean sandstones as a function of depth.....	93
46.	Secondary porosity volume in clean sandstones as a function of depth.....	94
47.	Estimated original feldspar volume of clean sandstones as a function of depth.....	95
48.	Semilog plot showing inverse relationship between total cement volume and porosimeter porosity in clean sandstones.....	100
49.	Semilog plot showing inverse relationship between calcite cement volume and porosimeter porosity in clean sandstones.....	102
50.	Minus-cement porosity as a function of depth in clean sandstones.....	103
51.	Log-log plot of porosimeter porosity versus stressed permeability in 422 sandstones.....	105
52.	Fractures in core from five Frontier Formation wells in Green River Basin.....	115
53.	Closely spaced vertical fractures in Frontier Formation core, Blue Rim Federal No. 1-30 well.....	118
54.	Map showing stress directions detected in GRI Tight Gas Sands wells in the Green River Basin; natural fracture strikes in Frontier Formation core and selected outcrops are also shown.....	120
55.	Balanced cross section of the Absaroka and Hogsback thrust sheets, north of Kemmerer in T23N, Lincoln County, Wyoming.....	124
56.	Map showing traces of vertical fractures on Frontier Formation sandstone bedding plane east of Kemmerer, Wyoming.....	125
57.	Map showing traces of dominantly east-striking vertical fractures on east-dipping sandstone bedding plane, Frontier Formation, north of Kemmerer, Wyoming.....	126
58.	Schematic map showing traces of dominantly north-striking vertical fractures on sandstone bedding plane, Frontier Formation, north of Kemmerer, Wyoming.....	127
59.	Fracture strike versus fracture length, Frontier Formation sandstone.....	130
60.	Histogram of fracture spacing in Frontier Formation outcrops, north of Kemmerer, Wyoming.....	131

61.	Fractures in outcrop traverses in Frontier Formation and in Cretaceous Pictured Cliffs Sandstone and horizontal core from Cretaceous Cozzette Sandstone, Piceance Basin, Colorado.....	133
62.	Fracture swarms in outcrop traverse, Frontier Formation.....	134
63.	Fractures in outcrop traverses, Frontier Formation, from various locations north of Kemmerer, Wyoming.....	135
64.	Map illustrating definition of constricted fracture terminations.....	137
65.	Proportions of fracture-termination types in representative Frontier sandstone outcrop.....	139
66.	Schematic maps of fracture traces, Frontier Formation sandstone, Kemmerer, Wyoming, showing contrasting fracture-network connectivity.....	141
67.	Graph showing number of counting elements containing fracture traces versus inverse of length of counting element sides for Frontier and Pictured Cliffs maps.....	143
68.	Map view of deformation fronts of various shapes and fracture strikes in adjacent foreland areas resulting from foreland lateral extension.....	148
69.	Depth versus $S_{Hmax}$ direction for SFE No. 4-24 well by means of several techniques.....	155
70.	Box plots of $S_{Hmax}$ for various stress-direction indicators in the Frontier Formation, SFE No. 4-24 well.....	156
71.	Diagram illustrating the point-load apparatus.....	163
72.	Disks of Frontier Formation core having anisotropic strength in axial point-load test.....	165
73.	Direction of hydraulic fracture growth from circumferential microseismic monitoring.....	168
74.	Generalized stress map of the western United States.....	173

#### Tables

1.	Frontier cores used in this study.....	6
2.	Average composition of Frontier sandstones by depositional environment.....	61
3.	Semiquantitative X-ray diffraction mineralogy data.....	70
4.	Stratigraphic data used to construct burial-history curves.....	88
5.	Calculated time-temperature indices and corresponding vitrinite-reflectance values for the Second Frontier.....	109

6. Characteristics of clean First, Second, and Third Bench Frontier sandstones in four areas along the Moxa Arch .....	87
7. Petrographic data from pay zones of GRI cooperative wells.....	111
8. Data showing maximum horizontal compression direction, Frontier Formation, Green River Basin, Wyoming .....	154



## INTRODUCTION

The Frontier Formation in the Green River Basin, Wyoming, produces gas from sandstone reservoirs that are generally low in permeability. Many Frontier reservoirs along the Moxa Arch, a major area of Frontier gas production in the western Green River Basin, have been designated as "tight gas sandstones." Stratigraphic, diagenetic, and structural variations, however, contribute to significant reservoir quality differences within and between the fields along the Moxa Arch. This report summarizes the results of integrated geologic studies of the Frontier Formation on the Moxa Arch in the Green River Basin that were conducted by the Bureau of Economic Geology.

The Frontier Formation was studied as part of the Tight Gas Sands project, a research program supported by the Gas Research Institute (GRI) that focuses on low-permeability sandstones. Many of the data used in this study were derived from three Frontier cooperative wells and the GRI Staged Field Experiment No. 4-24 well (SFE No. 4-24). (Cooperative wells are gas wells from which operating companies allow GRI contractors to collect data necessary for formation evaluation.) Information gained from the cooperative wells, combined with geologic characterization of the Frontier throughout the study area, led to the drilling by GRI of SFE No. 4-24 in 1990. SFE No. 4-24 was a research well drilled by GRI on a lease acquired through the cooperation and assistance of Enron Oil and Gas Company.

The Frontier Formation in the Green River Basin contained an estimated 36 Tcf of original gas in place, of which an estimated 1.7 Tcf had been produced by 1988 (Haas and others, 1988). The goal of the GRI Tight Gas Sands project is development of advanced technology that can be applied to the Frontier and other tight gas sandstones to enable greater recovery of gas in place in low-permeability reservoirs. Geologic research is one aspect of this broad, multidisciplinary program designed to increase knowledge about, and ultimate recovery of, unconventional gas resources by integrating geologic characterization, log analysis, reservoir engineering, and hydraulic fracture modeling to complete low-permeability sandstone reservoirs more effectively.

The fundamental objective of the geologic study of the Frontier Formation was to develop a complete description of the physical characteristics of the reservoir sandstones, which is necessary to (1) understand the distribution and reservoir behavior of the tight gas resource and (2) test and apply new technologies for resource extraction. Geologic studies can explain the physical characteristics of Frontier sandstones and provide information necessary for accurate formation evaluation, reservoir modeling, and fracture analysis. Geologic characteristics that are critical to an understanding of Frontier reservoirs, or any other tight gas sandstone, are (1) depositional systems and the distribution of reservoir sandstones, (2) diagenetic history of the formation and mineralogic composition of the reservoir, and (3) structural history and current structural setting of the basin and its contained reservoirs.

Stratigraphic studies help us place reservoirs in the context of a depositional systems framework in order to identify productive facies and determine lateral continuity of individual sandstone bodies. Depositional history helps us determine the regional distribution, geometry, and texture of reservoir sandstones, as well as the characteristics of the nonreservoir facies that may act as barriers to hydraulic fracture growth. Field-scale reservoir analyses provide geologic information necessary for engineering simulation studies. This report discusses (1) regional stratigraphic framework, (2) depositional patterns and sandstone geometries on the La Barge Platform, and (3) depositional facies and reservoir development in GRI cooperative wells. Potential stratigraphic and depositional controls on Frontier reservoir distribution and quality are discussed in each section.

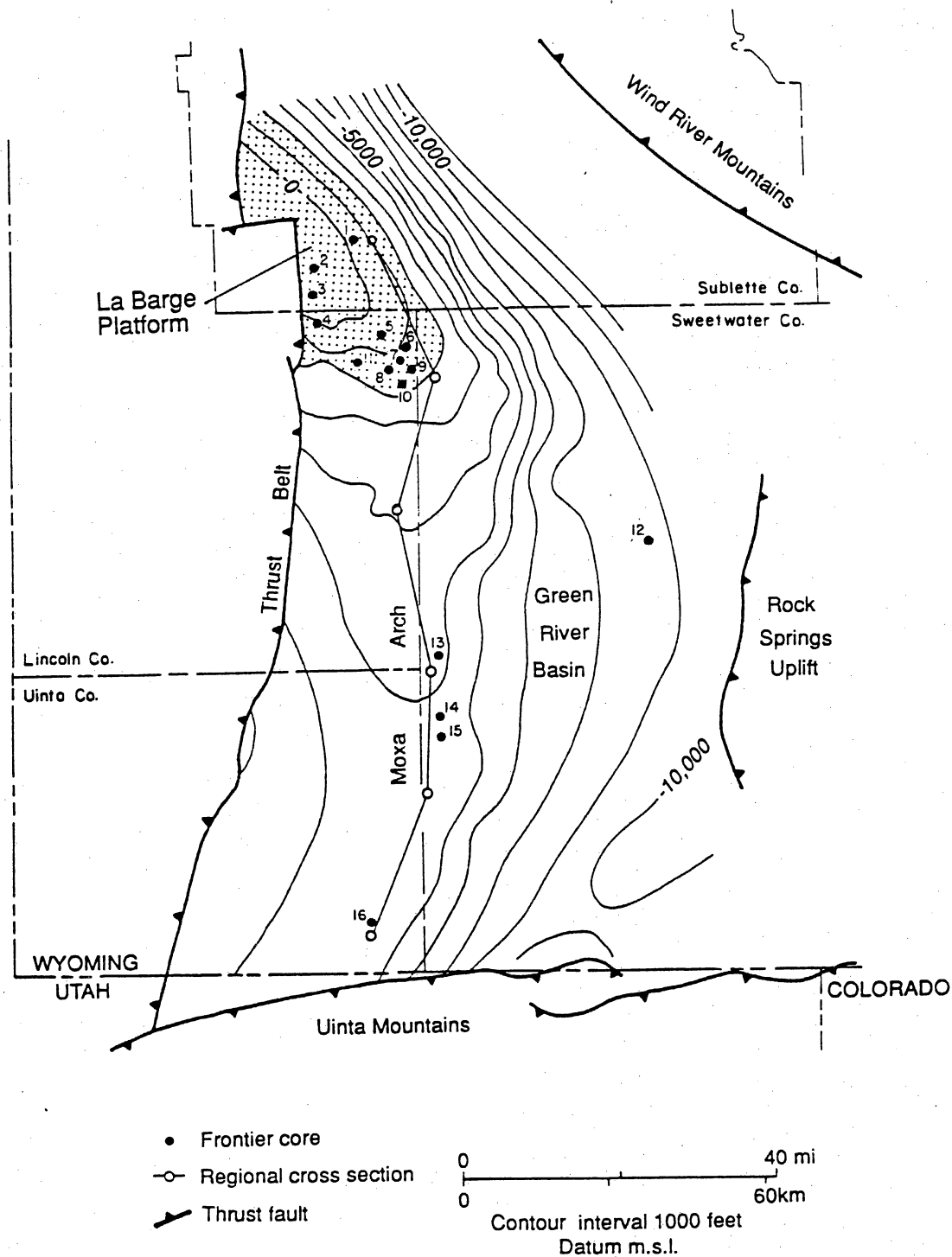
Production characteristics of tight gas reservoirs are partly controlled by diagenetic modifications to the reservoirs; extensive cementation is commonly the reason for low permeability. An understanding of the diagenetic history can help to predict zones of low permeability in a formation and to determine appropriate production methods. Petrographic studies of Frontier core samples were used to investigate the effects of diagenetic history on reservoir porosity and permeability. Composition of detrital minerals and authigenic cements, as well as the type of pores, were correlated with petrophysical properties such as porosity and

permeability, and the effect of diagenetic changes on reservoir properties was thereby identified.

Structural setting significantly influences the producibility of a tight gas sandstone because structural setting controls the state of stress and the abundance and pattern of natural fractures. Natural fractures are potential fluid conduits in low-permeability-sandstone gas reservoirs such as the Frontier Formation. Attributes of fracture networks in the subsurface are, however, difficult to measure, which hampers efficient exploration and development of tight gas resources. The identification of fractures in Frontier Formation core and on borehole-imaging logs and limited gas- and water-production data indicate that fractures are present in the subsurface and that fracture permeability is probably important, at least locally, in this formation. Analysis of fractures in Frontier outcrops provided descriptions of fracture attributes such as fracture spacing, orientation, length and connectivity, and the size and shape of fracture clusters and intervening unfractured areas. In the section on natural fractures, p. 112, we describe fractures in Frontier Formation core and outcrops and show that fractures are appropriate targets for gas exploration and should be incorporated into reservoir models.

### STRATIGRAPHY AND DEPOSITIONAL SYSTEMS

In the Green River Basin of southwest Wyoming (fig. 1), the Frontier Formation comprises marine and nonmarine sandstone and shale facies, which record early Late Cretaceous foreland-basin sedimentation. Frontier shorelines, composed of wave-dominated deltaic headlands and delta-flank strandplains, prograded eastward into the western interior Cretaceous seaway (Myers, 1977; Winn and others, 1984; Moslow and Tillman, 1986, 1989) during Cenomanian and Turonian times (Merewether and others, 1984). The formation thickens and becomes increasingly more dominated by nonmarine facies westward into the Wyoming-Utah-Idaho Thrust Belt, whereas it thins and becomes increasingly more marine to the east. In the west part of the Green River Basin, both nonmarine (fluvial or distributary) channel-fill sandstone and marine shoreline sandstone are well developed in the Frontier and form important low-



QA 15391

Figure 1. Structure-contour map on the top of the Second Frontier, showing major structural elements of the western Green River Basin (from Dutton and Hamlin, 1991). Location of thrust faults (surface traces) based on Love and Christiansen, 1985, and Ryder, 1988. Locations of wells from which Frontier cores were collected for this study are also shown; see table 1 for well names. The north-south cross section along the Moxa Arch is shown in figures 4 and 6.

permeability gas reservoirs. Frontier sandstone reservoirs are enclosed in coastal-plain and nearshore-marine shale and sandy shale. Stratigraphy and depositional environment are important controls on reservoir geometry and quality in the Frontier.

This section presents results of a study of Frontier stratigraphy and depositional environments along the Moxa Arch, which is the main area of Frontier gas production in the western Green River Basin (Crews and others, 1973; Law and others, 1989). Drilling activity has provided abundant well log and core data for mapping and characterizing Frontier sandstone along the Moxa Arch. Previous studies on Frontier stratigraphy in this area (for example, McDonald, 1973; De Chadenedes, 1975; Myers, 1977; Moslow and Tillman, 1986; Hamlin and Buehring, 1990; Hamlin, 1991) provided a starting point and context for this study, which extends the earlier work by using more abundant and closely spaced well log and core data and by focusing on subsurface mapping on the La Barge Platform. Additionally, local Frontier geology is described for several wells (GRI cooperative wells and a staged field experiment well) for which extensive engineering, reservoir modeling, and log and core analysis data are publicly available through the GRI Tight Gas Sands program.

## Methods

Logs from more than 800 wells and cores from 16 wells form the data base for subsurface geologic analysis of the Frontier Formation along the Moxa Arch (fig. 1, table 1). Most of the cores and about 500 of the logs are from wells on the La Barge Platform at the north end of the arch. The La Barge Platform (also known as the Big Piney-La Barge area) is the largest Frontier gas-producing area in the basin and includes Hogsback, Tip Top, Chimney Butte, Fontenelle, and other important fields (fig. 2). GRI cooperative wells were completed in Fontenelle and South Hogsback fields on the La Barge Platform and in Church Buttes field near the south end of the Moxa Arch (fig. 2, table 1). SFE No. 4-24 was completed in Chimney Butte field near the northeast margin of the La Barge Platform (fig. 1). The cooperative wells and SFE No. 4-24 provided complete log suites and continuous cores through the main Frontier sandstone

Table 1. Frontier cores used in this study.

	Well and field	County	Depth (ft)
1.	S. A. Holditch & Associates SFE No. 4-24 Chimney Butte field	Sublette	6,777-6,796; 7,226-7,240.2; 7,310-7,493; 7,607-7,647; 7,753-7,785; 7,963-8,004
2.	Mobil Tip Top No. T71X-6G-27N-113W Tip Top field	Sublette	6,970-7,030
3.	Mobil Hogsback No. T72X-29G-27N-113W Hogsback field	Sublette	6,369-6,396; 6,856-6,941
4.	Enron South Hogsback No. 13-8A South Hogsback field (cooperative well)	Lincoln	7,006-7,284
5.	Natural Gas Corporation of California Fontenelle No. 22-22B, Fontenelle field	Lincoln	7,600-7,660
6.	Natural Gas Corporation of California Federal No. 32-31, Fontenelle field	Lincoln	8,541-8,572
7.	Natural Gas Corporation of California Federal No. 23-7F, Fontenelle field	Lincoln	8,722-8,782
8.	Natural Gas Corporation of California Federal No. 41-14E, Fontenelle field	Lincoln	8,613-8,640; 8,652-8,710
9.	Terra Resources (Pacific Enterprises) Anderson Canyon No. 3-17, Fontenelle field (cooperative well)	Lincoln	9,015-9,142; 9,151-9,188
10.	Natural Gas Corporation of California Federal No. 2-19, Fontenelle field	Lincoln	8,941-8,982
11.	Natural Gas Corporation of California Federal No. 32-8, Fontenelle field	Lincoln	8,252-8,288; 8,302-8,322
12.	Energy Reserves Group Blue Rim Federal No. 1-30, Megas field	Sweetwater	16,053-16,134
13.	Texaco State of Wyoming UNCT 2 No. 1 Bruff field	Sweetwater	11,501-11,550
14.	Wexpro Church Buttes No. 41 Church Buttes field	Sweetwater	12,186-12,245
15.	Wexpro Church Buttes No. 48 Church Buttes field (cooperative well)	Sweetwater	12,045-12,072; 12,145-12,203
16.	Forest Oil Corporation Henry Unit No. 2, Henry field	Uinta	13,025-13,072

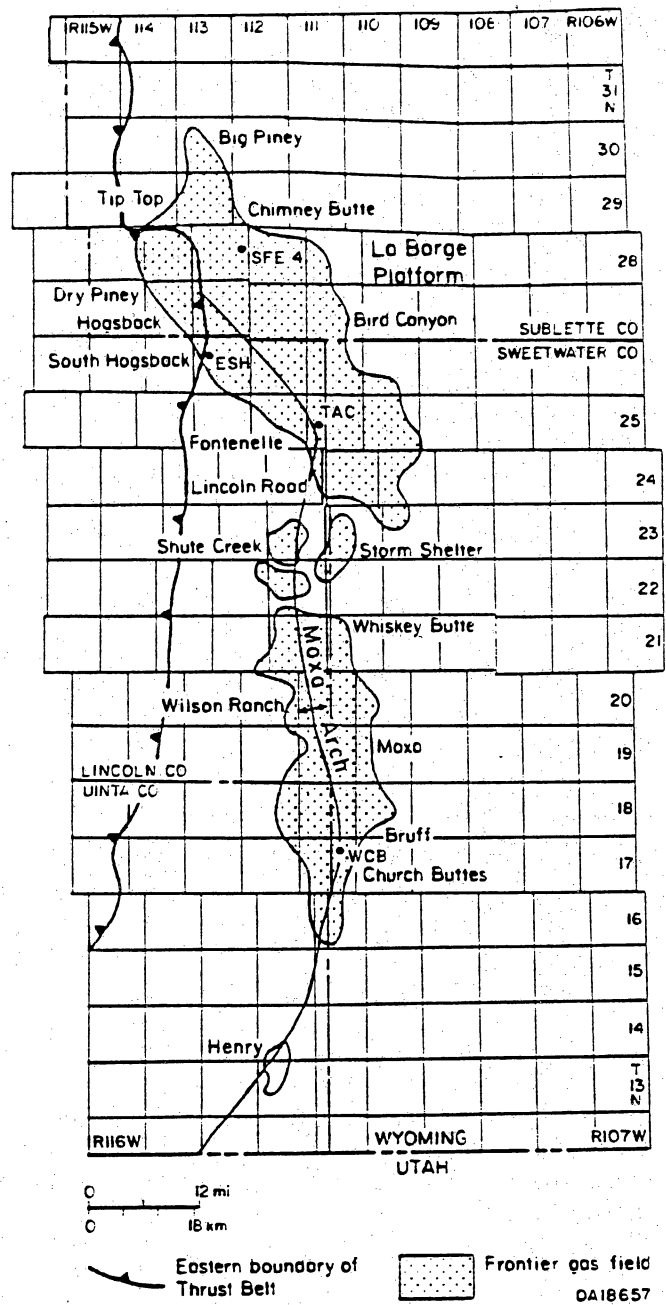


Figure 2. Map of major Frontier fields associated with the Moxa Arch, western Green River Basin (modified from Gregory and De Bruin, 1991). Names of selected Frontier gas fields are shown. The Big Piney-La Barge area at the north end of the Moxa Arch is commonly referred to as the La Barge Platform in this report. Locations of S. A. Holditch & Associates SFE No. 4-24 (SFE 4), Enron South Hogsback No. 13-8A (ESH), Terra Anderson Canyon No. 3-17 (TAC), and Wexpro Church Buttes No. 48 (WCB) wells are shown.

intervals. Additional cores and many well logs used in this study were made available by operators. Other logs were purchased from commercial sources.

Correlation and interpretation of gamma-ray, resistivity, and spontaneous potential (SP) logs established the stratigraphic framework of the Frontier at regional and local scales. A series of generally continuous horizons in marine shale facies were correlated throughout the Moxa Arch study area. Although of undetermined origin, these correlation horizons are recognized by recurring resistivity and gamma-ray signatures. Moreover, because these horizons are interbedded with the Frontier sandstone-bearing intervals, they help establish the equivalency and continuity of individual sandstone bodies.

Cores were used for depositional facies interpretations and lithologic calibration of well logs. Detailed descriptions of lithologies, sedimentary structures and textures, grain sizes, and accessory components were made for each core. Facies interpretations, such as fluvial channel or marine shoreface, were based on core descriptions in the context of the regional depositional systems framework. Calibrated log responses were used to determine sandstone thicknesses, and these thickness values were then used to map the distribution and geometries of Frontier reservoir sandstones. A more limited data base of porosity logs (density, neutron, and acoustic) was also used for sandstone mapping.

Frontier gas production data for wells along the Moxa Arch were compiled by the Geological Survey of Wyoming as a part of this project. Data were collected on initial potential, completion date, and cumulative production for most of the wells in the well log data base on the La Barge Platform. Production data from wells perforated in the Second Bench of the Second Frontier were mapped and compared with sandstone development to better determine the influence of geologic parameters (such as shale content and depositional facies) on gas productivity.



## Regional Geologic Framework

### Structural Setting

The Green River Basin is part of the Rocky Mountain foreland region, an extensive foreland basin that has been segmented by Laramide uplifts. Foreland basins are elongate asymmetric troughs that commonly occur on the cratonic side of thrust belts. In a foreland basin, strata thicken and dips steepen toward the thrust belt. Thrust loading causes the thickest sediment to accumulate near the thrust front (Jordan, 1981). Because the thrust belt also forms the sediment source area, foreland basins typically fill with thick, dominantly nonmarine strata that thin and become more marine dominated down depositional dip (away from the thrust front). The Frontier Formation conforms to this structurally related depositional pattern. The present form of the Green River Basin resulted from folding and faulting during the Late Cretaceous–early Tertiary Laramide orogeny. The Thrust Belt, which bounds the Green River Basin to the west, is a region of north-trending folds and thin-skinned, imbricate thrust faults that dip westward: thrust movement occurred from the latest Jurassic to the early Eocene (Wiltschko and Dorr, 1983). Basement-cored Laramide uplifts, such as the Wind River and Uinta Mountains, formed in the foreland area predominantly in early Tertiary time. They structurally subdivide the foreland area and define Tertiary depositional basins.

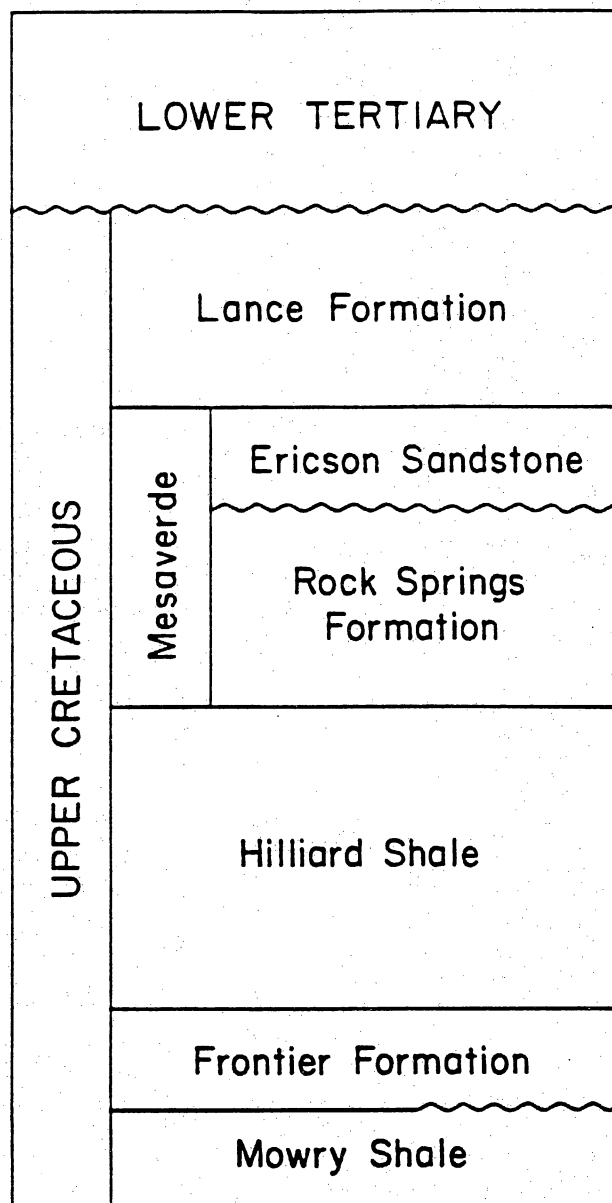
A major structure within the Green River Basin is the Moxa Arch, a broad north-trending uplift near the east margin of the Thrust Belt (fig. 1). Major uplift of the Moxa Arch apparently occurred during the Late Cretaceous (Wach, 1977), related partly to deep-seated thrust-fault movement (Kraig and others, 1987). Uplift largely postdated Frontier deposition, but stratigraphic thinning indicates that some uplift was occurring along the south part of the Moxa Arch during Frontier deposition (Thomaidis, 1973; Wach, 1977). The present attitude of the Moxa Arch indicates that more recent uplift has been concentrated in the north and has resulted in a southward tilt (fig. 1). Depth to the Frontier Formation increases from north to south along the Moxa Arch, ranging from about 6,000 to 15,000 ft (1,830 to 4,600 m) below

ground surface. The north segment of the Moxa Arch, which trends northwest and intersects the Thrust Belt (fig. 1), is called the La Barge Platform (fig. 2). The La Barge Platform encompasses some Frontier gas fields along the margin of the Thrust Belt, such as Tip Top and Hogback, that are structurally complex. Most of the Frontier gas fields along the Moxa Arch, however, consist of simple unfaulted anticlines or mixed structural/stratigraphic traps (McDonald, 1973).

### Stratigraphy

The stratigraphy of Upper Cretaceous and Tertiary formations in the Green River Basin (fig. 3) was shaped by the interplay of tectonics and sedimentation. Early Tertiary sediments comprise a heterogeneous suite of alluvial plain and lacustrine facies, which was deposited in an extensive intermontane basin system (Sullivan, 1980). Intermittent uplift of peripheral and intrabasinal structures provided varied sources and volumes of sediment to subsiding areas in the basin. The Moxa Arch is buried by a northward-thinning wedge of Paleocene-Eocene sediments, ranging from 10,000 to 3,000 ft (3,050 to 900 m) in thickness (fig. 4). The main sources for Moxa Arch Tertiary sediments were the Uinta Mountains (south part of arch), the Wind River Range (north part of arch), and the Thrust Belt (entire arch) (Sullivan, 1980).

Uppermost Cretaceous stratigraphy is also highly variable and includes major unconformities (figs. 3 and 4). In the west part of the Green River Basin, the uppermost Cretaceous Mesaverde Formation (Rock Springs Formation and Ericson Sandstone) and the Lance Formation form the proximal parts of several eastward-prograding regressive/transgressive cycles composed of interbedded fluvial, shoreline, and marine-shelf facies (Law and others, 1989). Along the Moxa Arch uppermost Cretaceous strata are dominantly nonmarine, although the lower part of the Rock Springs Formation includes shoreline sandstones that interfinger eastward and southward with the marine Hilliard Shale. The Rock Springs Formation is erosionally truncated across the crest of the south part of the arch (fig. 4); thick Ericson channel-fill sandstones overlie this unconformity (Thomaidis, 1973). Uppermost Cretaceous



QA19473

Figure 3. Upper Cretaceous stratigraphy in the western Green River Basin. Modified from Law and others (1989).

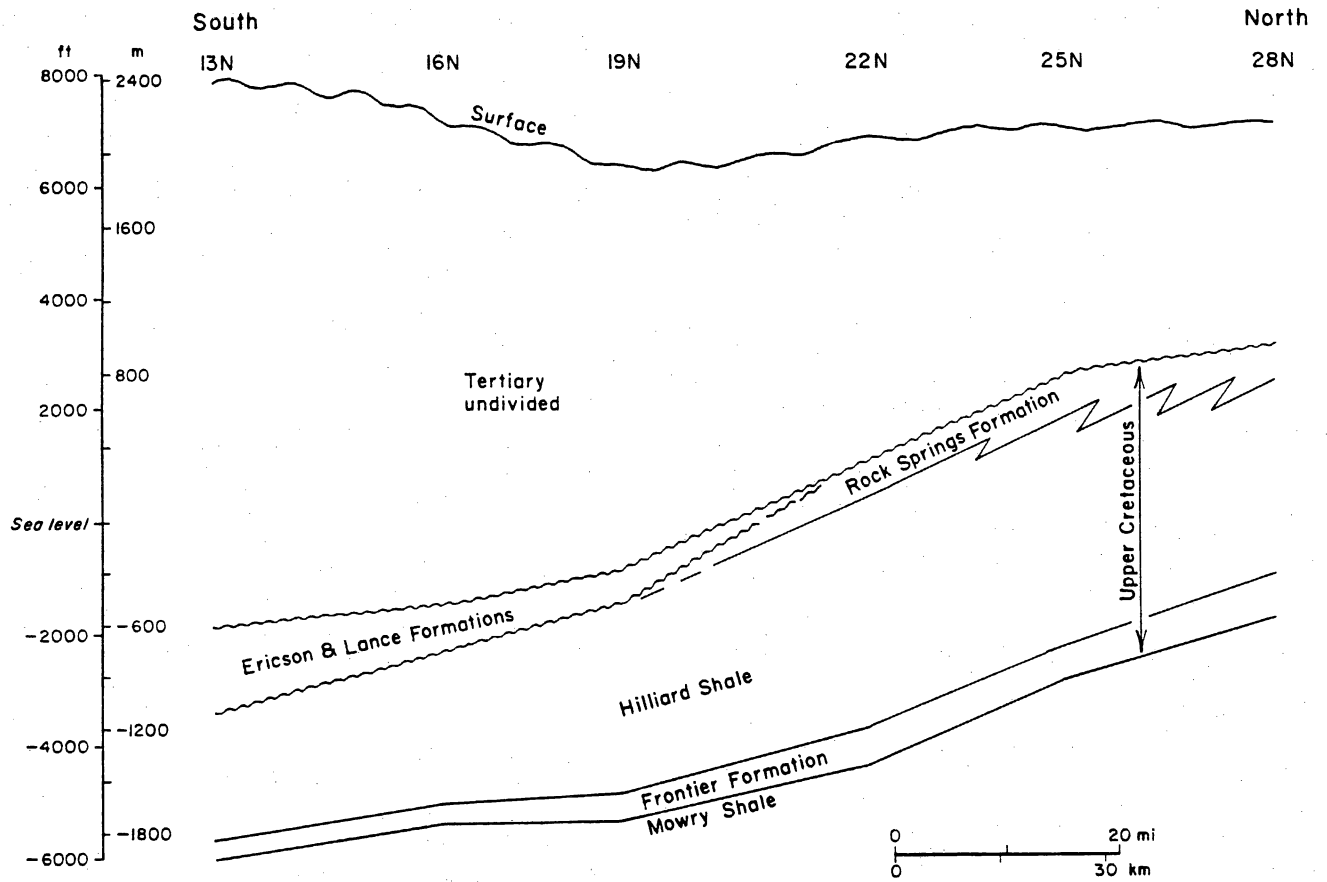


Figure 4. Regional north-south cross section along the Moxa Arch showing thicknesses and structural attitudes of Upper Cretaceous and Tertiary formations. Line of section shown in figure 1.

strata are variably truncated by the regional unconformity at the base of the Tertiary, which rests on Ericson and Lance strata along the south part of the arch and on Rock Springs strata at the north end (Asquith, 1966; Law and others, 1989) (fig. 4). Thus, uplift and erosion along the Moxa Arch were greatest in the south during most of the Late Cretaceous (Frontier through Ericson deposition, Cenomanian to Campanian), but shifted to the north at the end of the Cretaceous and in the early Tertiary.

The Frontier Formation along the Moxa Arch contains marine shoreline sandstone and nonmarine fluvial channel-fill sandstone enclosed in thick, regionally extensive marine shales. Overlying the Frontier, the Hilliard (or Baxter) Shale is 2,000 to 3,000 ft (600 to 900 m) thick and extends throughout the Green River Basin. The Hilliard Shale is partly chronostratigraphically equivalent to the Mancos Shale in Utah and Colorado (Molenaar and Wilson, 1990); the Hilliard–Mancos interval records a time of widespread marine-shelf conditions in the Rocky Mountain foreland region. Underlying the Frontier is the Mowry (or Aspen) Shale, which also records a time of widespread marine-shelf deposition. The Mowry Shale (uppermost Lower Cretaceous) is only 200 to 300 ft (60 to 90 m) thick but extends throughout Wyoming and parts of adjacent states (Byers and Larson, 1979). Both the Hilliard Shale and the Mowry Shale include some sandstone in the Thrust Belt to the west.

The uppermost sandstone in the Frontier Formation is the First Frontier (fig. 5), a distal-deltaic to nearshore marine sandstone that occurs only on the La Barge Platform (McDonald, 1973; De Chadenedes, 1975). First Frontier sandstone and sandstones in the overlying Hilliard Shale are similar in well log expression, stratigraphic position, and geographic distribution. First Frontier sandstone is separated from underlying Frontier sandstones by several hundred feet of regionally continuous marine shale (fig. 5).

Second Frontier sandstone extends the length of the Moxa Arch (fig. 6) and contains the most prolific Frontier gas reservoirs in the western Green River Basin. The Second Frontier is composed of several sandstone “benches” interbedded with shale (fig. 5). The First, Fourth, and Fifth Benches are laterally discontinuous fluvial channel-fill sandstones, whereas the Second

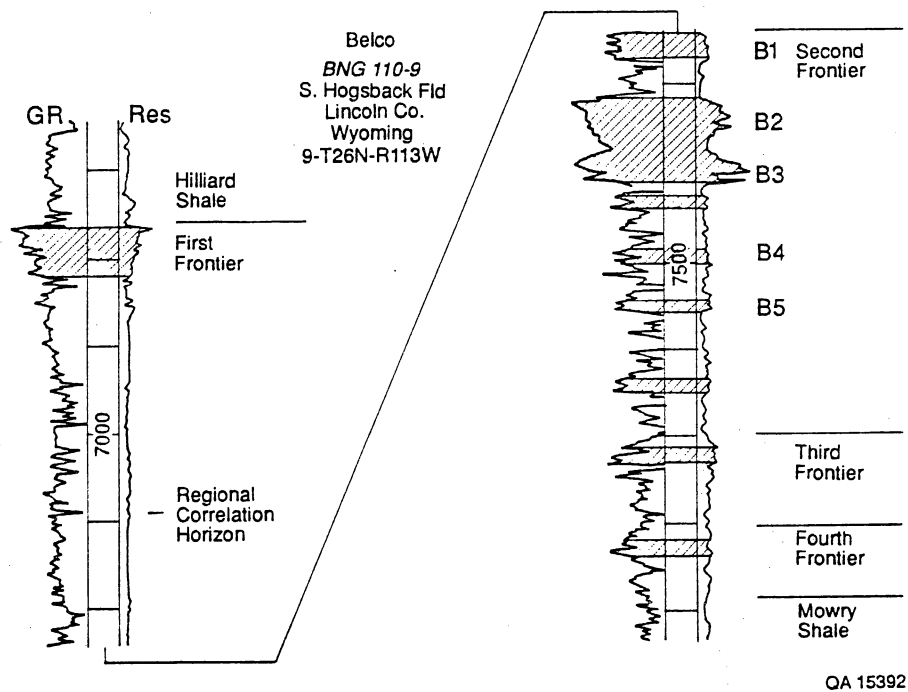


Figure 5. Typical gamma-ray/resistivity log, Frontier Formation, north Moxa Arch (from Dutton and Hamlin, 1991). Frontier sandstones are shaded.

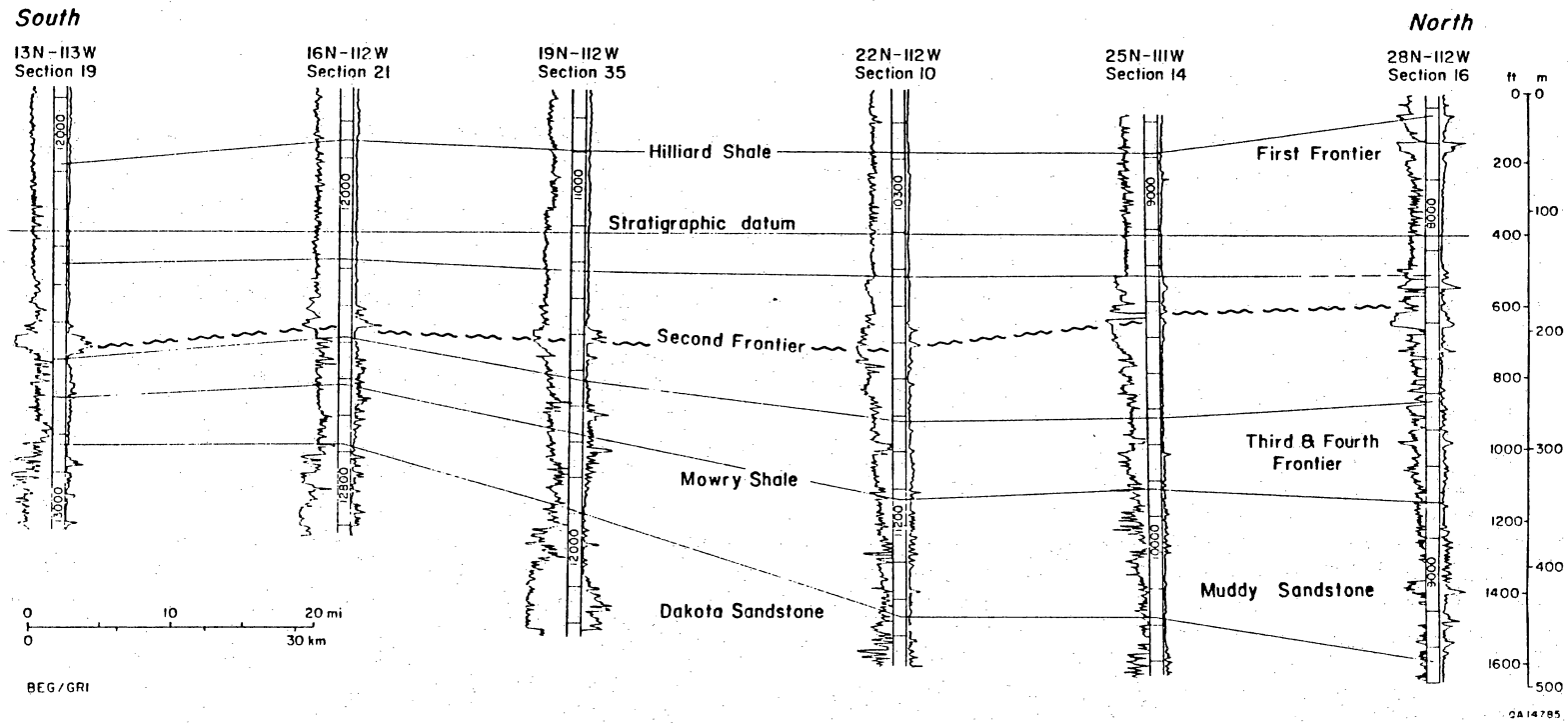


Figure 6. Regional north-south, gamma-ray/resistivity cross section along the Moxa Arch (modified from Dutton and Hamlin, 1991). Line of section same as in figure 4. An erosional unconformity (dashed wavy line) within the Second Frontier separates First Bench fluvial channel-fill sandstone from underlying Second Bench marine shoreline sandstone. A transgressive surface of erosion occurs at the base of the Second Bench (see fig. 11). Other (straight) lines shown on this section are correlation-based chronostratigraphic horizons. Formation boundaries (lithostratigraphic) are not shown.

Bench is a marine shoreline sandstone having widespread continuity. Correlation of facies sequences suggests that the Second Bench is continuous with the Oyster Ridge Sandstone that crops out in the Thrust Belt. The Third Bench is a shoreline sandstone that underlies and merges with the Second Bench in the west part of the La Barge Platform. Nonmarine organic-rich shales, thin coal beds, and bentonites (altered volcanic ash) are associated with the fluvial channel-fill sandstones, whereas marine and marginal marine shale and sandy shale commonly bound Second Bench shoreline sandstone.

The Second Frontier thins southward along the Moxa Arch, owing mainly to erosional truncation (fig. 6). On the La Barge Platform in the north, the First Bench includes erosionally based fluvial channel-fill sandstone, which is typically separated from the underlying Second Bench shoreline sandstone by 5 to 20 ft (2 to 6 m) of transitional, fine-grained facies (bay/lagoon, swamp, and marsh). In fields along the middle and south parts of the arch, such as Whiskey Butte and Church Buttes (fig. 2), erosional downcutting by First Bench channels generally removed the transitional shale and variable amounts of the underlying Second Bench shoreline sandstone. Whereas Second Bench shoreline sandstone forms the most productive reservoirs in the north, First Bench fluvial channel-fill sandstone forms the most productive reservoirs in the south (Moslow and Tillman, 1986, 1989). The Fourth and Fifth Benches of the Second Frontier also disappear southward along the arch, apparently owing to a combination of stratigraphic pinch-out and erosional truncation. Fourth and Fifth Bench fluvial channel-fill sandstones form reservoirs locally, but only on the La Barge Platform.

The Second Frontier formed in an eastward-prograding fluvial-deltaic depositional system, in which the reservoir sandstone facies are primarily fluvial channel fill and marine shoreline (strandplain). Sandstone thickness in the Second Frontier generally decreases to the east and south (fig. 7), partly because the Second Frontier interval thins in those directions. Net thickness of sandstone is greatest in northeast Lincoln County and northwest Sweetwater County (fig. 7), delineating a major deltaic depocenter in the Frontier along this part of the western interior Cretaceous seaway. Because the map of Second Frontier sandstone thickness



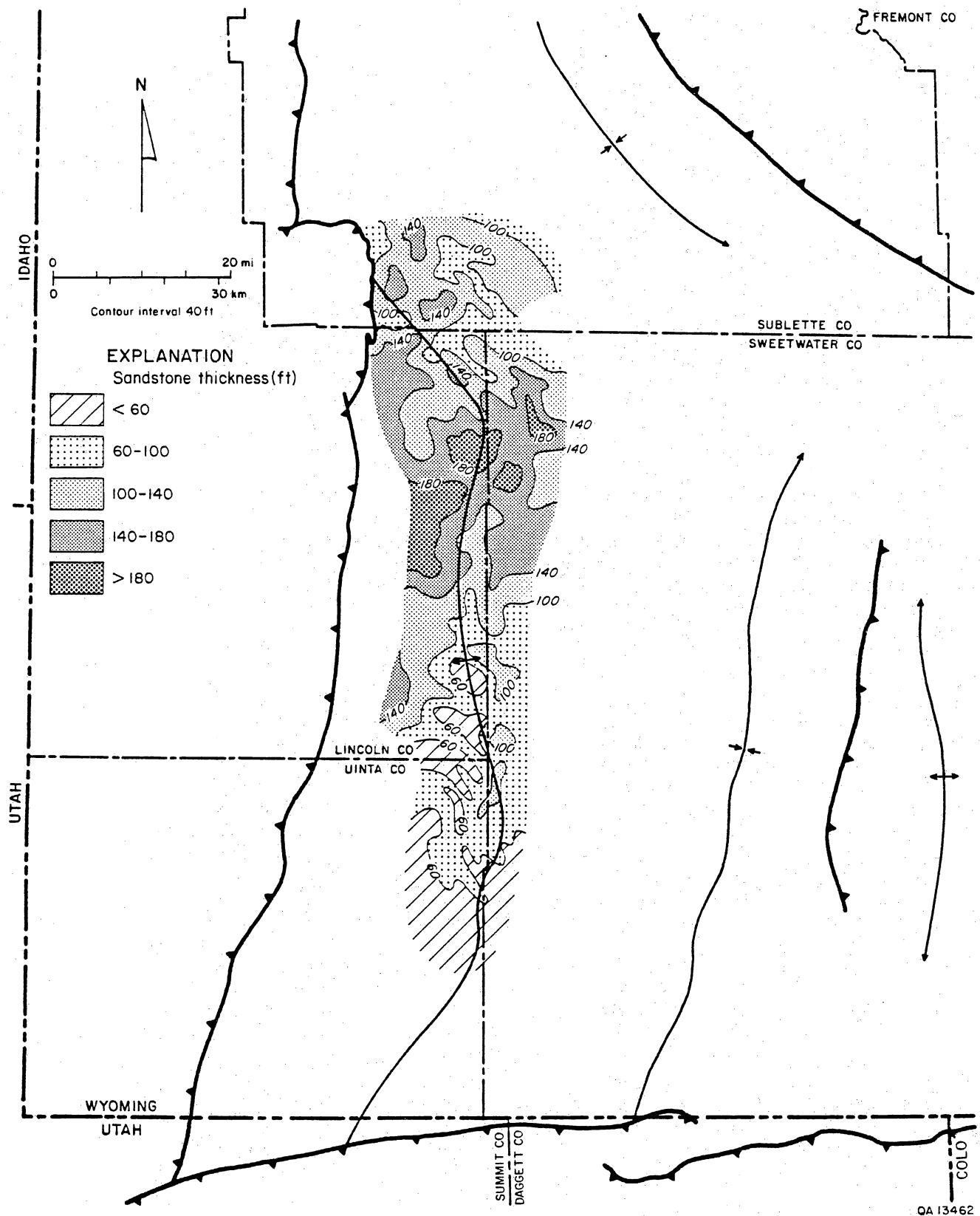


Figure 7. Map showing thickness of sandstone in the Second Frontier along the Moxa Arch. Several sandstone bodies (the benches) are combined on this map. Thick sandstone in northeast Lincoln County and northwest Sweetwater County delineates a major deltaic depocenter.

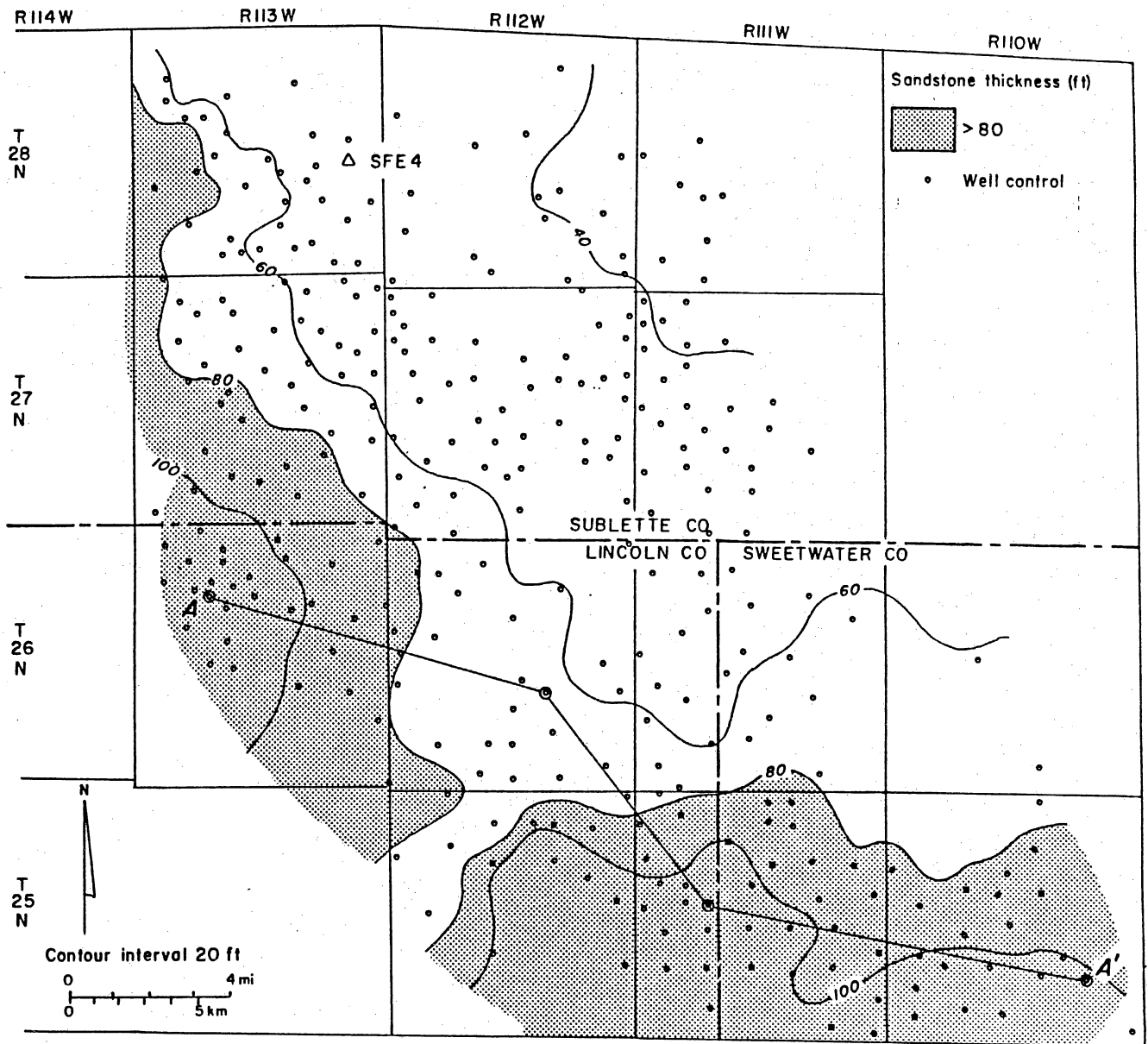
(fig. 7) includes multiple sandstone bodies of varying origins, facies-related trends are not clearly displayed. Nevertheless, southeast-trending contours along the southern Moxa Arch reflect the dominance of dip-oriented fluvial channel-fill sandstones, and crudely developed northeasterly trends in the north suggest the presence of thick strike-aligned marine shoreline sandstone (fig. 7). Previous studies (McDonald, 1973; Moslow and Tillman, 1989), as well as more detailed sandstone mapping (to be discussed), confirm that Second Frontier shorelines trended generally northeastward.

On the La Barge Platform, the Second Frontier is underlain by interbedded marine shales and shoreline sandstones known as the Third and Fourth Frontier (fig. 5). Sandstones are thin and laterally discontinuous in the Third and Fourth Frontier; these intervals are generally transitional with the underlying Mowry Shale. Southward along the Moxa Arch, the Third and Fourth Frontier intervals thin and become shalier, essentially grading into the upper part of the Mowry Shale (fig. 6).

## Second Frontier Sandstone on the La Barge Platform

### Sandstone Depositional Patterns

Second Frontier sandstone bodies display thicknesses, continuities, and elongations inherited from the depositional environment but modified by shoreline progradation and variable subsidence. On the La Barge Platform, the Second and Third Benches of the Second Frontier together form a continuous, northeast-thinning sheet of sandstone (fig. 8). Distinguishing the Second Bench from the Third Bench using well logs alone is difficult, and because they were deposited in similar environments, both benches will be discussed as a single unit, and (following common usage) will be termed "Second Bench." Studies of core indicate that the Second Bench of the Second Frontier was deposited in a marine shoreline environment comprising lower shoreface (below wave base) shaly sandstone and upper shoreface (above wave base) clean sandstone. The sandy shoreface was relatively narrow but



QA16285

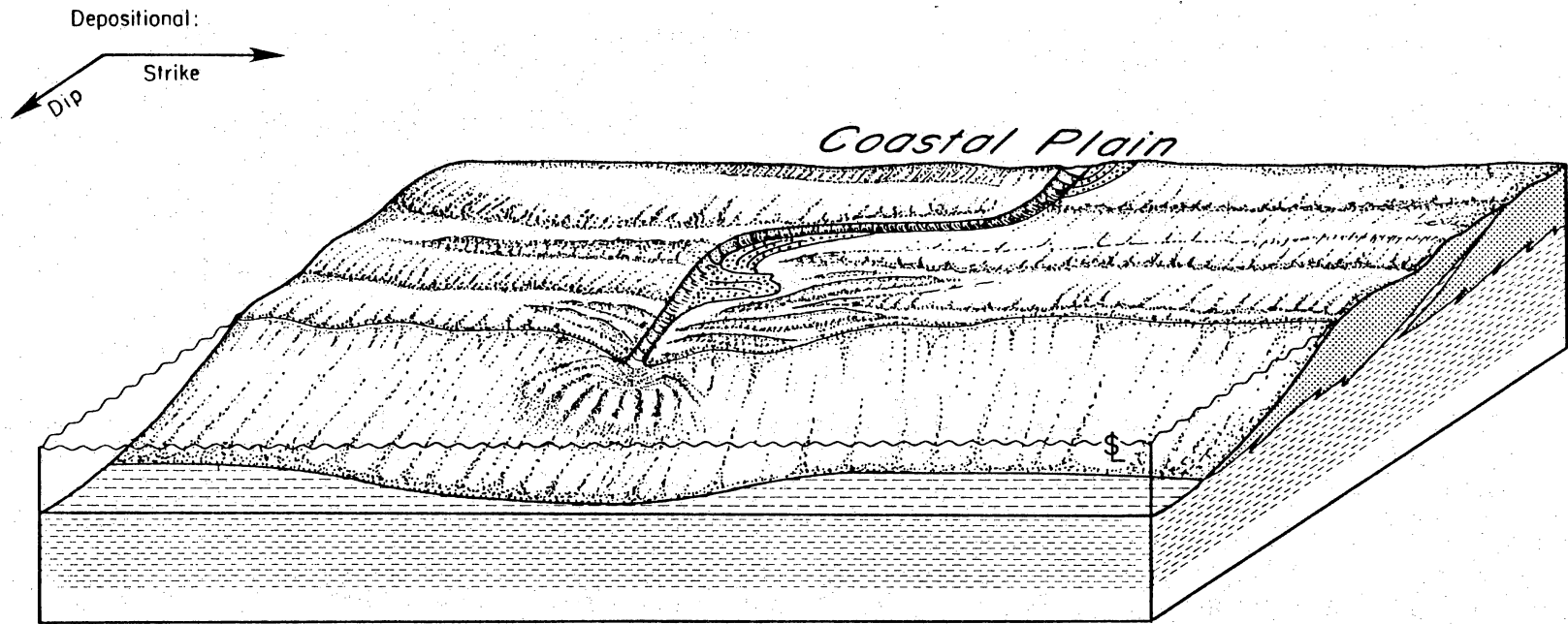
Figure 8. Map showing thickness of sandstone in the Second and Third Benches of the Second Frontier on the La Barge Platform. The Second and Third Benches merge across much of this area. Cross section shown in figure 11.

built seaward (prograded) through time by longshore sand transport and deposition. Sediment was supplied to the shoreline by rivers and reworked along the shoreface by wind- and wave-driven currents. Shoreline progradation resulted in a laterally continuous sheet of sandstone composed of amalgamated shoreface sequences (fig. 9). Although the dominant Second Bench shoreline trend was probably northeast, differential subsidence during deposition and proximity to the deltaic depocenter (fig. 7) are probably responsible for southwestward-increasing sandstone thickness (fig. 8).

The First Bench of the Second Frontier was deposited on a lower coastal plain (delta plain) and includes discontinuous fluvial channel-fill sandstone bodies. Southeast-trending belts of sandstone (fig. 10) delineate the positions occupied by river channels on the coastal plain. Through time the channels migrated laterally or changed course abruptly, preserving a network of lenticular sandstone bodies (fig. 10). During floods, overbank flow spread sand across the coastal plain, causing the First Bench to have at least some thin sandstone in most wells. Thicker, more lobate First Bench sandstone near the southeast margin of the La Barge Platform reflects deposition in a deltaic shoreline environment.

Second Frontier stratigraphy and sandstone development in the vertical dimension are displayed on a well log cross section (fig. 11). The Fourth and Fifth Benches of the Second Frontier together comprise a heterogeneous zone of fluvial channel-fill sandstones, nonmarine and transitional-marine shales, and volcanic ash deposits. This zone apparently becomes more marine to the southeast. Semicontinuous volcanic ash deposits (bentonites), identified by high gamma-ray spikes, form chronostratigraphic horizons useful for dividing the Fourth and Fifth Benches (fig. 11). The upper boundary of the Fourth Bench is a transgressive surface of erosion (marine facies abruptly overlying nonmarine facies), recording a time when relative sea level rose and the shoreline encroached on the coastal plain.

After the sea had completely transgressed the Fourth Bench coastal plain on the La Barge Platform, renewed sediment input and shoreline progradation resulted in the Second and Third Benches. The lateral continuity of sandstone in this interval was caused by seaward building of



**Sand-Rich Strandplain**

Figure 9. Depositional model of a sand-rich strandplain (from Galloway and Cheng, 1985). Closely offlapping shoreface sandstone wedges (stippled) amalgamate into a continuous sheetlike sandstone body, which is compartmentalized internally by thin shale layers along relict depositional surfaces and by facies changes.

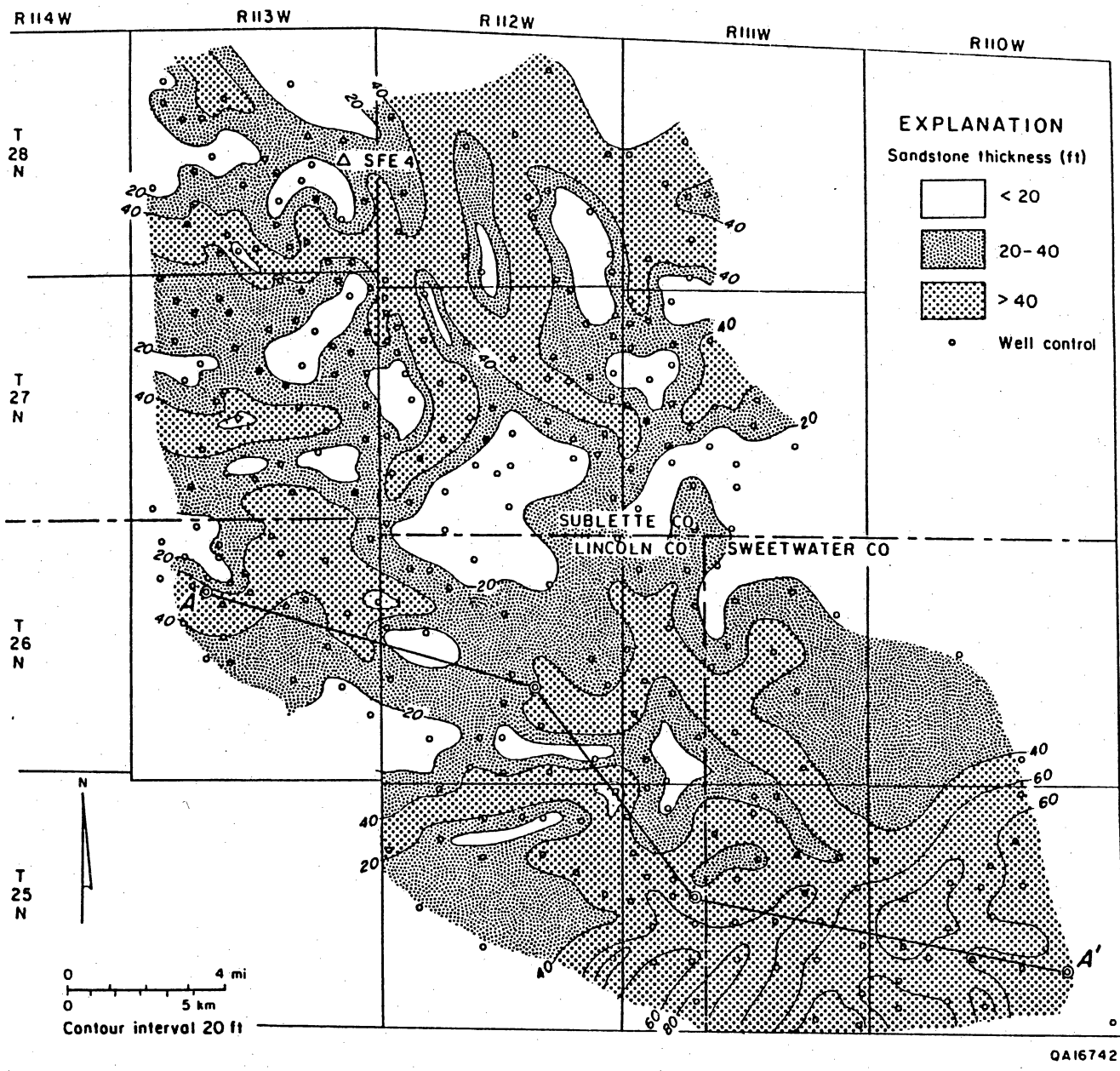


Figure 10. Map showing thickness of sandstone in the First Bench of the Second Frontier on the La Barge Platform.

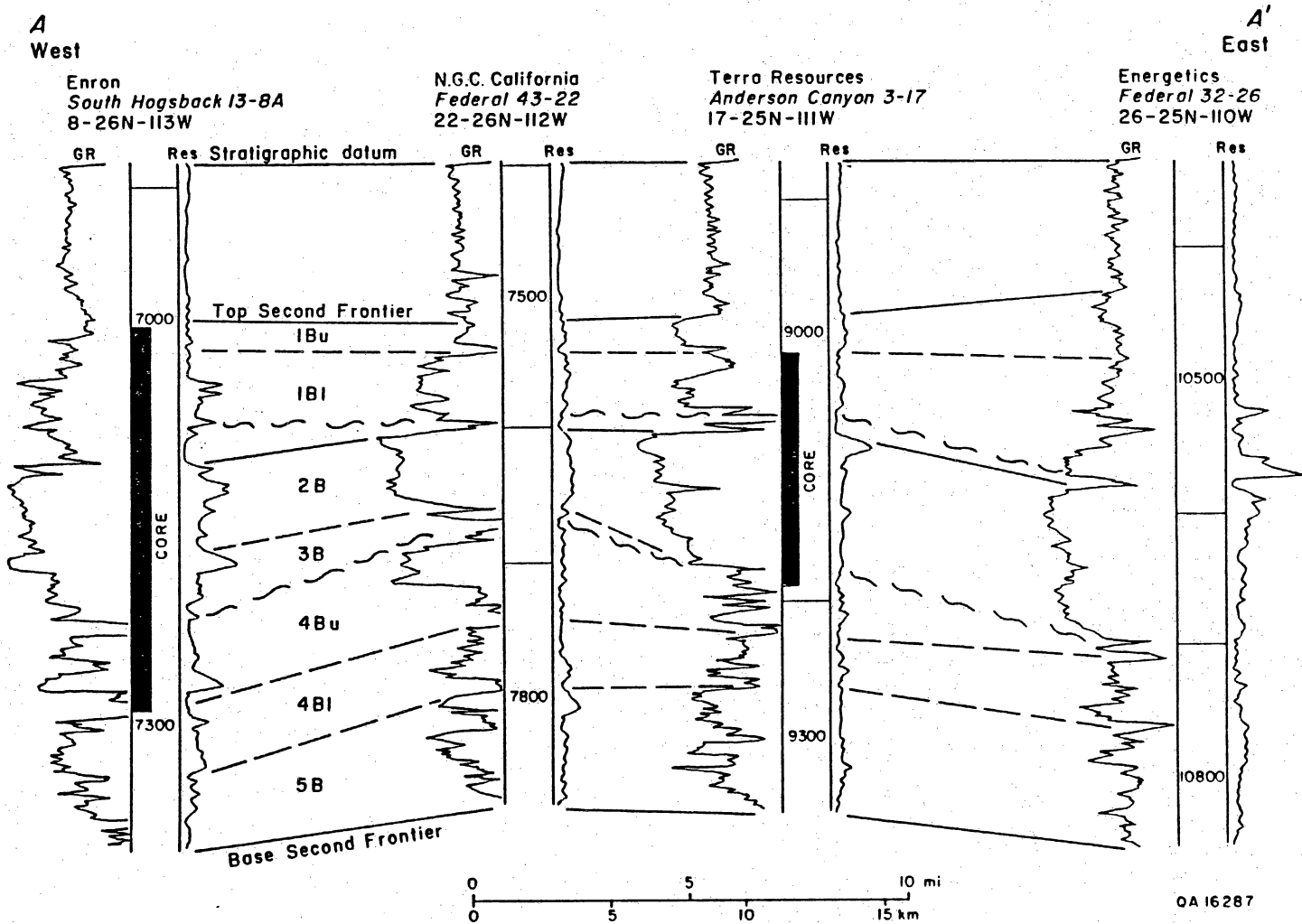


Figure 11. West-east gamma-ray/resistivity stratigraphic cross section of the Second Frontier on the La Barge Platform. Line of section shown in figure 8. Cored intervals in two GRI cooperative wells are also shown. The straight lines are correlation horizons, and the wavy lines represent unconformities (dashed where approximately located). Benches of the Second Frontier are labelled 1B-5B.

the shoreface at a rate sufficient to keep pace with subsidence. This process effected a sheetlike geometry that is superficially homogeneous but is actually compartmentalized internally by facies boundaries and depositional surfaces (fig. 9). In individual wells the Second Bench commonly forms a single progradational shoreline sequence of lower shoreface shaly sandstone overlain by upper shoreface clean sandstone. Gradational "upward cleaning" is reflected in upwardly decreasing gamma-ray response and upwardly increasing resistivity. The Third Bench forms a poorly defined upward cleaning sequence, which apparently pinches out toward the east (fig. 11).

The First Bench is separated from the Second Bench by a widespread high gamma-ray/low resistivity shale (fig. 11). Origin of this shale is problematic. In core it appears to be composed of depositional facies, such as bay/lagoon or coastal marsh, that are transitional between the marine Second Bench and the nonmarine First Bench. Its widespread distribution, however, suggests that this shale may actually record a relative sea-level rise and partial flooding of the coastal plain. The First Bench is a heterogeneous zone of primarily nonmarine facies, which is similar to the Fourth and Fifth Benches. Fluvial channel-fill sandstone is best developed in the lower part of the First Bench, where it generally causes blocky to upward increasing gamma-ray responses (fig. 11). The upper part of the First Bench forms an eastward-thickening zone that is transitional into the overlying, regionally extensive marine shale. Sandstone of probable shoreface origin occurs in the upper First Bench in the southeast part of the La Barge Platform (fig. 11).

#### Clean Sandstone Distribution

Studies of core show that the clay content of Frontier reservoirs influences porosity and permeability. Frontier pay zones commonly lie in sandstones having low detrital clay contents, although framework grain composition and postdepositional diagenesis severely limit reservoir quality even in clean Frontier sandstone. Therefore, net clean sandstone does not necessarily equal net pay, but distinguishing low-clay (clean) sandstone from clay-rich (shaly) sandstone is



an important first step in determining the distribution of potential Frontier reservoirs. By comparing core properties with corresponding log responses, gamma-ray and resistivity cutoffs were established for measuring thicknesses of clean sandstone (sandstone having less than about 10 percent clay content). Neutron/density logs, where available, aided in the determination of clean sandstone. Other variables besides clay content influence well log responses so that core-calibrated log measurements of clean sandstone are most accurate in limited areas where these other variables, such as connate water composition and formation mineralogy, are relatively constant. Net clean sandstone maps reveal depositional-facies-related trends, such as shorelines and channels, that can be projected into sparsely drilled areas and that lead to areas having potentially favorable reservoir development.

The apparent distribution of clean sandstone in the Second Bench (fig. 12) is influenced by factors other than depositional processes. Increasing thickness of clean sandstone to the west is related partly to increased subsidence and thicker gross sandstone in that area (fig. 8). Carbonate cement and calcareous shell debris are more abundant in the west part of the La Barge Platform and cause high resistivity responses, which can lead to overestimation of clean sandstone thicknesses. Thus, figure 12 probably most accurately reflects clean sandstone distribution in the east half of the mapped area.

Within the Second Bench sheet sandstone, net clean sandstone displays distinct northeast trends (fig. 12). Clean sandstone in the Second Bench lies primarily in upper shoreface facies, where waves and vigorous currents strongly agitate the sediment and winnow finer particles (silt and clay). In a progradational, wave-dominated delta and delta-flank strandplain system, foreshore and beach-ridge facies, also composed of clean sandstone, generally overlie the upper shoreface (Heward, 1981) but apparently are poorly preserved in the Second Bench. Thus, the Second Bench clean sandstone map (fig. 12) is essentially a map of the thickness of upper shoreface facies, and the northeast trends probably delineate successive positions of the shoreline as it prograded seaward (southeastward). The fact that northeast trends are absent in the gross thickness of Second Bench sandstone (fig. 8) is problematic, but it apparently can be

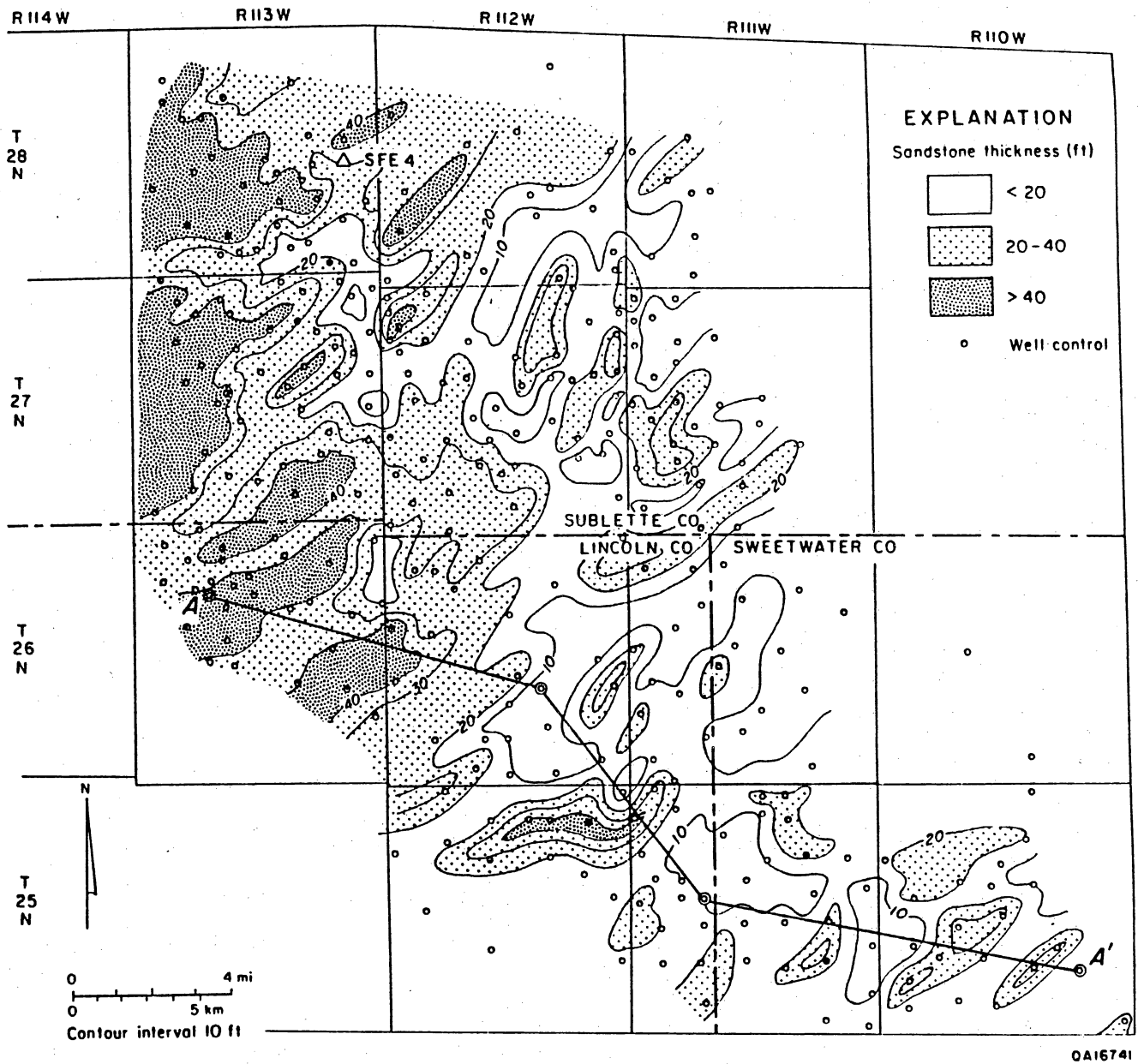


Figure 12. Net clean sandstone map of the Second Bench of the Second Frontier on the La Barge Platform. Cross section shown in figure 11.

attributed to westward- and southwestward-increasing subsidence and sedimentation rates that deemphasize the influence of depositional environment on sandstone thickness patterns.

In the First Bench, clean sandstone forms narrow southeast-trending belts (fig. 13), which are similar to but thinner than those seen on the map of First Bench gross sandstone (fig. 10). These sandstone belts record the positions of fluvial channels. The rivers that deposited First Bench sandstones did not supply sediment to Second Bench shorelines. First Bench shoreline facies occur mainly east and southeast of the Moxa Arch and postdate the Second Bench. Fluvial channel-fill facies in the Second Bench are located west of the Moxa Arch and were rarely observed in core from wells on the La Barge Platform.

On the La Barge Platform, the First and Second Benches of the Second Frontier contain most of the clean sandstone in the lower (Second, Third, and Fourth) Frontier interval (fig. 14). The Fourth and Fifth Benches of the Second Frontier and the underlying Third Frontier and Fourth Frontier are more discontinuous and contain only isolated clean zones. The Third Frontier and the Fourth Frontier probably represent isolated shoreface sequences in a mud-dominated shoreline system. The Fourth and Fifth Benches are fluvial channel-fill deposits that formed on a mud-rich coastal plain that had isolated fluvial channels. The First Bench, in contrast, formed on a relatively sand-rich coastal plain. First Bench fluvial channels migrated laterally, forming belts of sandstone that are several times wider than the original river channel and that are flanked by broad aprons of thinner sandstone (fig. 10), which were deposited by overbank flow during floods. First Bench clean sandstone is more limited and discontinuous (figs. 13 and 14), occurring primarily within thicker channel-fill facies. Clean sandstone is most continuous in the Second Bench (fig. 14), but even there its thickness is highly variable (fig. 12). Lateral continuity is characteristic of progradational shoreface sandstone sequences (Heward, 1981).

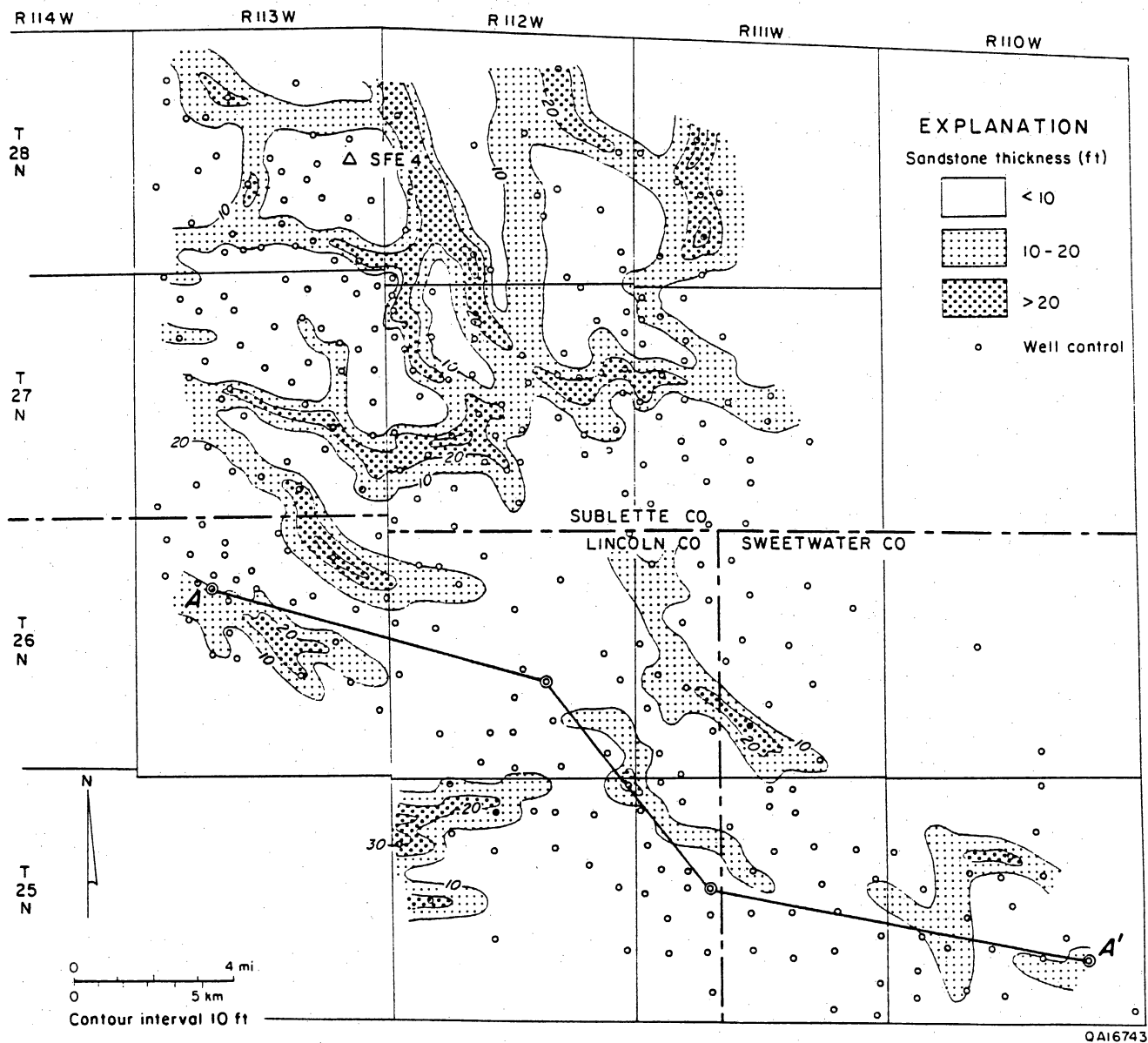


Figure 13. Net clean sandstone map of the First Bench of the Second Frontier on the La Barge Platform. Cross section shown in figure 11.

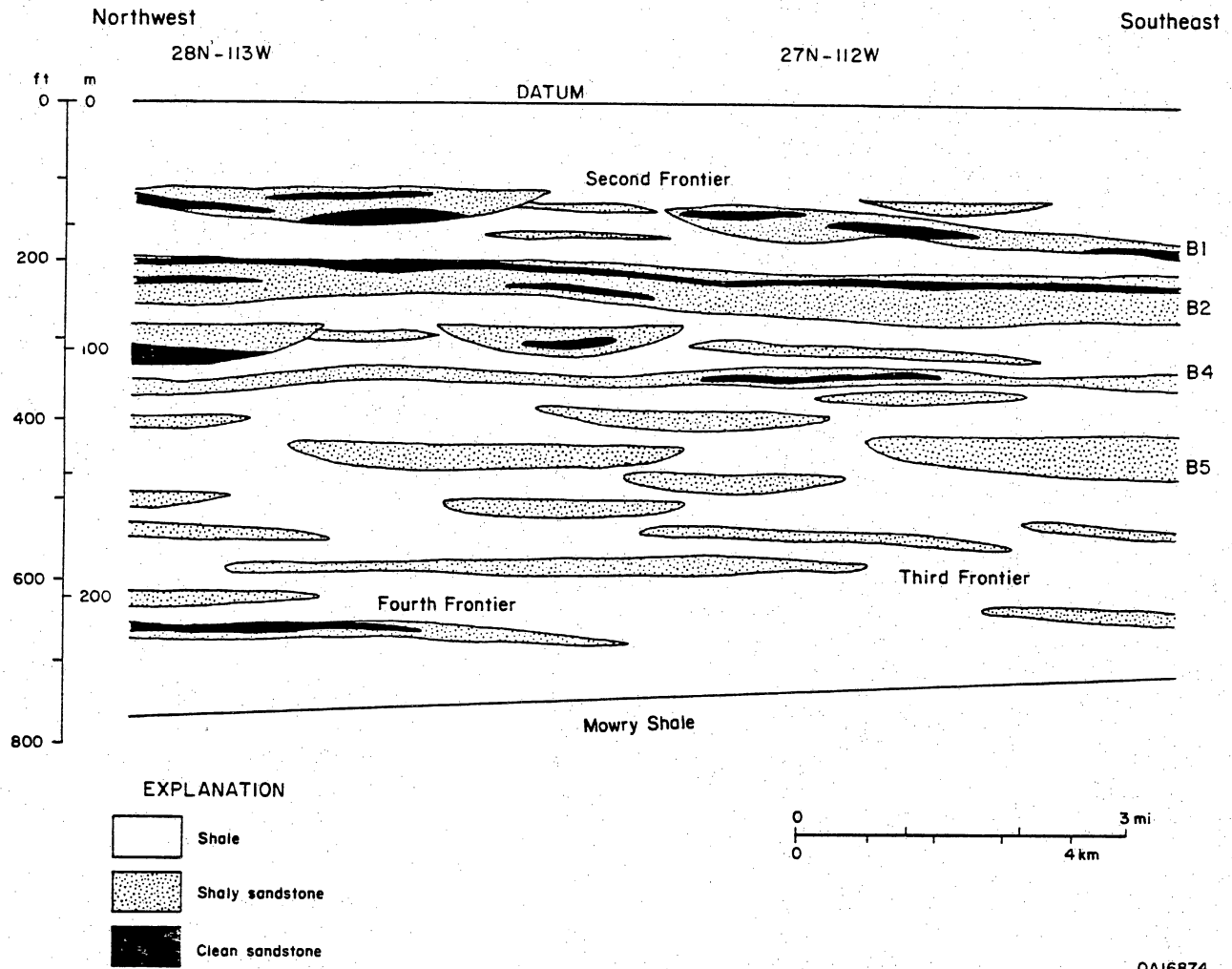


Figure 14. Northwest-southeast schematic cross section showing distribution of shaly sandstone and clean sandstone in the lower (Second, Third, and Fourth) Frontier interval, north La Barge Platform. (B = Bench.)

## Sandstone Porosity Maps

Density, neutron, and acoustic logs were also used to help determine the distribution and quality of Frontier reservoirs. In Frontier sandstones, porosity determined from logs has a weak correlation with permeability determined from core analysis. Even the correlation between core-measured porosity and permeability is relatively weak, and porosity commonly is thus a poor predictor of permeability in Frontier sandstones. However, porosity maps are useful, especially when compared with net clean sandstone maps, to help delineate potential reservoir rock.

Because the relationship between porosity and permeability in Frontier sandstone is poor, the cutoff used for measuring porosity thickness from logs was set at 15 percent. This value yielded thickness variations that were readily mappable. Additionally, this cutoff yielded results that are qualitatively valuable: log porosities are typically highest in areas where sandstone having at least 15 percent log porosity is thickest. To avoid significant shale effects, only clean sandstone and slightly shaly sandstone (clay volume less than approximately 20 percent) were included in porosity-thickness measurements.

In the northwest part of the La Barge Platform (Tip Top-Hogsback area), Second Bench sandstone having at least 15 percent log porosity displays thickness trends (fig. 15) that are similar in orientation, although not always in location or magnitude, to those on the clean sandstone map (fig. 12). Porosity in Frontier clean sandstone is commonly low, because of postdepositional compaction and cementation. In slightly shaly sandstone, abundant microporosity may cause total porosity to be greater than 15 percent. Thus, the distribution of clean sandstone (fig. 12) only imprecisely matches that of porous sandstone (fig. 15), but permeability is likely to be highest in areas where the two coincide.

In the southeast part of the La Barge Platform (Fontenelle area), net porous Second Bench sandstone occurs in lobate bodies that display no clear trend (fig. 16) but that coincide approximately with areas having thick gross sandstone (fig. 8). In this area sandstone having at least 15 percent log porosity includes not only the clean upper shoreface facies but also much

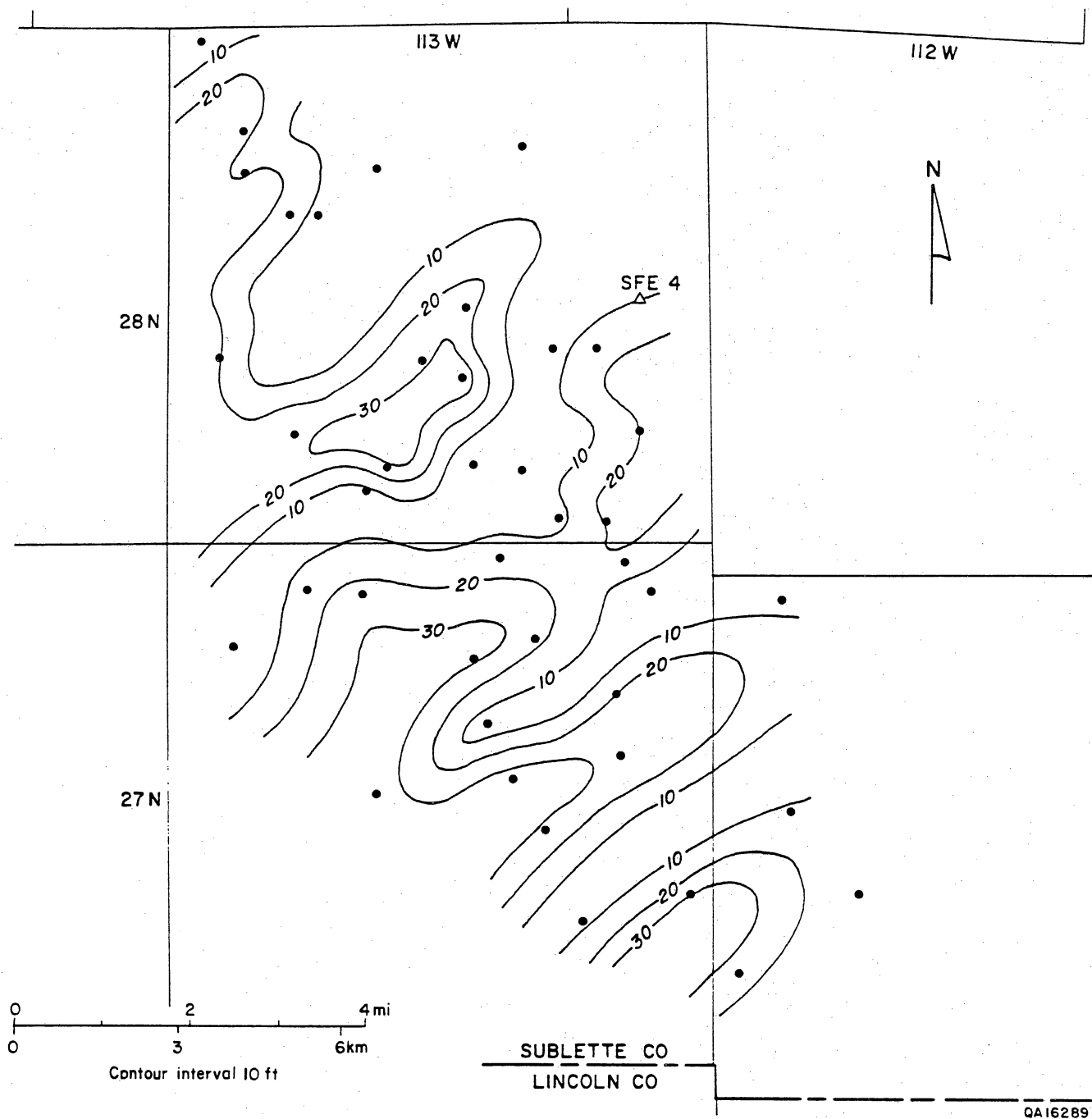


Figure 15. Map showing net thickness of Second Bench sandstone having at least 15 percent log porosity, northwest part of the La Barge Platform. Location of GRI research well, SFE No. 4, is also shown.

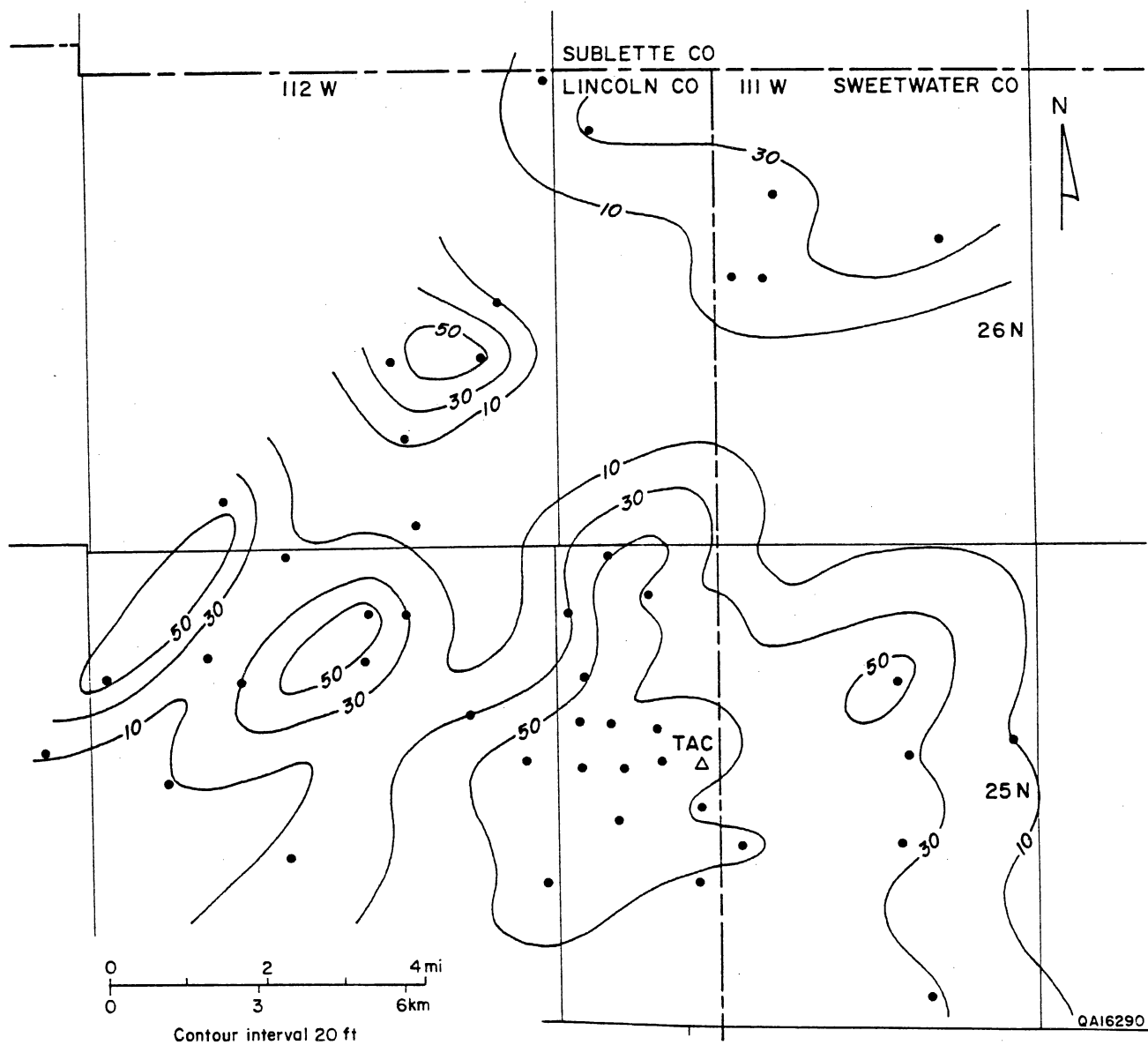


Figure 16. Map showing net thickness of Second Bench sandstone having at least 15 percent log porosity, southeast part of the La Barge Platform. Location of Terra Anderson Canyon No. 3-17 well (TAC) is also shown.



of the underlying, slightly shaly, lower shoreface facies. Core data indicate that Second Bench lower shoreface sandstone in the Fontenelle area commonly has 15 percent porosity but rarely has appreciable (stressed) permeability (0.009 md average). Of the maps illustrated here, the clean sandstone map (fig. 12) probably best indicates the distribution of permeable Second Bench sandstone in the southeast part of the La Barge Platform, although studies of core show that much of this clean sandstone has low permeability (<0.1 md).

### Second Bench Production Trends

Second Bench production trends reflect sandstone depositional patterns, but other variables also influence well productivity, as illustrated by an initial potential (IP) map (fig. 17). Most Frontier wells on the La Barge Platform have perforations in the Second Bench, and although net pay zones on the platform are typically much thinner than in other areas, a rough correlation exists between well productivity (fig. 17) and gross sandstone thickness (fig. 8). Production trends (fig. 17) also show some coincidence with clean sandstone (fig. 12) and porous sandstone (fig. 15). Although the productive limits of the Second Bench may be more attributable to sandstone thinning and low permeability than to structural position (McDonald, 1973; Schultz and Lafollette, 1989), the distribution of wells having high initial potentials coincides roughly with the structurally highest part of the La Barge Platform. Permeabilities in many of the wells having high initial potentials apparently are anomalously high for Frontier sandstone, and sandstone maps based on SP logs reveal a correlation between high IP in the Second Bench and large negative SP deflections. The initial potentials shown on figure 17 are typically measured or calculated after the wells received a hydraulic fracture treatment, and variations in the effectiveness of these stimulation treatments can influence well productivity. Natural fractures may be important to Second Bench productivity, but the location, abundance, and orientation of natural fractures in the subsurface is difficult to measure directly (Laubach, 1991). Finally, commingling of gas production from several Frontier zones is a common

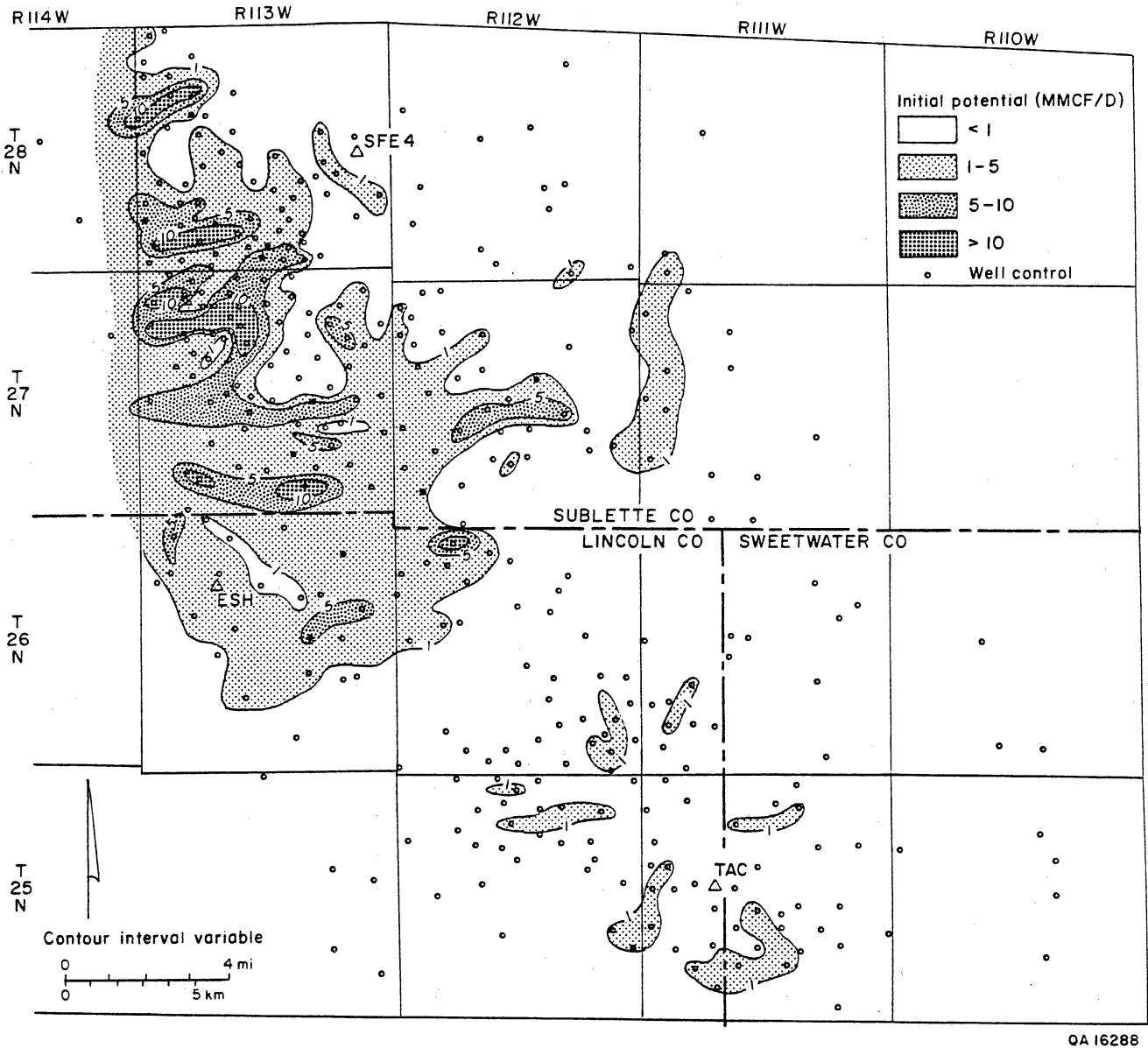


Figure 17. Initial potential map of wells on the La Barge Platform having Second Bench perforations. These wells commonly have additional perforations in other Frontier zones, and in those cases production is commingled. Locations of S. A. Holditch & Associates Staged Field Experiment No. 4 well (SFE 4), Terra Anderson Canyon No. 3-17 (TAC), and Enron South Hogsback No. 13-8A (ESH) are shown.

completion practice and further obscures causal relationships, although the Second Bench is typically the dominant contributor in such cases.

### GRI Cooperative Wells

Core and log data gathered in GRI/industry cooperative wells allowed field-scale and well-site studies of Frontier reservoir sandstones at several locations along the Moxa Arch (fig. 1).

#### Terra Resources Anderson Canyon No. 3-17

The Terra Resources (now Pacific Enterprises) Anderson Canyon No. 3-17 cooperative well is located at Fontenelle field on the southeast margin of the La Barge Platform (well 9 in fig. 1; fig. 2). Fontenelle field lies in a broad, unfaulted, structural nose, which dips 200 ft/mi (38 m/km) ( $2^\circ$ ) to the southeast. Continuous core was taken in Terra Anderson Canyon No. 3-17 from 9,015 to 9,188 ft (2,747 to 2,800 m). The cored interval includes the lower First Bench, all of the Second Bench, and a small part of the upper Fourth Bench (fig. 11).

The deepest core recovered is about 15 ft (5 m) of shale and sandy shale (9,172.5 to 9,188 ft [2,796 to 2,800 m]) from below the Second Bench, which displays the indistinct mottling and root traces commonly observed in soil profiles. This is the uppermost part of the Fourth Bench coastal-plain depositional facies. The Third Bench is generally indistinguishable at Fontenelle field (fig. 11). A sharp erosional surface occurs at 9,172.5 ft (2,796 m) and is overlain by bioturbated shaly sandstone in the lower part of the Second Bench. This surface, which forms the lower boundary of the Second Bench shoreface sequence throughout the La Barge Platform, was cut into the underlying Fourth Bench by shoreface erosion that accompanied westward shoreline retreat.

At the Terra Anderson Canyon No. 3-17 well site, the Second Bench is a well-developed progradational shoreface sequence, comprising 74 ft (23 m) of lower shoreface shaly sandstone (9,098 to 9,172.5 ft [2,773 to 2,796 m]) overlain by 20 ft (6 m) of upper shoreface clean sandstone (9,078 to 9,098 ft [2,767 to 2,773 m]) (fig. 18). The lower shoreface facies are

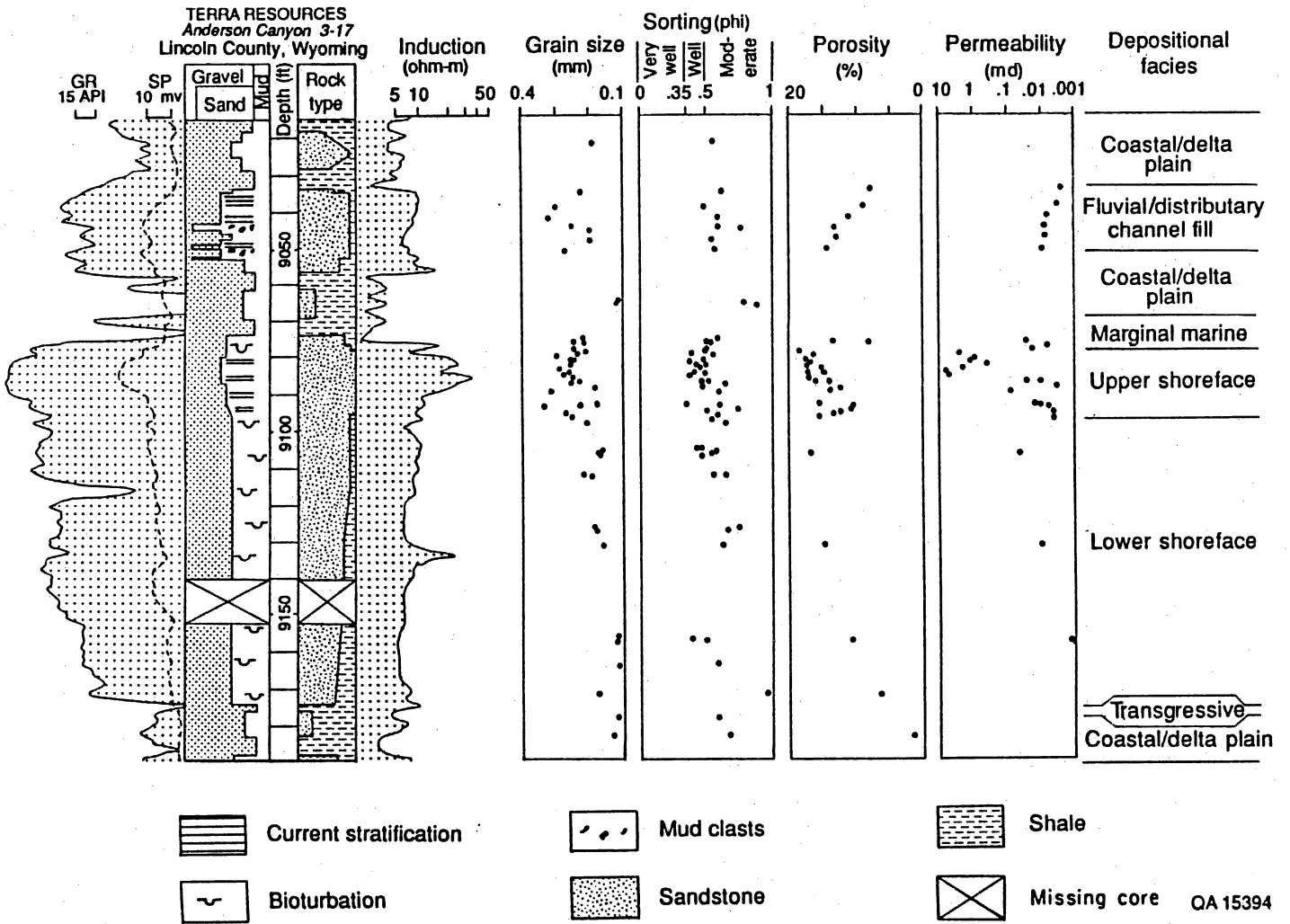


Figure 18. Log responses and rock properties in core from the First and Second Benches of the Second Frontier (fig. 11), Terra Anderson Canyon No. 3-17 well, Fontenelle field (from Dutton and Hamlin, 1991). Porosity and stressed permeability data from core are shown.

thoroughly bioturbated mixtures of sand, silt, and clay; primary stratification was destroyed by burrowing organisms. Clay content decreases gradationally upward, ranging from 50 to 10 percent of rock volume. This upward cleaning reflects gradual shoaling as the shoreline approached the position of this well. The upper part of the lower shoreface contains 1- to 2-ft-thick (0.3- to 0.6-m) clean sandstone beds that were deposited during storms. The upper shoreface facies comprise clean, well-sorted sandstone having prominent horizontal lamination and crossbeds. The upper shoreface facies were deposited in shallow water where wave- and wind-driven currents agitated and winnowed the bottom sediments and inhibited the activity of burrowing organisms.

The Second Bench is capped by a shale (9,057 to 9,074 ft [2,760 to 2,766 m]) (fig. 18), having a widespread distribution and a complex depositional history. This shale, together with a 3-ft (1-m) transition zone of bioturbated shaly sandstone at the top of the Second Bench, apparently records an episode of relative sea-level rise, partial flooding and reworking of the upper part of the shoreface sequence, and then relative sea-level fall accompanied by a return to a coastal-plain setting. Most of this interval (9,070 to 9,057 ft [2,764 to 2,760 m]) contains well-developed root mottling and abundant plant debris, indicating a heavily vegetated floodplain environment.

On the La Barge Platform, First Bench fluvial channel-fill sandstone commonly overlies the organic-rich nonmarine shale described above. At the Terra Anderson Canyon cooperative well, a 19-ft (6-m) channel-fill sandstone was cored (9,034 to 9,053 ft [2,753 to 2,759 m]) (fig. 18). An erosional base and internal erosional surfaces, mud-clast conglomerates, large crossbeds, and soft-sediment deformation are distinctive features of the First Bench sandstone from the Terra Anderson Canyon well. The sand-sized fraction in the First Bench is coarser and less well sorted than it is in the Second Bench (fig. 18). Clay volume in this First Bench sandstone averages about 10 percent and occurs mainly as sand- and gravel-sized rip-up mud clasts, which were eroded from the muddy river banks and incorporated into the sandy bed load of the river channel. A zone in the middle part of the sandstone (9,044 to 9,050 ft [2,756 to 2,758 m])

contains several 1-ft (0.3-m) beds in which volume of mud clasts exceeds 50 percent. A higher gamma-ray response marks this clay-rich zone (fig. 18). First Bench channel-fill sandstone is overlain by channel-flank shaly sandstone and shale in the uppermost part of the core.

At Terra Anderson Canyon No. 3-17, as is the case with most of the wells in Fontenelle field, the Second Bench is the primary reservoir. The pay zone is about 7 ft (2 m) thick (9,079 to 9,086 ft [2,767 to 2,769 m], approximate core depth) and lies within Second Bench upper shoreface facies. This zone is distinguished by higher core permeabilities than those in adjacent, apparently similar, upper shoreface sandstone (fig. 18), and it contains a lower percentage of ductile rock fragments than does the closely adjacent sandstone (Dutton, 1991). These factors, along with subtle variations in stratification type, suggest that the pay zone was deposited either in a foreshore (intertidal) environment or in a very high energy subenvironment of the upper shoreface. The strong bottom currents in this environment winnowed not only the silts and clays but also the less durable sand-sized particles (Dutton, 1991). Clearly, depositional environment exerted a strong control on reservoir quality in the Frontier at the Terra Anderson Canyon well site.

#### Wexpro Church Buttes No. 48

The Wexpro Church Buttes No. 48 cooperative well is located in Church Buttes field along the south part of the Moxa Arch (well 15 in fig. 1; fig. 2). The field lies in a north-trending, doubly plunging anticline, which is about 14 mi (22 km) long and coincides with the crest of the Moxa Arch. The Church Buttes cooperative well is located on the north end of the anticline near the fold hinge. The top of Frontier sandstone is at 12,153 ft (3,704 m) in this well. A single Second Frontier sandstone interval is present in this area. Core was taken in marine shale above the sandstone (12,045 to 12,072 ft [3,671 to 3,680 m]) and through most of the Second Frontier sandstone (12,144 to 12,204 ft [3,701 to 3,718 m]).

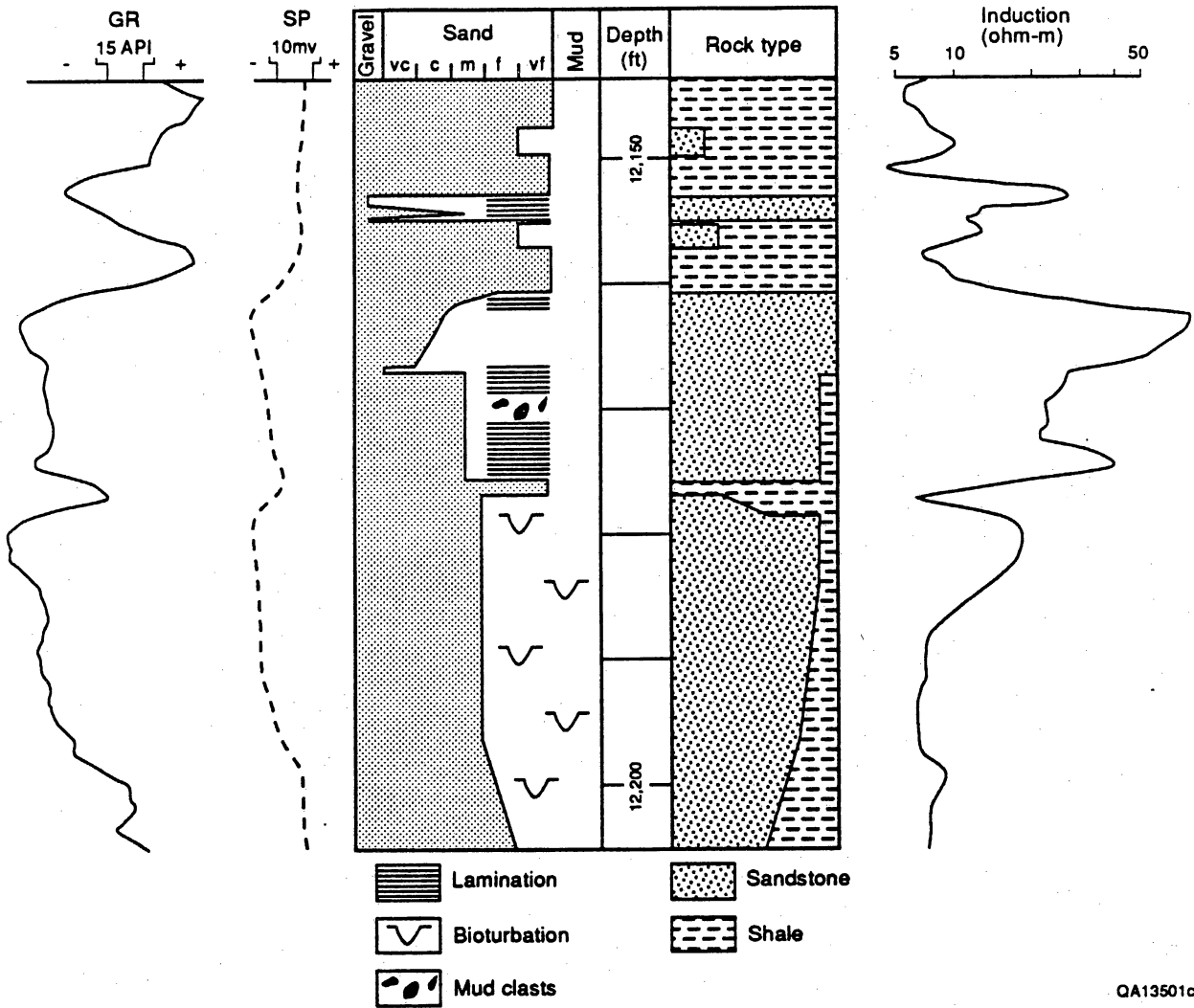
At Wexpro Church Buttes No. 48, the Second Frontier sandstone comprises a progradational shoreface sequence truncated by a fluvial channel. The lower part of the core

(12,177 to 12,204 ft [3,712 to 3,718 m]) consists of bioturbated lower shoreface shaly sandstone in which stratification was almost completely destroyed by pervasive burrowing. Upwardly increasing grain size and sandstone percent are well displayed (fig. 19). The lower shoreface is capped by 2 ft (0.6 m) of marine mudstone, which is abruptly overlain by fluvial channel-fill sandstone (12,161 to 12,175 ft [3,707 to 3,711 m]) containing abundant mud clasts, crossbeds, soft-sediment deformation, and upwardly decreasing grain size (fig. 19). A heterogeneous suite of nonmarine, organic-rich shale and thin sandstone (12,144 to 12,161 ft [3,701 to 3,707 m]) overlies the fluvial channel-fill sandstone.

Regional stratigraphic correlations indicate that the Second Bench shoreface sequence was erosionally truncated by downcutting of First Bench fluvial channels along the south part of the Moxa Arch. Studies of cores such as this one reveal a shoreline sequence in which the upper shoreface and transitional-marine facies are commonly missing, and fluvial channel-fill sandstone rests directly on offshore marine facies. This erosional unconformity can be traced northward on well logs into the shale that separates the Second and First Benches on the La Barge Platform. Erosional truncation and interval thinning increase southward along the Moxa Arch (fig. 6), indicating that subsidence increased northward during Frontier deposition.

The geometry and quality of Frontier reservoirs are affected by these variations in deposition and erosion. Along the south part of the Moxa Arch, where upper shoreface facies are commonly missing, First Bench fluvial channel-fill sandstone forms the primary reservoir facies (Moslow and Tillman, 1986, 1989). First Bench fluvial sandstone forms dip-oriented, laterally discontinuous reservoirs, whereas Second Bench shoreface sandstone reservoirs are strike aligned and more continuous (figs. 12 and 13). At the Wexpro Church Buttes cooperative well site, the upper part of the fluvial channel fill (12,161 to 12,167 ft [3,707 to 3,709 m]) has the highest core (stressed) permeabilities (0.28 to 0.79 md), probably because the upper fluvial channel-fill sandstone is coarser grained and contains much fewer mud clasts than does the lower part (fig. 19). Lesser quality reservoir rock exists in the lower part of the channel fill and

WEXPRO  
Church Buttes Unit 48  
Sweetwater County, Wyoming



QA13501c

Figure 19. Log responses and core description, Wexpro Church Buttes Unit No. 48 well, Church Buttes field (fig. 2). The core includes bioturbated sandstone (Second Bench) overlain by laminated, mud-clast-bearing sandstone (First Bench).



the upper part of the lower shoreface (approximately 12,167 to 12,187 ft [3,709 to 3,715 m]), where core (stressed) permeabilities average 0.23 md.

#### Enron South Hogsback No. 13-8A

The Enron South Hogsback No. 13-8A cooperative well is located in South Hogsback field on the west part of the La Barge Platform (well 4 in fig. 1; fig. 2). The easternmost of the major Thrust Belt faults (Darby Thrust) crops out near this well. In South Hogsback field, Frontier strata are folded into a south-plunging anticline between two smaller reverse faults (fig. 20). Several reverse faults in the Hilliard Shale intersect the Enron S. Hogsback cooperative well (fig. 21).

The geometries and orientations of Frontier fluvial and shoreface sandstones are well displayed in South Hogsback field and probably influence production patterns. The Second Bench forms a continuous sheet of shoreface sandstone that is 50 to 70 ft (15 to 21 m) thick throughout the field (fig. 22). Within this sheet upper shoreface clean sandstone occurs in discontinuous northeast-trending belts (fig. 23). Southeast-trending belts of fluvial channel-fill sandstone are prominent on a map of the First Bench, and wells that are perforated in and produce gas from the First Bench are located within these belts (fig. 24). Because the First Bench interchannel areas are composed largely of shale, they are unlikely to be productive. Thus, no wells having First Bench perforations lie outside the channel belts (fig. 24). Wells having Second Bench perforations, however, do occur outside of the upper shoreface clean sandstone trends (fig. 23) because these areas do contain abundant, although shaly, lower shoreface sandstone. The Enron S. Hogsback No. 13-8A well is located within but near the margins of these high-sandstone belts (figs. 23 and 24). Nearly continuous core was taken in this well from 7,007 to 7,285 ft (2,136 to 2,220 m), including the First through the Fourth Benches of the Second Frontier (fig. 25).

In South Hogsback field the Fourth Bench includes several laterally discontinuous fluvial channel-fill sandstones, but only the uppermost of these was cored (fig. 22). The Fourth Bench

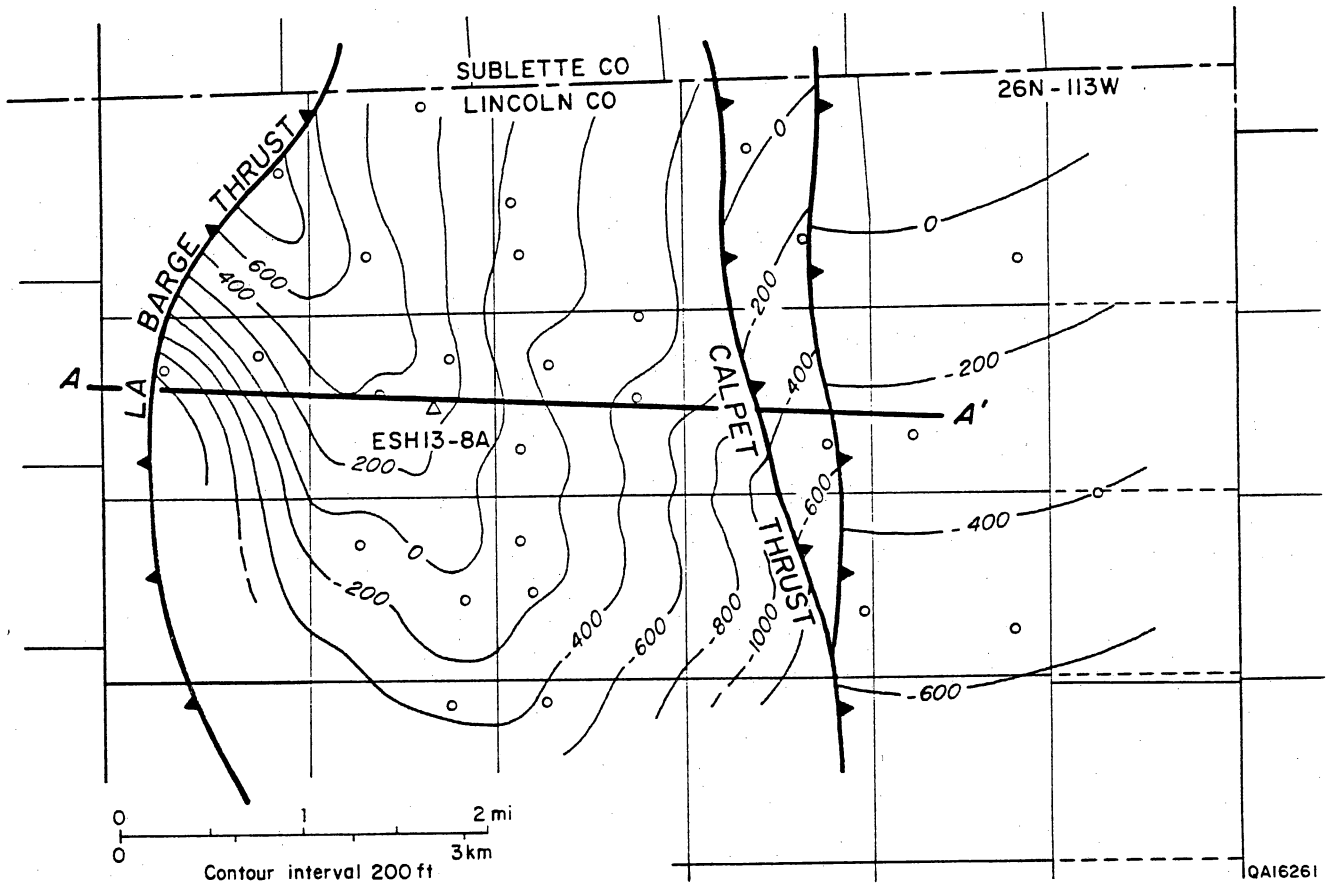


Figure 20. Structure-contour map on the top of the Second Frontier, South Hogsback field; location of Enron S. Hogsback No. 13-8A well (ESH 13-8A) also shown. The positions of the La Barge and Calpet Thrust faults (Blackstone, 1979) are shown at the mapped horizon. The much larger Darby Thrust carries Paleozoic rocks to the surface near the Enron well. Cross section shown in figure 21.

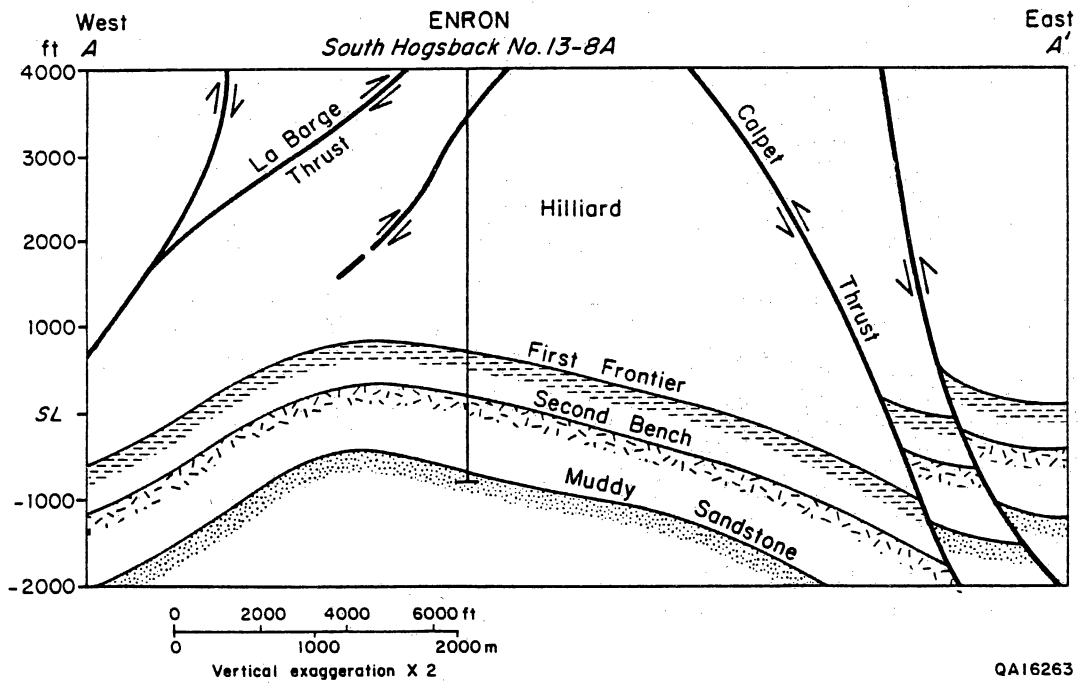


Figure 21. West-east structural cross section in South Hogsback field showing the attitudes of several prominent horizons in the Frontier Formation and the Muddy Sandstone. Line of section shown in figure 20.

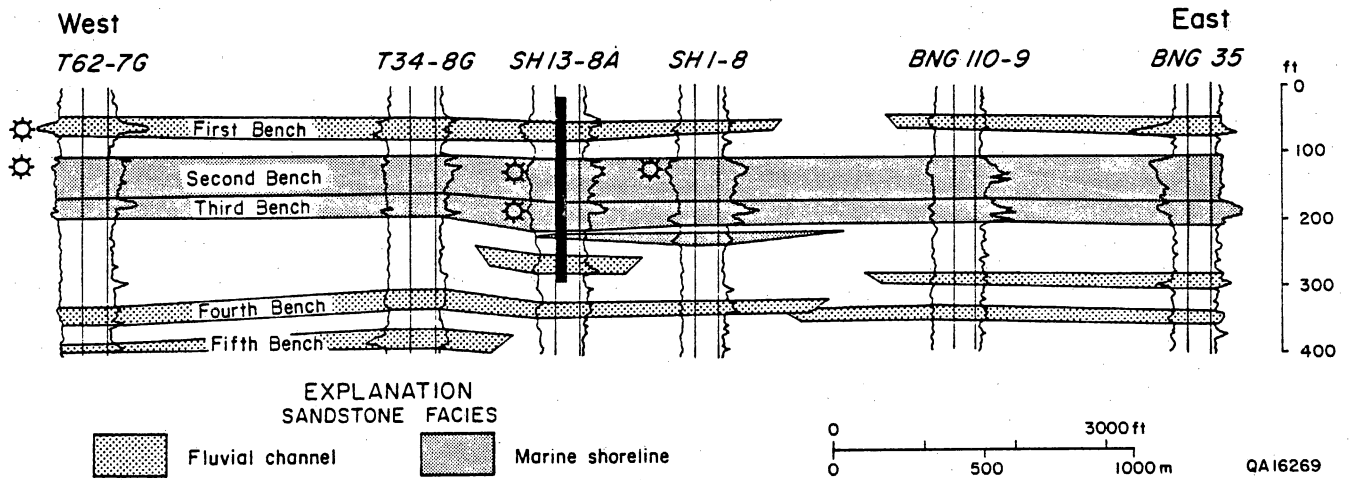


Figure 22. West-east stratigraphic cross section showing SP and resistivity logs from the Enron S. Hogsback No. 13-8A well (SH 13-8A) and the nearest offset wells. Line of section shown in figure 23. Second Frontier producing intervals in these wells are shown as stars.

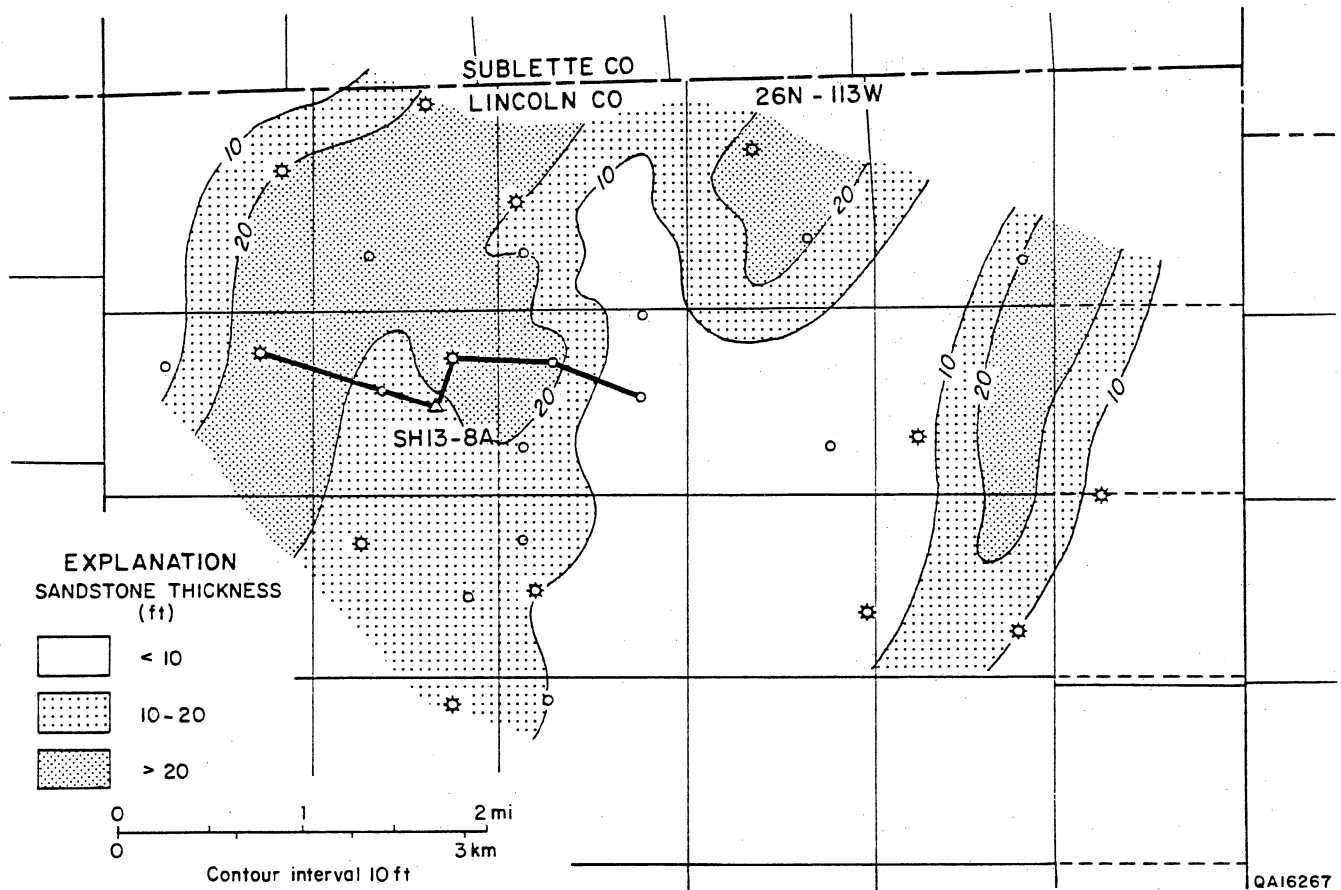


Figure 23. Thickness map of high-resistivity (low clay content) sandstone in the Second Bench of the Second Frontier, South Hogsback field. The Third Bench, although present in this field, is not included on this map. Wells producing gas from the Second Bench are shown as stars. Cross section shown in figure 22.

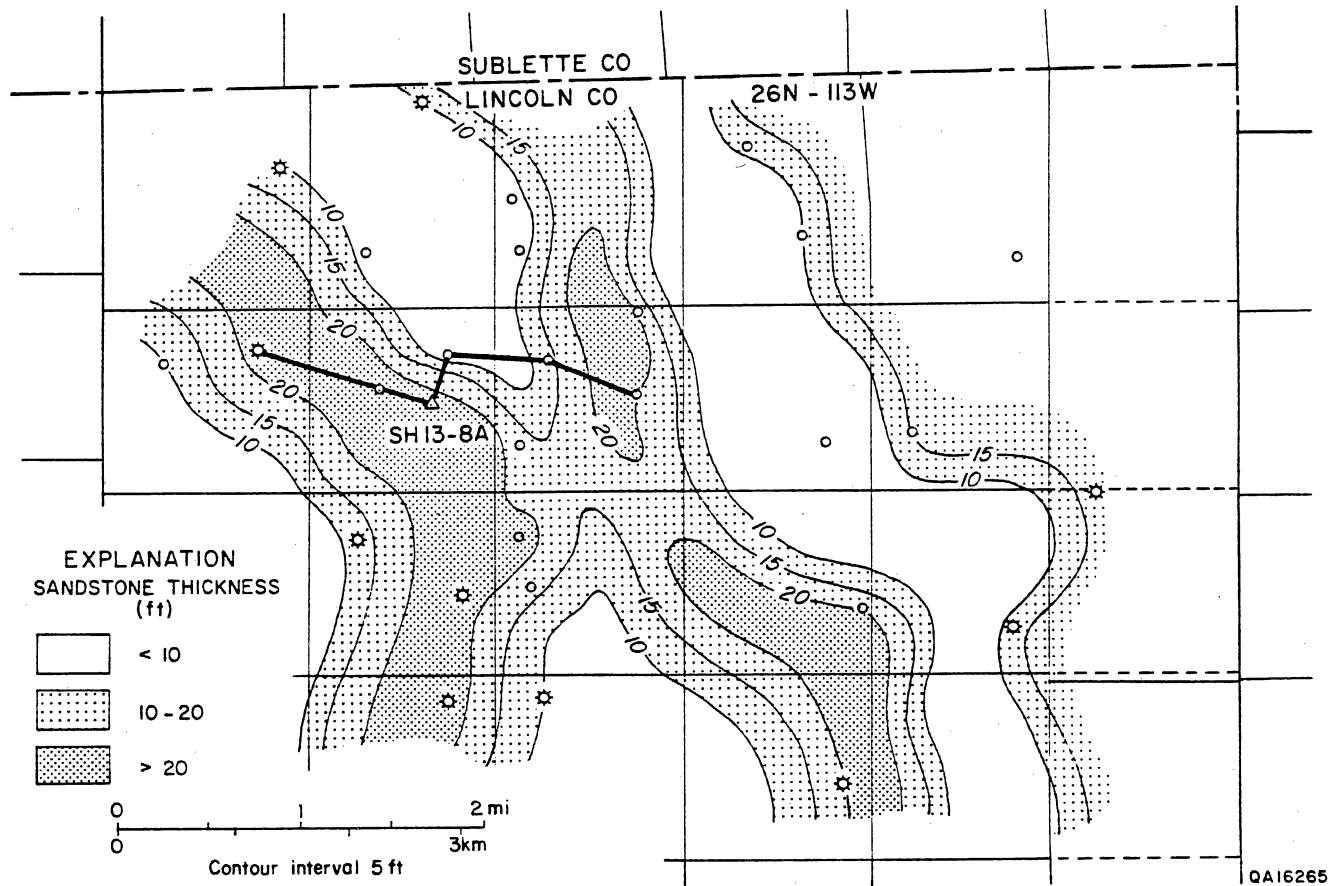
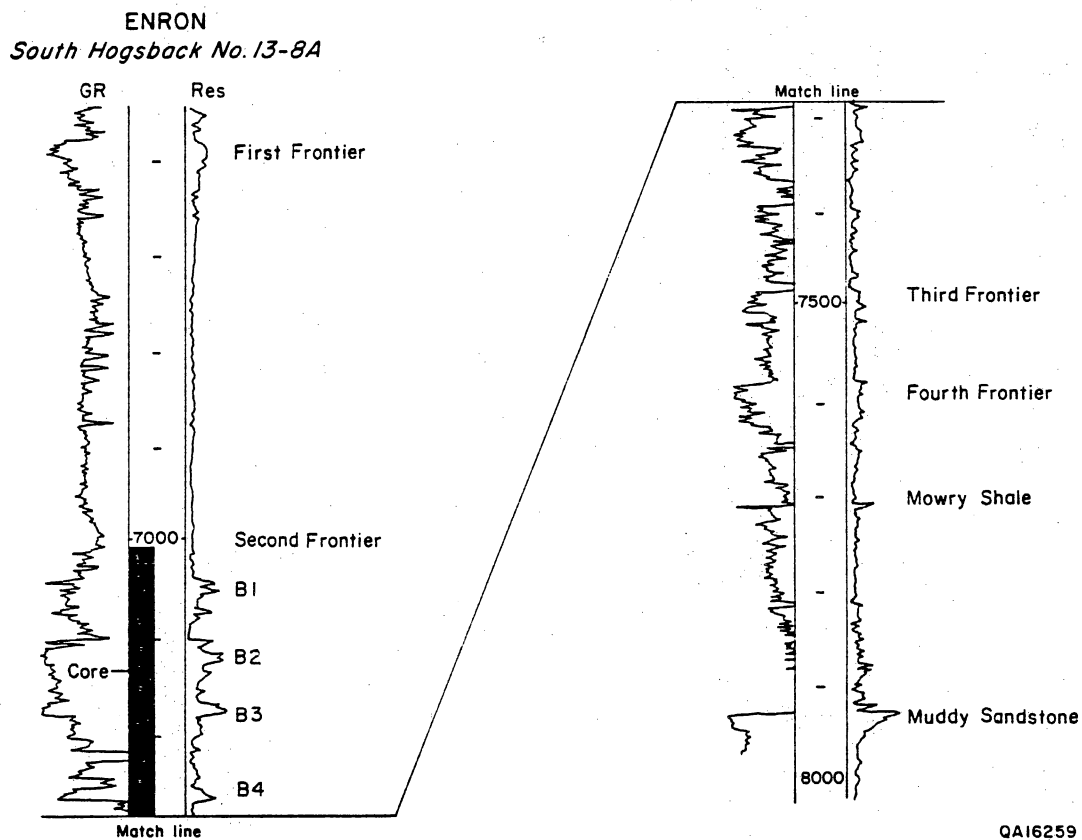


Figure 24. Thickness map of sandstone in the First Bench of the Second Frontier, South Hogsback field. SP, gamma-ray, and resistivity logs were qualitatively analyzed to determine this gross (clean plus shaly) sandstone thickness. Wells producing gas from the First Bench are shown as stars. Cross section shown in figure 22.



QA16259

Figure 25. Gamma-ray/resistivity log from the Enron S. Hogsback No. 13-8A cooperative well showing Frontier sandstone zones and cored interval.

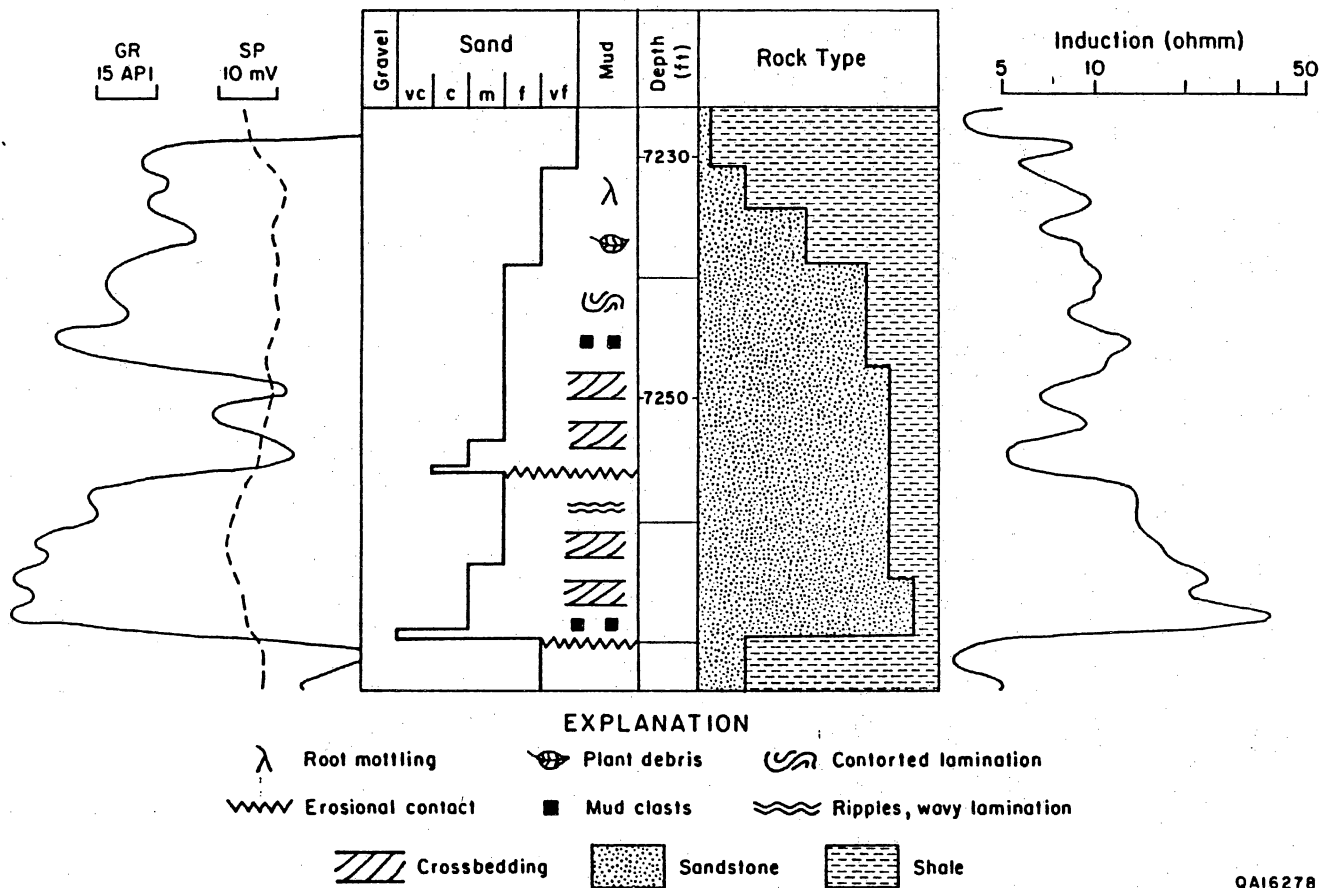
core contains many features that typify Frontier fluvial channel-fill facies: erosional surfaces, upwardly decreasing grain size, large crossbeds, mud rip-up clasts, and soft-sediment deformation (fig. 26). Clay volume increases from 10 percent near the base of the channel (7,270 ft [2,216 m]) to 30 percent near the top (about 7,240 ft [2,207 m]). Abundant biotite (probably volcanoclastic) between 7,249 and 7,255 ft (2,209 to 2,211 m) may be responsible for the high gamma-ray response in this zone (fig. 26). In this Fourth Bench core, porosity averages 9 percent, and permeability is less than 0.01 md (from core analysis). The Fourth Bench sandstone is enclosed in nonmarine and transitional-marine, organic-rich shale, sandy shale, and bentonite, which cause very high (off-scale) gamma-ray responses (fig. 25). The same transgressive surface that was cored in the Terra Anderson Canyon cooperative well occurs in the shale that overlies the Fourth Bench in this well (fig. 11).

At Enron S. Hogsback No. 13-8A, the Second and Third Benches form an amalgamated marine shoreline sandstone (fig. 22), which is composed of two progradational shoreface sequences (7,109 to 7,207 ft [2,167 to 2,197 m]) (fig. 27). In both benches, lower shoreface facies are thoroughly bioturbated and contain abundant clay (10 to 40 percent). The Third Bench lower shoreface (7,185 to 7,207 ft [2,190 to 2,197 m]) includes abundant sandstone/shale interlamination, whereas the Second Bench lower shoreface (7,145 to 7,171 ft [2,178 to 2,186 m]) consists of a more homogeneous mixture of sand and mud, discrete lamination having been destroyed by burrowing. The Second Bench upper shoreface sandstone (7,113 to 7,145 ft [2,168 to 2,178 m]), which has the highest core permeabilities (fig. 27), is also pervasively bioturbated but is relatively clean (less than 10 percent clay) and has well-preserved medium- to small-scale trough crossbedding. The Third Bench upper shoreface (7,171 to 7,185 ft [2,186 to 2,190 m]) contains local shale laminations and abundant carbonate cement.

The Second Bench is overlain by 8 ft (2.4 m) of interbedded sandstone and shale (7,101 to 7,109 ft [2,164 to 2,167 m]) having abundant bioturbation and oyster shells in the upper 2 ft (0.6 m). The oyster shells are overlain by 19 ft (6 m) (7,082 to 7,101 ft [2,159 to 2,164 m]) of marine and marginal-marine shale. This shale caps the Second Bench throughout the La Barge



ENRON SOUTH HOGSBACK No. 13-8A  
Second Frontier, Fourth Bench



QA16278

Figure 26. Log responses and core description from the Fourth Bench of the Second Frontier (fig. 25), Enron S. Hogsback No. 13-8A well, South Hogsback field.

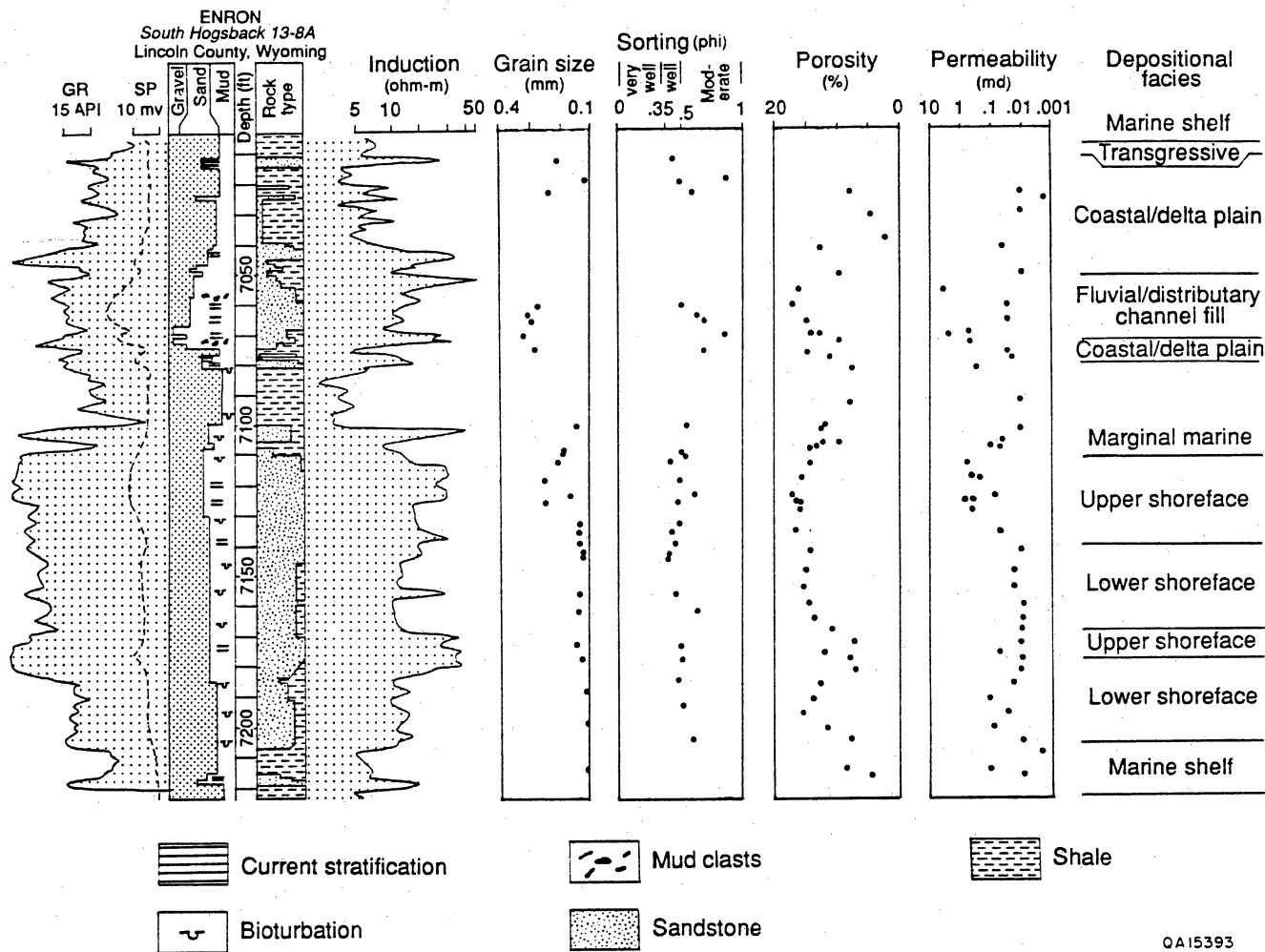


Figure 27. Log responses and rock properties in core from the First, Second, and Third Benches of the Second Frontier (fig. 25), Enron S. Hogsback No. 13-8A well, South Hogsback field. Porosity and stressed permeability data from core are shown.

Platform (fig. 11), although it appears to be more marine-dominated in the Enron S. Hogsback well than it is in the Terra Anderson Canyon well.

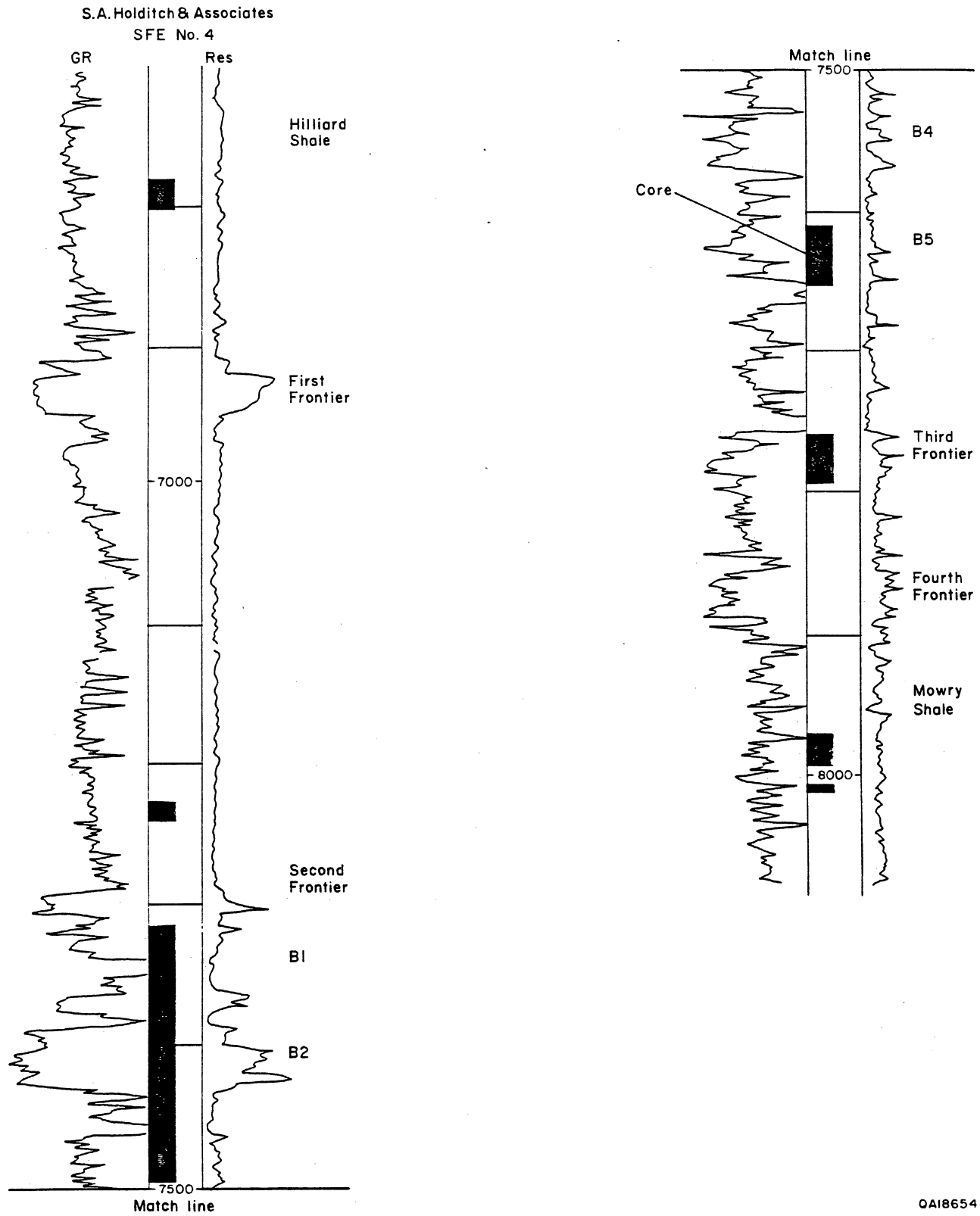
At the Enron S. Hogsback cooperative well site, the First Bench comprises a fluvial channel-fill sandstone enclosed in coastal-plain shale and thin sandstone (fig. 27). The lower part of the channel-fill sandstone (7,067 to 7,075 ft [2,154 to 2,156 m]) includes large mud rip-up clasts and coal fragments, which together make up 10 to 70 percent of the rock volume. The upper part of the channel-fill sandstone (7,060 to 7,067 ft [2,152 to 2,154 m]) consists of crossbedded sandstone having about 20 percent sand-sized clay clasts. Abundant mud rip-up clasts significantly limit First Bench reservoir quality on the La Barge Platform. Locally high core (stressed) permeabilities (0.5 to 1.5 md) in the First Bench in this well (fig. 27) occur in isolated thin zones.

A thick (7,015 to 7,060 ft [2,138 to 2,152 m]) zone of root-mottled organic-rich shaly sandstone and sandy shale lies between the First Bench channel-fill sandstone and marine sandstone and shale contained in the uppermost 8 ft (2.4 m) of core. A thin, transgressive marine sandstone (7,012.5 to 7,014.5 ft [2,137 to 2,138 m]) (fig. 27) marks the top of the Second Frontier in the Enron S. Hogsback cooperative well.

Perforations (7,110 to 7,202 ft [2,167 to 2,195 m]) extend across both the Second and Third Benches in Enron S. Hogsback No. 13-8A (fig. 22), encompassing lower and upper shoreface facies. Core permeabilities, however, are generally very low throughout the perforated interval, except in a 17-ft-thick (5-m) zone (7,113 to 7,130 ft [2,168 to 2,173 m]) within the Second Bench upper shoreface, where stressed permeability averages 0.36 md (fig. 27). Unlike the Terra Anderson Canyon well, no high-energy subenvironment or foreshore facies appears within the upper shoreface in the Enron S. Hogsback cooperative well.

S. A. Holditch & Associates SFE No. 4-24

The SFE No. 4-24 well is a research well drilled by GRI on leases acquired through the cooperation and assistance of Enron Oil and Gas Company. SFE No. 4-24 is located in Chimney



QA18654

Figure 29. Gamma-ray/resistivity log from the S. A. Holditch & Associates SFE No. 4 well showing Frontier sandstone zones and cored intervals.

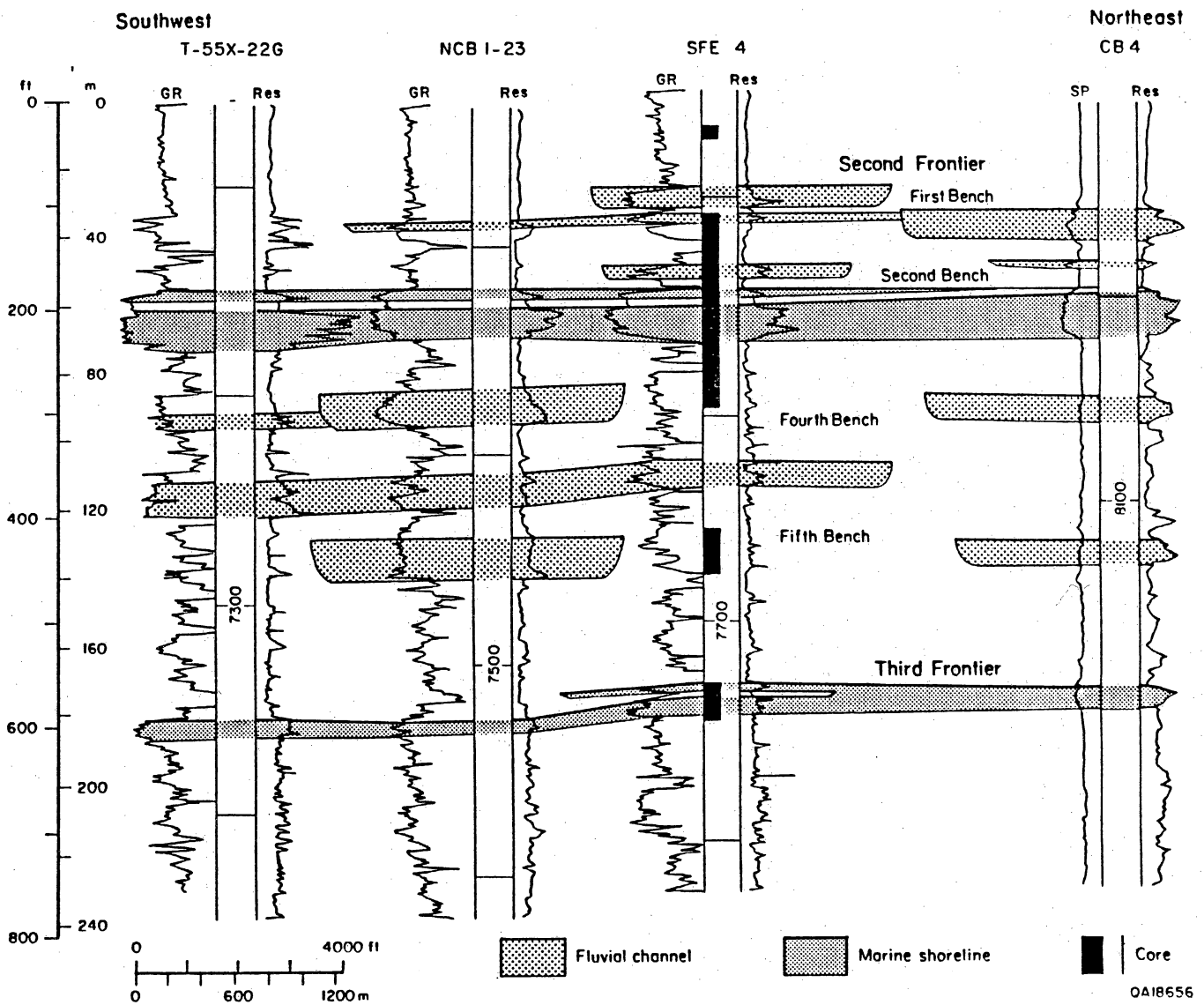
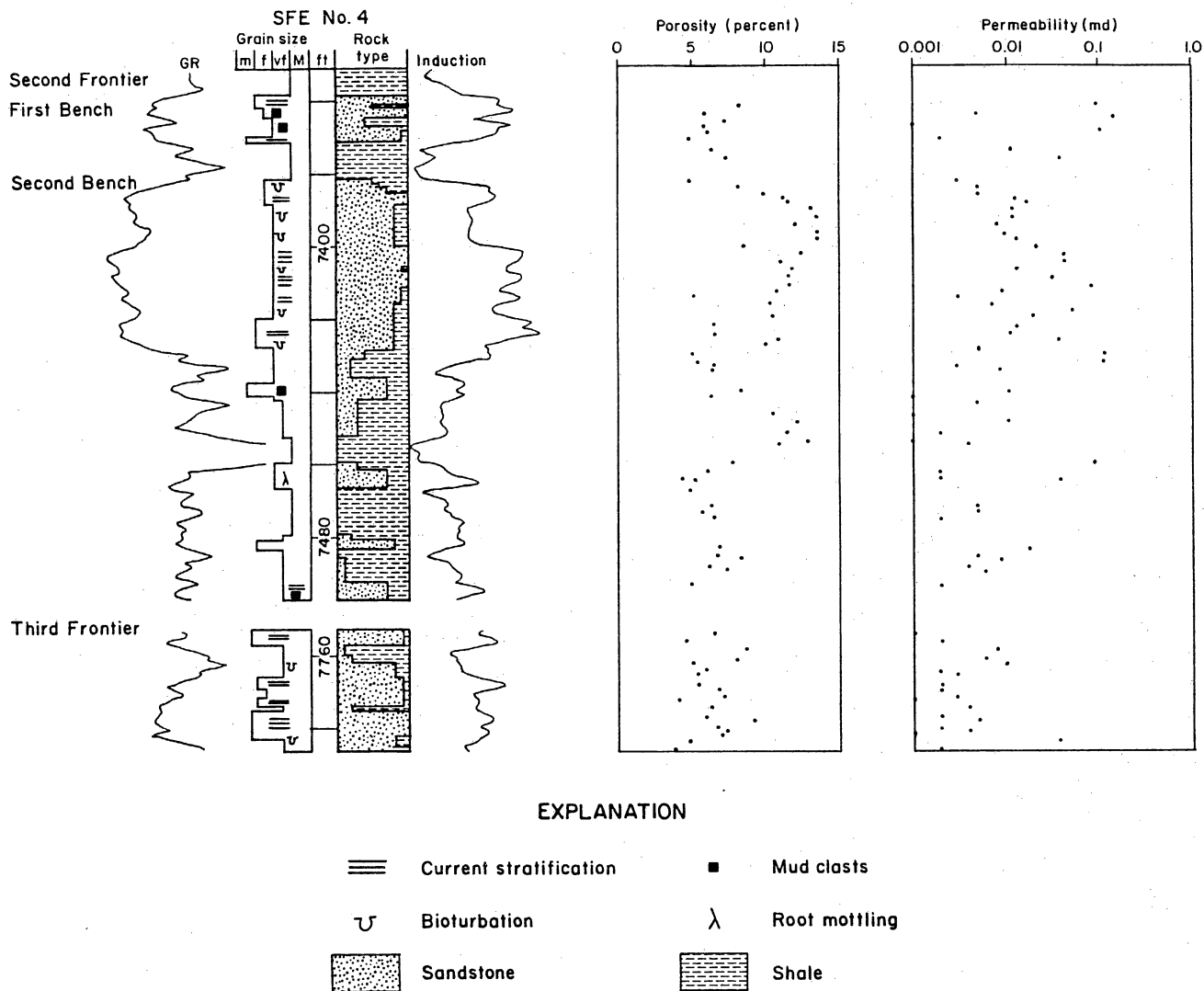


Figure 30. Southwest-northeast stratigraphic cross section showing well logs from SFE No. 4 and offset wells, Chimney Butte and Tip Top fields. Line of section shown in figure 28.

shoreline that could supply coarse-grained detritus to the inner shelf. The Hilliard and Frontier marine shales both include less sand than does the Mowry and were probably deposited farther from areas of active shore-zone sedimentation.

At the SFE No. 4-24 well site, the Second Bench marine shoreface sandstone (7,382 to 7,428 ft [2,250 to 2,264 m]) (fig. 31) is thinner and less permeable than it is at the other cooperative wells on the La Barge Platform (figs. 18 and 27). The lower shoreface facies (approximately 7,411 to 7,428 ft [2,259 to 2,264 m]) consists of interbedded shaly sandstone and clean sandstone. Ripple and wavy lamination, pervasive bioturbation, and thin shale layers are distinctive features. Clay content decreases upward through this interval. Clean sandstone beds (0.2 to 2.0 ft [6 to 60 cm] thick) within the lower shoreface are probably storm deposits. Upper shoreface facies (7,400 to 7,411 ft [2,256 to 2,259 m]) overlie the lower shoreface facies and form the main Frontier reservoir zone in the SFE No. 4-24 well. The clean, well-sorted, fine- to very fine grained sandstone of the Second Bench upper shoreface facies is characterized by horizontal and gently inclined lamination, vertically oriented bioturbation, and minor thin muddy layers. Permeabilities are mostly less than 0.1 md throughout the Second Bench (fig. 31), and the upper shoreface reservoir zone (7,400 to 7,411 ft [2,256 to 2,259 m]) does not appear to be more permeable than the lower shoreface (7,411 to 7,428 ft [2,259 to 2,264 m]). Porosities, however, display an upwardly increasing trend through the Second Bench (fig. 31). The uppermost part of the Second Bench (7,382 to 7,400 ft [2,250 to 2,256 m]) is largely composed of thoroughly bioturbated shaly sandstone, although a thin zone of relatively clean sandstone occurs near the top (7,386 to 7,389 ft [2,251 to 2,252 m]). This interval, which has the characteristics of a lower shoreface deposit, has the lowest permeabilities in the Second Bench sandstone (fig. 31).

Core from the Third Frontier (7,753 to 7,785 ft [2,363 to 2,373 m]) (fig. 31) comprises interbedded sandstone and shale of probable marine shoreface origin. Bioturbation is present throughout this interval, although not as abundant here as it is in Second Frontier shoreface facies. Organic debris and rip-up mud clasts are common. Relatively clean sandstone beds,



QA18658

Figure 31. Log responses and rock properties in core from the Second and Third Frontier (fig. 29), SFE No. 4, Chimney Butte field. Porosity and stressed permeability data from core are shown.

1 to 4 ft (0.3 to 1.2 m) thick, are interbedded with shaly sandstone and sandy shale beds having similar thicknesses. Horizontal, inclined, and ripple-trough lamination occur in the sandstones.

Core from the First Bench of the Second Frontier includes a fluvial channel-fill sandstone (7,360 to 7,372 ft [2,243 to 2,247 m]) (fig. 31). This sandstone has an erosional base, ripple trough and climbing ripple lamination, organic debris, and thin mudstone layers. Rip-up mud clasts are abundant and generally concentrated in layers 0.1 to 1.0 ft (3 to 30 cm) thick, where they compose as much as 50 percent of the rock volume.

The rest of the core from the First Bench (7,311 to 7,360 ft [2,228 to 2,243 m]), as well as the cores from the Fourth and Fifth Benches (7,439 to 7,494 ft [2,267 to 2,284 m] and 7,607 to 7,648 ft [2,319 to 2,331 m]), consists of nonmarine shale, sandy shale, and siltstone. Coal fragments, traces of plant roots, and pyrite are abundant in these rocks, which were deposited on a vegetated coastal plain (delta plain). Wavy and contorted lamination are common, although many intervals appear massive and structureless. The presence of bentonitic shales and thin bentonites record volcanic ash-fall events. The bentonite, yellowish tan to greenish gray, typically contains abundant mica flakes and is composed largely of sticky clay (probably smectite). Thin shaly sandstones that occur in these coastal plain facies probably were deposited near the margins of fluvial channels.

#### DIAGENESIS OF FRONTIER SANDSTONES

The Frontier Formation produces gas along the Moxa Arch from sandstone reservoirs that are generally low in permeability. However, diagenetic variations contribute to significant reservoir quality differences within and between fields along the Moxa Arch. The purpose of the petrographic study of Frontier sandstones was to investigate how the diagenetic history has modified reservoir porosity and permeability. Previous studies of the diagenesis of the Frontier Formation along the Moxa Arch (Winn and Smithwick, 1980; Stonecipher and others, 1984; Winn and others, 1984; and Schultz and Lafollette, 1989) have provided the foundation for this study. Most of the previous work concentrates on the central Moxa Arch (T20N to T24N). This



study extended evaluation of the Frontier Formation farther to the north (to T28N) and south (to T17N), as well as to the east of the Moxa Arch in the Green River Basin.

### Methods

Thin sections were examined from Frontier cores from 13 wells on and adjacent to the Moxa Arch (fig. 1). Twelve of the cores were from four areas along the Moxa Arch: (1) the Hogsback area (wells 1-4, fig. 1) on the La Barge Platform; (2) the Fontenelle area (wells 6-9, fig. 1) southeast of Hogsback, where the arch changes from northwest-southeast to north-south orientation; (3) the Church Buttes-Bruff area (wells 13-15, fig. 1) near the middle of the arch; and (4) the Henry area (well 16, fig. 1) at the south end of the arch. One core samples the Frontier in the Green River Basin to the east of the Moxa Arch (well 12, fig. 1). Most cores were from the First and Second Benches of the Second Frontier, but cores of the First and Third Frontier and the Third, Fourth, and Fifth Benches of the Second Frontier also were studied.

Analyses of 899 core plugs form the data base for porosity and permeability. All samples were measured under unstressed conditions, that is, under ambient, or near ambient pressure (0 or 800 psi confining pressure), and some were also measured under stressed conditions, at calculated in situ overburden pressure. Porosity was measured by helium injection, and permeability measurements were made on dried, extracted plugs using nitrogen gas or air as the fluid. Contribution to effective reservoir permeability by natural fractures was not evaluated.

The composition of Frontier sandstones was determined from 247 thin sections selected from different facies and from the total depth range in each core. Of these, 172 thin sections are from the ends of core-analysis plugs. Only thin sections made from core-analysis plugs were used to compare petrographic and petrophysical data. The chemical composition of detrital and authigenic components of sandstone and mudstone was determined by standard thin-section petrography, scanning electron microscopy (SEM) using an energy-dispersive X-ray spectrometer (EDX), electron microprobe analysis, stable-isotope analysis, and X-ray analysis.

Thin sections were stained using sodium cobaltinitrite (potassium feldspars), potassium ferricyanide, and alizarin red-S (carbonates). Point counts (200 points) determined mineral composition and porosity. Grain size and sorting of framework grains were measured by grain-size point counts (50 points) of the apparent long axis of grains. By comparing point-count data of thin sections with core analyses, the influence on porosity and permeability of parameters such as grain size, sorting, compaction, volume of authigenic cements, and pore type (primary versus secondary) was determined.

## Frontier Composition

### Grain Size and Sorting

The Frontier Formation in the study area is mainly composed of sandstones, muddy sandstones, and sandy mudstones. Of 149 clean Frontier Formation sandstones (defined as containing  $\leq 2$  percent detrital clay matrix), 82 are fine grained ( $3.0$  to  $2.0 \phi$  [ $0.125$  to  $0.25$  mm]) and 45 are medium grained ( $2.0$  to  $1.0 \phi$  [ $0.25$  to  $0.5$  mm]). Clean Frontier sandstones are mostly well sorted ( $0.35$  to  $0.5 \phi$ ) to moderately well sorted ( $0.5$  to  $0.71 \phi$ ), according to the definition of Folk (1974). Because grain size was measured only on sand and silt grains, mean grain size and sorting in sandstones having abundant detrital clay-sized grains refer only to the population of framework grains.

Frontier Formation sandstones, particularly those that were deposited in lower shoreface environments, have varying amounts of clay matrix mixed with the sand- and silt-sized grains. The volume of matrix in lower shoreface sandstones ranges mostly from 5 to 30 percent; volume of clay typically decreases upward in these progradational shoreline sandstones. Fluvial channel-fill and upper shoreface sandstones contain an average of 1 percent matrix (table 2).

Mudstones in the Frontier Formation formed in nonmarine floodplain and marine-shelf environments. Floodplain mudstones typically contain between 30 and 75 percent clay-sized grains; the remaining volume is mostly sand- and silt-sized grains of quartz. Marine-shelf deposits

Table 2. Average composition of Frontier sandstones by depositional environment.

	Fluvial channel fill Q <sub>59</sub> F <sub>6</sub> R <sub>36</sub> (n = 66)	Upper shoreface Q <sub>66</sub> F <sub>5</sub> R <sub>29</sub> (n = 73)	Lower shoreface Q <sub>67</sub> F <sub>6</sub> R <sub>27</sub> (n = 60)
Grain size (mm)	0.23	0.17	0.14
Sorting (phi standard deviation)	0.58	0.50	0.58
Detrital clay matrix (%)	1	1	8
Quartz cement (%)	8	5	2
Calcite cement (%)	3	3	6
Total cement (%)	16	13	10
Thin-section primary porosity (%)	0.8	2.2	0.8
Thin-section secondary porosity (%)	2.4	5.6	3.2
Microporosity (%)	6.8	6.4	8.5
Minus-cement porosity (%)	14	13	8
Porosimeter porosity (%)	10.0 (n = 136)	14.2 (n = 66)	12.5 (n = 284)
Unstressed permeability (md) (Geometric mean)	0.13 (n = 132)	0.19 (n = 65)	0.08 (n = 271)
Stressed permeability (md) (Geometric mean)	0.01 (n = 57)	0.05 (n = 48)	0.01 (n = 169)

above the Second Frontier sandstone were cored in the Enron S. Hogsback No. 13-8A and Wexpro Church Buttes No. 48 wells. These deposits are also mudstones that contain 30 to 75 percent clay-sized grains.

The finest grained deposits in the Frontier Formation are bentonite beds in the First, Fourth, and Fifth Benches of the Second Frontier. Bentonite consists of aggregates of clay, largely smectite, formed by in situ alteration of volcanic ash (Blatt and others, 1972). These thin beds (generally <2 ft [ $<0.6$  m] thick) are composed of more than 90 percent clay-sized grains and are classified as claystones.

#### Framework Grains

Essential framework grains are those used to classify sandstones: quartz, feldspar, and rock fragments. Although the relative proportion of the essential framework grains in the Frontier Formation varies, Frontier sandstones are mainly litharenites to sublitharenites having an average composition of 64 percent quartz, 6 percent feldspar, and 30 percent rock fragments ( $Q_{64}F_6R_{30}$ ) (fig. 32). Detrital quartz composes an average of 48 percent of the total rock volume in clean sandstones and forms between 26 and 89 percent of the essential constituents.

Plagioclase composes an average of 4 percent of the total sandstone volume and 0 to 67 percent of the essential framework grains, whereas orthoclase feldspar is absent in most samples. Estimation of the original feldspar content from petrographic data indicated that feldspar content was greater at the time of deposition: some feldspar has been lost by dissolution or replacement by carbonate cements. Secondary porosity constitutes an average volume of 4.4 percent of Frontier sandstones, and approximately half is estimated to have formed by feldspar dissolution. Carbonate cement has an average volume of 4.7 percent; approximately half is estimated to replace feldspar. Therefore, the original feldspar content may have been about 8 percent of the total rock volume, and the original sandstone composition was approximately  $Q_{61}F_{11}R_{29}$ . The volume of feldspar in First, Second, and Third Bench Frontier sandstones at the time of deposition differed from north to south along the

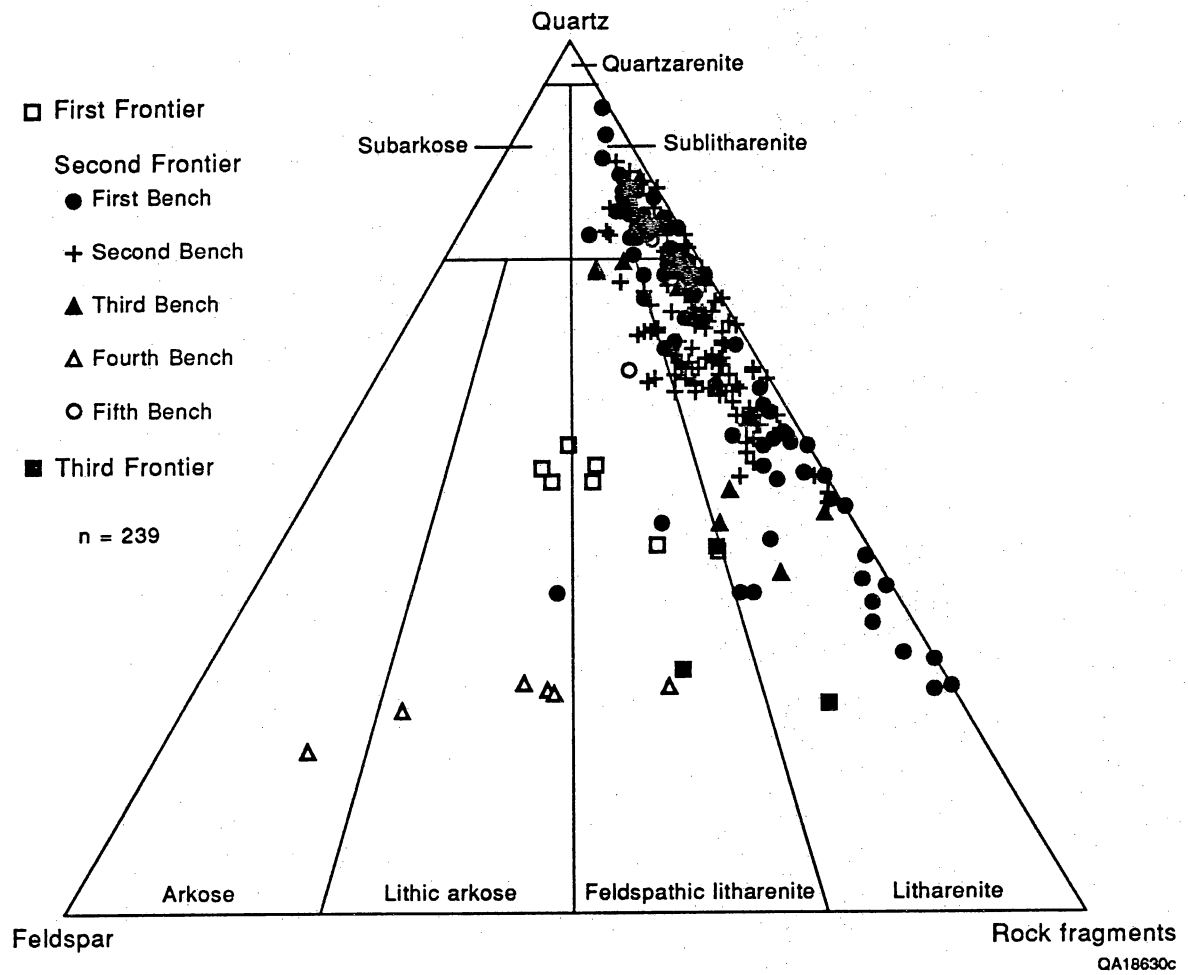


Figure 32. Compositional classification of First, Second, and Third Frontier Sandstones.

Moxa Arch. Original feldspar volume averaged 9 percent at the north end of the arch but only 4 percent at the south. The north end retains slightly greater volumes of feldspar today, an average of 3 percent in clean sandstones in the north versus 2 percent in the south.

Some plagioclase grains are fresh, but others have been partly altered to sericite or vacuoles (fluid-filled bubbles). Partial to complete dissolution of plagioclase along cleavage planes results in delicate honeycombed grains and secondary pores.

Plagioclase grains in the Frontier Formation have been extensively albitized. Feldspars from four Frontier sandstones were analyzed by electron microprobe to determine major-element composition. Plagioclase composition in 156 analyses ranges from  $Ab_{86}$  to  $Ab_{100}$ . Eighty percent of the grains have compositions of greater than  $Ab_{98}$ ; the average composition of all Frontier plagioclase is  $Ab_{98}$ . The original detrital composition of the plagioclase is unknown, but it was probably more calcic than it is now. The presence in the Frontier Formation of plagioclase of composition  $Ab_{86}$  indicates that the source area contained feldspars as calcic as oligoclase. Therefore, at least some of the Frontier feldspars were probably albitized after burial, although some of the albite may have been inherited from older, albitized sandstones or from low-grade metamorphic rocks in the source area.

Rock fragments range from 10 to 75 percent of the essential framework grains. Sedimentary rock fragments, particularly chert but also chalcedony, shale, sandstone, and phosphate, are the most common lithic grains. The total volume of chert in Frontier sandstones and mudstones ranges from 0 to 47 percent and averages 14 percent. Detrital chert in the Frontier probably was derived from the Permian-age Phosphoria Formation and other Paleozoic units (Stonecipher and others, 1984). Low-rank metamorphic rock fragments, common in some samples, appear to be slightly metamorphosed sandstone or mudstone grains. Volcanic rock fragments and ripped up and transported pieces of bentonite occur mainly in the Fourth Bench sandstones in the Second Frontier. Whereas plutonic rock fragments are rare, accessory grains such as biotite and glauconite are locally common.

Framework-grain composition of Frontier sandstones is influenced both by depositional environment and by stratigraphic position. Sandstones deposited in fluvial channels contain less quartz than do sandstones deposited in shoreface environments (fig. 33). Fluvial-channel sandstones have an average composition of  $Q_{59}F_6R_{36}$ , upper shoreface sandstones average  $Q_{66}F_5R_{29}$ , and lower shoreface sandstones average  $Q_{67}F_6R_{27}$  (table 2). The relation between depositional environment and sandstone composition in the Frontier Formation was observed previously (Winn and Smithwick, 1980; Stonecipher and others, 1984; Winn and others, 1984). Shoreface sandstones probably contain a high percentage of detrital quartz because wave abrasion removed many of the mechanically unstable rock fragments (Winn and others, 1984) and because differences in hydraulic properties allowed wave action to winnow quartz from chert. Fluvial-channel sandstones contain abundant chert because they were not winnowed and are coarser grained than shoreface sandstones, and chert and other rock fragments tend to occur in the coarser sand fraction. The average grain size of fluvial-channel sandstones is  $2.1 \phi$  (0.23 mm), compared with  $2.5 \phi$  (0.17 mm) for upper shoreface sandstones and  $2.8 \phi$  (0.14 mm) for lower shoreface sandstones (table 2). Upper shoreface sandstones are well sorted ( $\phi$  standard deviation of 0.50), whereas fluvial and lower shoreface sandstones are moderately well sorted ( $\phi$  standard deviation of 0.58).

In core from Church Buttes field, differences in framework grain composition were observed at a millimeter scale between individual laminations. Small differences in density and hydraulic properties between quartz and chert resulted in some laminations having abundant detrital quartz grains and laminations only a few millimeters away containing abundant chert grains. Much of the primary porosity in quartz-rich laminae was filled by quartz cement, but because quartz does not nucleate as effectively on chert grains as on quartz grains, the chert-rich laminae retained more intergranular porosity than did the quartz-rich laminae.

The composition of fluvial channel-fill sandstones is strongly dependent on stratigraphic position. Most First Bench fluvial channel-fill sandstones contain abundant rock fragments, primarily chert, and little feldspar (fig. 32). In contrast, fluvial channel-fill deposits from the

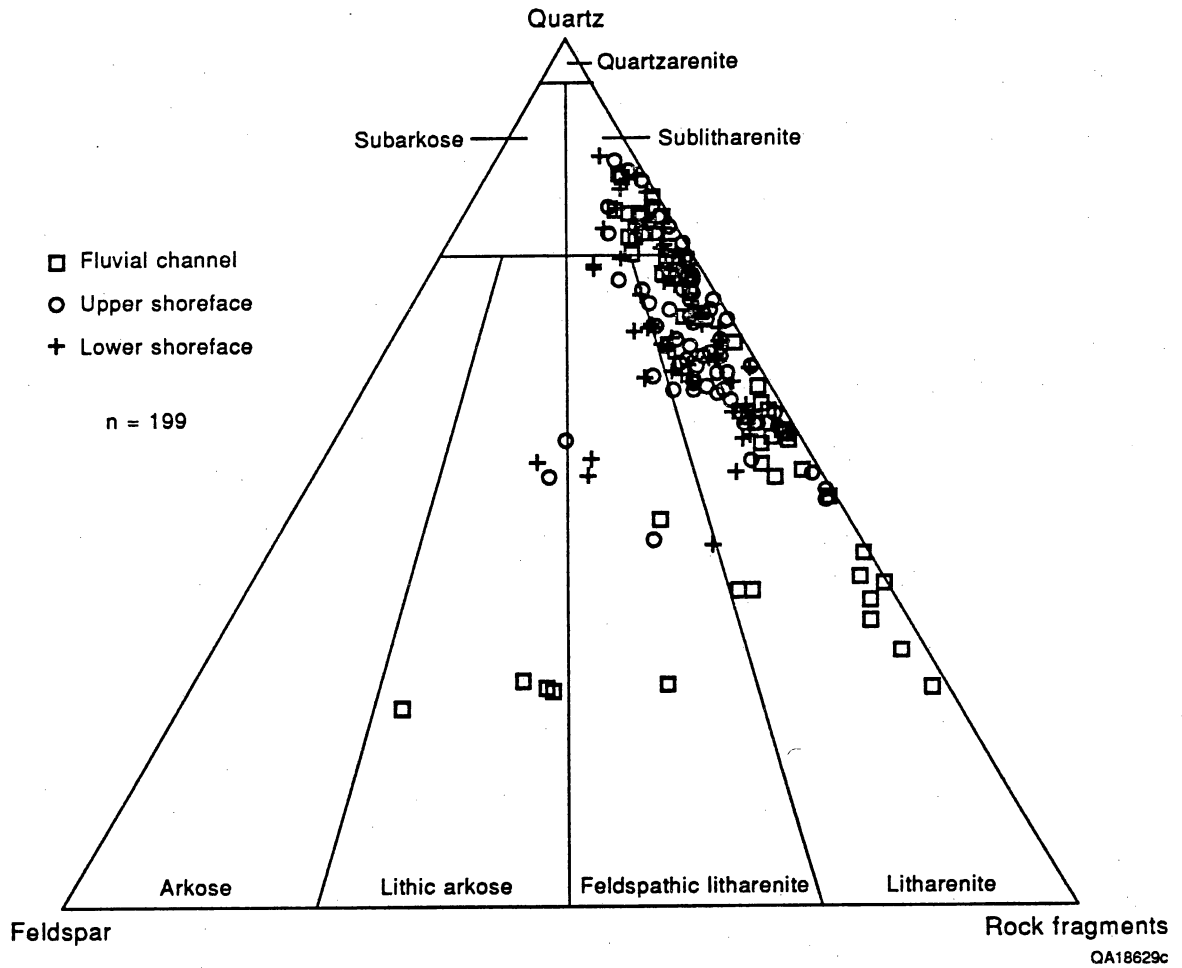


Figure 33. Compositional classification of Frontier sandstones by depositional environment.



Fourth Bench contain abundant plagioclase and biotite. The Fourth Bench sandstones also contain volcanic rock fragments and bentonite clasts and thus were derived from a source terrain that included volcanic rocks. Marine sandstones of the First Frontier have a similar composition (fig. 32) and probably were derived from a source area similar to that of the Fourth Bench sandstones. The quartz- and chert-rich sandstones of the First, Second, and Third Benches probably were derived primarily from older sedimentary rocks and slightly metamorphosed sedimentary rocks, although bentonite layers occur within the First Bench.

Differences in provenance and depositional environment of Frontier sandstones resulted in sandstones at the north end of the Moxa Arch containing a wide range of volumes of feldspar and rock fragments but sandstones at the south end being more uniformly quartz rich. Both the range and the average volume of feldspars and ductile grains (metamorphic and volcanic rock fragments, mudstone, sandstone, glauconite, and mica grains) decrease from north to south along the arch. Therefore, at the time of deposition, Frontier sandstones at the north end of the arch contained greater volumes of chemically reactive grains and ductile grains susceptible to mechanical compaction than did sandstones at the south end.

### Matrix

Detrital clay matrix, defined as detrital grains too small to be identified in thin section, composes 0 to 94 percent of the volume of Frontier sandstones, mudstones, and claystones. Matrix occurs in sandstones that either were affected by burrowing organisms and had clay-sized grains mixed into an originally well-sorted sandstone or were deposited in an alternating high- and low-energy environment (such as rippled sandstones that have clay laminations). X-ray diffraction analysis (<5  $\mu\text{m}$  size fraction) indicates that clay minerals constitute an average of 75 weight-percent of the matrix. Clay-sized quartz forms most of the remainder of the matrix. Mixed-layer illite-smectite (MLIS) and illite are the most abundant clay minerals; kaolinite and chlorite are also present. The MLIS contains approximately 20 percent expandable smectite layers, a value similar to those previously reported (Stonecipher and others, 1984). No X-ray

diffraction analysis was performed on bentonite layers, but they are thought to be composed of smectite and MLIS.

## Cements

Cements and replacive minerals constitute between 0 and 38 percent of the sandstone volume in Frontier Formation samples. Pore-filling cement is most abundant in clean sandstones that contain little detrital clay matrix; the average volume of cement in clean Frontier sandstones is 16 percent. Fluvial sandstones contain a volume of cement greater than that in shoreface sandstones (table 2). Total cement does not correlate significantly with depth.

Quartz, calcite, and MLIS and illite (which cannot be distinguished in thin section) are the most abundant authigenic minerals in Frontier sandstones. Less abundant authigenic minerals include chlorite, kaolinite, ankerite, albite, and pyrite. On the basis of petrographic evidence, the relative order of occurrence of the major events in the diagenetic history of Frontier sandstones was found to be (1) mechanical compaction by grain rearrangement and deformation of ductile grains, (2) formation of illite and MLIS rims, (3) precipitation of quartz overgrowths, (4) precipitation of calcite cement, (5) generation of secondary porosity by dissolution of calcite cement and detrital feldspar, chert, and mudstone, (6) precipitation of kaolinite in secondary pores, and (7) chemical compaction by intergranular pressure solution and stylolitization and additional precipitation of quartz cement (Dutton, 1990). Many of these events overlapped in time, as will be described in later sections.

## Authigenic Clays

Authigenic clays occur in most clean Frontier sandstones, where they affect permeability (Winn and Smithwick, 1980; Stonecipher and others, 1984; Schultz and Lafollette, 1989; Luffel and others, 1991). Illite and MLIS that has approximately 20 percent smectite layers are the most common authigenic clays in general, but in two wells in the Hogsback area, kaolinite is

most abundant (table 3). Authigenic chlorite is more abundant in the deep samples from the southern Moxa Arch than in shallow samples from the north end (table 3). No kaolinite was observed in sandstones at the south part of the study area, in Church Buttes and Bruff fields (T17N to T19N; fig. 2), and kaolinite is absent in Frontier sandstones at least as far north as Wilson Ranch field (T20N) (Stonecipher and others, 1984).

Some of the illite and MLIS occur as rims of tangentially oriented flakes that developed around detrital grains early in the diagenetic history (fig. 34). The tangentially oriented illite and MLIS crystals may have entered the sandstone by mechanical infiltration or burrowing and may have been recrystallized during burial diagenesis. In the Terra Anderson Canyon No. 3-17 well, some illite and MLIS rims apparently were thick enough to inhibit the precipitation of quartz cement. Later dissolution of detrital feldspar grains generated secondary porosity and resulted in many of the illite and MLIS rims being left as delicate rims around secondary pores. Tangentially oriented illite and MLIS rims are most abundant in samples from Fontenelle field.

Other illite and MLIS having a flaky to fibrous morphology are clearly authigenic and extend into and across primary pores (figs. 35, 36 and 37). Fibrous illite and MLIS line most primary pores, but they are less abundant in secondary pores, indicating that much of the authigenic illite and MLIS precipitated before the dissolution of feldspar. Fibrous illite and MLIS in primary pores are more abundant in samples from Fontenelle field than from any other area.

The relatively low expansibility of the authigenic MLIS suggests that it may be only moderately sensitive to fresh water. In tests conducted to evaluate fluid sensitivity of Frontier sandstones (Luffel and others, 1991), permeability to fresh water was 25 to 50 percent lower than permeability to brine. A more important effect of clays on permeability seems to be a function of clay distribution and morphology. Fibers and sheets of illite and MLIS that bridge intergranular pores and pore throats significantly lower permeability (Luffel and others, 1991). Stressed permeability to air measured on dried, extracted plugs in which the fibrous illite and MLIS have matted against the pore walls is 10 to 100 times higher than in situ gas permeability at connate water saturation in plugs having undisturbed illite and MLIS (Luffel and others,

Table 3. Semiquantitative X-ray diffraction mineralogy data (less than 5  $\mu\text{m}$  in diameter fraction).

Depth (ft)	Wt. % bulk rock		Clay minerals normalized to 100%				Illite in MLIS (%)
	Total fines <5 $\mu\text{m}$	Total clay minerals	Kaolinite	Chlorite	Illite	MLIS <sup>1</sup>	
<b>Mobil Tip Top (MT)</b>							
6,982.7 <sup>2</sup>	11.1	8.2	56	07	14	23	79
6,986.5	8.1	6.1	54	02	15	29	78
6,999.6 <sup>2</sup>	3.5	2.5	67	03	08	22	79
<b>Mobil Hogsback (MH)</b>							
6,889.0 <sup>2</sup>	3.0	1.9	73	—	10	17	86
6,894.3 <sup>2</sup>	1.7	1.1	68	—	12	20	82
6,907.8*	6.8	5.0	49	06	16	29	81
6,912.0*	6.4	4.2	50	06	17	27	79
<b>Enron South Hogsback (ES)</b>							
7,104	N.R.	14	21	—	14	64	80
7,120	N.R.	17	6	6	29	59	80
7,137	N.R.	19	21	Tr	16	63	80
7,148	N.R.	22	23	—	18	59	80
<b>Terra Resources Anderson Canyon 3-17 (TA)</b>							
9,064.0	44.8	31.5	08	09	21	62	72
9,082.9 <sup>2</sup>	5.2	3.7	27	03	19	51	77
9,085.3 <sup>2</sup>	3.3	1.9	—	—	27	73	78
9,088.0 <sup>2</sup>	3.1	1.7	—	—	26	74	80
9,095.7 <sup>2</sup>	7.8	5.5	—	—	24	76	80
9,110.0	6.1	4.9	—	03	20	77	74
9,118.0	6.1	4.9	—	05	23	72	76
<b>Texaco State of Wyoming #1 (TW)</b>							
11,515.5 <sup>2</sup>	3.8	2.2	—	11	22	67	83
11,527.9	4.8	3.9	—	07	23	70	84
<b>Church Buttes (WC)</b>							
12,163.2 <sup>2</sup>	7.1	4.3	—	17	26	57	85
12,165.1 <sup>2</sup>	1.8	0.9	—	13	30	57	79
12,169.6 <sup>2</sup>	3.8	2.8	—	13	31	56	86
12,173.5 <sup>2</sup>	5.3	3.8	—	14	19	67	84

<sup>1</sup>Mixed-layer illite-smectite

<sup>2</sup>Samples containing only authigenic clay

N. R. = Not reported

Tr = Trace

— = Below detection limit

\*Sample contains abundant calcite cement, some of which probably was ground to <5  $\mu\text{m}$  during sample preparation

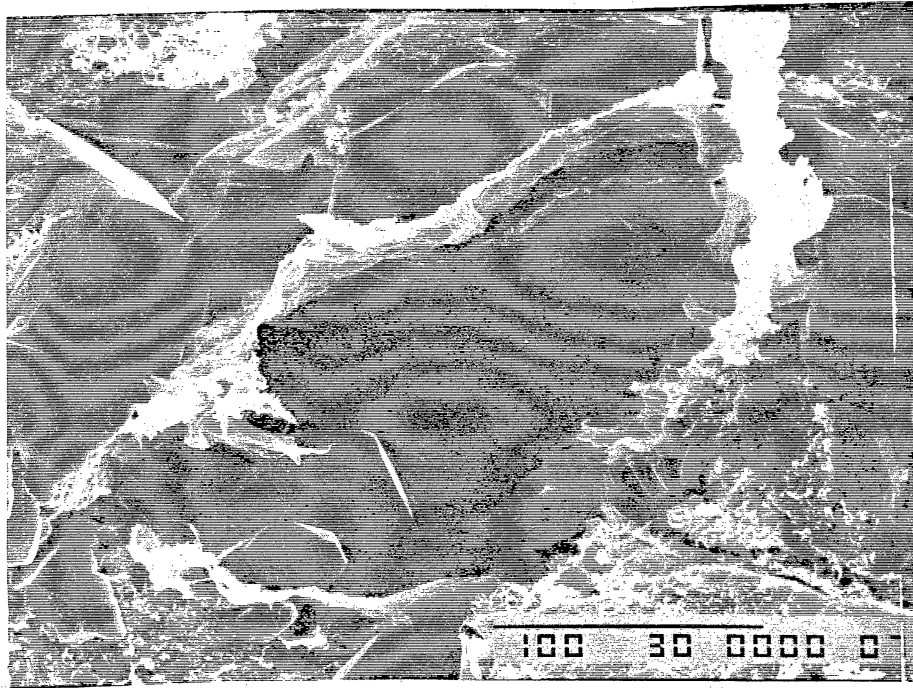


Figure 34. SEM photo of illite tangentially oriented around a secondary pore; quartz crystals project into pore. Sample from a depth of 9,084.7 ft (2,769.0 m), Terra Anderson Canyon No. 3-17 well. Sample was prepared by critical point drying. SEM photo by K. L. Herrington; scale bar is 100  $\mu\text{m}$ .

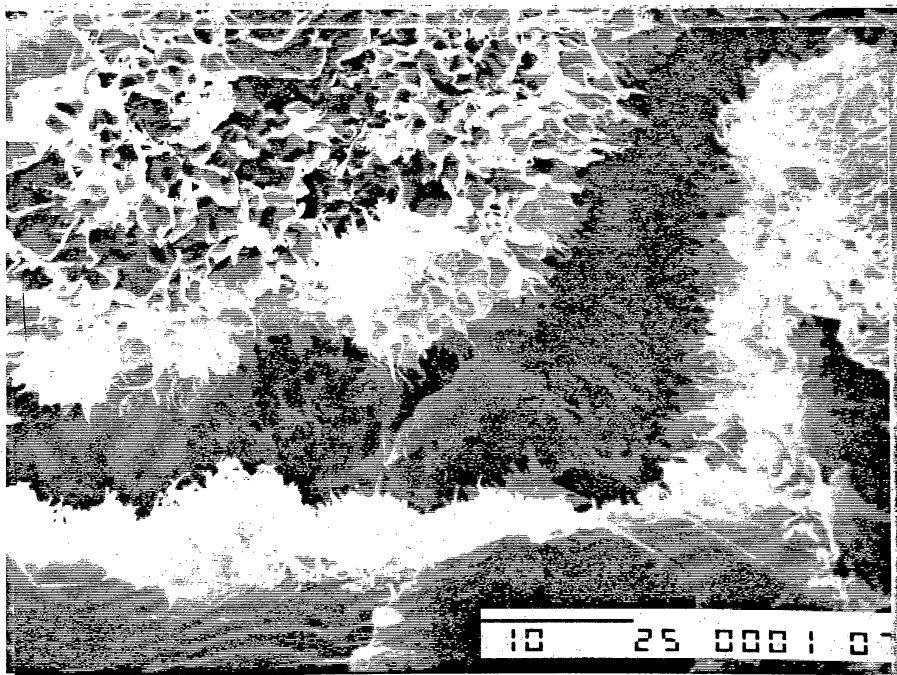


Figure 35. SEM photo of authigenic fibrous illite lining primary pore. Sample from a depth of 9,079.9 ft (2,767.6 m), Terra Anderson Canyon No. 3-17 well. Sample was prepared by freeze drying. SEM photo by K. L. Herrington; scale bar is 10  $\mu\text{m}$ .

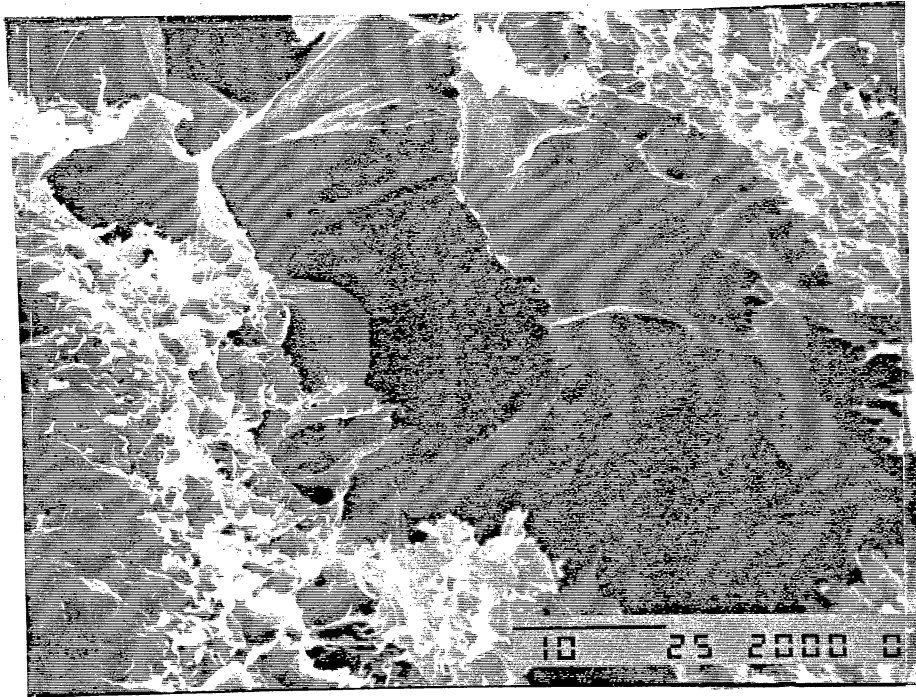


Figure 36. SEM photo of sheets of authigenic illite bridging a pore. Sample from a depth of 9,079.5 ft (2,767.4 m), Terra Anderson Canyon No. 3-17 well. Sample was prepared by air drying. SEM photo by K. L. Herrington; scale bar is 10  $\mu\text{m}$ .

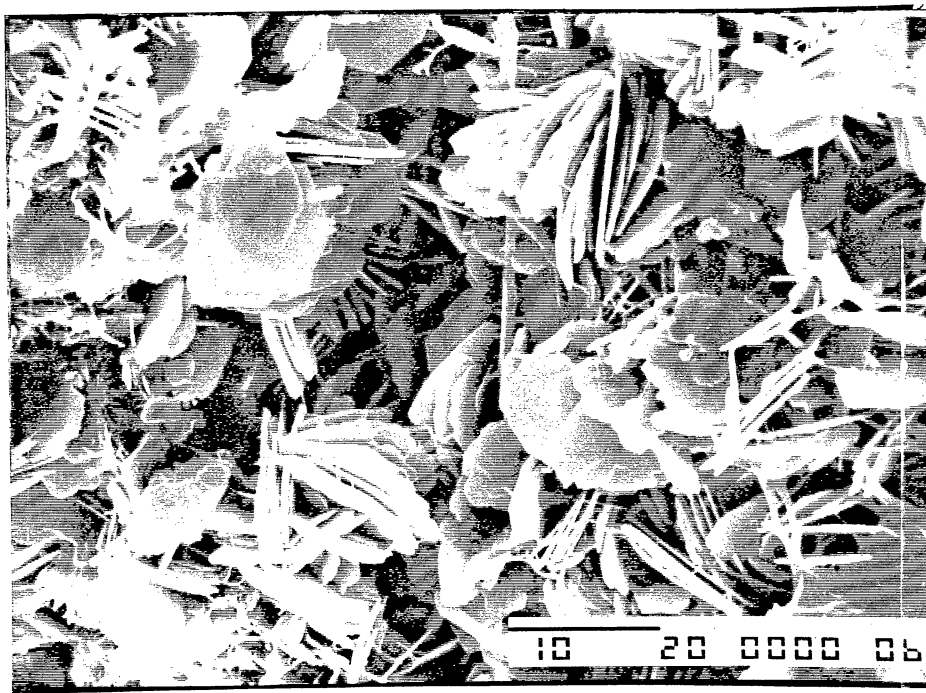


Figure 37. SEM photo of cluster of authigenic chlorite flakes. Sample from a depth of 12,175 ft (3,711 m), Wexpro Church Buttes No. 48 well. SEM photo by K. L. Herrington; scale bar is 10  $\mu\text{m}$ .

1991). Thus, permeability to air, measured in dried core samples, may be one or two orders of magnitude higher than actual reservoir permeability.

Authigenic flakes and rosettes of chlorite (figs. 36 and 37) precipitated relatively early in the burial history, before precipitation of quartz overgrowths. In sandstones from Church Buttes field, chlorite around detrital grains commonly is engulfed by quartz overgrowths (fig. 38), resulting in small, chlorite-filled pores between detrital quartz grains and overgrowths. Chlorite rims around detrital grains are more common in samples from the south end of the Moxa Arch. Clean fluvial sandstones from the south contain an average of 2.6 percent chlorite cement, compared with 0.6 percent at the north end of the arch. The reason for a greater abundance of chlorite rims on detrital grains at the south end of the Moxa Arch and illite rims at the north end is unknown, but the composition of early burial fluids in the different areas must have differed. Pore fluids at the south end probably were richer in iron, causing chlorite to precipitate instead of illite.

Kaolinite is found mainly within secondary pores (fig. 39). Because it is a reaction product of feldspar dissolution, it must have formed after the grain-rimming illite and chlorite. Kaolinite probably has less impact on sandstone permeability in the Frontier than does illite and MLIS because it is somewhat isolated within secondary pores. Kaolinite only occurs in the shallower Frontier sandstones at the north end of the Moxa Arch; no kaolinite was observed in sandstones deeper than 9,100 ft (2,770 m) (table 3, fig. 40).

### Quartz Overgrowths

Quartz is volumetrically the most abundant cement in Frontier sandstones, ranging from 0 to 18 percent of bulk rock volume. Volume of quartz cement in clean Frontier sandstones increases significantly with depth (fig. 41). In clean sandstones at the north end of the Moxa Arch, quartz cement does not occlude porosity significantly, filling an average volume of only 5 percent. In contrast, at the south end of the arch (including well 12, fig. 1), the average volume of quartz cement in clean sandstones is 11 percent, quartz cementation being a main

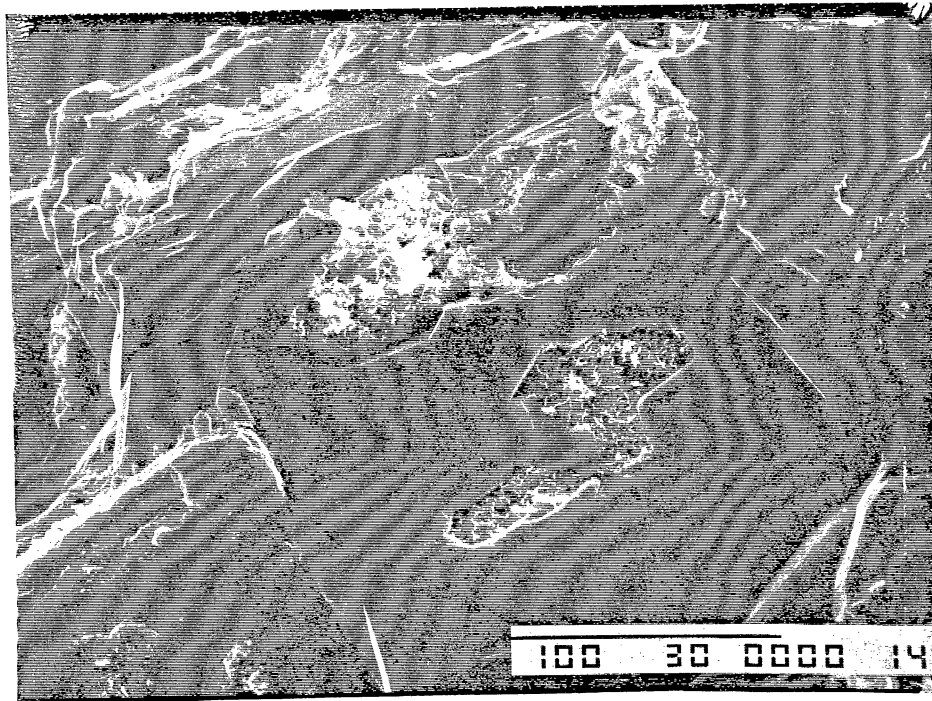


Figure 38. SEM photo of quartz overgrowth engulfing illite and chlorite cement. Sample from a depth of 12,163.2 ft (3,707.3 m), Wexpro Church Buttes No. 48 well. SEM photo by K. L. Herrington; scale bar is 100  $\mu$ m.

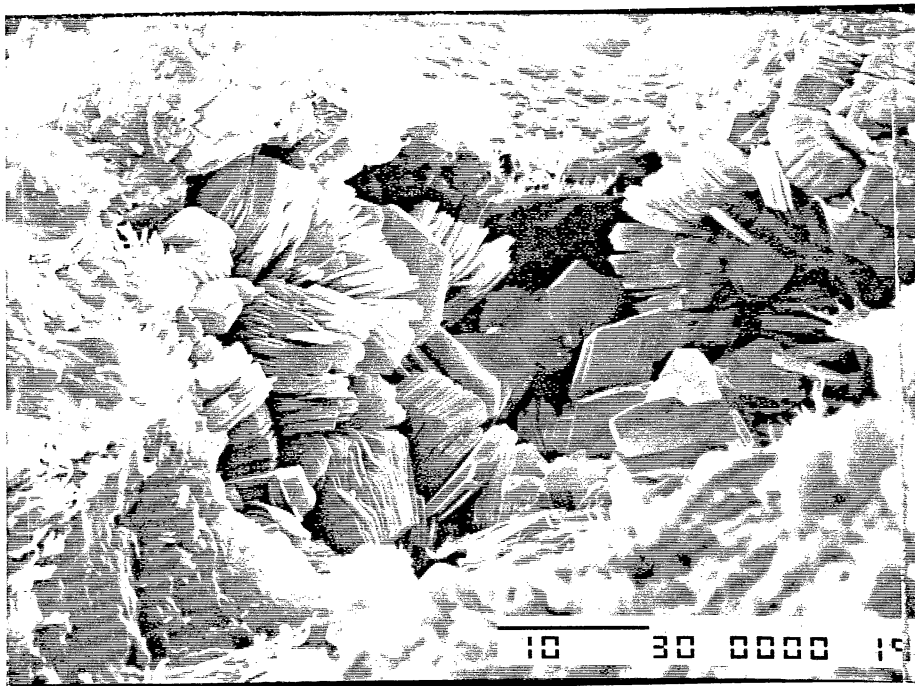


Figure 39. SEM photo of authigenic kaolinite within a secondary pore. Sample from a depth of 6,985.5 ft (2,129.2 m), Mobil Tip Top No. T71X-6G-28N-113W well. SEM photo by K. L. Herrington; scale bar is 10  $\mu$ m.



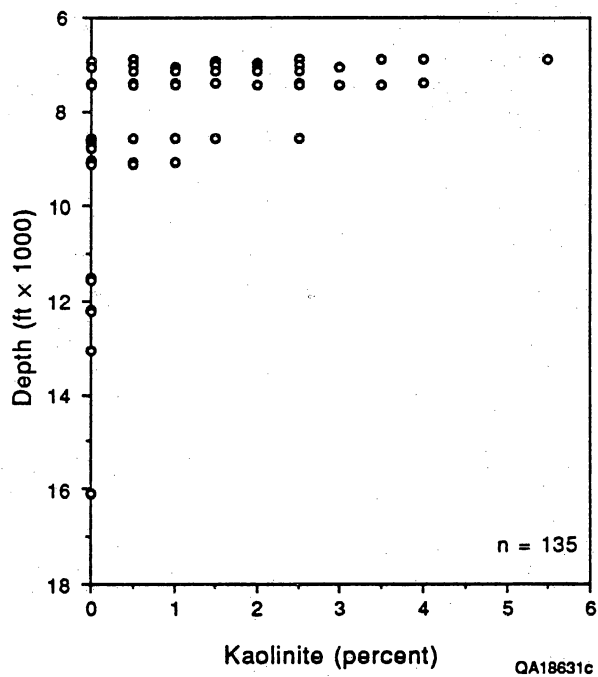


Figure 40. Kaolinite cement volume in clean ( $\leq 2$  percent matrix) First, Second, and Third Bench sandstones as a function of present burial depth. No kaolinite was observed in Frontier sandstones deeper than 9,000 ft (2,750 m).

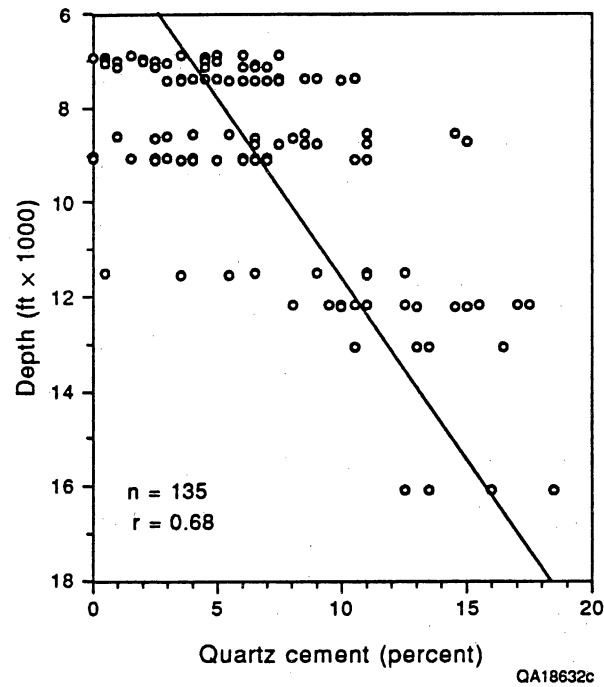


Figure 41. Quartz cement volume in clean ( $\leq 2$  percent matrix) First, Second, and Third Bench sandstones as a function of present burial depth. Quartz cement increases significantly with depth. Linear regression equation relating depth and quartz cement is

$$\text{quartz cement (\%)} = -5.4 + 1.3 \times \text{depth (ft)} \times 10^{-3}.$$

cause of porosity loss. Quartz cement probably is more abundant at the south end of the Moxa Arch and in the basin because Frontier sandstones are more deeply buried there and have developed numerous stylolites, a source of silica. In addition, many chert grains in the deeper Frontier sandstones appear to be partly dissolved and to have undergone intergranular pressure solution; chert dissolution could be another source of silica for quartz cement.

Fluvial channel-fill sandstones contain significantly more quartz cement than do shoreface sandstones (table 2), probably because of the greater depth of the fluvial samples. Because of the sample distribution, the average depth of fluvial sandstones is 10,800 ft (3,292 m), compared with 8,300 ft (2,530 m) for shoreface sandstones. No correlation exists between volume of quartz cement and grain size or sorting.

Chert cement occurs in Fourth Bench sandstones of the Second Frontier (Enron S. Hogsback No. 13-8A well) and in Third Frontier sandstones (SFE No. 4-24 well), both of which are associated with volcanic ash beds. Silica liberated from the volcanic ash probably was the source of the chert cement. Chert cement volume ranges from 1 to 5 percent.

Quartz is interpreted to have precipitated relatively early in the burial history of Frontier sandstones because it was the first cement to precipitate in primary pores after clay rims. However, some petrographic evidence suggests multiple or prolonged periods of quartz cementation. For example, some quartz cement clearly precipitated before feldspar dissolution because quartz overgrowths do not extend beyond where the feldspar grains used to be, although quartz overgrowths project into secondary pores in other cases (fig. 34). We have also observed quartz cement that envelops kaolinite inside a secondary pore, indicating that both the kaolinite and quartz precipitated after feldspar dissolution.

### Calcite

Calcite was the last of the volumetrically significant cements to precipitate in Frontier sandstones. Textural relationships between quartz and calcite show that calcite precipitation generally followed quartz overgrowths. Calcite cement abundance in clean sandstones averages

4.6 percent and ranges from 0 to 35 percent, which includes both pore-filling and grain-replacing calcite. In clean sandstones, an average of 2 percent calcite cement fills primary pores, and an average of 2.6 percent replaces framework grains, mainly feldspars.

Calcite cement is more abundant in lower shoreface sandstones (average of 6 percent) than in either upper shoreface or fluvial channel-fill sandstones (average of 3 percent in both) (table 2). Of the 35 sandstones having particularly abundant calcite cement (>10 percent), 8 are in fluvial sandstones, 5 in upper shoreface, and 20 in lower shoreface and marine-shelf sandstones. No other clear pattern exists in the distribution of abundant calcite cement. In several cases, extensive calcite cement occurs at the top of a clean, well-sorted sandstone, directly below the contact with a fine-grained, poorly sorted muddy sandstone. In other cases, calcite cement is most abundant in clean sandstone beds within an overall poorly sorted interval, such as laminated storm deposits within a burrowed, lower shoreface sequence. Clean sandstones in the Hogsback area have significantly greater volumes of calcite cement (7 percent) than do clean sandstones from either the Fontenelle (1 percent) or Church Buttes areas (4 percent). Of the 35 Frontier samples containing more than 10 percent calcite cement, 28 are from the Hogsback area.

Nine clean Frontier sandstone samples contain more than 20 percent pore-filling and grain-replacing calcite cement, and seven of them are from the Hogsback area. The other two are from a 2.3-ft-thick (0.7-m) calcite-cemented interval at the top of a fluvial channel-fill sandstone in a well from the south part of the Moxa Arch (well 13, fig. 1). In the nine extensively calcite cemented sandstones, the average volume of quartz cement is only 1.4 percent, whereas an average of 6.9 percent quartz cement occurs in all other clean Frontier sandstones containing calcite cement. The low volume of quartz cement in the extensively calcite-cemented zones may be due to calcite replacement of quartz. Experimental dissolution of calcite using dilute HCl revealed numerous replacement features seen in SEM, such as pits, v-shaped notches, and embayments on detrital quartz grains and quartz overgrowths. These

textures were described by Burley and Kantorowicz (1986) as indicating calcite replacement of quartz grains and overgrowths, probably as the result of surface-reaction-controlled dissolution.

The average composition of the calcite cement is  $(\text{Ca}_{0.96}\text{Mg}_{0.01}\text{Fe}_{0.01}\text{Mn}_{0.02})\text{CO}_3$ , determined by 92 microprobe analyses of calcite cement in 3 sandstone samples from Fontenelle field. Most calcite has a low iron content, but values range from 0.003 to 0.02 mole-percent iron. Carbon and oxygen isotopic compositions of calcite cements were determined for four samples from the north and south ends of the Moxa Arch (wells 3, 9, 13, and 15, fig. 1). Calcite  $\delta^{18}\text{O}$  compositions have a narrow range of values from  $-12.2$  to  $-13.8$  o/oo relative to the Peedee belemnite standard (PDB). The average  $\delta^{18}\text{O}$  composition is  $-12.9$  o/oo (PDB), which is equivalent to  $+17.6$  o/oo relative to Standard Mean Ocean Water (SMOW). Carbon isotopic composition ( $\delta^{13}\text{C}$ ) ranges from  $-2.0$  to  $-6.6$  o/oo and averages  $-3.7$  o/oo (PDB). These light values of carbon indicate that there was a contribution from  $^{13}\text{C}$ -depleted carbon derived from oxidation or decarboxylation of organic matter, which has a  $\delta^{13}\text{C}$  composition of approximately  $-23$  o/oo, but that most of the carbon was derived from skeletal carbon from marine organisms. Modern carbonate sediment has  $\delta^{13}\text{C}$  values that range from  $+4$  to  $-2$  o/oo (Land, 1980). Interpretation of the oxygen isotopic values will be discussed in the section Interpretation of Diagenetic History, p. 89.

Dissolution of calcite in some sandstones may have reopened intragranular and intergranular pores that were formerly filled with cement (Schultz and Lafollette, 1989). For example, the top of the upper-shoreface sandstone that constitutes the pay zone in the Terra Anderson Canyon No. 3-17 well has extensive secondary porosity and remnants of dissolved calcite cement. Secondary porosity is abundant throughout the entire pay zone, but remnants of partly dissolved calcite cement only occur at the top of the sandstone. It is unclear whether calcite formerly pervaded the sandstone and completely dissolved everywhere but at the top, or whether calcite was only present at the top of the sandstone and has partly dissolved there.

## Porosity

Porosity in Frontier sandstones observed in thin section ranges from 0 to 19 percent; porosimeter-measured porosity ranges from 1.4 to 19.3 percent. Average porosimeter porosity in clean Frontier sandstones is 12.3 percent, compared with an average of 5.8 percent thin-section porosity. In general, thin-section porosity is lower than porosimeter porosity because accurately identifying the volume of microporosity in thin section is difficult. The two measures of porosity in Frontier sandstones are related by the following equation: porosimeter porosity =  $8.4 + 0.62 \times (\text{thin-section porosity})$  ( $r = 0.68$ ). The largest difference between thin-section and porosimeter porosity is at low porosity values; samples having no thin-section porosity have an average of 8.4 percent porosimeter porosity. Both primary and secondary porosity identified in thin section correlate significantly with porosimeter porosity ( $r = 0.56$  and  $0.63$ , respectively).

Thin-section porosity was divided into (1) primary, intergranular pores and (2) secondary pores that result from dissolution of framework grains or cements. On the basis of thin-section identification, average primary porosity in clean Frontier sandstones has been found to be 1.6 percent, and average secondary porosity, 4.2 percent. Most secondary pores formed by the dissolution of framework grains, particularly feldspar, chert, clay clasts, and biotite; secondary pores are thus approximately the same size as detrital grains. Some secondary pores contain remnants of the original detrital grains or reaction products such as kaolinite (fig. 39). Dissolution of calcite cement probably also generated some intergranular and intragranular secondary porosity (Schultz and Lafollette, 1989).

Microporosity, defined as pores having pore-aperture radii  $<0.5$  mm (Pittman, 1979), is abundant in Frontier sandstones, where it occurs between authigenic clay crystals (figs. 35, 37, and 39) and within detrital clay matrix. Micropores also developed by dissolution of some of the tiny (0.2 mm) quartz crystals that compose chert grains (figs. 42 and 43). Microporosity cannot be accurately quantified by routine thin-section point counts, but an estimate of the volume of microporosity can be obtained by taking the difference between porosimeter-measured porosity and thin-section porosity. This method is predicated on the fact that pores that cannot

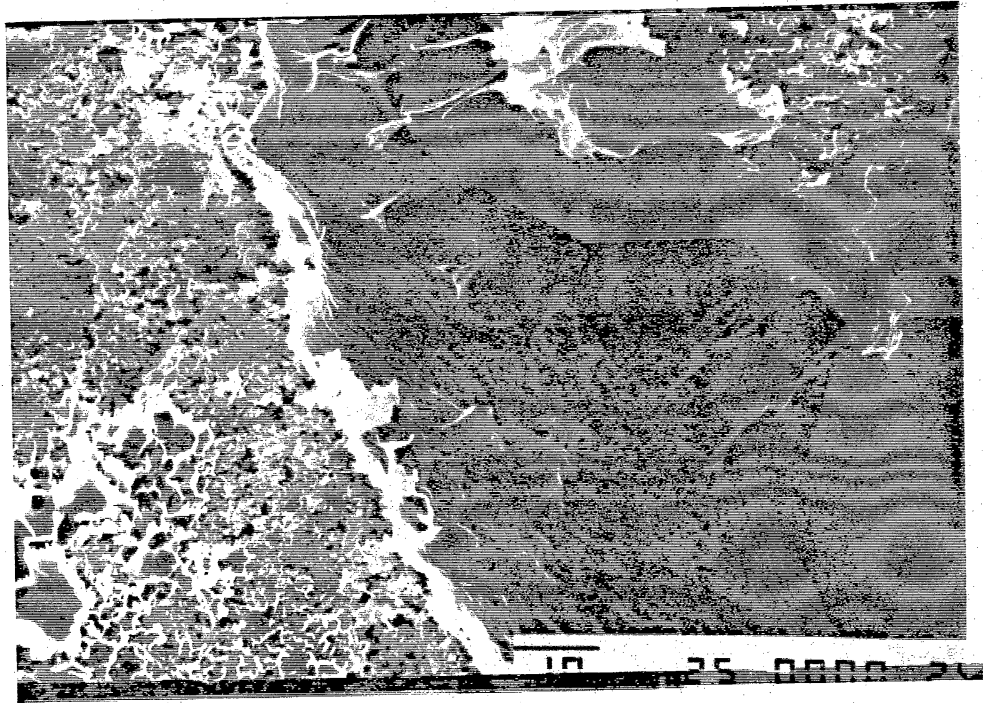


Figure 42. SEM photo of chert grain (left side) showing abundant microporosity. Note thin rim of tangentially oriented clay around detrital chert grain. Sample from a depth of 9,087.8 ft (2,770.0 m), Terra Anderson Canyon No. 3-17 well. SEM photo by K. L. Herrington; scale bar is 10  $\mu\text{m}$ .

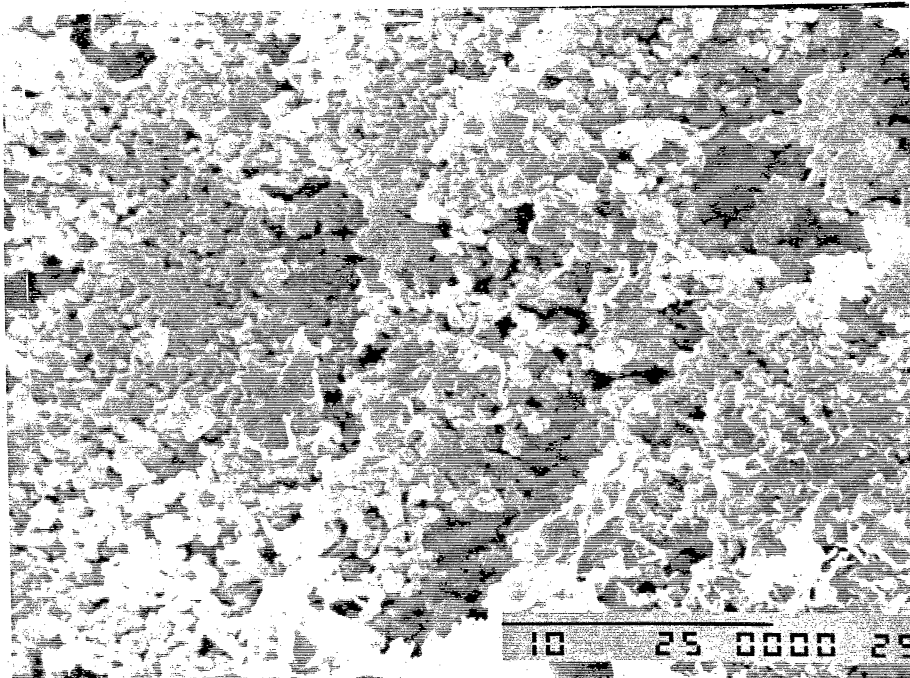


Figure 43. Close-up of surface of chert grain shown in figure 17. Partial dissolution of chert has resulted in abundant micropores. SEM photo by K. L. Herrington; scale bar is 10  $\mu\text{m}$ .

be distinguished in thin section are micropores. The average volume of microporosity in Frontier sandstones estimated by this method is 8.3 percent. Capillary-pressure data from three Frontier cores provide a check on this method of estimating microporosity. Significant correlation ( $r = 0.66$ , significant at the 99-percent confidence level) exists between microporosity calculated from thin-section data and microporosity determined by capillary-pressure data, but most thin-section-derived values are higher. The average microporosity for 22 Frontier samples is 7.6 percent based on capillary-pressure data, compared with an average of 8.8 percent microporosity based on thin-section data. The difference probably is caused by differences in what is being measured to determine microporosity. Using capillary-pressure data, a pore-aperture radius of  $0.5 \mu\text{m}$  (equivalent to an air-brine capillary pressure of 237 psi) is considered to be the lower size limit for macropores (Pittman, 1979). In thin sections, the smallest pore diameter that can be discriminated is approximately  $5 \mu\text{m}$ , which consequently becomes the lower size limit of macropores. Therefore, microporosity calculated as the difference between thin-section porosity and porosimeter porosity tends to overestimate microporosity slightly, compared with capillary-pressure measurements of microporosity. Nevertheless, the difference between porosimeter and thin-section porosity provides a reasonably good estimate of microporosity.

Much of the depositional porosity in Frontier sandstones has been lost by mechanical and chemical compaction. Intergranular pressure solution and stylolitization are examples of chemical compaction. Many chert grains have undergone intergranular pressure solution; stylolites, oriented both parallel and perpendicular to bedding, are common in sandstones from the south end of the Moxa Arch and in the basin. Whereas chemical compaction reduces porosity by causing closer packing of framework grains, mechanical compaction is bulk volume reduction resulting from processes other than framework-grain dissolution, such as reorientation of competent grains and deformation of ductile grains (Houseknecht, 1987). Many of the sedimentary and metamorphic rock fragments in Frontier sandstones are ductile and have been deformed during compaction, causing a reduction of primary porosity. Minus-cement porosity,



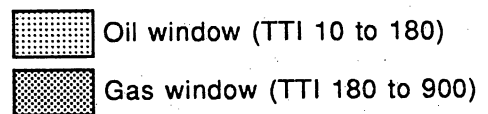
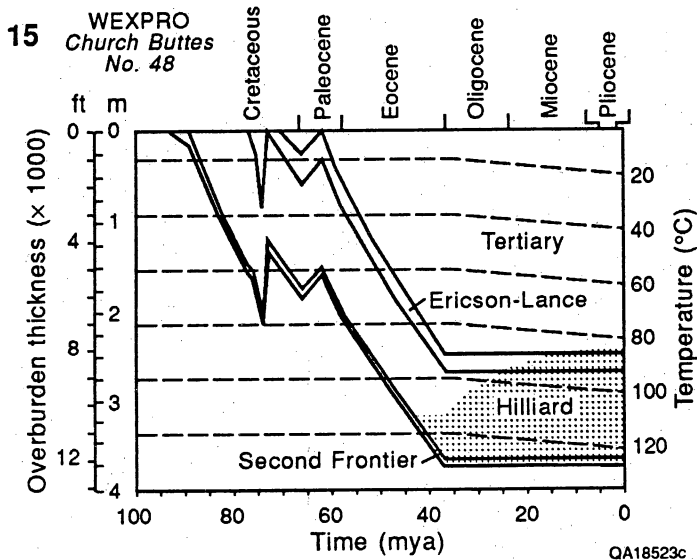
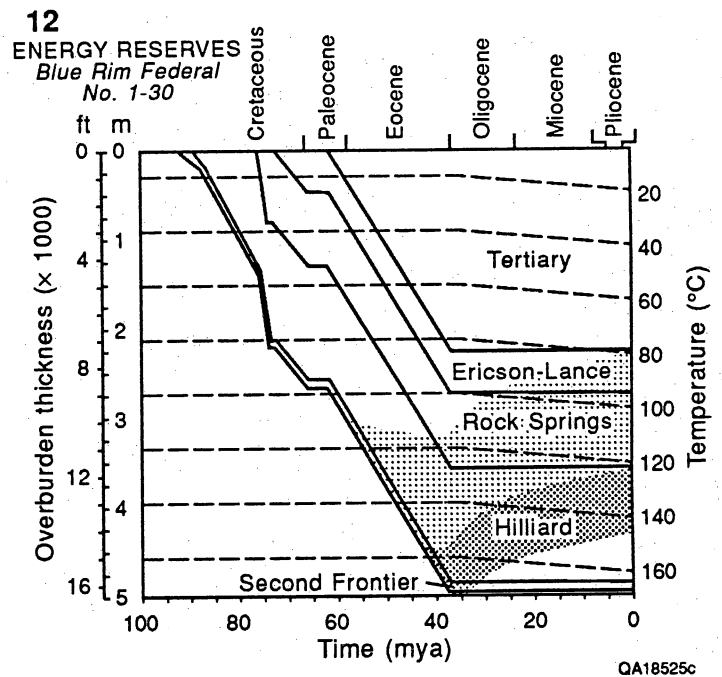
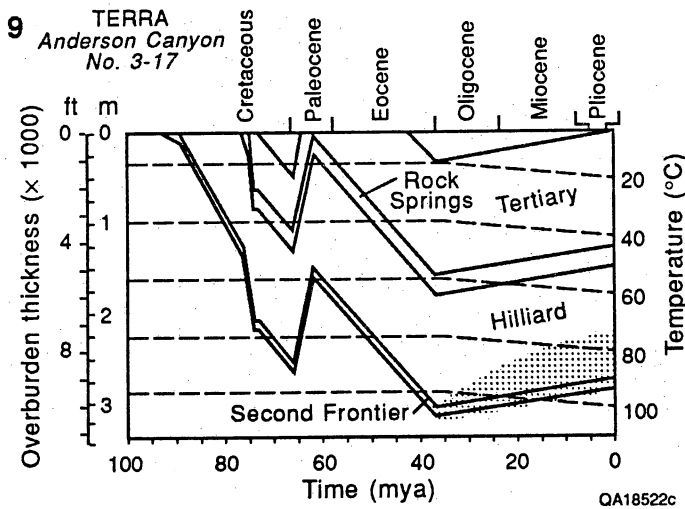
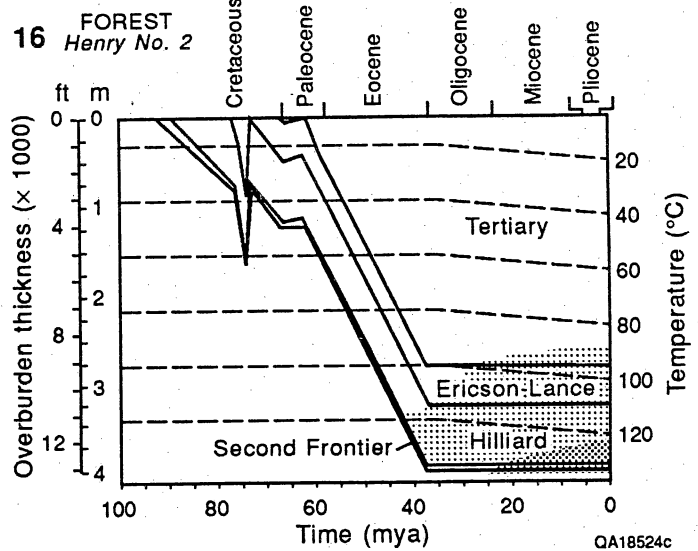
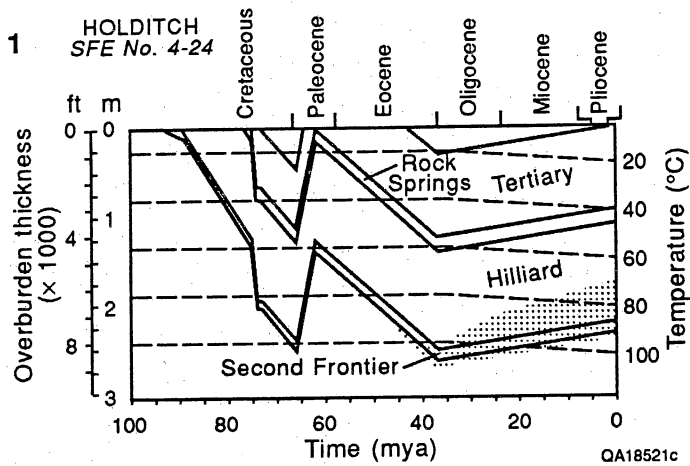
which is the amount of porosity that remained after compaction but before cementation, averages only 14 percent in clean Frontier sandstones. At the time of deposition, well-sorted Frontier sandstones probably had a porosity of at least 40 percent (Pryor, 1973; Atkins, 1989). Thus, about 26 percent porosity (65 percent of the original porosity) was lost by compaction. Much of the remaining intergranular porosity was occluded by precipitation of an average of 12 percent pore-filling cement in clean Frontier sandstones.

### Burial and Thermal History

To interpret the diagenetic history of the Frontier Formation more completely, the burial depth and temperature of the formation must be estimated through time. Stratigraphic information was used to reconstruct the burial history of wells along the Moxa Arch and in the Green River Basin (Dutton and Hamlin, in press), and the modern geothermal gradient was extrapolated into the past to estimate paleotemperatures. With this information, burial-history curves were plotted using the program BasinMod™, which was also used to calculate the thermal maturity of the Frontier Formation in the wells.

### Burial-History Curves

Burial-history curves of the tops of the Second Frontier, Hilliard, Rock Springs Formations (lower Mesaverde Group), the Ericson-Lance Formation (upper Mesaverde Group and uppermost Cretaceous deposits), and undifferentiated Tertiary formations (fig. 4) were plotted for five wells along the length of the Moxa Arch and in the basin (fig. 44). These burial-history curves plot total overburden thickness versus time and correct sediment thickness for compaction. The burial-history curves use stratigraphic-thickness data taken directly from geophysical logs of each of the wells, except in intervals that have a section missing. Ages of the stratigraphic units were estimated from a variety of sources (McGookey, 1972; Thomaidis,



**9** Well numbers on figure 1 and table 1

Figure 44. Burial history curves for the tops of the Second Frontier, Hilliard, Rock Springs, Ericson-Lance, and undifferentiated Tertiary in five wells on the Moxa Arch and in the Green River Basin. See figure 1 for well locations. The times during which the formations were in the oil and wet-gas windows are shown. Burial-history curves were plotted using the program Basin Mod™, which also calculated oil and gas windows.

1973; Edman and Surdam, 1984; Merewether and Cobbin, 1986; Weimer, 1986; Ryder, 1988). Stratigraphic data used to make the burial-history curves are summarized in table 4.

During deposition of the Frontier and Hilliard, subsidence was greater at the north end of the Moxa Arch; consequently these two formations are thicker at the north than they are at the south (table 4). Because of erosion of post-Hilliard Cretaceous units on the Moxa Arch, the original thickness of these formations was estimated from their thickness in the basin using the Energy Reserves Group Blue Rim Federal No. 1-30 well (well 12, fig. 1), which has a nearly complete Upper Cretaceous section. Original thickness of Tertiary deposits was estimated from published studies of the Tertiary in the Green River Basin (Curry, 1973; Sullivan, 1980).

Three episodes of uplift and erosion were incorporated into the burial-history curves (Dutton and Hamlin, in press). The first episode involves movement of the Moxa Arch during the Late Cretaceous (early late Campanian time; Ryder, 1988) and erosion of the lower Mesaverde Rock Springs Formation and uppermost Hilliard deposits. The greatest amount of uplift and erosion occurred at the south end of the Moxa Arch, as indicated by burial-history curves for the Forest Henry No. 2 and Wexpro Church Buttes No. 48 wells (fig. 44). The amount of Hilliard deposited and later removed was estimated by correlating marker units within the Hilliard along the length of the arch and determining which markers have been removed from the top of the Hilliard in the two southern wells. No erosion is interpreted as having taken place in early late Campanian time at the north end of the Moxa Arch or in the basin.

The second period of uplift occurred at the end of the Cretaceous, and it was at this time that the arch acquired its present south-plunging configuration. The greatest uplift occurred at the north end of the arch, where all the Ericson-Lance deposits were removed, as well as some of the underlying Rock Springs lower Mesaverde deposits (Asquith, 1966; McDonald, 1973) (fig. 44). Less erosion occurred at the south end of the arch, and some Ericson-Lance deposits remain in the Forest Henry No. 2 and Wexpro Church Buttes No. 48.

The final period of erosion took place from about 37 mya to the present at the north end of the arch. Approximately 1,000 ft (305 m) of Tertiary deposits have been removed at the SFE No. 4-24 and Terra Anderson Canyon No. 3-17 wells, but no Tertiary is interpreted to have been eroded at the south end of the arch or in the basin (Curry, 1973; Sullivan, 1980) (fig. 44). Erosion is arbitrarily shown as taking place continuously from 37 mya to the present.

### Thermal History

Geothermal gradients were calculated from bottom-hole temperatures (BHT) for the five wells for which burial-history curves were plotted (Dutton and Hamlin, in press) (table 4). The log with the highest BHT was used if the well had more than one logging run. The present-day geothermal gradient in the study area varies from 1.71°F/100 ft (3.12°C/100 m) to 2.03°F/100 ft (3.70°C/100 m) after correction for nonequilibration of BHT (DeFord and others, 1976). The correction was not applied to SFE No. 4-24 because a logging run was made a year after the well was drilled, and the measured BHT was assumed to have reached equilibrium with the formation. Following the work of Law and others (1980), a linear temperature gradient has been assumed because data were not available to refine the temperature profile further.

The calculated geothermal gradients for these five wells are higher than the geothermal gradient of 1.4°F/100 ft (2.55°C/100 m) shown for this area on a map of geothermal gradients in North America (DeFord and others, 1976). The wells used in making the map may not have had several logging runs each, and thus the BHT's that were used may have been further from equilibrium than the temperatures in the wells used for this study.

The modern geothermal gradient was assumed to have been in place since 95 mya, throughout the burial history of the Frontier Formation. On the basis of the work of Spencer (1987), we assumed the mean annual surface temperature was 40°F (4.4°C) from 0 to 4 mya, 50°F (10°C) from 37 to 95 mya, and uniformly declining from 50° to 40°F (10° to 4.4°C) between 37 and 4 mya. Thermal maturity values calculated from the burial-history curves are in reasonable agreement with measured vitrinite reflectance values (Merewether and others,

Table 4. Stratigraphic data used to construct burial-history curves

Formation	Time deposition began (mya)	Present formation thickness (ft)	Missing thickness (ft)
Holditch SFE No. 4			
Second Frontier	93	370	0
Hilliard	89	3,660	0
Rock Springs	76	520	2,190
Hiatus	74		
Ericson-Lance	73	0	1,550
Erosion	66		-3,740
Tertiary	62	3,100	1,000
Erosion	37		-1,000

Geothermal gradient = 2 °F/100 ft [3.7°C/100 m.]

Terra Anderson Canyon No. 3-17			
Second Frontier	93	370	0
Hilliard	89	4,110	0
Rock Springs	76	720	1,990
Hiatus	74		
Ericson-Lance	73	0	1,550
Erosion	66		-3,540
Tertiary	62	4,160	1,000
Erosion	37		-1,000

Geothermal gradient = 1.7 °F/100 ft [3.12°C/100 m.]

Wexpro Church Buttes No. 48			
Second Frontier	93	280	0
Hilliard	89	3,140	200
Rock Springs	76	0	2,710
Erosion	74		-2,910
Ericson-Lance	73	670	880
Erosion	66		-880
Tertiary	62	8,170	0
Hiatus	37		

Geothermal gradient = 1.8 °F/100 ft [3.26°C/100 m.]

Table 4 (cont.)

Formation	Time deposition began (mya)	Present formation thickness (m)	Missing thickness (m)
Forest Henry No. 2			
Second Frontier	93	240	0
Hilliard	89	2,290	200
Rock Springs	76	0	2,710
Erosion	74		-2,910
Ericson-Lance	73	1,380	170
Erosion	66		-170
Tertiary	62	9,210	0
Hiatus	37		

Geothermal gradient = 1.8 °F/100 ft [3.26°C/100 m.]

Energy Reserves Group Blue Rim Federal No. 1-30

Second Frontier	93	370	0
Hilliard	89	4,180	0
Rock Springs	76	2,710	0
Hiatus	74		
Ericson-Lance	73	1,550	0
Hiatus	66		
Tertiary	62	7,480	0
Hiatus	37		

Geothermal gradient = 1.8 °F/100 ft (3.29°C/100 m.)

For all wells, assume surface temperature = 40 °F (4.4°C) from 0–4 mya, 50 °F (10°C) from 37–95 mya, and uniform decrease from 50 °F to 40 °F (10°C to 4.4°C) between 37 and 4 mya.

Table 5. Calculated time-temperature indices (TTI) and corresponding vitrinite reflectance ( $R_o$ ) values for the Second Frontier.

Well Name	Top Second Frontier	
	Calculated TTI	Calculated $R_o$
Holditch SFE No. 4	30	0.83
Terra Anderson Canyon No. 3-17	32	0.84
Wexpro Church Buttes No. 48	190	1.29
Forest Henry No. 2	334	1.47
ERG Blue Rim Federal No. 1-30	3,079	2.50

1987), supporting the assumption that a significantly different geothermal gradient did not exist in the past. Time-temperature index (TTI) values calculated by the method of Waples (1980) for the top of the Second Frontier range from a low of 30 in the SFE No. 4-24 well to a high of 3,079 in the Energy Reserves Blue Rim Federal No. 1-30 well (table 5). Equivalent  $R_o$  values range from 0.83 to 2.50 in these same wells (table 5).

Burial-history curves indicate that the Second Frontier has entered the oil window at the north end of the Moxa Arch and the wet-gas window at the south end (fig. 44). In the deep part of the Green River Basin, off the arch, the Frontier has passed out of the wet-gas window into the dry-gas zone. Law (1984) reported that no evidence exists for linking Green River Basin nonassociated gas to thermal cracking of oil and concluded that the gas is a primary catagenetic product from source-rock organic matter. Identification of the source of gas in the Frontier Formation is beyond the scope of this study, but marine shales of the Mowry and Hilliard Formations are likely source rocks. The top of the Mowry (base of the Frontier Formation) entered the wet-gas window at 43.3 mya in the Energy Reserves Group Blue Rim Federal No. 1-30 well, and the base of the Hilliard entered the wet-gas window at 41.5 mya (fig. 44). If the gas in reservoirs on the Moxa Arch was generated in Mowry and Hilliard Shales in the basin and then migrated updip and was trapped in structures along the Moxa Arch, gas probably entered Frontier reservoirs approximately 43 mya. If the gas was generated in older, deeper formations, then it would have migrated into Frontier reservoirs at an earlier time.

#### Interpretation of Diagenetic History

The paragenetic sequence of authigenic phases in Frontier reservoirs was determined primarily from petrographic relations. Major phases occurred in this order: (1) illite and MLIS rims, (2) quartz overgrowths, (3) calcite cement, (4) kaolinite, and (5) additional precipitation of quartz cement. The actual timing of precipitation was not determined for any of the authigenic phases (for example, by radiometric age-dating of illite), but isotopic composition data of calcite cement can help constrain the temperature, and thus timing, at which it precipitated. This, in

turn, constrains the timing of formation of earlier cements. Isotopic data from cements in Muddy Formation sandstones in the Powder River Basin, Wyoming (Law, 1983), provide information on composition of subsurface fluids in an area not far from the Green River Basin.

#### Early Diagenetic Reactions

As previously described (p. 77), calcite cement in Frontier reservoirs on the Moxa Arch has an average  $\delta^{18}\text{O}$  composition of  $-12.9$  ‰ (PDB), or  $+17.6$  ‰ (SMOW). An infinite number of combinations of temperature and water compositions could have precipitated calcite with this isotopic composition. Work by Law (1983) suggests that meteoric water in Wyoming in the Cretaceous was no lighter than  $-12$  ‰ (SMOW). Calcite in the Muddy Formation precipitated at a range of depths, from formation water diluted to varying extents by meteoric water. Calcite cement that formed at shallow depths (4,500 ft [1,370 m]) precipitated from fluids only slightly heavier than meteoric, with a  $\delta^{18}\text{O}$  composition of  $-10$  ‰, whereas calcite that precipitated at depths of 8,000 ft (2,440 m) precipitated from formation fluids of  $-1$  ‰ (SMOW), which had experienced much less dilution by meteoric water (Law, 1983). Calcite cement in Muddy sandstones, with  $\delta^{18}\text{O}$  compositions of  $+17$  to  $+18$  ‰ (SMOW) (similar to those in the Frontier Formation) are interpreted as having precipitated from fluids with  $\delta^{18}\text{O}$  composition of  $-5$  to  $-6$  ‰ (SMOW).

If calcite in the Frontier Formation had precipitated from fluids of similar composition, it would have formed at temperatures of about  $120^\circ$  to  $160^\circ\text{F}$  ( $50^\circ$  to  $70^\circ\text{C}$ ) (using calcite fractionation equation of Friedman and O'Neil, 1977), which occurred at burial depths of approximately 3,700 to 5,900 ft (1.1 to 1.8 km). The Frontier Formation was buried to this depth and temperature approximately 75 mya, toward the end of Hilliard deposition and the beginning of Rock Springs deposition (fig. 44).

If this interpretation of the timing and fluid composition at which Frontier Formation calcite precipitated is correct, then quartz cement, which clearly precipitated before calcite, probably precipitated from meteoric water (or formation water extensively diluted by meteoric



water) with  $\delta^{18}\text{O}$  composition of between  $-6$  and  $-12$  ‰ (SMOW) at moderate burial depths (<3,700 ft [ $<1.1$  km]). Quartz cement in Frontier sandstones would have precipitated during deposition of the Hilliard Formation. Isotopic composition of quartz overgrowths in Frontier sandstones was not measured, so this interpretation cannot be supported directly, but when Law and others (1990) determined the  $\delta^{18}\text{O}$  composition of quartz cement in Muddy Formation sandstones in the Powder River Basin, they concluded that the quartz overgrowths precipitated from predominantly meteoric fluids at depths of 1,000 to 3,300 ft (0.3 to 1.0 km). On the basis of existing data, we conclude that quartz cement in the Frontier Formation precipitated under similar conditions.

The paleogeographic setting of the Green River Basin during the Upper Cretaceous should have permitted deep circulation of meteoric water. Deposition of nonmarine sandstone and conglomerate (Frontier and Henefer Formations) continued in updip areas during deposition of the marine Hilliard shale in the downdip position of our study area (Ryer, 1977), implying that areas of topographic relief occurred to the west and southwest. Thus, meteoric water could have entered the coarse clastics in the updip recharge area and circulated downdip through buried Frontier sandstones, driven by gravitational head.

The volume of quartz cement that precipitated in Frontier sandstones during this early phase of cementation may have been approximately 7 percent throughout the study area, which is the volume of quartz cement in clean sandstones that contain calcite cement. We speculate that the volume of quartz that precipitated in Frontier sandstones during this period of cementation was uniform throughout the area because meteoric water circulated equally through all buried Frontier sandstones. The southerly plunge of the Moxa Arch had not developed yet (Dutton and Hamlin, in press), so Frontier sandstones in the Hogsback area were buried at depths similar to those in the Church Buttes area at this time.

Authigenic illite and MLIS rims, the earliest cement to precipitate, probably formed in the shallow subsurface, perhaps within the first 1,000 ft (300 m) of burial. They probably formed

from meteoric water because of the apparent predominance of meteoric fluids during early diagenesis of Frontier sandstones.

#### Late Diagenetic Reactions

Late-stage diagenesis included feldspar albitization, secondary porosity generation, and kaolinite, chlorite, illite, and quartz precipitation. Dissolution of feldspar, clay clasts, chert, and biotite resulted in secondary pores. The extent to which calcite cement precipitated and later dissolved is uncertain, but most calcite cement is not corroded. Thus, most secondary porosity apparently formed by silicate dissolution. Some secondary pores contain reaction products of feldspar dissolution, specifically kaolinite and illite in the north (at depths <10,000 ft [ $<3,050$  m]) and chlorite and illite in the south (at depths >10,000 ft [ $>3,050$  m]). Small quartz crystals that project into secondary pores indicate that some late quartz cementation occurred.

Late-stage diagenesis differed between Frontier sandstones at the north and south ends of the arch. Sandstones at the north end of the Moxa Arch are characterized by more abundant kaolinite (fig. 40) and calcite cement (fig. 45), as well as greater volumes of secondary porosity (fig. 46). Sandstones at the south end of the arch and in the basin contain significantly greater volumes of quartz cement (fig. 41).

The greater volume of secondary porosity at the north end of the arch is probably caused by differences in framework grain composition, specifically the greater volume of detrital feldspar (fig. 47). Because much of the secondary porosity in the Frontier was formed by feldspar dissolution, sandstones that contained greater volumes of feldspar developed more secondary porosity. In addition, a somewhat greater percentage of the original feldspar apparently dissolved at the north end than in the south, 67 versus 50 percent feldspar dissolution.

The reasons for the greater volumes of carbonate cement at the north end of the Moxa Arch are unknown. One possibility is that erosion of part of the Second Bench shoreface sandstones at the south end of the arch removed much of the section that contained shell

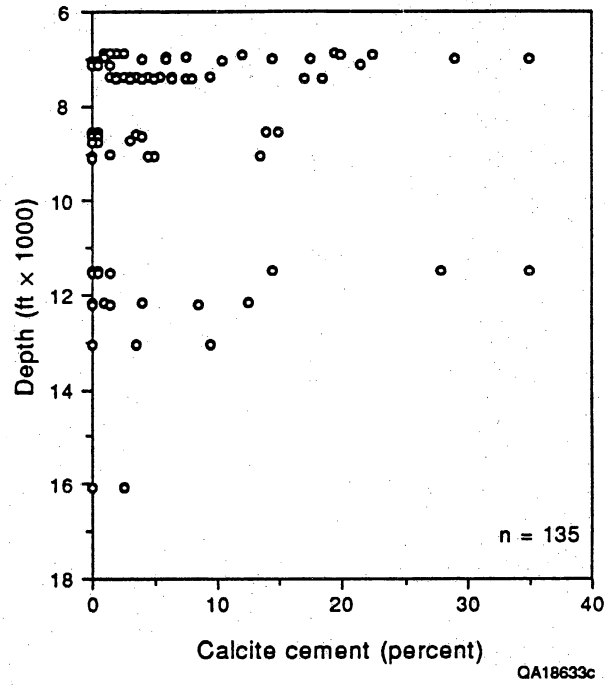


Figure 45. Calcite cement volume in clean ( $\leq 2$  percent matrix) First, Second, and Third Bench sandstones as a function of depth. In general, the average and maximum volumes of calcite cement decrease with depth.

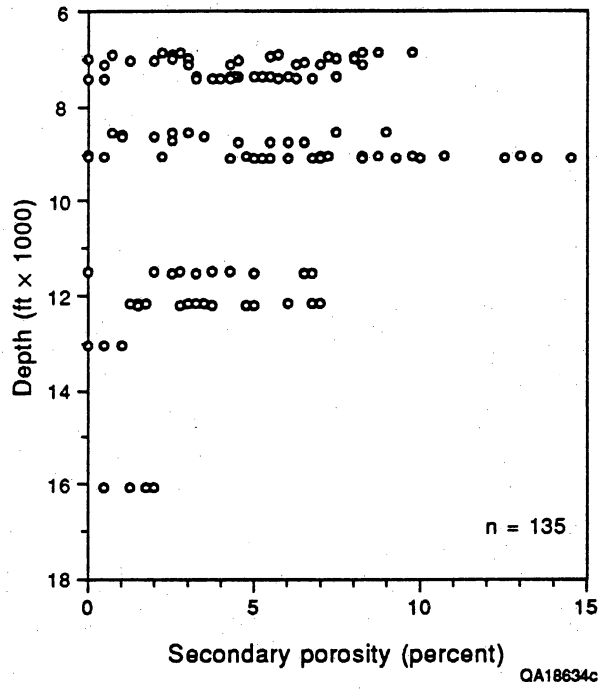


Figure 46. Secondary porosity volume in clean ( $\leq 2$  percent matrix) First, Second, and Third Bench sandstones as a function of depth. In general, the average and maximum volumes of secondary porosity decrease with depth.

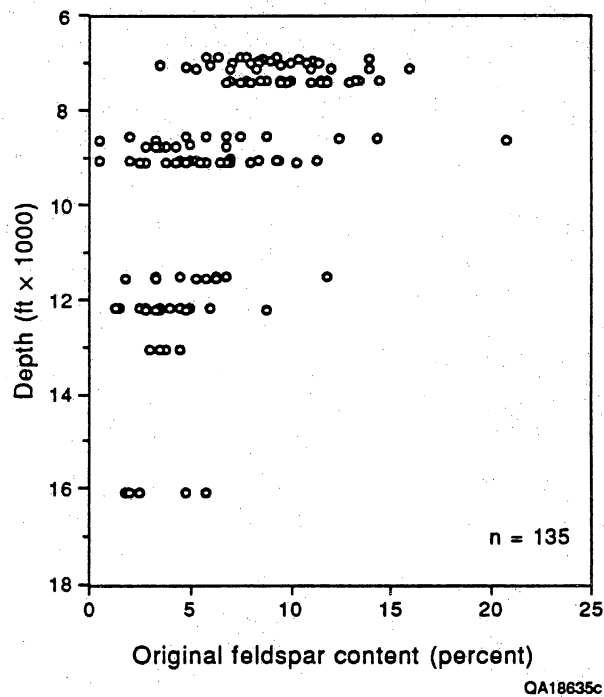


Figure 47. Estimated original feldspar volume of clean ( $\leq 2$  percent matrix) First, Second, and Third Bench sandstones as a function of depth. Original feldspar volume was greatest at the north end of the Moxa Arch, which is presently at the shallowest burial depths. See text for discussion of method by which original feldspar volume was calculated, p. 62.

fragments. The source of the calcium carbonate for calcite cement may have been internal, from shell fragments in the Frontier shoreface deposits. Sandstones at the south end may have lacked an abundant source of calcium carbonate and, therefore, less calcite cement precipitated.

Another possible explanation for the greater abundance of calcite cement at the north end may relate to differences in the buffering capabilities of Frontier sandstones. Milliken and Land (1991) suggested that interaction of sandstones with acidic formation fluids is largely controlled by feldspar content of the sandstones. We speculate that acidic formation fluids were expelled from Frontier and Hilliard shales in the deep basin as a result of illitization of smectite. These acidic pore waters may also have dissolved skeletal carbonate from the shales and thus transported  $H^+$ ,  $Ca^{++}$ , and  $CO_2$  into the Frontier sandstones on the Moxa Arch. According to Milliken and Land (1991), as long as sandstones contain reactive feldspars, acid from the shales will be buffered by feldspar dissolution and albitization, allowing calcite to precipitate. Once the supply of feldspar is exhausted, the partial pressure of  $CO_2$  ( $pCO_2$ ) rises and calcite cement dissolves. Sandstones at the north end of the Moxa Arch started with a greater volume of feldspar, which may have effectively buffered most of the acidic formation waters that migrated updip from the deep basin. As a result, abundant calcite cement precipitated from the buffered, low- $pCO_2$  fluids. In contrast, sandstones at the south end of the arch contained less reactive feldspar, so the fluids were not buffered and developed high  $pCO_2$ . Less calcite cement precipitated—or it precipitated but later dissolved.

A possible explanation for the absence of kaolinite in the deeper, hotter Frontier sandstones at the south end of the Moxa Arch, and in the basin, is that it may have been altered to chlorite or illite, or both. According to this hypothesis, kaolinite originally occurred everywhere along the Moxa Arch, forming as a reaction product of feldspar dissolution, but in the deeper Frontier sandstones it was later altered to other clay minerals. Kaolinite becomes unstable at temperatures of 250° to 265°F (120° to 130°C) (Bjorlykke and others, 1989). If potassium is present in the pore fluids, kaolinite alters to illite (Bjorlykke and others, 1989), but

if magnesium and iron are present, kaolinite alters to chlorite (Kaiser, 1984; Bjorlykke and others, 1989). Frontier sandstones at the south end of the Moxa Arch and in the Green River Basin are at temperatures higher than those at the north end (fig. 44) and may be in the stability field for chlorite and illite, not kaolinite. In the wells in which kaolinite is present, the Frontier Formation has never experienced temperatures greater than 230°F (110°C) (fig. 44), and TTI is  $\leq 32$ . In contrast, in the wells without kaolinite, the Frontier Formation has been at temperatures of at least 250°F (120°C) for the past 40 my (fig. 44), and TTI is  $\geq 190$ .

A different explanation, suggested by Stonecipher and others (1984), is that kaolinite only occurs in sandstones at the north end of the Moxa Arch because this part of the arch experienced more uplift and erosion during Late Cretaceous folding. As a result, Frontier sandstones at the north end of the arch were exposed to dilute, acidic meteoric water. Meteoric fluids that reached the south end of the arch had experienced more rock-water interaction because they followed a longer flow path, and thus may have contained too high a solute concentration to precipitate kaolinite (Stonecipher and others, 1984). However, isotopic data from calcite cements suggest that sandstones from both the north and south ends of the Moxa Arch were exposed to meteoric fluids. Similarly, early quartz cement in Frontier sandstones along the entire arch is interpreted as having precipitated from deeply circulating meteoric water that was recharged in the updip area to the west. Thus, new data that were not available to Stonecipher and others in 1984 suggest that their explanation for the distribution of kaolinite (that only the north end of the arch was exposed to meteoric water) is unlikely.

The final diagenetic difference between Frontier sandstones at the north and south ends of the Moxa Arch is the greater abundance of quartz cement in the deeper sandstones at the south end and in the basin (fig. 41). In the five wells for which TTI was calculated, an excellent correlation ( $r = 0.95$ ) exists between thermal maturity of the sandstone (TTI) and average volume of quartz cement (Dutton and Hamlin, in press). The equation relating quartz cement to TTI in Frontier sandstones is:

$$\text{volume of quartz cement (percent)} = -2.1 + 5.5 \times \log \text{TTI.}$$

We interpret the increase of quartz cement with depth to indicate that a second, later episode of quartz cementation occurred that added more quartz cement to what had previously precipitated from meteoric water. On the basis of comparison with other quartz-cemented sandstones (Dutton and Diggs, 1990), we think the later generation of quartz cement may have been derived internally. Because the Frontier sandstones at the south end of the Moxa Arch and in the basin were buried deeper, they experienced more intergranular pressure solution of chert and stylolitization, thereby liberating silica for quartz cement. In addition, more chert grains at the south end of the arch are partly leached (figs. 42 and 43), indicating that partial dissolution of chert grains was another source of silica. The late episode of quartz cementation may have occurred during the Tertiary, perhaps 37 to 62 mya, when the south end of the arch was buried most deeply.

The second episode of quartz cementation apparently enlarged existing quartz overgrowths in optical continuity and without dust lines or other inclusions, making it difficult to distinguish different generations of quartz cement. Petrographic evidence of a second generation of quartz cement includes quartz overgrowths that engulf kaolinite cement and prismatic quartz crystals, termed "outgrowths" by McBride (1989), that grow into secondary pores.

On the basis of burial-history curves (fig. 44), gas is interpreted to have migrated into Frontier reservoirs approximately 40 mya. The major diagenetic events are interpreted as having already taken place by this time.

The diagenetic history outlined above interprets meteoric water to be important during early phases of diagenesis, particularly at depths <5,900 ft (<1.8 km), but less involved in later diagenetic reactions that occurred at greater depths. The reason for the change may be a lower depth limit for meteoric water circulation into the basin or the erosion in the updip areas to the west that lowered gravitational head in the hydrologic system. Later diagenesis apparently was influenced more by basin-derived fluids and may have occurred in a less active hydrologic system.



## DIAGENETIC CONTROLS ON RESERVOIR QUALITY

### Porosity

Matrix-free sandstones deposited in high-energy upper shoreface and fluvial channel-fill environments had the highest porosity and permeability at the time of deposition. However, porosity was reduced by compaction and cementation during burial diagenesis. Loss of porosity by compaction in clean sandstones was most severe where ductile grains, such as chert, mud rip-up clasts, biotite, glauconite, and metamorphic rock fragments, were abundant. For example, because many fluvial channel-fill sandstones contain abundant chert and mud rip-up clasts, they have lost considerable porosity by mechanical compaction.

The most quartz-rich sandstones were deposited in upper shoreface environments, and these sandstones have lost the least porosity by compaction. However, even within the upper shoreface, variations in depositional energy resulted in variable framework-grain composition and extent of compaction. In the Terra Anderson Canyon No. 3-17 well, Fontenelle field, the most quartz-rich sandstones (Q<sub>79</sub>F<sub>2</sub>R<sub>19</sub>) (fig. 18, depth 9,078 to 9,086 ft [2,767 to 2,769 m]) were deposited in a high-energy foreshore environment. Average primary porosity in this section is 5 percent, porosimeter porosity is 15.9 percent, and average stressed permeability to air is 0.75 md. Sandstones deposited in a slightly lower energy environment, but still on the upper shoreface (fig. 18, depth 9,087 to 9,098 ft [2,768 to 2,773 m]), contain more ductile rock fragments (Q<sub>63</sub>F<sub>2</sub>R<sub>35</sub>). As a consequence of greater mechanical compaction in this interval, average primary porosity in this section is 3 percent, porosimeter porosity is 13.2, and average stressed permeability to air is 0.009 md.

Porosity has also been lost in Frontier sandstones by cementation. The most effective control on porosity in clean Frontier sandstones is the total volume of cement (fig. 48), for more than half of the variation in porosity is explained by variation in total cement volume ( $r^2 = 0.56$ ). Fluvial sandstones have undergone the most cementation, containing an average of

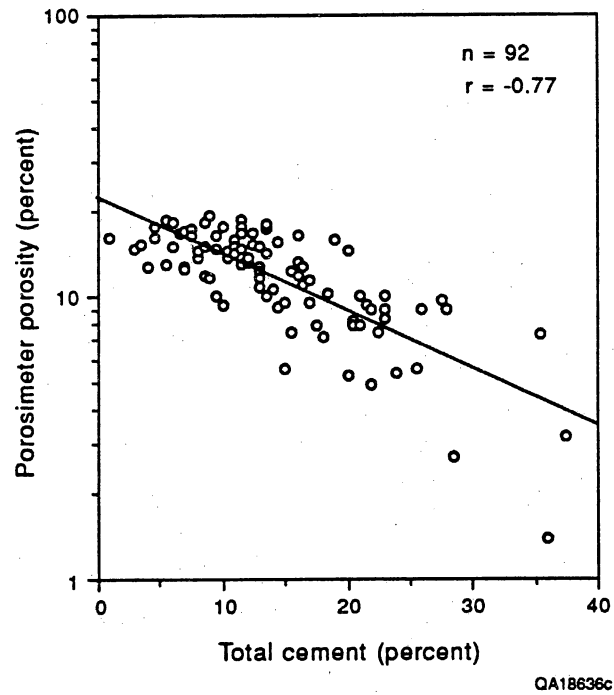


Figure 48. Semi-log plot showing inverse relationship between total cement volume and porosimeter porosity in clean ( $\leq 2$  percent matrix) First, Second, and Third Bench sandstones. Volume of authigenic cement is a major control on porosity in Frontier sandstones.

15 percent cement, compared with an average of 10 to 11 percent in upper and lower shoreface sandstones (table 2). Calcite is the individual cement that has the largest effect on porosity. In clean sandstones containing less than 5 percent calcite cement, porosity is highly variable, but in sandstones having more than 5 percent calcite, an excellent inverse relationship exists between log porosimeter porosity and calcite cement (fig. 49). No significant relationship exists between porosity and grain size, sorting, or quartz cement.

Given our current understanding, to predict the presence of extensive calcite cement in a particular well or sandstone bed is impossible, but patterns in the distribution of calcite cement exist and can provide general guidelines to its occurrence. Abundant calcite cement is most likely to occur in lower shoreface sandstones. However, because of the large volume of detrital clay matrix, lower shoreface sandstones probably will be poor reservoirs, whether or not they contain calcite cement. Within clean sandstones, calcite cement is most abundant at the north end of the Moxa Arch, especially in the Hogsback area on the northwest part of the La Barge Platform. The amount of calcite cement in sandstones in this area may be controlled by original feldspar distribution or by an abundance of shell fragments. In other areas, calcite cement commonly is most abundant at the top of clean, well-sorted sandstones, directly below the contact with an overlying muddy sandstone. Once a well has been drilled, zones of intense calcite cementation can be recognized on logs as zones of low porosity with high resistivity response. Intervals of intense calcite cementation should not be counted as part of the pay in a well.

Average porosimeter porosity in Frontier sandstones does not change from north to south along the Moxa Arch. At any given depth, a wide range of porosity exists, but the average is approximately 10 percent along the entire length of the arch. Minus-cement porosity, however, increases significantly with increasing depth (fig. 50), indicating that sandstones at the south end of the arch retained more primary, intergranular porosity following compaction than did sandstones at the north end. Northern Moxa Arch sandstones contain a greater volume of ductile grains, and thus they experienced more porosity loss by mechanical

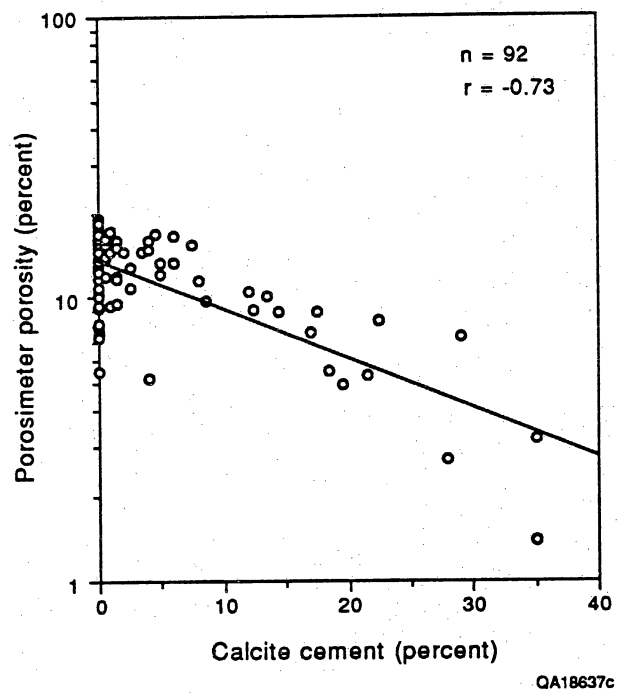


Figure 49. Semi-log plot showing inverse relationship between calcite cement volume and porosimeter porosity in clean First, Second, and Third Bench sandstones ( $\leq 2$  percent matrix).

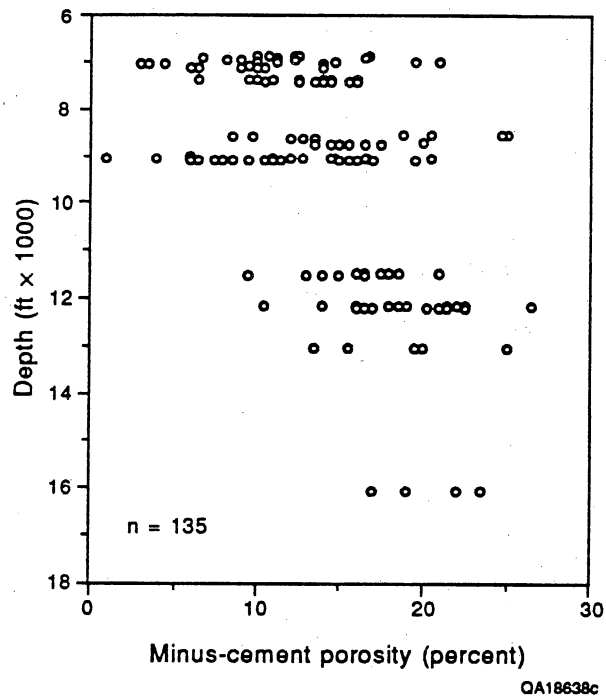


Figure 50. Minus-cement porosity as a function of depth in clean ( $\leq 2$  percent matrix) First, Second, and Third Bench sandstones. Sandstones at the north end of the Moxa Arch, which are at the shallowest burial depths now, experienced more mechanical compaction and have lower minus-cement porosity than do sandstones at the south end of the Arch.

compaction early in their burial history than did sandstones from the south end of the arch. However, subsequent precipitation of quartz cement was more extensive in sandstones at the south end of the arch (fig. 41). The result was uniformly low average porosity in Frontier sandstones all along the Moxa Arch. Sandstones at the north end of the arch lost primary porosity by extensive mechanical compaction and minor quartz cementation, whereas sandstones at the south end lost porosity by relatively minor mechanical compaction and extensive quartz cementation.

### Permeability

Stressed permeability in Frontier sandstones ranges from 0.003 to 22 md. Average stressed permeability (geometric mean) in all Frontier sandstones is 0.014 md; average unstressed permeability is 0.076 md. In clean sandstones, which are most likely to be reservoirs, average stressed permeability is 0.07 md, and average unstressed permeability is 0.22 md. As is true for porosity, no significant trend exists in the relationship of permeability versus depth.

Porosity is not always a good predictor of permeability in Frontier sandstones because the correlation between porosimeter porosity and stressed permeability in clean Frontier sandstones is relatively low (fig. 51). Primary and secondary porosity are interpreted to contribute about equally to permeability in Frontier sandstones. The correlation coefficient between primary porosity and unstressed permeability is 0.53, and it is 0.55 between secondary porosity and unstressed permeability. (Unstressed permeability has been compared with petrographic parameters because there are 102 thin sections of clean Frontier sandstones that have corresponding unstressed permeability measurements but only 55 that have stressed permeability measurements.) The correlation between total cement volume and permeability is low ( $r = -0.34$ ), but statistically significant at the 99-percent confidence level. Weak but statistically significant relationships also exist between volume of calcite cement and permeability ( $r = -0.51$ ) and between grain size and permeability ( $r = -0.40$ ; the correlation coefficient is negative because grain size is in  $\phi$  units). No significant relationship (at the

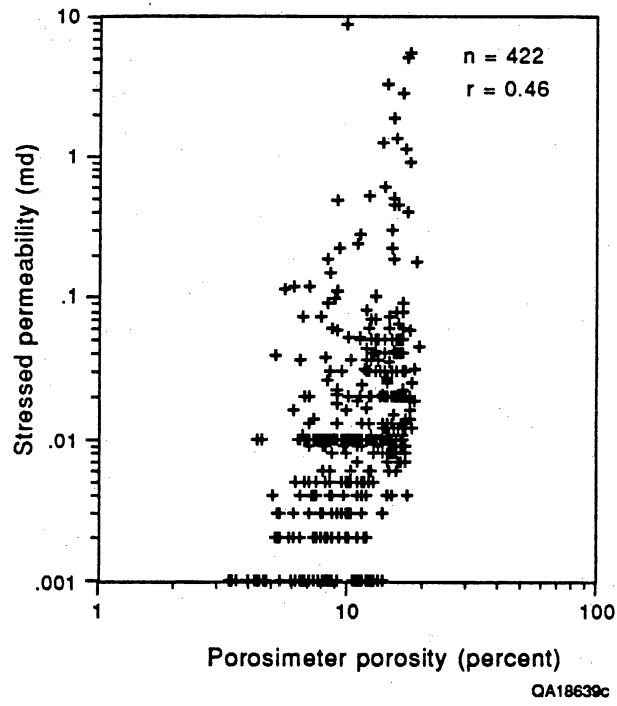


Figure 51. Log-log plot of porosimeter porosity versus stressed permeability in 422 Frontier sandstones.

99-percent confidence level) exists between permeability and volume of quartz cement or sorting in clean Frontier sandstones. Permeability decreases significantly in clean sandstones in the Fontenelle area as the volume of ductile grains increases ( $r = -0.67$ ). However, no relationship between volume of ductile grains and permeability was observed for Church Buttes or Hogsback clean sandstones.

One reason for the scatter in the porosity-versus-permeability plot (fig. 51) is the abundance of microporosity, which is measured by porosimeter but contributes insignificantly to permeability. Another reason for the low correlation is the presence of abundant fibrous illite and MLIS in many Frontier sandstones. The fibrous clay has little effect on porosity, but it dramatically lowers permeability. The presence of variable amounts of fibrous illite and MLIS in Frontier sandstones makes the porosity-permeability relationship less predictable than in other low-permeability sandstones, such as the Lower Cretaceous Travis Peak Formation in East Texas (Luffel and others, 1989). In general, the highest permeability in the Frontier occurs in sandstones having at least 3 percent primary porosity. Clean sandstones that have <3 percent primary porosity have an average (geometric mean) unstressed permeability of 0.16 md, but clean sandstones having  $\geq 3$  percent primary porosity have an average (geometric mean) unstressed permeability of 1.1 md.

### Depositional Environment

In our study area, important differences in average porosity and permeability exist among sandstones from the three major depositional environments—fluvial channel fill, upper shoreface, and lower shoreface—as a result of depositional differences in grain size and sorting and subsequent diagenetic modifications, particularly compaction and cementation (table 2). Fluvial sandstones have average porosimeter porosity of 10.0 percent and unstressed permeability of 0.13 md. Upper shoreface sandstones have average porosimeter porosity of 14.2 percent and unstressed permeability of 0.19 md. Lower shoreface sandstones have average porosimeter porosity of 12.5 percent and unstressed permeability of 0.08 md. Thus, in our



study area, upper shoreface sandstones have the best reservoir quality. They are well sorted and probably had good porosity and permeability at the time of deposition. Because of their quartz-rich composition, they have undergone less compaction than have sandstones from lower shoreface environments. They have lost less porosity by cementation than have fluvial sandstones because of their average shallower burial depth (table 2).

Frontier reservoirs in fluvial channel-fill sandstones in the study area generally have lower porosity and permeability than do upper shoreface sandstones (table 2). Important differences exist between clean fluvial sandstones at the north end of the Moxa Arch (Hogsback and Fontenelle areas) and those at the south end and in the Green River Basin. Clean fluvial sandstones at the south end of the arch are relatively quartz rich ( $Q_{68}F_3R_{29}$ ) and thus have not lost much porosity by ductile grain deformation (minus-cement porosity = 18 percent). However, the average volume of quartz cement in these sandstones is 11 percent, and the total volume of cement is 19 percent. As a result, fluvial sandstones at the south end of the Moxa Arch have poor reservoir quality, mainly because of extensive cementation. In contrast, fluvial sandstones from the north end of the Moxa Arch have an average of only 11 percent total cement, including 4 percent quartz cement. However, the average framework-grain composition of the northern fluvial sandstones is  $Q_{46}F_5R_{49}$ . The large volume of rock fragments suggests that mechanical compaction by ductile grain deformation was the most important porosity-reducing process in the north fluvial sandstones (minus-cement porosity = 10 percent). Therefore, at the north and south ends of the Moxa Arch, different but equally effective diagenetic modifications have resulted in low average porosity and permeability in fluvial channel-fill sandstones.

Lower shoreface sandstones have the lowest permeability in the study area (table 2). They probably had low porosity and permeability at the time of deposition because of their fine grain size and abundance of detrital clay matrix. As much as 80 percent of the depositional porosity was lost by compaction (minus-cement porosity = 8 percent), and most of the remaining primary porosity has been occluded by calcite cement. Of the 35 Frontier sandstone

samples that contain more than 10 percent calcite, 20 are in lower shoreface sandstones. Lower shoreface sandstones may contain abundant calcite cement because they probably contained more shell fragments than did either the upper shoreface or fluvial sandstones, and the shells provided an internal source of calcium carbonate. As a result of both compaction and cementation, permeability is lowest in the lower shoreface sandstones. Lower shoreface sandstones are volumetrically more abundant in the study area than are either fluvial channel-fill or upper shoreface sandstones.

### Geographic Area

Diagenetic differences occur among sandstones in the three areas studied along the Moxa Arch. However, comparison of diagenesis in the three geographic areas presupposes the limited volume of sample available from each area to be representative of that area. The total volume of cement in clean sandstones from the Fontenelle area is significantly lower, and the average porosity and permeability significantly higher, than in sandstones from either the Hogsback or Church Buttes areas (table 6). As noted previously, sandstones from the Church Buttes area have low porosity and permeability because they contain variable amounts of calcite cement and very abundant quartz cement, probably as a result of their greater burial depth. Low porosity and permeability in sandstones from the Hogsback area probably result from the finer grain size and heavier calcite cementation compared with those of sandstones from the other two areas (table 6). Shoreface sandstones in Hogsback wells contain more calcite cement than do shoreface sandstones in either the Church Buttes or Fontenelle areas. Upper shoreface sandstones from the Hogsback area contain an average of 6 percent calcite, compared with an average of 1 percent in Fontenelle upper shoreface sandstones. (No upper shoreface sandstones occur in the Church Buttes cores.) Similarly, lower shoreface sandstones from the Hogsback wells contain an average of 8 percent calcite. Fontenelle lower shoreface sandstones average 1 percent calcite, and Church Buttes samples average 3 percent.

Table 6. Characteristics of clean First, Second, and Third Bench Frontier sandstones in four areas along the Moxa Arch.

	Hogsback	Fontenelle	Church Buttes <sup>1</sup>	Green River Basin <sup>2</sup>
Grain size (mm)	0.15	0.22	0.23	0.22
Sorting (phi)	0.50	0.51	0.58	0.49
Original feldspar (%)	9	6	4	3
Present feldspar (percent)	3	2	2	2
Quartz cement (%)	5	6	11	16
Calcite cement (%)	7	1	4	1
Kaolinite cement (%)	2	0.3	0	0
Total cement (%)	16	11	19	20
Primary porosity (%)	1	3	1	1
Secondary porosity (%)	5	6	3	1
Total thin-section porosity (%)	6	9	4	2
Ductile grains (%)	26	25	23	17
Minus-cement porosity (%)	12	14	18	21
Porosimeter porosity (%)	12.2	15.3	9.3	—
Unstressed permeability (md)	0.17	0.46	0.18	—
Stressed permeability (md)	0.07	0.09	—	—
Depth (ft)	7,000	8,900	12,500	16,100
QFR ratio <sup>3</sup>	Q <sub>63</sub> F <sub>5</sub> R <sub>32</sub>	Q <sub>66</sub> F <sub>3</sub> R <sub>31</sub>	Q <sub>67</sub> F <sub>2</sub> R <sub>30</sub>	Q <sub>75</sub> F <sub>3</sub> R <sub>22</sub>

<sup>1</sup>Includes data from Forest Henry No. 2 (well 16, fig. 1)

<sup>2</sup>Green River Basin data from Energy Resources Group No. 1-30 Blue Rim Federal well (well 12, fig. 1)  
— = No data

<sup>3</sup>Quartz:feldspar:rock fragments

An empirical relationship between porosity in sandstones and TTI was developed by Schmoker and Gautier (1989). The equation for porosity is  $\phi = 30 (TTI)^{-0.33}$ , where TTI is time-temperature index calculated by the Waples (1980) method. This equation does not work well for Frontier sandstones. Predicted porosity for the Holditch SFE No. 4-24 well is 9.8 percent, which is fairly close to the average measured porosimeter porosity of 10.8 percent. However, predicted porosity for the Terra Anderson Canyon No. 3-17 well is 9.6 percent, compared with the average measured porosity of 14.3 percent. Predicted porosity for the Wexpro Church Buttes No. 48 well is 5.3 percent, significantly lower than the average measured porosity of 8.5 percent. The equation may not be applicable because of the different mechanisms, compaction versus cementation, that control porosity in the Frontier Formation at different ends of the Moxa Arch.

#### Comparison of Diagenesis in Three Frontier Wells

Diagenetic differences in the pay zones of three wells from the north end of the arch, the SFE No. 4-24, Enron South Hogsback No. 13-8A, and Terra Anderson Canyon No. 3-17, may explain some of the differences in initial gas production among the three wells (table 7). The Enron S. Hogsback No. 13-8A well had the highest prefracture production of 170 Mcf/d. The Terra Anderson Canyon No. 3-17 well had a prefracture flow rate of 70 Mcf/d, and the Holditch SFE No. 4-24 had a flow rate of 9 Mcf/d. On the basis of thin-section analysis of the reservoir sandstones, SFE No. 4-24 would be expected to have the lowest prefracture flow rate of the three wells, and it did. Sandstones in the pay zone from the Holditch SFE No. 4-24 contain more total cement, as well as finer grain size, and consequently have lower porosity and permeability than do sandstones in the other two wells (table 7).

The reason that the flow rate in the Enron S. Hogsback No. 13-8A well is higher than that of the Terra Anderson Canyon No. 3-17 well is unclear. In thin sections, sandstones from the Terra Anderson Canyon well have significantly more porosity than do sandstones from the Enron S. Hogsback well, and permeability to gas measured in dried core plugs is an order of

Table 7. Petrographic data from pay zones of GRI cooperative wells.

	Holditch SFE No. 4 (7,400–7,412 ft)	Enron S. Hogsback No. 13-8A (7,114–7,140 ft)	Terra Anderson Canyon No. 3-17 (9,079–9,086 ft)
Grain size (mm)	0.13	0.17	0.24
Sorting (phi)	0.52	0.48	0.45
Quartz cement (%)	7	5	6
Calcite cement (%)	5	1	1
Pore-filling calcite (%)	1	0.1	0.4
Total cement (%)	17	9	11
Primary porosity (%)	2	2	5
Secondary porosity (%)	5	5	9
Total thin-section porosity (%)	7	7	14
Porosimeter porosity (%)	11.9	15.7	17.6
Unstressed permeability (md) (measured on dry core plugs)	0.10	0.22	2.79
Stressed permeability (md) (measured on dry core plugs)	0.03	0.11	1.32
Reservoir permeability (md) <sup>1</sup>	0.005 <sup>2</sup>	0.1	0.05
Prefracture flow rate (Mcf/d)	9	170	70

<sup>1</sup>Reservoir permeability calculated from pressure build-up tests (personal communication, Bradley M. Robinson, S. A. Holditch & Associates, January 1991)

<sup>2</sup>Because of low flow rate, calculated reservoir permeability could be 50 percent higher or lower

magnitude higher in samples from the Terra Anderson Canyon than from the Enron S. Hogsback well (table 7). One reason for the higher gas flow rate in the Enron S. Hogsback well is the thicker pay interval of 26 ft (8 m), compared with only 7 ft (2 m) in the Terra Anderson Canyon well (table 7). The Enron S. Hogsback well had a flow rate of 6.5 Mcf/d/ft, whereas the Terra Anderson Canyon well had a higher flow rate per foot of net pay, 10 Mcf/d/ft. In addition, the flow rate in the Terra Anderson Canyon well may be lower than expected because of the presence of abundant fibrous illite in the pore network of the reservoir sandstones. Fibrous illite has little effect on porosity, but it drastically lowers permeability to gas at connate water saturation (Luffel and others, 1991). The Enron S. Hogsback well apparently contains less fibrous illite in the pay zone, which may explain why it has higher well-test permeability than does the Terra Anderson Canyon well (Luffel and others, 1991). Reservoir permeability calculated from pressure-buildup tests is 0.1 md for the Enron S. Hogsback well, and only 0.05 md for the Terra Anderson Canyon well.

#### NATURAL FRACTURES

The purposes of this section are (1) to show that fractures occur in Frontier Formation cooperative-well and SFE-well core in the Green River Basin and (2) to present observations of fracture patterns in Frontier sandstone outcrops of reservoir facies that illustrate the types of fracture networks that are likely to exist at depth.

In rocks having low-matrix permeability, open fractures are potential fluid conduits. In fractured, low-permeability rock, overall pattern and connectivity of fractures control size and shape of the rock volume contacted by a given borehole; thus, information on fracture patterns can be used in design of exploration, development, and completion strategies. Some general aspects of fracture patterns, such as fracture orientation, can be determined from borehole and core observations and forecast with current structural models, but on the prospect scale, predicting fracture attributes such as clustering and connectivity and size of the fracture target has proven challenging. One reason is that in mildly deformed and flat-lying sedimentary rocks,

fracture-detection methods, such as geophysical well logs and core (particularly from vertical wells), may fail to detect fractures and, at best, sample only small parts of fracture networks. Consequently, the types of fracture patterns to be expected in the subsurface are uncertain, and planning appropriate drilling and stimulation strategy may be hindered.

Frontier Formation core collected in this study contains widespread but sparse natural fractures. Because they are vertical fractures sampled in vertical wells, the abundance of such fractures is not a reliable guide to their importance in the reservoir. Production and hydraulic-fracture-treatment results provide qualitative evidence that natural fractures are important reservoir elements in the Frontier Formation. Natural fracture permeability is one of the numerous factors that can account for local high gas and/or water production and abrupt differences in well performance that cannot be explained by other aspects of reservoir geology or completion practices. For example, in one Frontier Formation well, the Enron S. Hogsback No. 13-8A, a twentyfold increase in gas production after fracture treatment (from 170 Mcf/d to 3 to 4 MMcf/d) was interpreted to imply that stimulation fractures intersected an area of greater permeability away from the wellbore—possibly a natural fracture system (W. Whitehead, personal communication, 1990; Laubach, in press). Higher-than-expected leakoff coefficients needed in hydraulic fracture models of the Frontier Formation to fit pressure data also might reflect dilation of natural fractures (Chris Wright, RES, personal communication, 1992). Opening of natural fractures could account for wide scatter in the location of microseismic signals detected following hydraulic fracture treatments monitored using in-well geophones (Laubach and others, in press). In the Holditch SFE No. 4-24 well, high treatment pressures and apparent near-wellbore constrictions to fluid flow detected during minifrac tests are most likely caused by development of multiple fracture strands in naturally fractured intervals (Laubach, 1989a; S. A. Holditch, personal communication, 1992).

Outcrop observations show that natural fractures in Frontier Formation sandstones are in patterns that are far different from those envisioned in traditional fractured reservoir models. That such models fully or accurately portray the role of fractures in Frontier Formation

production is unlikely. Core and outcrop observations, coupled with the structural setting of the Frontier Formation in a basin that has experienced an active tectonic history where widespread fracture development is expected, suggest that natural fractures need to be taken into account in exploration, development, and reservoir modeling.

### Natural Fractures in Core

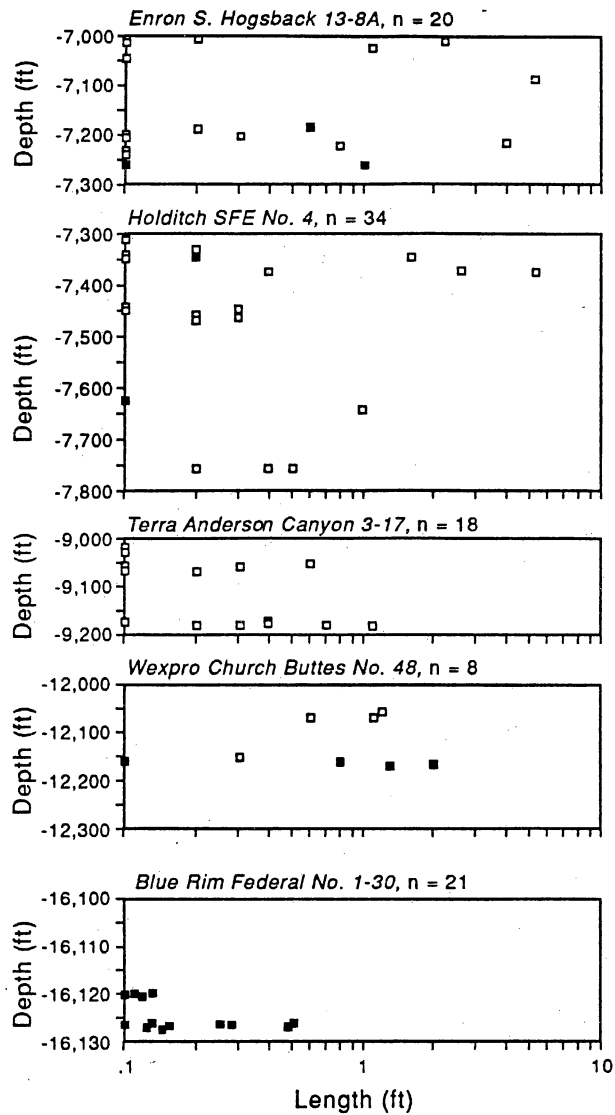
Natural fractures are sparse but persistent features of Frontier Formation core. They include vertical to subvertical extension (opening mode) fractures and small faults. Natural fractures were distinguished from drilling-induced fractures by the presence of vein-filling minerals in natural fractures and by surface marks and distinctive shapes (such as downward-steepening profiles of petal-centerline fractures) that are typical of drilling-induced fractures. The criteria we used to identify drilling-induced fractures are described by Kulander and others (1990). Not all natural fractures contain infilling minerals that are readily apparent, and some induced fractures lack distinctive surface marks and shapes, so the classification of a few fractures is uncertain.

### Fracture Abundance in Core

Fractures in five cores were studied in detail. Six additional cores were surveyed for fracture occurrence. Despite the low probability of vertical fractures intersecting with vertical core, 92 fractures were encountered in 10 Frontier wells having more than 1,580 ft (481 m) of core. Fracture abundance in five cores is illustrated in figure 52, which shows the depth and vertical lengths (height) of fractures in core. From these wells, 32 vertical or steeply inclined extension fractures were recovered in approximately 470 ft (143 m) of sandstone core.

Extension fractures are in sandstones from all five wells. They occur over a depth range of 7,195 to 16,130 ft (2,193 to 4,916 m). The deepest fractures are from 16,130 ft (4,916 m) in the Energy Reserves Group Blue Rim Federal No. 1-30 well in Sweetwater County. Calcite-filled





QA15574c

Figure 52. Fractures in core from five Frontier Formation wells in the Green River Basin (Laubach, 1991).

fractures in one interlaminated sandstone and mudstone interval have heights of 6 inches (140 mm), widths of as much as 0.25 mm, and spacing of 0.4 to 1.2 inches (10 to 30 mm). For all natural fracture types in these cores, no obvious, consistent difference is apparent in style, number, or height of fractures with depth. Maximum heights of vertical fractures in shallow and deep cores are comparable. The abundance of fractures and the proportion of different fracture types per length of cored interval are generally similar for all five wells.

Core from the SFE No. 4-24 well illustrates typical proportions of natural fracture types encountered in these wells. The core contains three steeply inclined calcite-lined extension fractures and 22 gently to moderately dipping, striated fractures or small faults. The latter are primarily compaction/dewatering features in mudstones, but several calcite-lined slip surfaces are small tectonic faults (shear fractures). Other fractures include extension fractures (cleat) in coal, and eight vertical, nonmineralized fractures in mudstone that may be either natural or drilling induced.

Closely spaced fractures in Frontier Formation core from depths of 16,130 ft (4,916 m) in the Energy Reserves Group Blue Rim Federal No. 1-30 well suggest that fractures can occur at great depth in the Green River Basin, distant from major tectonic folds and faults. Outcrop observations of fractures in exposed sandstones and fracture observations in closely spaced vertical and horizontal wells in other low-permeability sandstones and other flat-lying sedimentary rocks (Laubach, 1991; Lorenz and Hill, 1991; Collins and others, in press) make it clear that a quantitative measure of vertical fracture abundance cannot readily be obtained from vertical cores. Nevertheless, the occurrence of a few natural fractures in most cored Frontier Formation wells we studied is qualitative evidence that fractures are widespread in the subsurface of the Green River Basin.

#### Fracture Dimensions in Core

Mineralized extension fractures in Frontier Formation core, typically narrow, are commonly <0.25 mm wide, and they have lens-shaped cross sections. Wide fractures are filled

or partly filled with minor quartz and calcite. Only a few show petrographic evidence, such as euhedral crystals lining fractures, indicating that fractures were persistently open in the subsurface. Vertical fractures are the only type for which meaningful height measurements in vertical core can be obtained. These fractures are short, generally less than 1 ft (30 cm). The tallest fracture of this type is about 2 ft (60 cm). Fractures in Frontier Formation core tend to be confined to individual sandstones and generally end at shale interbed intersections or at blind terminations within sandstone (fig. 53). Some fractures are also composed of vertically discontinuous fracture strands, suggesting that fractures may not form continuous networks of interconnected fractures from the top to the base of a sandstone.

Length (plan-view dimension) and spacing cannot be measured in vertical core, but Frontier Formation outcrop observations, described later, suggest fracture length is probably much greater than fracture height (>10:1). The appearance and style of extension fractures in these cores is similar to that of fractures in core from other Mesozoic low-permeability sandstones, such as the Cotton Valley and Travis Peak Formation of the East Texas Basin (Laubach, 1989b), the Pictured Cliffs Sandstone of the San Juan Basin (Laubach and others, 1991a), or Mesaverde sandstone of the Piceance Basin (Lorenz and Finley, 1991).

#### Petrography of Fracture-Filling Minerals

The sequence in which vein-filling minerals precipitated is evident in thin section from overprinting and cross-cutting relations among minerals. In a few fractures, overlapping relations suggest that quartz precipitated first, followed by calcite. In these fractures only small amounts of quartz are present, forming faceted crystal faces on grains adjacent to fractures. It is possible that this quartz precipitated before fractures developed, as quartz overgrowth cement in pores. Fracturing subsequently exposed quartz crystals on the fracture walls. This interpretation is supported by the discontinuous pattern of quartz on fracture surfaces and the widespread unfaceted quartz grains on fracture walls overgrown with calcite—implying that a phase of quartz precipitation preceded fracture development.

BLUE RIM  
Federal 1-30

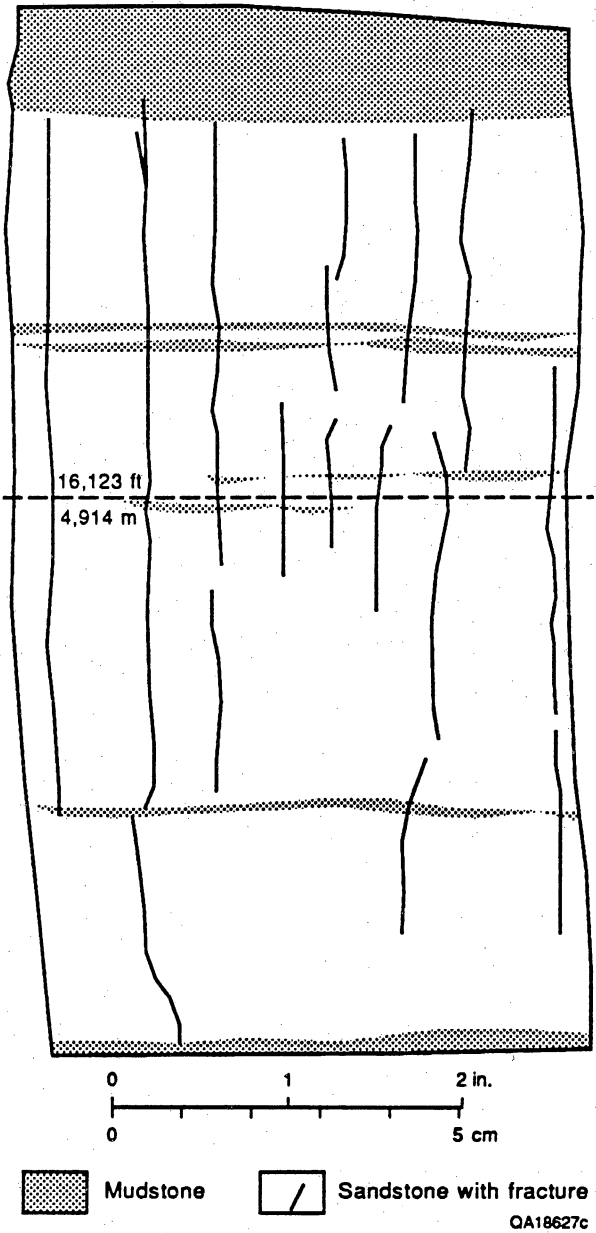


Figure 53. Closely spaced vertical fractures in Frontier Formation core, Blue Rim Federal No. 1-30 well. Core depth 16,123 ft (4,914 m).

Fractures typically are filled or partly filled with calcite, which is commonly massive and blocky or slender and having crystals oriented normal to the fracture surfaces. Locally, euhedral crystal faces are evident, indicating minerals grew into open fracture pore space. In some examples, late blocky calcite encloses older, acicular calcite crystals. On the basis of these overprinting relationships, and differences in crystal habit and color, several generations of vein-filling calcite can locally be inferred.

In the Mobil Tip Top No. T71X-6G well, Sublette County, cross-cutting relations in a calcite-filled vein show the timing of fracture genesis relative to calcite precipitation and feldspar dissolution. The vein occurs at 6,912 ft (2,106 m). Vein-filling calcite that crosses open or clay-filled pores that formerly contained feldspar grains is evidence that fractures formed and vein calcite precipitated before feldspar dissolution. In this example, the calcite that filled the vein remains after the surrounding feldspar grain was dissolved. Feldspar dissolution following calcite precipitation is a sequence that also occurs in the diagenetic history of these rocks.

Vein-filling minerals in fractures from outcrop are similar to those in core, but commonly calcite is highly twinned in outcrop examples, and locally it is microfractured. A thin veneer of clay minerals coats euhedral vein calcite in some fractures. Wide, north-striking calcite-filled veins from outcrops southeast of Kemmerer (Sec. 36, T21N, R116W) have vertical stylolites that cross cut and are superimposed on acicular crystals oriented normal to the fracture wall. Such features generally indicate shortening and pressure solution normal to the stylolite seam, so this relationship marks east-west shortening following vein formation. Subvertical stylolite seams unassociated with preexisting veins occur in Wexpro Church Buttes No. 48 core, from the southern Moxa Arch.

#### Fracture Orientations in Core

Only seven extension fractures were reliably oriented in the cores we studied (fig. 54), so conclusions on subsurface fracture orientations are tentative. In the Wexpro Church Buttes No. 48 well, one fracture strikes east-northeast and three others strike northeast. Subvertical

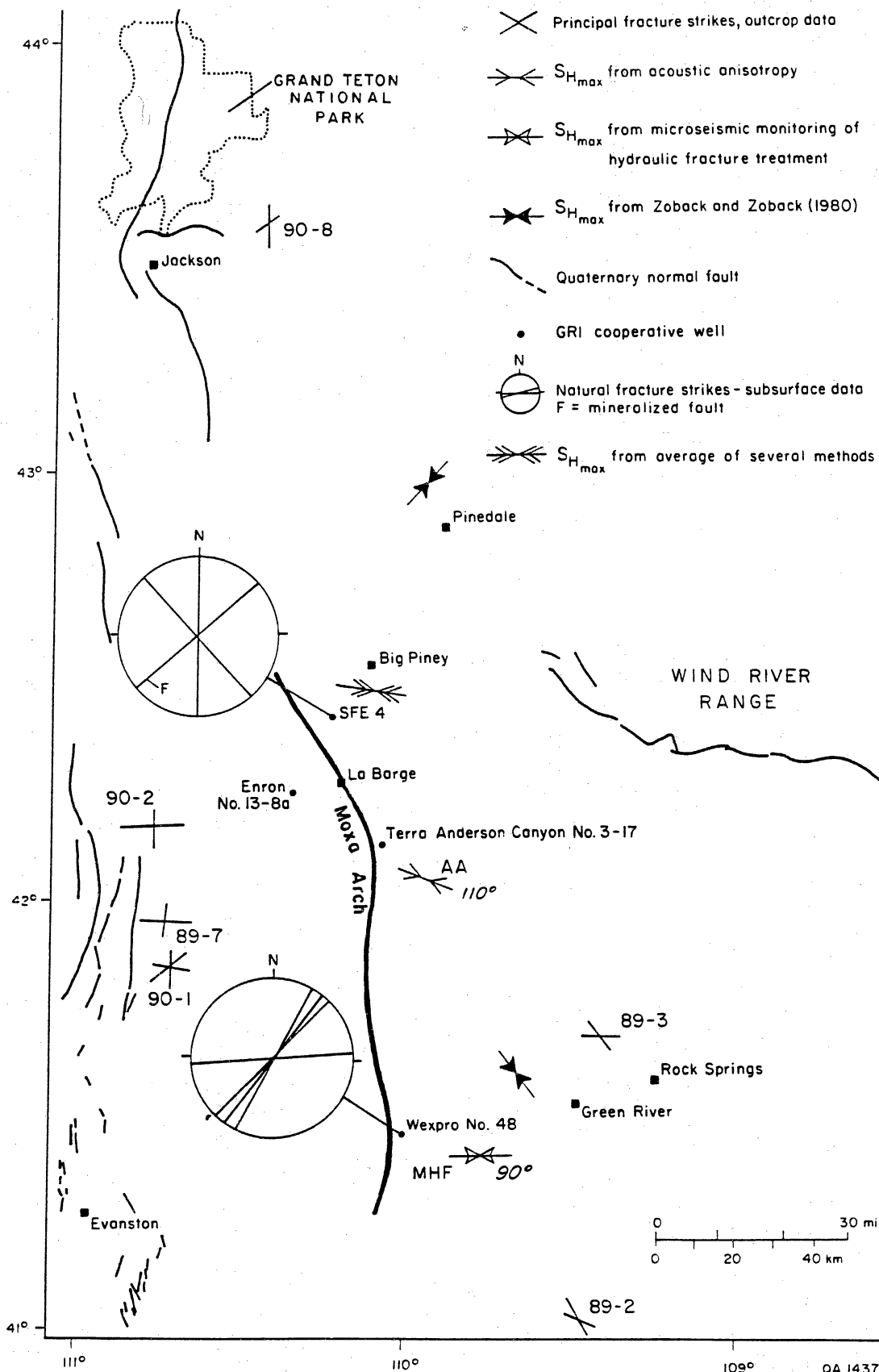


Figure 54. Map showing stress directions detected in GRI Tight Gas Sands wells in the Green River Basin, published stress direction determinations, and young fault scarps (reflecting current tectonic deformation). Natural fracture strikes in Frontier Formation core and selected outcrops are also shown. Inward-pointing arrows indicate the direction of  $S_{H_{max}}$ . Locations of young normal faults from Case (1986).

fractures in SFE No. 4-24 core strike northwest, north, and northeast. These results show that in the Frontier Formation, fractures having east, northeast, and north strikes locally occur in the subsurface, indicating that multiple fracture sets may exist. These results need to be viewed with caution, however. In addition to the uncertainty associated with the small number of samples and core orientation results, outcrop data show that even in local areas, fractures in a set may not have uniform strike (fracture-strike dispersion can be large). Moreover, it is unlikely that regional fractures have constant orientation throughout the basin, and the wells we sampled are widely separated.

Borehole-imaging geophysical logs provide limited additional information on fracture strike because few fractures were imaged, and of these, most images were of single traces of vertical fractures and so cannot be uniquely oriented (Laubach and others, 1990a). Formation Microscanner observations in SFE No. 4-24 predominantly sampled the northeast and southwest and northwest and southeast faces of the borehole wall, although few fracture traces are visible in these quadrants. If fractures striking in the direction of these quadrants are more likely to be visible because they intersect the borehole wall at a high angle in these quadrants, then this observation suggests that fractures striking in these directions are uncommon in the borehole wall. Features interpretable as fractures are locally visible in parts of the borehole where fractures that have north and east strikes would intersect the borehole at a high angle. This is consistent but far from compelling evidence that natural fractures have predominantly north and east strikes.

Evidence from axial point-load tests shows that sandstones in SFE No. 4-24 have tensile strength anisotropy (Clift and others, in press). Preliminary petrographic evidence suggests that this anisotropy results from aligned microfractures. In the Cretaceous Travis Peak Formation of East Texas, similar microfractures parallel macrofractures, and microfracture orientations are useful guides to orientations of large fractures (Laubach, 1989b). In SFE No. 4-24, the trend of strength anisotropy shifts from northward to eastward in adjacent sandstone beds. If microfractures and macrofracture orientation are the same, then these results suggest that

north- and east-striking macrofractures exist in the subsurface at the site of SFE No. 4-24, and fracture strikes shift over short distances between adjacent beds.

### Natural Fractures in Outcrop

Fracture patterns in outcrops of producing units are guides to patterns in reservoirs because many fractures in outcrop have counterparts in the subsurface. Maps of outcrops that show fracture traces portray fracture-network characteristics such as spatial distribution, spacing, connectivity, trace length, and fracture-bounded-block size and shape in a way that measurements of core cannot. Restrictions of this approach are threefold: (1) fractures caused by surficial processes in outcrops need to be recognized and discounted; (2) similar fracture-causing processes, such as folding or mild, pervasive regional deformation of flat-lying rocks, should predominate in reservoir rock and outcrop analog; and finally, (3) such maps at best provide insight into patterns that can occur in buried reservoir rocks, rather than showing actual fracture locations in the subsurface.

Fracture patterns in Frontier sandstone outcrops were mapped on aerial photographs and topographic base maps. Fractures are represented on these maps as a two-dimensional array of thin line segments. Locations of individual fractures were surveyed using plane table and electronic distance-measuring devices. Fracture descriptions are based on petrographic observations, large-scale outcrop descriptions, scanline measurements, and field maps at scales of 1:50, 1:100, 1:300, and 1:12,000. Fracture attributes in map areas were compared to regional fracture patterns observed during basinwide reconnaissance.

### Setting of Frontier Formation Exposures

The Frontier Formation is exposed on the east, south, and west sides of the Green River Basin. Fractures in basin-margin rocks could differ from those at depth in the basin because rocks on the basin margins have had a structural history separate from those in basin centers;



rocks on the basin margins are in folds and near fault zones rather than in nearly flat-lying homoclines. Nevertheless, these rocks may preserve fractures that are representative of the basin interior. The style, orientation, and distribution of fractures in the outcrops we studied led us to conclude that many, if not most, of the fractures in Frontier Formation on the west side of the Green River Basin predate folding and formed in rocks that were nearly flat lying and therefore valid guides of subsurface fractures. Other attributes of the Frontier Formation in the exposures we mapped, such as unit thickness, depositional environments, and aspects of the burial history, are similar to those of Frontier reservoirs in the basin to the east.

Frontier Formation exposures on the west side of the Green River Basin are in the limbs of north-trending folds (fig. 55). The folds were produced by fault-bend folding and other processes related to fault movement in the overthrust belt, and rocks in these folds have been displaced to the east relative to their original site of deposition. Many exposures we studied are in an open, angular-hinged syncline above the Darby thrust and close to the edge of the thrust belt. The evolution of this structure is described by Delphia and Bombolakis (1988).

#### Dominant Fracture Directions

Sets of fractures having north and east to east-northeast strikes are dominant in Frontier Formation sandstone outcrops near Kemmerer, Wyoming. Northeast-striking fractures are dominant in a few outcrops. Fractures having an easterly strike are younger; they cut across or abut north-striking fractures where the two sets occur together (fig. 56). The age of northeast-striking fractures is unestablished, but locally fractures that have this orientation are younger than east-striking fractures.

In many beds, only one set of fractures is well developed (fig. 57). In some beds, only one set is present (fig. 58). Adjacent beds commonly contain only one or the other of the dominant sets. The presence of a given fracture set is therefore unrelated to structural position. No obvious correlation is evident between rock type and fracture direction. Studies in progress suggest that subtle differences may exist in the original composition or diagenesis of beds

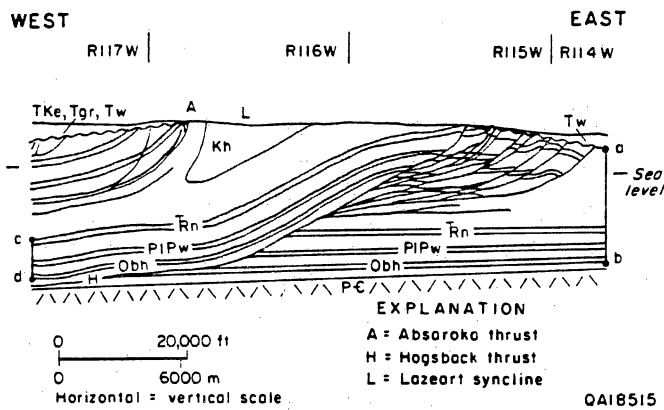


Figure 55. Balanced cross section of the Absaroka and Hogsback thrust sheets, north of Kemmerer in T23N, Lincoln County, Wyoming. From Delphia and Bombolakis (1988). Pc, Precambrian Crystalline Complex; Obh, Bighorn Dolomite; PIPw, Weber Sandstone; Rn, Nugget Sandstone; Kh, Hilliard Formation; Tw, Wasatch Formation. Lazeart Syncline is marked by a solid-line curve drawn along the contact between the Frontier Formation and overlying Hilliard sequence (Kh). Both a-b and c-d are pin lines for palinspastic restorations (see original reference). SL is sea-level reference elevation.

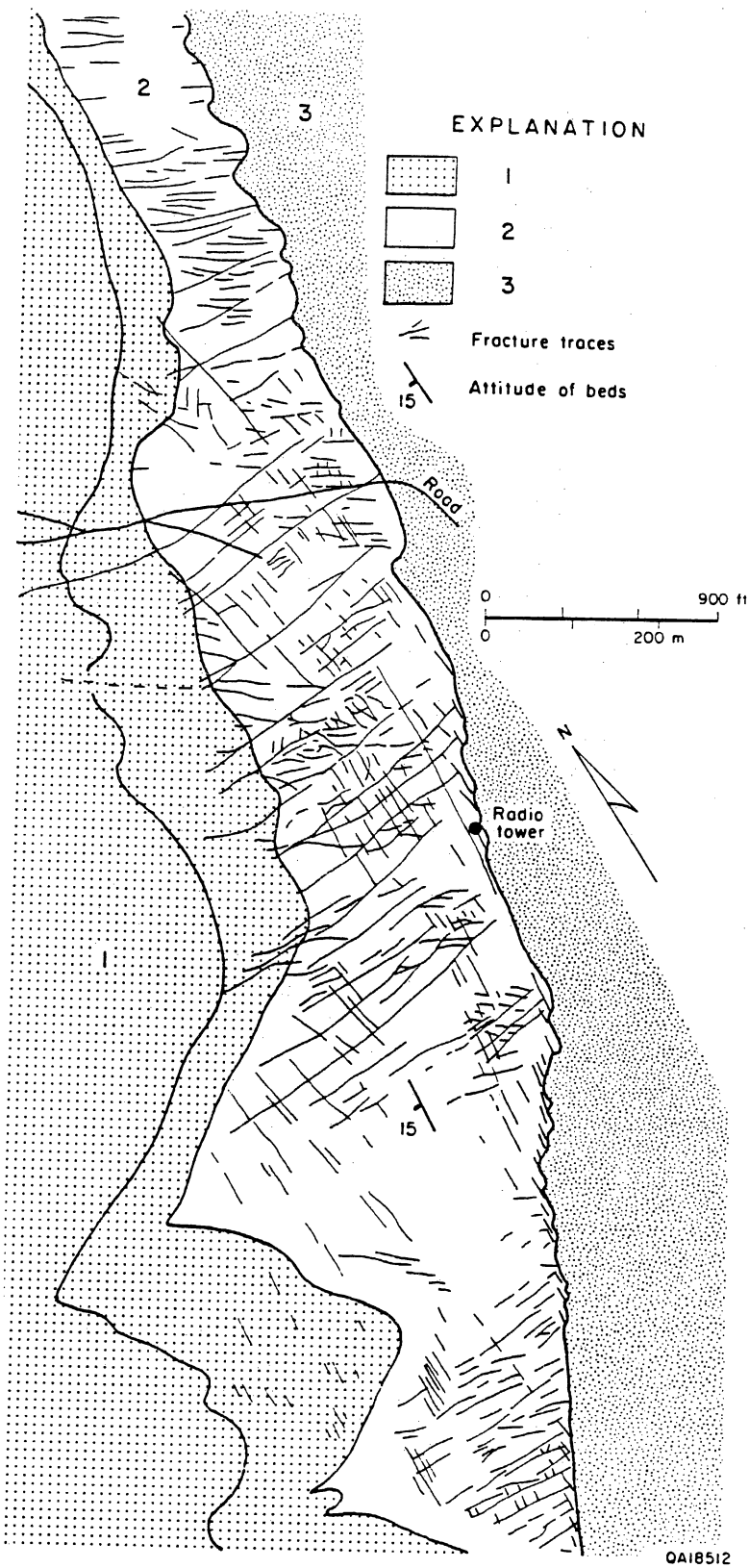


Figure 56. Map showing traces of vertical fractures on Frontier Formation sandstone bedding plane, illustrating abutting and crossing relations. Exposure near Radio Tower (T21N, R115W), east of Kemmerer, Wyoming.

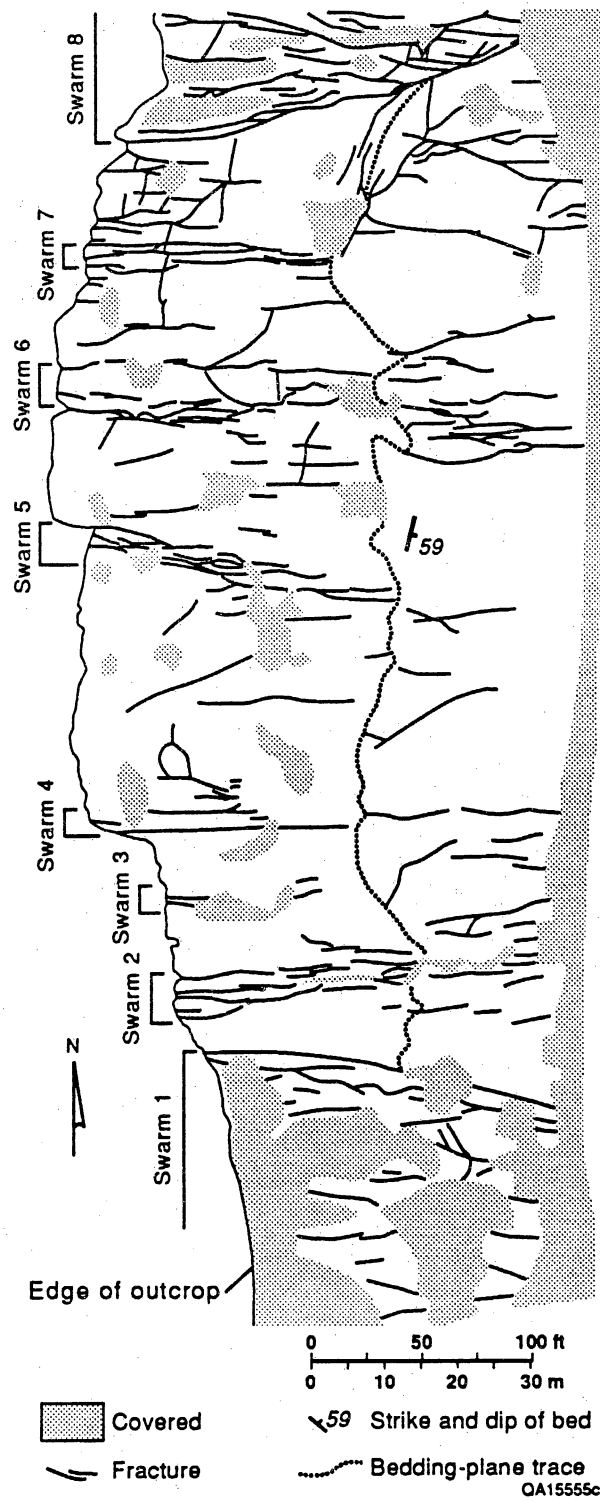


Figure 57. Map showing traces of dominantly east-striking vertical fractures on east-dipping sandstone bedding plane, Frontier Formation, north of Kemmerer, Wyoming (Commissary Ridge; T24N, R116W).

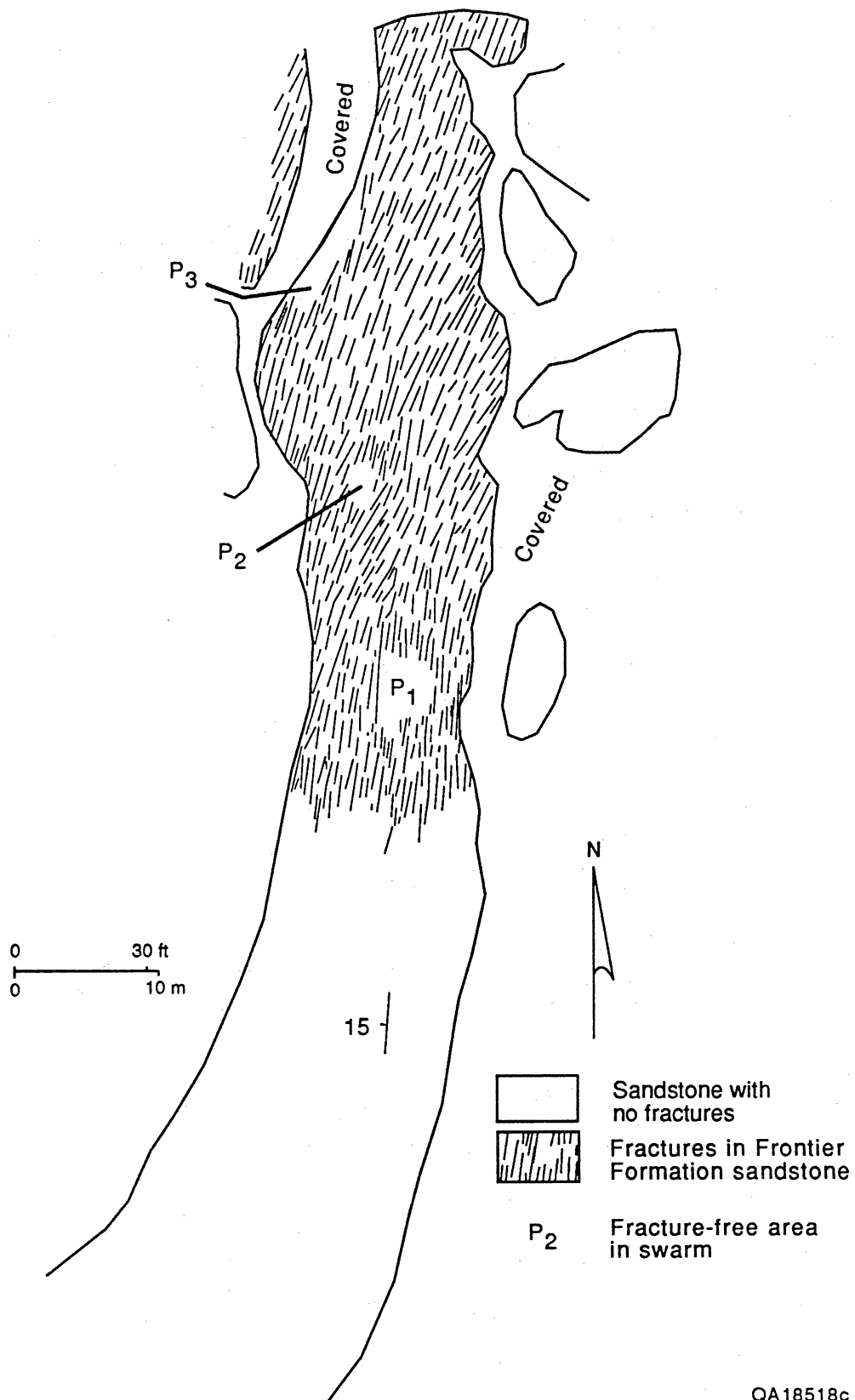


Figure 58. Schematic map showing traces of dominantly north-striking vertical fractures on sandstone bedding plane, Frontier Formation, north of Kemmerer, Wyoming (Sec. 36, T23N, R116W). Note fracture "front" where fracture abundance abruptly changes.

having different prominent fracture directions. Diagenetic contrasts could change the rock's strength and therefore affect its propensity to fracture (Laubach and others, 1989).

In this report we have not attempted to describe all of the fracture patterns visible in Frontier Formation outcrops around the margin of the Green River Basin. Some of these fracture patterns appear to be associated with specific folds and faults on the south, east, and north margins of the basin. As will be discussed in more detail, we sought fracture exposures having the least amount of structural overprint related to basin-margin faults and folds.

### Style of Fracture Sets

Fractures are perpendicular to beds. Joints and the veins we mapped are extension fractures that show no evidence of shear offset. Locally, fractures have visible surface marks, crack-seal microstructures, and wall-rock inclusions that indicate an origin by opening mode (Mode I) growth. Where surficial leaching of fracture fill has not occurred, fractures are typically filled with fibrous, blocky, or euhedral calcite.

The relative age of fractures is determined using cross cutting and abutting relations among fractures. North-striking fractures are common in many Frontier Formation outcrops, but they rarely occur in the same beds as have east- to northeast-striking fractures. Where they occur together, east-striking fractures abut or cross north-striking fractures (fig. 56), indicating that north-striking fractures are older. The older north-striking fractures and younger east-striking fractures differ in style of occurrence.

In outcrop, north-striking fractures are locally closely spaced (4 inches to 3 ft [10 cm to 1 m]), with small dispersion in strike (fig. 58). Planar, they have abundant infilling calcite, and commonly no visible aperture. For thin beds at least, fracture spacing is similar to (and generally less than) bed thickness. In contrast, east-striking fractures have highly variable spacing, and locally spacing is wide. These fractures have wide dispersion in strike, and locally are strongly curved. An example of east-striking fractures is shown in figure 57. The sandstone is nearly 15 ft (4.6 m) thick, and it dips eastward about 60° (fig. 57). It is bounded above and below by

siltstone and muddy sandstone. Fracture traces are clustered in north and south parts of the outcrop. Fractures generally strike east, but strike varies by more than 40° (fig. 59). Many of the longest fractures are curved.

#### Fracture Dimensions

Fractures commonly end vertically at subtle changes in sandstone rock type or at mudstone interbeds, so they are generally confined to individual sandstone beds and their height is equal to or less than bed thickness. In plan view, the longest fractures observed in outcrop are on the order of hundreds to thousands of meters in length (fig. 56), with length to height ratios greater than 10:1. Fractures have a range of lengths (fig. 57). In one example, fracture-trace lengths range from inches to more than 125 ft (38 m) (fig. 59). For fractures more than 3 ft (1 m) long, mean fracture length is 23 ft (7 m). Such fractures are composed of long, planar segments that are colinear, but that step to the right or left in an echelon or relay patterns. In plan view, where fracture strands overlap, overlapping segments are straight, with little tendency to hook toward or away from one another. Typically a large number of short fractures are in a given map area (fig. 60).

East-striking fractures range in width from fractions of a millimeter to several centimeters. North-striking fractures are typically narrower, but the range of widths overlaps and some of the widest fractures strike north. North-striking fractures are commonly partly filled with calcite and, locally, subsidiary minor quartz and clay minerals. Both calcite and quartz locally have euhedral crystal faces that suggest they grew into open cavities. Vein calcite from outcrops is variably twinned and fractured, and north-striking fractures locally have stylolitic seams subparallel to vein walls.

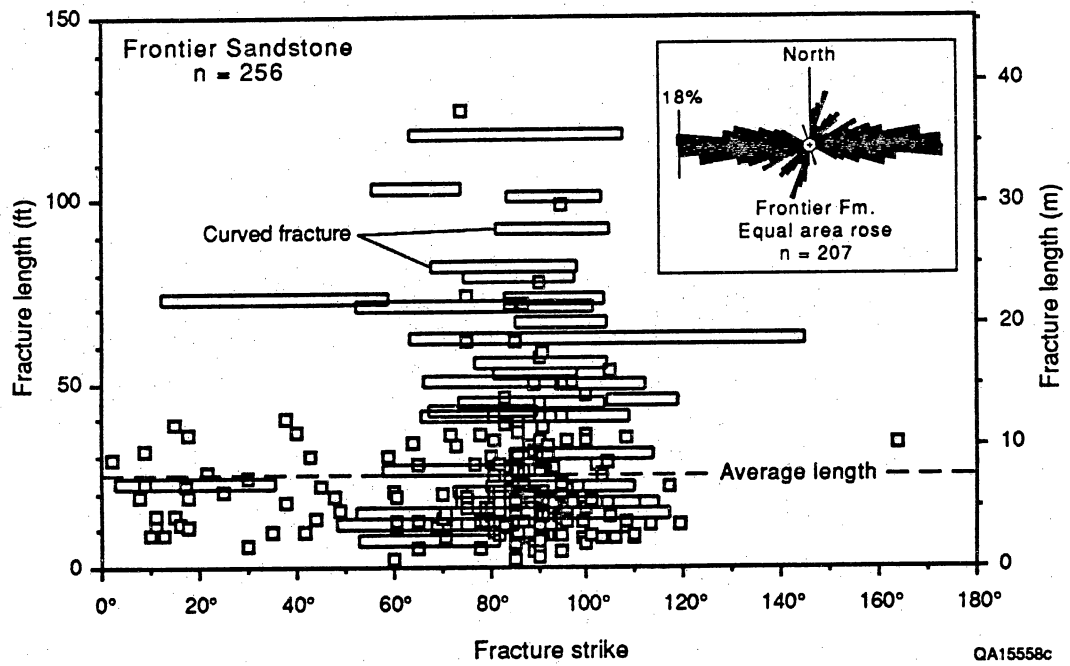


Figure 59. Fracture strike versus fracture length, Frontier Formation sandstone. Open boxes show range of strike of curved fractures. Inset shows rose diagram of fracture strikes. Data from outcrop depicted in figure 57.



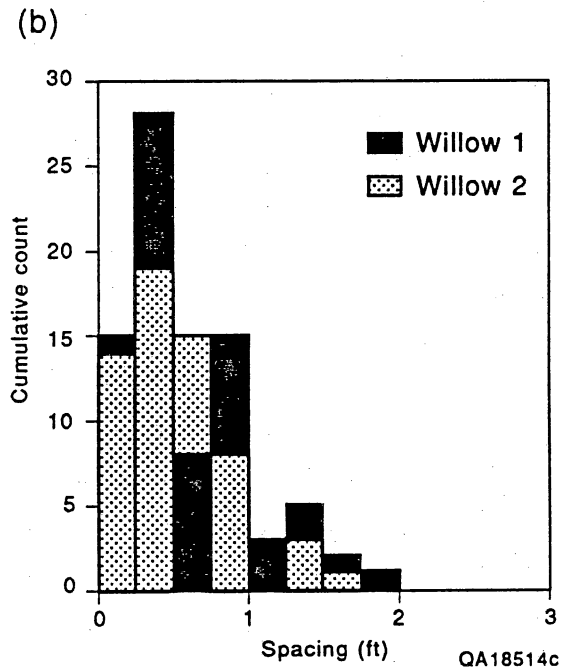
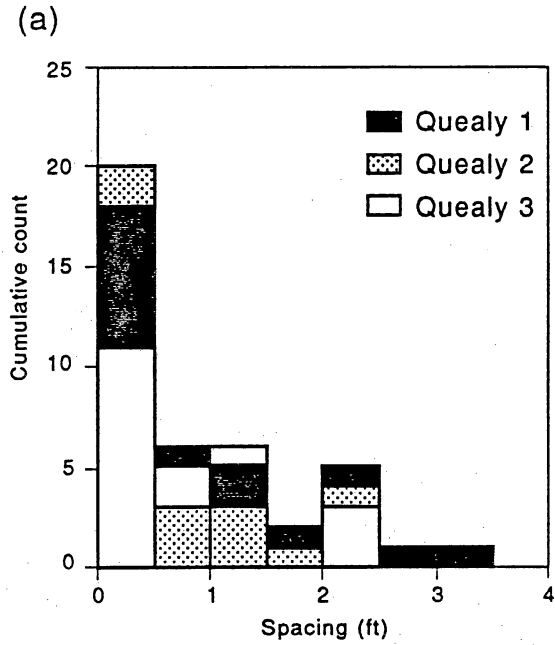


Figure 60. Histogram of fracture spacing in Frontier Formation outcrops, north of Kemmerer, Wyoming. (a) Northeast-striking fractures, Quealy Peak outcrop (28-91), Sec. 31, T22N, R115W. (b) East-northeast-striking fractures, Willow Creek outcrop (29-91), Sec. 12, T22N, R116W.

## Fracture Spacing

Fracture spacing ranges from inches to tens of feet. Spacing between fractures is commonly not uniform. Instead, clustering of fractures into swarms is evident at several scales, and typically fracture spacing ranges widely in a given bed (figs. 60 and 61). Swarms are defined by areas of close fracture spacing (figs. 57 and 61). Scanlines from north-striking fractures show clustering, but overall fracture spacing is much closer than that of east-striking fractures (figs. 62 and 63). Contrasts in fracture density between swarm and interswarm areas are most pronounced for east-striking fractures.

We mapped one area where spacing of large east-striking swarms is about 400 to 500 ft (120 to 150 m), but generally swarm separations are not uniform. Small swarms in this area are separated by rock without fractures, but between map-scale swarms, numerous fractures and small swarms are present. Many isolated fractures are fairly evenly spaced. Swarm widths range from 2 inches (5 cm) to more than 160 ft (50 m). Narrow swarms, having widths of 30 ft (10 m) or less, consist of 3 to more than 10 fractures. The widest swarms in this example are 65 ft (20 m) and 145 ft (45 m) (swarms 1 and 8, fig. 57). Fracture spacing within these swarms also shows clustering and ranges from less than 1 inch (2.5 cm) to 15 ft (5 m). Spacing cannot be delineated accurately in wide swarms because of preferential erosion along fractures, but short trace-length fractures are more prevalent and fracture intensity is at least 2 to 3 times greater than in adjacent areas.

Because bed thickness is nearly constant but fracture spacing varies, the systematic increase in fracture spacing with greater bed thickness (Ladeira and Price, 1981) that occurs in some sandstones is not evident for sandstones thicker than about 6 ft (2 m). On the other hand, for some thin beds, fractures are generally slightly more closely spaced than bed thickness, and spacing increases for thicker beds. The relationship holds for beds of as much as about 3 ft (1 m) in thickness. Locally, fracture spacing decreases near the edges of lenticular sandstones as beds thin.

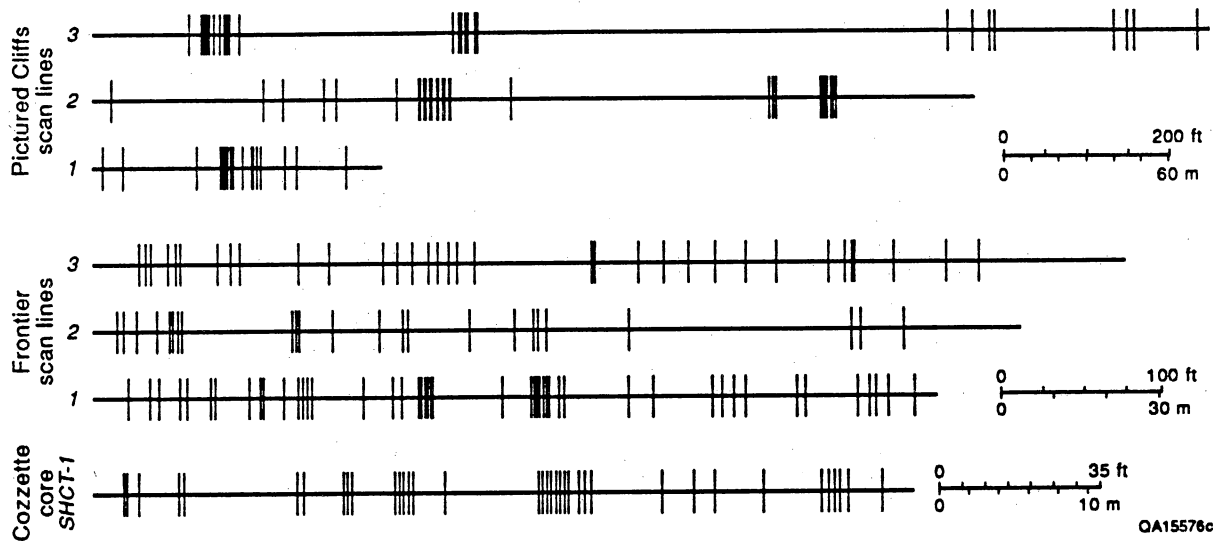


Figure 61. Fractures in outcrop traverses (scan lines) in Frontier Formation and in Cretaceous Pictured Cliffs Sandstone (San Juan Basin, New Mexico and Colorado) and horizontal core from Cretaceous Cozzette Sandstone, Piceance Basin, Colorado. Scan lines show fractures that would be encountered in a horizontal borehole across the outcrop. Clustering is less apparent on some Frontier scan lines than in examples from the other units because small, isolated fractures are not distinguished from large fractures on the scanlines. From Laubach, 1991.

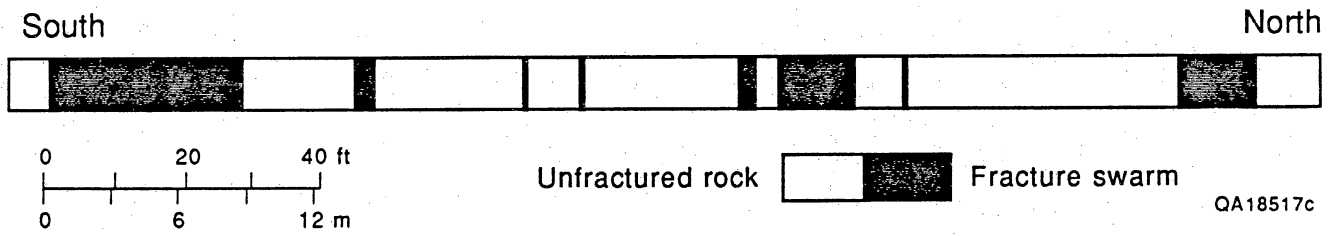


Figure 62. Fracture swarms in outcrop traverse (scan line), Frontier Formation, from near Coalville, Wyoming. Scan lines show fractures encountered in a north-south traverse across the outcrop.

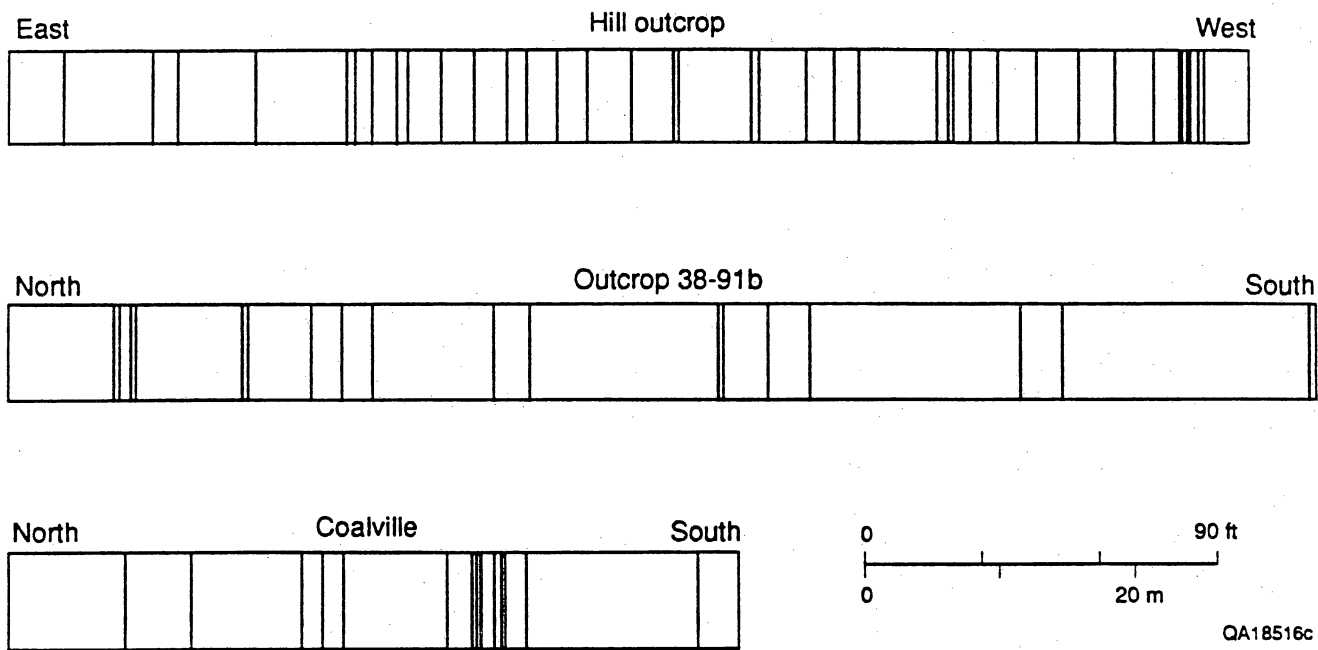


Figure 63. Fractures in outcrop traverses (scan lines), Frontier Formation, from various locations north of Kemmerer, Wyoming. Scan lines show fractures encountered in traverses across the outcrops. "Hill" outcrop (41-91a) and outcrop 38-91b are on east limb of Lazeart Syncline, north of Windy Gap.

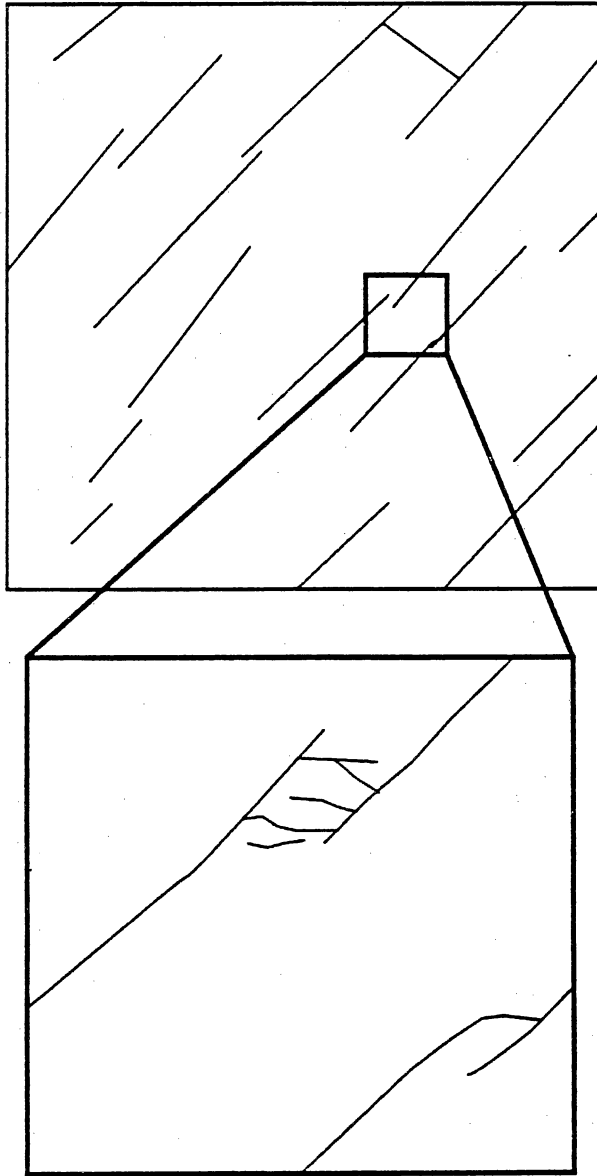
## Fracture Patterns

Fracture patterns in the Frontier Formation are apparent in simplified maps that show traces of nearly vertical fractures on sandstone bedding planes (figs. 56, 57, and 58). Many beds have a single, uniformly oriented fracture set, but some beds have multiple fracture directions, and fractures intersect at high angles. Where only one set is present, fracture patterns range from relatively uniformly spaced to highly clustered. Scanlines across outcrops show the various scales of clustering evident in Frontier Formation outcrops. Many clusters or swarms of fractures have linear or lens-shaped outlines in plan view (fig. 57), but some are in more irregular, patchlike or subcircular distributions (fig. 58).

Because fractures formed perpendicular to paleohorizontal and are aligned at right angles to beds (mapped surfaces), overall trace arrangement represents three-dimensional patterns, but details may vary with depth within a given sandstone layer. For instance, fractures that intersect in the plane of the map may not intersect at depth and vice versa. Moreover, because fractures are not equant and those having short traces in plan view may have limited vertical extent, the number of short fractures in a given volume of sandstone is likely to be underrepresented on any given mappable horizon.

Maps presented here have been simplified from field maps because of space limitations. Map scale dictates the size of fracture that can be shown because at every map scale a fracture is too small to conveniently depict. Thus, some fractures that are shown as a single line may actually be composed of several strands, and two adjacent fractures that appear isolated from one another at one scale may actually be connected by arrays of smaller fractures that would be visible on larger-scale maps. The size of the mapped area can influence the appearance of fracture patterns because parts of patterns may be unrepresentative of the whole. An example of a feature that would be missed if maps are at too small a scale is a constricted termination (fig. 64), where small fractures connect large fractures.

The patterns represented in these outcrops are of a scale that is relevant to gas production. Bedding-plane exposures have areas ranging from hundreds to thousands of square



Scale arbitrary

QA18520c

Figure 64. Map illustrating definition of constricted fracture terminations. Fractures with a range of sizes make up fracture networks, and small fractures that interconnect larger fractures may play an important role in how networks transmit fluid.

meters and are therefore as wide as the extent of the longest fractures created in hydraulic fracture treatments, typical horizontal reaches of directionally drilled wellbores (~2,000 ft [-600 m]), or interwell distances in oil and gas fields having 160-acre vertical well spacing.

### Fracture Networks and Connectivity

Isolated fractures can have little impact on flow properties of a fracture system. A basic control on fracture-network flow properties is the degree of interconnection among fractures (Long and Witherspoon, 1985; Long and Billaux, 1987; Barton and Hsieh, 1989). In a fracture-trace-map study, connectivity can be assessed by cataloging numbers of intersection types. Dead-end, connected, and constricted intersections are three common fracture-intersection types in these networks. Dead-end terminations are those in which fractures end without touching another fracture. Connected fractures intersect by abutting, crossing, or contacting tangentially. Constricted intersections are those in which narrow, constricted fracture segments or microfractures connect adjacent fractures (fig. 64). The latter is really a type of connection in the fracture network but one that may represent a constriction to fluid flow. Definition of the last intersection type depends in part on the scale at which fractures are shown. Constricted intersections exist where mapped fractures are linked by visible fractures that are too small to represent at map scale (on our maps those having trace lengths less than 3 ft [1 m]). Connectedness is assessed from measurements on large-scale field maps and is represented on a triangular graph that shows ratios of connected, constricted, and dead-end termination types (fig. 65).

Some fracture networks in the Frontier Formation have an orthogonal pattern that assures numerous abutting or crossing intersections (fig. 56). In contrast, the connectivity of many Frontier fracture networks is low (figs. 57 and 58). Few abutting or crosscutting fractures occur within swarms; most connections are at low-angle intersections and through microfracture arrays where strands overlap (constricted connections). Such intersections tend to connect fractures parallel to swarm length but not across swarm width, so some sections of swarms may be partly



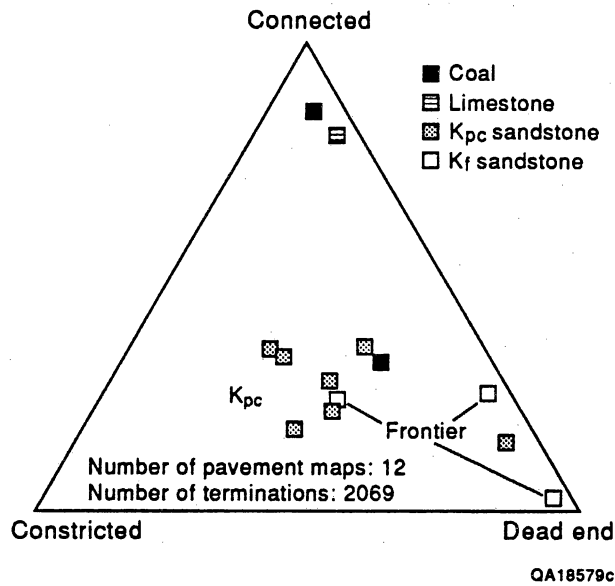


Figure 65. Proportions of fracture-termination types in representative Frontier sandstone outcrop. Shown for comparison are examples of Pictured Cliffs Sandstone (K<sub>pc</sub>), coal (Cretaceous Fruitland Formation, San Juan Basin, Colorado) and limestone (Cretaceous Austin Chalk, Balcones Fault Zone, Texas) (Collins and others, 1990; Laubach and others, 1991a). See text for discussion.

or completely isolated from others. Moreover, fractures tend to end vertically at bedding planes, so swarm height is typically limited by sandstone thickness or by spacing of interbeds. Thus, fracture arrays are confined to specific beds rather than being continuous or well interconnected vertically. More important, swarms also are isolated laterally within sandstones having uniform composition. This partitioning of the fracture network implies that sandstones have compartments of differing fracture permeability.

In some exposures connectivity may vary drastically for fracture networks of the same set, where rock type, bed thickness, depositional environment, and structural setting are similar. For example, schematic maps of two pavement exposures of north-striking fractures show non-interconnected and partly interconnected fracture networks (fig. 66). The cause of such differences is currently unknown.

Degree of along-strike connectivity in Frontier fracture networks where fractures dominantly strike eastwards differs from networks in the Cretaceous Pictured Cliffs Sandstone, a low-permeability sandstone gas reservoir rock exposed on the margins of the San Juan Basin in Colorado and New Mexico (Laubach, 1991; in press). Adjacent segments of Frontier fractures tend to be straight, with few curving, intersecting tips or small cross fractures. As a result, along-strike connectivity in Frontier networks is low. About half the fractures that occur between major swarms do not intersect other fractures and are therefore isolated from the fracture network. Fracture segments in the Pictured Cliffs, on the other hand, are commonly strongly curved, with fractures hooking toward one another where they overlap, causing greater connectivity parallel to the strike of the fracture swarm. If fractures are all open-fluid conduits, such differences would affect the size of areas drained by fractures.

### Scaling Attributes and Clustering

Fracture patterns that maintain the same characteristics at a wide variety of scales are said to be self-similar. A qualitative sign of scale invariance in Frontier fracture patterns is their similar appearance when viewed at different magnifications. Aspects of this include a tendency

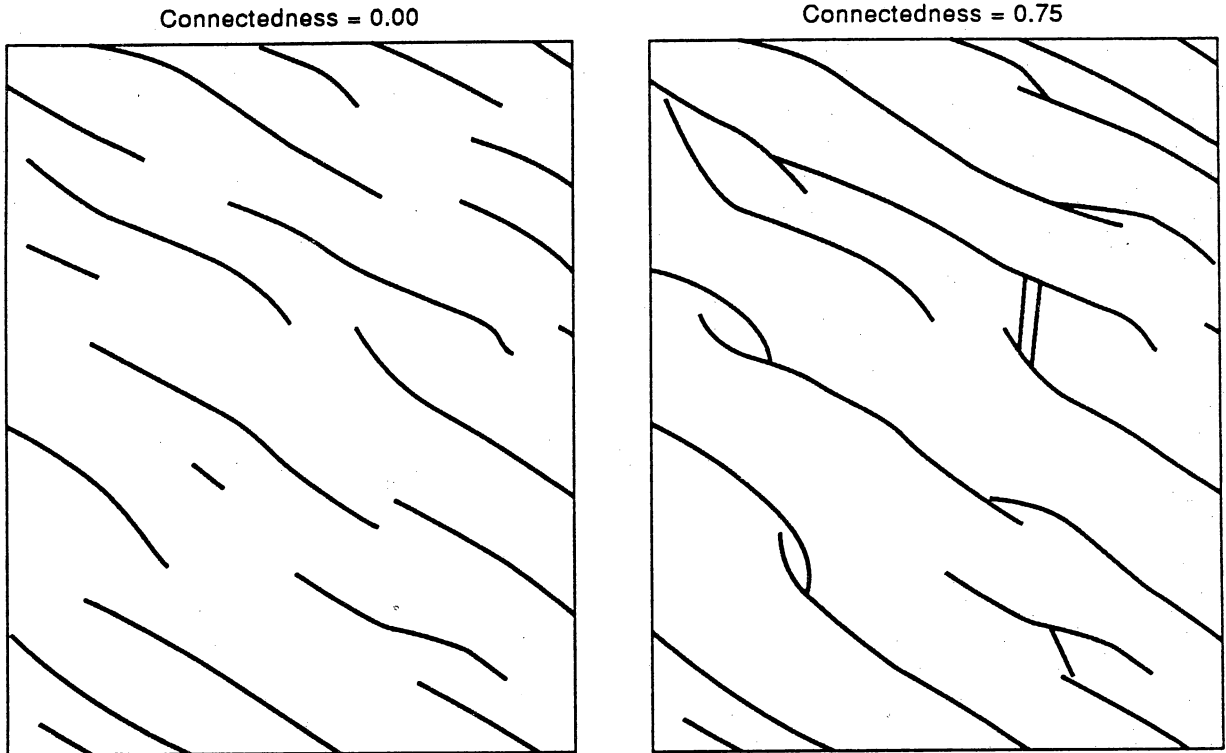


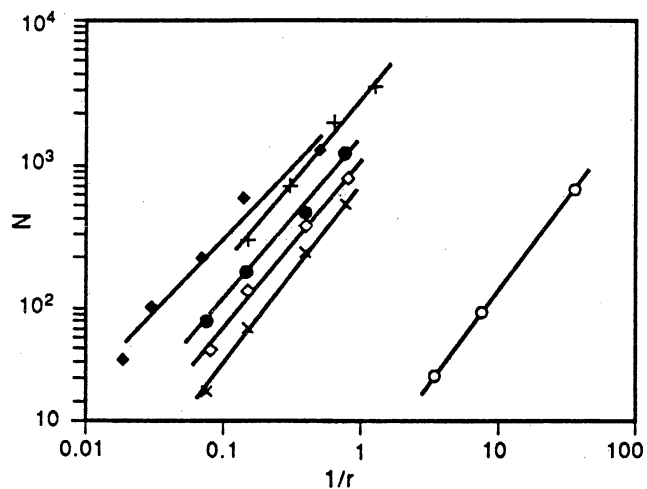
Figure 66. Schematic maps of fracture traces, Frontier Formation sandstone, showing contrasting fracture-network connectivity (based on outcrops northeast and southeast of Kemmerer, Wyoming). Connectedness is the ratio of connected and constricted fracture to dead-end terminations, as measured on large-scale field maps or as calculated by counting termination types in the outcrop.

for fractures to cluster in swarms having nearly parallel strikes and for subsidiary fractures to have similar patterns over a wide range of scales.

Quantifying characteristic ways that fracture traces fill space improves fracture network description and can help model fluid flow in such systems. Fractal geometry is useful for quantifying scaling properties of intricate patterns, including fracture traces (Barton and Larsen, 1985; LaPointe, 1988). Such information is being incorporated increasingly in fractured-reservoir models because researchers realize that flow processes in fractal fracture systems are likely to be substantially different from those in nonfractal fracture networks (Adler, 1989). Reservoir simulations using a fractal network of fractures may provide useful predictions of hydrocarbon reservoir production characteristics (Matthews and others, 1989). Information on characteristic scaling properties of fracture systems may be useful for extrapolating outcrop observations of fractures to subsurface exploration and development (LaPointe, 1988); eventually, this approach could help define optimal horizontal well spacing and length needed to tap fracture networks efficiently. Fractal properties can also be used as an objective standard of comparison between fracture patterns.

Fractal dimension (D) characterizes the tendency of fracture trace patterns to fill space. For lines on a two-dimensional surface, D can range between 1.0 (a line) and 2.0 (filled space). We used the box method to estimate fractal dimensions of Frontier fracture networks (Barton and Larsen, 1985; LaPointe, 1988). This method involves successively placing grids of square elements of side-length  $r$  over a map and counting the number of grid elements (N) containing a fracture trace. A fractal distribution of lines on a map is defined by  $D = \log N / \log (1/r)$ , where D (fractal dimension) is the slope of the best-fit line on a log-log plot. Box sizes in this study range from 0.1 inch (0.29 cm) to 167 ft (51 m), which is an indication of the range of scales studied.

Results are shown in figure 67. The observed smooth lines on the fractal plots indicate a power law relationship and imply that the fracture pattern is in some sense scale invariant over the range of scales studied. Although a larger range of box-size increments would have been



EXPLANATION

- + F100-103
- ◆ P001-005
- P011-014
- × P021-024
- ◇ P031-034
- P041-043

QA17505c

Figure 67. Graph showing number of counting elements containing fracture traces (N) versus inverse of length of counting element sides (r) for Frontier (F) and Pictured Cliffs (P) maps. Slope of each plot (line) is the fractal dimension D. F100-103 are data from Frontier Formation map shown in figure 57.

preferred for this type of analysis, the slopes determined using a few boxes are linear on the plot of  $\log N/\log (1/r)$ . Similar slopes were obtained for Frontier maps and examples from the Cretaceous Pictured Cliffs Sandstone of the San Juan Basin (Laubach, in press). For seven maps, fractal dimension  $D$  ranges between 1.1 and 1.4 and averages 1.29 (fig. 67). For maps of the best exposed Frontier outcrop,  $D$  is  $\sim 1.2$  ( $r^2 = 0.99$ ), reflecting the clustered nature of the fracture distribution.

This result is evidence that fractal concepts are a valid approach to describing some attributes, such as aspects of fracture density distribution, in low-permeability sandstones. The fractal dimensions of fracture patterns obtained in this study are similar to those of Merceron and Velde (1991) but lower than those of Barton and others (1987) for fracture networks in rocks.

### Fracture Origins

Knowledge of fracture origins is important because it can be used to predict fracture strike and the location of highly fractured areas. Because a variety of loading paths could, in principle, lead to development of fractures, specifying fracture origins can be challenging. Evidence for the timing of fracturing is critical for interpreting fracture origins. We conclude that the oldest fractures in the Frontier Formation in outcrop, and probably in the subsurface, strike north and likely result from lateral stresses associated with subsidence of the north-trending Cretaceous foredeep. The orientation of east- and northeast-striking fractures may reflect east-west shortening during Cretaceous/early Tertiary orogenesis.

### Timing and Style of Fracturing

On the west side of the Green River Basin, most fractures in Frontier Formation sandstone are joints and veins (extension fractures) that are normal to bedding. Such fractures probably form under conditions of high pore fluid pressures and low differential stress. Of the two most

prominent fracture sets in outcrops on the west margin of the basin, north-striking fractures formed first and were either held shut by lateral compression or were cemented when east-striking fractures grew. Plume axes on fracture faces (where visible) are parallel to bedding (paleohorizontal). These observations suggest that the direction of extension (minimum principal stress axis) and the axis of maximum compressive stress were horizontal during fracture initiation but that through time the extension direction switched by 90°. Fracture style is similar to that of fractures found in core from within the basin. Abutting relations show that north-striking fractures formed before east-striking fractures. The sequence of vein-filling minerals in unoriented fractures in core suggests that at least some fractures formed early in the rock's burial history, during precipitation of calcite cement, after an early phase of quartz cementation, and before feldspar dissolution. Fibrous crystals and crack-seal structures in some north-striking fractures in outcrop show that they grew during east-west extension. Stylolites in these veins show that this east-west extension was followed by east-west shortening and development of vertical stylolites.

Stretching during basin subsidence can account for north-striking fractures. These fractures parallel the depositional axis of the Cretaceous foredeep, and preliminary petrogenetic evidence suggests that vein-filling minerals in north-striking fractures may be contemporaneous with early Frontier Formation cements. Simple geometric considerations, summarized by Laubach and Lorenz (in press), show that stretching (and fracturing) associated with subsidence is plausible. Isopachs in the western Green River Basin area show that more than 18,000 ft (5,486 m) of Upper Cretaceous strata were laid down in a basin that was only 40 mi (64 km) from edge to depocenter (Weimer, 1961; Monley, 1971). As the basin subsided, strata were stretched in the east-west direction due to lengthening parallel to bedding as the original, nearly flat depositional surface adjusted to conform to the asymmetric basin margin. This implies that older and more deeply buried strata may be more highly fractured because they have been subjected to the greatest stretching. This process also could have affected rocks deposited on the Moxa Arch.

The lengthening of strata during east-to-west extension, burial, and subsidence can produce significant east-west stretching (Laubach and Lorenz, in press). A critical strain of about 0.3 percent and a stress of nearly 435 psi (3 MPa) are necessary to fracture similar sandstones under laboratory conditions. However, under geologic conditions (slow strain rates, elevated temperatures, fracture growth assisted by chemical reaction, etc.), strata will fracture at lower stress levels especially if pore pressures are high. Burial rates of at least 650 ft/my (200 m/my) were common for the thickened strata in this basin, and elevated pore pressures were probably widespread.

Laubach and Lorenz (in press) calculated an east-west stretch of just more than 0.2 percent in Frontier strata as a result of subsidence by the end of Cretaceous time. An additional component of stretch caused by elastic flexure of the lithosphere by the weight of the overriding thrust plates can be calculated to be about 0.06 percent, assuming a conservative amount of flexure. Thus, total stretch because of these processes could have been at least 0.26 percent, or nearly the amount of strain needed to fracture samples in the laboratory. In the absence of other complications, this 0.26-percent stretch would probably be sufficient to have caused north-south fractures in the Frontier under geologic conditions. Although subsidence is a slow process, stress accumulation and intermittent rapid rupture could account for features such as plume structure on fracture surfaces, which may be due to abrupt fracture propagation. Regional extension at shallow depths in sedimentary basins such as the East Texas Basin can produce widespread open fractures in sandstone that parallel basin strike (Laubach, 1988, 1989a and b).

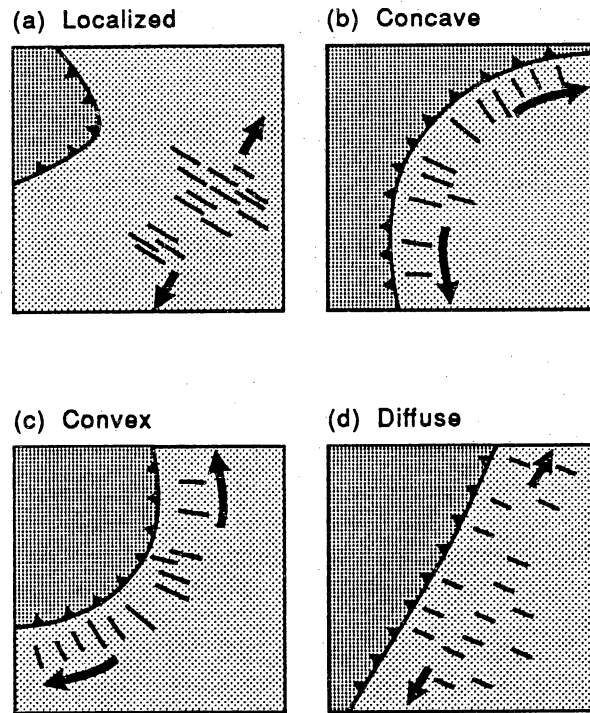
An alternative explanation for the north-striking fractures in outcrop is that they are b-c extension fractures produced by flexure at the hinges of large-scale folds. However, these fractures are not localized in fold hinges and do not increase in frequency in the exposed hinge of the Lazeart syncline near Fontenelle, Wyoming, and they predate vertical stylolites that mark east-west shortening. The fractures also strike 10° to 20° oblique to the fold axis and, except for variations that can be ascribed to folding of preexisting fractures, do not change






strike in sympathy with changes in fold-axis trend. Moreover, the fold has an abrupt, angular hinge, and limbs may be expected to have rotated with little internal deformation during folding. We therefore discount the possibility that flexure is a general explanation for this fracture set.

The Frontier Formation outcrops we studied are along the leading east edge of the Idaho-Wyoming thrust belt, and fracture sets likely developed when these rocks were in the foreland of the thrust belt. Fractures that accommodate lateral extension of forelands, even in flat-lying rocks far from a thrust front (>300 mi [ $>500$  km]), are a recognized mode of foreland deformation (Engelder and Geiser, 1980; Hancock and Bevan, 1987). Extensional structures that strike normal to thrust fronts in foreland areas have been ascribed to stretching at right angles to orogenic shortening directions (fig. 68) (Engelder, 1985; Hancock and Bevan, 1987; Laubach and others, 1991b; Lorenz and others, 1991).

Both north- and east-striking Frontier Formation fracture sets are normal to bedding where beds are tilted and are locally cross cut by fractures spatially associated with fold hinges and fault zones, implying that bed-normal fractures are older than local folds and faults. Similar joint sets in Jurassic and Cretaceous rocks are rotated about a vertical axis where the thrust belt is bent in the north salient of the overthrust belt near Jackson, Wyoming, implying fractures predated thrust development and were rotated along with the thrust sheet in which they occur (Craddock and others, 1988). Fractures of older, prefolding sets stop at thin shale partings, indicating low driving stresses for fracture growth, whereas younger fractures that are localized in fold hinges tend to cross interbeds. An illustration of this type of deformation on a large scale is the north-trending Rock Springs Uplift in the Green River Basin. Associated east- to northeast-striking normal faults mark concurrent east-west shortening and north-south extension, respectively. Syn-thrust movement on normal faults in the Green River Basin is consistent with extension parallel to the north- to northeast-trending long axis of the Rocky Mountain foreland area.



From Hancock and Bevan (1987)

-  Deformation front
-  Fractures
-  Regional extension direction

QA14859c

Figure 68. Map view of deformation fronts of various shapes and fracture strikes in adjacent foreland areas that may result from foreland lateral extension (modified from Hancock and Bevan, 1987). Lateral extension may result from stretching and crowding caused by salients and recesses in the orogenic front. (a) Convex front and localized extension. (b) Concave front and concave arc of extension. (c) Convex front and convex arc of extension. (d) Nearly rectilinear front and slightly convex arc of extension directions.

Stresses responsible for this deformation are likely transmitted by the ductile, stress-bearing section of the lithosphere. Episodic thrusting and foreland fracturing are both possible responses of the brittle carapace to flow of this underlying ductile substratum, and therefore movement of specific faults and foreland fracturing may not necessarily occur at exactly the same time. The precise timing of fracture formation may depend on the interplay of lateral and vertical loading history, the penetration of migrating fluids that serve to raise formation pore pressure, and diagenetic/compactional changes in rock physical properties that create brittle layers. In a foreland area, these processes are likely to be linked. Dutton and Hamlin (in press) charted the burial and diagenetic history of the Frontier Formation, and Wiltschko and Dorr (1983) summarized the timing of thrust events in the Idaho-Wyoming segment of the thrust belt.

We suggest that north-striking fractures formed early, during rapid subsidence associated with isostatic and flexural adjustment to nearby supracrustal thrust-sheet loads, and that east-striking fractures formed later, when compression related to mountain building was dominant. This compression would have tended to hold north-striking fractures closed. Moreover, east-west tectonic shortening associated with movements in the thrust belt probably tended to decrease the subsidence-related east-west component of stretching at some stratigraphic levels, while at the same time adding a component of north-south stretching. North-south crustal flow east of the Idaho-Wyoming segment of the thrust belt would have been amplified by stretching associated with the convex salient in the thrust belt at this latitude, accentuating the tendency to form fractures having generally eastward strikes.

The development of the Wind River and Uinta uplifts and Moxa Arch could have contributed to fracture formation by stretching and flexing strata, but their significance for regional fractures has yet to be evaluated. Of these, indentation of the basin by thrusts along the Uinta Mountain front may have been the most important ancillary factor in the formation of the north-striking fracture set (Laubach and Lorenz, in press). Major northward-directed, thick-skinned thrusting occurred during late Campanian to early Paleocene time (Hansen,

1965), concurrent with maximum stretching of the Frontier due to burial and flexure as described earlier.

In some exposures near thrusts or in tight fold hinges, fractures predominate that we interpret to be related to thrusts and folds. They are typically small faults. For example, in the Little Hogsback area north of Evanston, fractures are predominantly closely spaced faults having small (millimeter-scale) displacements. Faults are in conjugate patterns, and the eastward fault-slip direction matches that inferred from offset marker horizons and bedding-plane striations. Such fracture patterns are unlikely to be representative of nearly flat-lying rocks in the basin interior except near minor faults. Recent studies in the foreland basin of Alberta show that zones of minor faults may be widespread in the Cordilleran foreland basin (Skuce and others, 1992).

#### Predicting Subsurface Fracture Attributes

Fracture observations in outcrops near Kemmerer predict generally north- and east-striking fractures within the Green River Basin. If fractures are related to regional deformation, as outlined above, then elsewhere the set of fractures that strikes north in the vicinity of Kemmerer may vary in strike according to the structure of the Cretaceous foredeep. Because the younger fractures that strike east near Kemmerer may reflect the orientation of the Cretaceous-Tertiary orogenic front, fractures and swarms of this generation in flat-lying rocks should strike normal to fold and fault trends and form divergent fans around salients in the orogenic front (fig. 68). Orientation patterns similar to this have been documented for joint sets in the Appalachian foreland (Engelder, 1985 and references therein) and in fracture (cleat) patterns in coal in the Rocky Mountain region (Laubach and Tremain, 1991; Laubach and others, 1991b).

Outcrop observations show that regional fractures can occur in closely spaced swarms (Hodgson, 1961; Laubach, 1991), but swarms of vertical fractures are difficult to demonstrate

using vertical core because core or borehole diameters are too small to properly sample vertical fracture swarms wider than 8 inches (20 cm). Fractures in Frontier reservoir sandstone core resemble those in outcrop swarms in height, width, and mineral fill, but testing for the existence of fracture swarms in the Green River Basin may require horizontal drilling or high-resolution seismic studies. Abrupt contrast in fracture intensity (or density) between swarms and adjacent rocks suggests that swarms could provide a change in seismic-reflection character or a velocity contrast that might be detected as a velocity anomaly on conventional seismic reflections or by techniques designed to detect seismic velocity anisotropy. Fracture-trace maps provide an understanding of fracture-density patterns, and thus can help guide efforts to develop better methods of detecting drilling targets.

Direct evidence of the existence of subsurface swarms in rocks similar in composition and structural history to Frontier sandstone is apparent in subhorizontal core from Cretaceous Cozzette Sandstone (Mesaverde Group) in the Piceance Basin, Colorado (Lorenz and Hill, 1991) (fig. 61). Overall pattern of fracture clustering in this core is similar to that in Frontier outcrops. Swarm widths are similar to narrow swarms in Frontier sandstone (such as swarms 2-7, fig. 57).

Not all fractures are necessarily fluid conduits. North-striking fractures in particular are densely cemented with calcite and locally have stylolites resulting from deformation of the vein fill. Such processes tend to close fractures, and crossing relations indicate that north-striking fractures were largely closed during formation of the younger east-striking fracture set. Petrographic evidence from the Mobil Tip Top T71X-6G well that feldspar dissolution occurred after some veins formed and that this dissolution event did not remove vein calcite suggests that these filled fractures could be barriers to fluid flow through networks of secondary pores.

#### Natural Fracture Exploration Targets

Regional fracture patterns in which fractures are uniformly spaced and perhaps occur in sets having orthogonal map patterns can in principle be readily exploited by hydraulic fractures or deviated wellbores drilled perpendicular to closely spaced fracture sets or at some angle that

maximizes contact with fractures likely to be open in the ambient stress field. Where various fracture directions are isolated in different beds, and where fractures are arranged in clusters, exploration for swarms that are "sweet spots" in low-permeability-sandstone gas reservoirs is more challenging. For example, swarms that are discontinuous along strike are potentially elusive targets; hydraulic fractures or deviated wells in the most favorable orientation, directly across fracture strike, may miss such swarms entirely or tap only poorly interconnected fractures. Because swarms can be vertically confined and isolated in a given sandstone bed, they have limited height and may be narrow targets for horizontal wells. Such swarms could easily be missed by hydraulic fractures or indiscriminate horizontal drilling even if fractures or wells are oriented perpendicular to fracture strike. Where fractures have different orientations in adjacent beds, the optimum fracturing or drilling direction may change drastically in short vertical distances within the target formation.

#### STRESS DIRECTIONS

To accurately predict the azimuth of hydraulic fracture growth or optimum directions for horizontal drilling in fractured rocks, we must know the direction of the maximum and minimum horizontal stress. Knowledge of the principal horizontal compressive stress azimuth is a prerequisite for effective placement, completion, and stimulation of many wells because open natural and hydraulically induced fractures are commonly aligned parallel to maximum horizontal stress ( $S_{Hmax}$ ). In reservoirs such as the Frontier Formation, where matrix rock permeability is low, the need for credible measurements of principal stress directions is acute because permeable natural fractures may be an exploration target and hydraulic fracture treatments are used to stimulate wells. Estimates of  $S_{Hmax}$  azimuth can be obtained from information provided by core, geophysical well logs, or well tests.

Stress-direction indicators used in GRI's study of the Green River Basin include the orientation of remotely monitored microseismicity from hydraulic fractures, wellbore breakouts, coring-induced fractures, and core-scale phenomena such as anelastic strain recovery (ASR),

circumferential monitoring of acoustic P-wave velocity anisotropy (CVA), and rock-strength anisotropy measured using axial point-load tests. Regional neotectonic deformation, expressed in western Wyoming as earthquakes, young (Quaternary to Recent) fault scarps, and aseismic uplift or subsidence, also provides an indication of current stress directions. Here we summarize observations of stress directions in the Frontier Formation from cooperative wells and the SFE No. 4-24 well.

### Results of Stress-Direction Measurements

Stress directions are summarized in table 8 and on a regional map (fig. 54). Stress-direction indicators give inconsistent orientations of  $S_{Hmax}$  in the wells we studied. Borehole breakouts, coring-induced fractures, anelastic strain recovery, P-wave velocity anisotropy, and strength-anisotropy tests each show large dispersion in inferred maximum horizontal stress direction (figs. 54, 69, and 70). Wellbore breakouts and coring-induced fractures, which are generally among the most reliable methods, are poorly expressed. Some breakouts, one coring-induced fracture, and remotely monitored microseismicity from hydraulic fractures give a general east to east-southeast azimuth of maximum horizontal stress, and some core-based methods suggest east to east-northeast  $S_{Hmax}$  direction. On the other hand, the most reliably defined breakouts in two wells indicate north-trending  $S_{Hmax}$ .

#### Wellbore Breakouts

Among the most reliable phenomena for determining stress directions are wellbore breakouts (elliptical wellbore enlargements) (for example, Plumb and Hickman, 1985). Wellbore breakouts develop when stress concentrations in the vicinity of the wellbore surface exceed the rock strength. The symmetric elongations of the wellbore profile that result are aligned with the minimum horizontal stress. Wellbore breakouts were measured in three wells in this study (table 8). In the Holditch SFE No. 4-24 well, breakouts were detected using an oriented

Table 8. Data showing maximum horizontal compression direction, Frontier Formation, Green River Basin, Wyoming.

Operator	Well	Data	Result (SH <sub>max</sub> )
Terra Resources	Anderson Canyon No. 3-17	CVA	ESE 013°
		Breakouts	NE 050° (n=5)
Wexpro	Church Buttes No. 48	ASR	NNE 015° (n=7) E 092° (n=8)
		DSCA	NW 150° (n=4) NE 030° (n=2)
		PC	NE 026° (n=1)
		CMS	NE 070° E 090°
Wexpro	Church Buttes No. 41	ASR	N 358° (n=3) E 108° (n=2)
Enron Oil & Gas Co.	South Hogsback No. 13-8A	CVA	ENE 084° (n=11)
		CMS	NE 079°
		Breakouts	NNW (n=3)
S.A. Holditch	SFE No. 4-24	Breakouts	~NNW, E?
		APT	E & N (n=300)
		CVA	N 009° ESE 099°
		ASR	~E? 060-120°
		PC	NW? 134°
		CMS	NE 030°-035°

APT = Axial point-load test  
ASR = Anelastic strain recovery  
CMS = Circumferential microseismic monitoring  
CVA = Circumferential velocity analysis  
DSCA = Differential strain curve analysis  
PC = Petal-centerline fracture



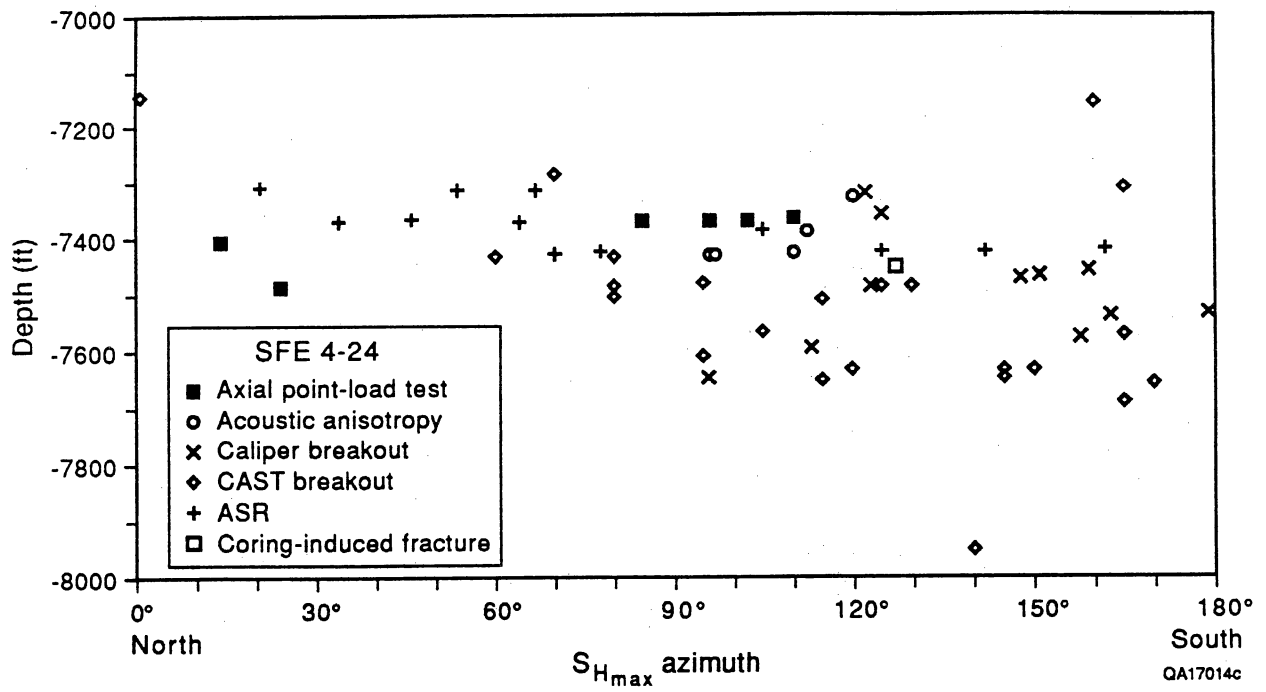


Figure 69. Depth versus  $S_{H_{max}}$  direction for Holditch SFE No. 4-24 well by means of several techniques.

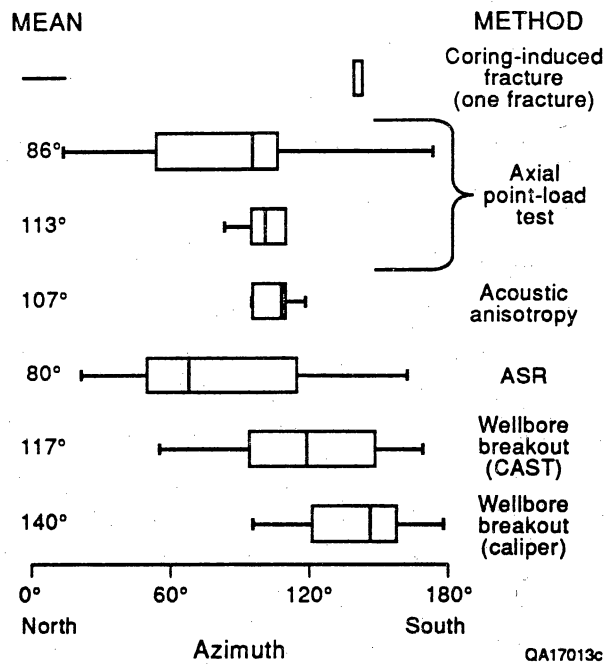


Figure. 70. Box plots of  $S_{Hmax}$  for various stress-direction indicators in the Frontier Formation, Holditch SFE No. 4-24 well. Box shows the center half of the data, and bar indicates median value.

caliper and the Circumferential Acoustic Scanning Tool (CAST), a type of borehole televiewer. Borehole viewers provide the most reliable method of detecting and measuring breakouts because they provide a high-resolution image of borehole surface topography that can be used to separate true breakouts from other types of borehole irregularities (such as washouts) and from natural and drilling-induced fractures.

Breakouts are not clearly indicated in the Holditch SFE No. 4-24 wellbore, and caliper results in particular have low reliability owing to an extensively washed-out borehole. Twenty breakouts were identified on borehole televiewer logs. The small number of breakouts over a logged interval of more than 900 ft (274 m) suggests that either (1) widespread breakouts did not develop in this borehole or (2) breakouts were undetected by the borehole televiewer. Breakouts may not have developed if stresses near the borehole wall did not exceed rock strength. On the other hand, the borehole televiewer may not have detected breakouts because of extensive borehole washout, drill-pipe wear on the borehole wall, or because the tool was not centered in the borehole. Drill-pipe wear produces an elliptical borehole, which shows up as vertical dark and light stripes on the log. Deviations from perfect centering of the borehole televiewer tool can cause the same effect. These stripes obscure the microtopography of the borehole wall and hide breakouts. Vertical stripes appear in more than 50 percent of the 950 ft (289 m) of borehole televiewer image. Fourteen of twenty breakouts (70 percent) on the borehole televiewer log are in zones where stripes do not obscure the borehole wall. The other six are in zones that are partially obscured. Clearly, this striping reduces visibility of breakouts and lowers the number of breakouts detected.

Orientations of breakouts detected using a borehole televiewer in the Holditch SFE No. 4-24 well are scattered, but almost twice as many breakouts are oriented northeast than northwest. Most northeast-southwest breakouts are between 040° and 080°. These sparse data suggest that  $S_{Hmax}$  is oriented in a northwest-southeast direction, probably between 130° and 170°. Breakouts in the depth interval between 7,300 and 7,400 ft (2,225 and 2,255 m) are aligned in a nearly north-south direction, consistent with east-trending  $S_{Hmax}$ .

Only one of the breakouts identified on the borehole televiewer logs corresponds to a wellbore breakout identified on caliper logs of this well. Six of the caliper breakouts appear on the borehole televiewer logs to be washouts. The borehole televiewer travel time log at each of these features displays a zone of high values about 1 ft (30 cm) wide that is continuous around the borehole. This indicates that a horizontal layer of weaker rock has washed out, increasing the circumference of the borehole. Three other breakouts occur in zones of vertical stripes that obscure the borehole wall or where quality of the borehole televiewer log is poor. Many breakouts have diffuse margins and no internal structure, but a few have features that are typical of progressive breakout development, and these can be used to find breakout azimuth.

Five distinct breakouts were shown in an assessment of borehole televiewer logs from the Terra Resources Anderson Canyon No. 3-17 well. Breakouts are mainly in the northwest and southeast quadrants of the borehole, giving a northeast average  $S_{Hmax}$  direction of approximately  $050^{\circ}$ . Breakouts were also detected in the Enron S. Hogsback No. 13-8A well. In this well, oriented calipers from the Formation Microscanner log were used to detect breakouts. Only three breakouts were evident on two logging runs over the same interval (6,820–7,308 ft [2,078–2,227 m]). These results indicate an  $S_{Hmax}$  direction of about  $340^{\circ}$ .

#### Petal-Centerline Fractures

Another indicator of  $S_{Hmax}$  is the strike of subvertical opening-mode fractures induced during coring and drilling, called petal and petal-centerline fractures (Kulander and others, 1990). These fractures are generally aligned parallel to maximum horizontal stress. In low-permeability sandstone, they are commonly visible in core and locally may be identified on borehole-imaging geophysical logs (Laubach and Monson, 1988; Lorenz and others, 1991). However, no diagnostic images of drilling-induced fractures were visible on borehole televiewer logs in the Terra Anderson Canyon No. 3-17 or Holditch SFE No. 4-24 wells or on Formation Microscanner logs from the Holditch SFE No. 4-24 or Enron S. Hogsback No. 13-8A wells.

Of the Frontier Formation cores we studied, only a few petal-centerline fractures were oriented, and only two of these measurements appear to be reliable (table 1). In the Wexpro Church Buttes No. 48 core, a petal-centerline fracture in sandstone strikes northeast ( $026^\circ$ ) at a depth of 12,169 ft (3,709 m). Only one petal-centerline fracture in Holditch SFE No. 4-24 was accurately oriented. It strikes northwest ( $134^\circ$ ) and occurs in a mudstone at 7,461 ft (2,274 m). Obviously, such limited petal-centerline data can only supplement results obtained by other methods.

The orientation of small hydraulic fractures that are deliberately created in boreholes and imaged using geophysical logs or sampled in core can also indicate horizontal stress anisotropy. An open-hole stress test was carried out in the Enron S. Hogsback No. 13-8A well, but the trace of the created fracture was undetected using a borehole-imaging Formation Microscanner log, and the fracture was absent in recovered core.

#### Anelastic Strain Recovery

When core is removed from the subsurface, in situ stresses are relieved and core relaxes. Core relaxation involves an instantaneous, elastic component and a time-dependent anelastic creep component that can persist for hours or days. Anelastic strain recovery (ASR) techniques measure the latter component of relaxation soon after core is removed from the core barrel (Teufel, 1983). Strain is manifested as change in core shape (displacement) and is measured using sensitive strain gauges. Anisotropic expansion is thought to result from the opening of numerous microcracks oriented perpendicular to the direction of in situ maximum compression. The direction of maximum expansion is inferred to be the direction of maximum horizontal compressive stress ( $S_{Hmax}$ ) in the subsurface. Because sedimentary and structural heterogeneities (such as bedding and fractures) can distort and mask stress relaxation-related displacements, homogeneous core is sought for the ASR method. In low-permeability rock, another complication that can occur is core contraction caused by slow release of pore fluids and concomitant reduction in pore pressure.

In the Holditch SFE No. 4-24 well, directions of ASR were measured by TerraTek and analyzed by TerraTek and Sandia Laboratories (Warpinski, in press). Many of the ASR data are of low quality owing to the effects of rock fabric, low strain magnitudes, and technical problems such as faulty gauges. We summarize the results of tests that were judged to be most reliable from the technical standpoint (Warpinski, in press). A single relaxation direction is not obvious from measurements of samples from the Holditch SFE No. 4-24 well. Results have a wide range of trends, but most of the reliable ASR  $S_{Hmax}$  directions fall between 060° and 120°. Warpinski (in press) interpreted the most reliable ASR results from this well to indicate northeast-trending  $S_{Hmax}$ . Sandstone samples have a preferred northeastward to east-northeastward expansion. Mudstone samples have northeast-trending displacement azimuth.

In core from the Wexpro Church Buttes No. 48 well, displacement patterns of seven samples imply north-northeast (015°)  $S_{Hmax}$ , and eight samples suggest east-trending (092°)  $S_{Hmax}$ . Five ASR samples from Wexpro Church Buttes No. 41 also suggest bimodal displacement directions, with three samples evincing north-trending (003°)  $S_{Hmax}$  and two samples showing eastward (108°) relaxation trends.

Differential strain curve analysis (DSCA) is based on anisotropic contraction of core when it is hydrostatically loaded in the laboratory (Strickland and Ren, 1980). The direction of maximum core contraction is inferred to be the direction of maximum horizontal stress, on the premise that differential contraction results from the closing of microfractures that opened during core relaxation. Five DSCA samples of Wexpro Church Buttes No. 48 core (TerraTek, 1989) gave a bimodal pattern of northwest (~150°; four samples), and northeast (~030°; two samples) inferred  $S_{Hmax}$  directions. Thus, for this well, both ASR and DSCA record north-northeast trends, but the northwest direction visible in some DSCA results does not match an ASR direction.

## Acoustic Anisotropy

Circumferential velocity analysis (CVA) involves measuring compressional acoustic wave velocity through a whole core sample in several directions using an ultrasonic velocity apparatus (Sayers, 1988; Hyman and others, 1991). The distribution of velocity through the core is affected by the distribution of microfractures. Open microfractures retard acoustic wave speed, so the fastest direction through the core is parallel to microfracture strike. Velocity analyses were carried out by TerraTek (Hyman and others, 1991).

The direction of fastest acoustic travel time in core indicates  $S_{Hmax}$  direction if (1) microfractures are created by ambient stresses in the subsurface or (2) a set of microfractures opens preferentially in the core expansion direction (and anisotropic expansion reflects in situ stress). The direction of minimum velocity is parallel to the maximum horizontal stress direction when the microfractures are the result of core strain recovery. However, if the microfractures formed in situ in response to the present stress field (that is, a type of natural fracture), then it is the maximum velocity that parallels the maximum horizontal stress. Thus, knowledge of the cause of velocity anisotropy is needed to assess stress directions from velocity measurements because at least two processes could create fractures that have differing strikes. Moreover, natural fractures that have strikes unrelated (or only coincidentally related) to contemporary stresses may exist in core and create acoustic anisotropy.

Petrographic observations of mineralization and irregular fracture shape were used to identify natural microfractures (Hyman and others, 1991), but in many cases microfracture origin is ambiguous owing to the absence of diagnostic natural microfracture traits such as mineralization or healed fractures (Laubach, 1989a). A key to identifying relaxation-induced fractures in Hyman and others' study was inspection of thin sections from samples that had been subjected to reservoir pressures in the laboratory, where they were injected with dye and epoxy. Under these conditions of sample preparation, microfractures caused by core relaxation tend to be closed and therefore do not fill with epoxy. Fractures open under these conditions were presumed to be natural. Nevertheless, because natural and relaxation-induced fractures

can have a similar appearance, distinguishing them in thin section is problematic. On the basis of our petrographic work on Holditch SFE No. 4-24 core, we could not confidently distinguish small preexisting natural fractures from fractures that could have been induced by other processes.

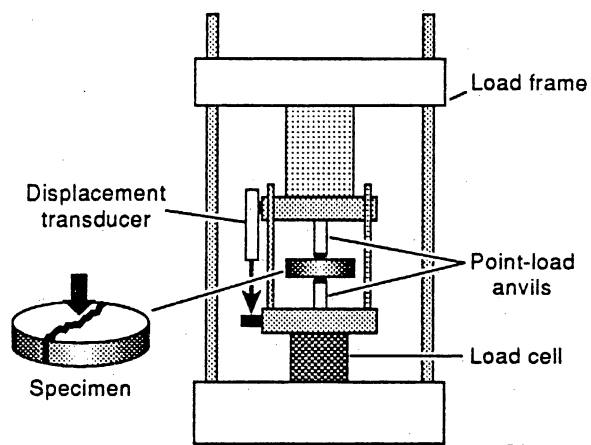
The fastest sonic velocity in Terra Resources Anderson Canyon No. 3-17 samples is in a north-northeast (013°) direction, and maximum velocity is in an east-northeast (084°) direction in Enron S. Hogsback No. 13-8A samples. Acoustic velocity measurements from Holditch SFE No. 4-24 have both east-southeast- (099°) and north- (009°) trending maximum velocity directions, with east-southeast directions being prevalent (Hyman and others, 1991). In the Terra Resources Anderson Canyon No. 3-17 well, where the maximum velocity direction is northeastward, Hyman and others (1991) interpreted dominant microfractures to have been induced by core expansion. Thus, they interpreted the anisotropy to show east-southeast (110°)  $S_{Hmax}$  direction. Hyman and others (1991) interpreted east-southeast maximum velocity in Holditch SFE No. 4-24 to be caused by natural microfractures unrelated to current in situ stresses. Microfractures interpreted to be natural have strikes that range between 100° and 110° in these samples.

#### Axial Point-Load Tests

Axial point-load tests (APT) measure rock-strength anisotropy by breaking small core samples and measuring the strike of the resulting fracture or fractures (Clift and others, 1992). Versions of this test have previously been used to determine rock properties such as compressive strength and strength anisotropy in surface engineering applications (see references in Clift and others, in press).

The point-load test we used involves loading a small rock sample to failure with two diametrically opposed indenting anvils that approximate point loads (fig. 71). Load was applied by a Soil Test 10,000-pound load frame, at a rate of about 1 lb/s. Load and time were indicated on an x-y recorder. Variation in loading rate, rock strength, and sample size can affect the way





QA17080c

Figure 71. Diagram illustrating the point-load apparatus. A disk of rock is loaded between two anvils that have rounded ends that approximate point loads.

samples break. We obtained simple fractures having preferred orientations by using thin disks of sample material (~0.10 to 0.45 inch [-0.25 to 1.1 cm] thick, ~1 inch [-2.54 cm] diameter) and low to moderate loading rates (~1 lb/s for precisely aligned 0.5-inch [1.2-cm] load platens). Our sample preparation and test procedures are detailed by Clift and others (1992). Point-load tests were carried out on more than 160 Frontier Formation sandstone samples from the Holditch SFE No. 4-24 well.

The stress field produced by axial point loads is axisymmetric, but the induced fracture preferentially aligns along a direction perpendicular to that of the rock's minimum tensile strength. A preferred direction of sample breakage indicates strength anisotropy, which for core samples may correspond to a principal direction of in situ stress or a preexisting structural (or sedimentary) anisotropy. As in ASR and velocity anisotropy tests, strength anisotropy will reflect current stress directions when fracture growth is guided by preferentially oriented microfractures that existed in the core as a result of in situ stresses or expansion caused by relief of subsurface stress. These directions, however, are not necessarily the same.

Point-load tests show that marked strength anisotropy exists in Frontier Formation sandstones (fig. 72), but samples from different beds have contrasting strikes, leading to an overall bimodal pattern of induced fracture strike. In some samples, strike is predominantly east and northeast, but in other samples fractures created in tests have north strikes. Within a sample or an individual sandstone, the strikes of fractures created by axial point-load tests are highly reproducible, and each APT data point represents the average of numerous point-load tests from a given depth. Four sets of results have fracture strikes that are generally east (~070° to 110°), and two sets have north to northeast strikes (~010° and ~025°).

No obvious aligned sedimentary grains are visible to account for the strength anisotropy. We interpret strength anisotropy to have resulted from aligned microfractures, but petrographic and scanning electron microscope study of these samples suggests that it is microfractures smaller than 10  $\mu\text{m}$  that grow and coalesce to produce the visible fractures that break the sample. The origin of such small fractures is difficult to diagnose. Such fractures may

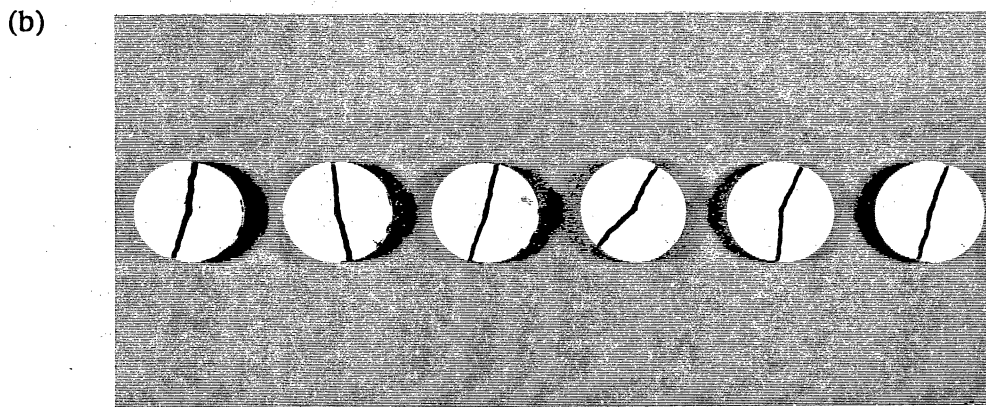
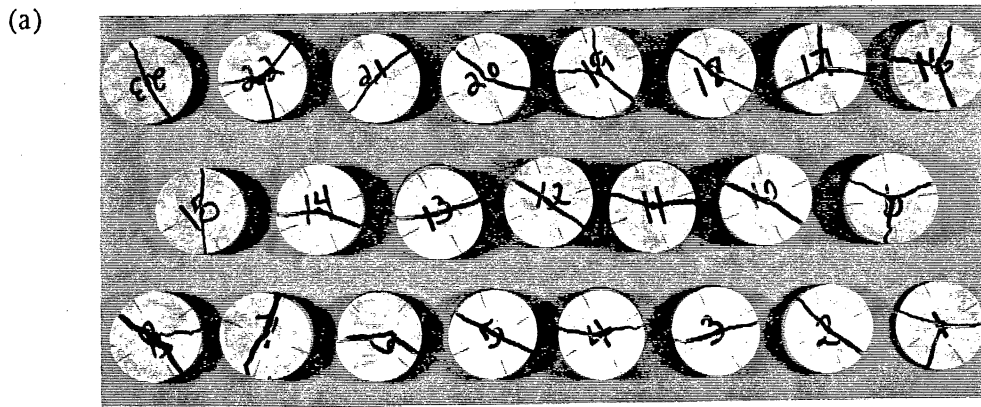


Figure 72. Disks of Frontier Formation core having anisotropic strength in axial point-load test. (a) Predominantly east-striking fractures created in Holditch SFE No. 4-24 samples, depth 7,486 ft (2,281 m). (b) Predominantly north-striking fractures in Holditch SFE No. 4-24 samples, depth 7,365 ft (2,244 m).

have been created by subsurface deviatoric stresses or by deformation related to core relaxation, or they may be natural fractures having strikes unrelated to current stresses. The bimodal pattern of sample breakage suggests that several processes may be responsible and that some microfractures are possibly natural fractures that are not necessarily aligned with current stress directions.

#### Hydraulic Fracture Microseismic Monitoring

Low-level seismicity induced by massive hydraulic fractures can be monitored to give an estimate of the strike of the stimulation fracture, as described later in detail. The strike of these induced fractures is commonly assumed to be aligned parallel to the maximum horizontal stress (Fix and others, 1990), although a previous study has shown that natural fractures may modify or even control the strike of induced fractures (Barton, 1986).

In the microseismic method, azimuth of the induced fracture is determined by analyzing the polarization of microseismic signals recorded in the treatment well during shut-in following hydraulic fracture treatment. In Frontier wells, analysis was based on particle motion during the first half cycle of each signal, in order to minimize contamination by tool-borehole resonances. Resonances are particularly severe if local casing or formation coupling is poor at the location of the recording tool. Experience has shown that most signals recorded in the treatment well following a hydraulic fracture treatment originate in the borehole, in the perforations, or within the cemented zone. Particle motions from these sources are generally unrelated to the orientation of the induced fracture. Hence, identification of signals from sources outside the borehole is necessary to estimate fracture orientation.

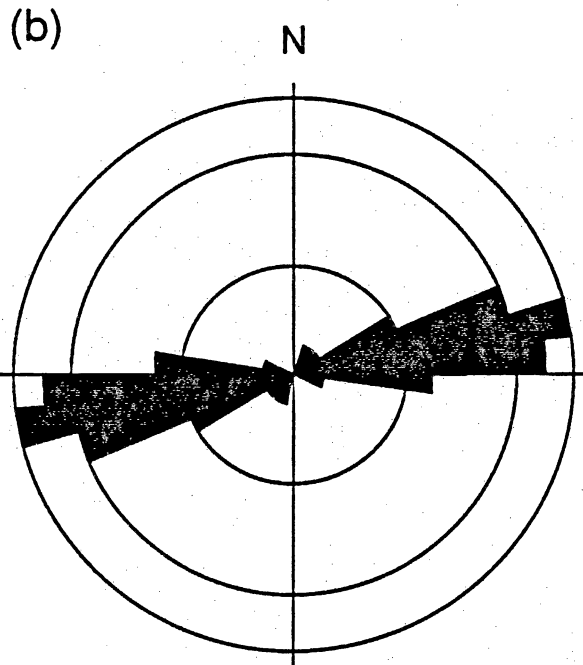
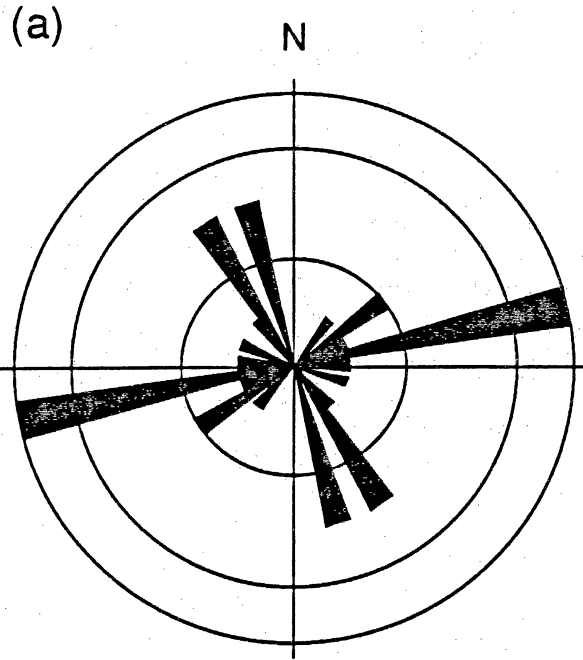
Teledyne Geotech's signal-detection algorithm was applied to 100 ms RMS values computed for the vector horizontal component at several depths. This algorithm requires an RMS peak-to-background ratio of 3 or greater for a signal to be declared. The detected signals were plotted and visually reviewed for evidence of tool-borehole resonances within the first half cycle of the signal; signals showing such evidence were deleted from the data set, as were tube-wave

signals. Particle-motion orientations of remaining signals were determined using a program that estimates a best linear fit to observed motion over a specified time and frequency band and calculates a measure of reliability of the statistical fit (F value). Azimuth estimates having F values less than 10 were removed from the data set. Fracture strikes were estimated from histograms of remaining azimuths.

In this study, three wells—the Enron S. Hogsback No. 13-8A, Wexpro Church Buttes No. 48, and Holditch SFE No. 4-24—were tested using this method. Rose diagrams of signal directions for three GRI research wells are shown in figure 73.

Induced-fracture strike in the three Frontier Formation wells is generally east to northeast (fig. 73). A fracture striking  $079^\circ$  and dipping  $078^\circ$  to the northwest was detected in the Enron S. Hogsback No. 13-8A. In the Wexpro Church Buttes No. 48 cooperative well, results indicate fracture growth with generally east ( $090^\circ$ ) to east-northeast ( $070^\circ$ ) strike, east strikes occurring in the lower part of the fractured interval and northeast strikes detected in the upper part. In Holditch SFE No. 4-24, induced seismicity indicates a fracture striking northeast ( $030^\circ$  to  $035^\circ$ ).

Evidence of possible diffuse microseismicity that may result from a wide hydraulic fracture zone or multiple fracture directions is visible in signal data from the Enron S. Hogsback No. 13-8A well (Laubach and others, in press, their figure 9). Such features may be a manifestation of natural fractures influencing hydraulic fracture growth. Alternatively, in the Enron well the signals that fall off the plane of the east-striking fracture may be spurious, possibly the result of detection of S-waves or other processes. Multiple directions of fracture growth possibly related to natural fractures have been inferred from tiltmeter data from tests of a well in the northern Green River Basin (Power and others, 1976).



QA19855c

Figure 73. Direction of hydraulic fracture growth from circumferential microseismic monitoring (from Teledyne Geotech, unpublished data, 1992). Rose diagram of orientation vectors of seismic signals from (a) Enron S. Hogsback No. 13-8A and (b) Holditch SFE No. 4-24.

## Interpretation of Stress Data

### Inconsistent Stress Directions

Our results show that in the western Green River Basin,  $S_{Hmax}$  orientations derived from several techniques are scattered. In the wells we studied, stress indicators give inconsistent orientations of the maximum horizontal compression direction. Wellbore breakouts, coring-induced fractures, anelastic strain recovery, P-wave velocity anisotropy, and strength anisotropy tests each show large dispersion or bimodal distributions of inferred maximum horizontal stress directions both within and between wells. Wellbore breakouts and coring-induced fractures, which are generally among the most reliable methods, are not clearly indicated, possibly because of the drilling procedures used in these wells or because of low stress (relative to rock strength) conditions near the wellbore. Core-based methods such as velocity analysis and point-load tests are challenging to interpret in terms of stress directions because the origin of fractures creating anisotropy cannot be unequivocally specified using available petrographic information.

Both north- and east-trending  $S_{Hmax}$  directions can be supported using test results. Although breakouts have a wide range of orientations and are poorly developed in the Holditch SFE No. 4-24 well, the most reliable breakout directions show north-trending  $S_{Hmax}$ . On the other hand, east-trending  $S_{Hmax}$  is indicated by breakouts in the depth range where a hydraulic fracture was created; microseismic monitoring of this fracture shows that it has a generally east strike, consistent with breakout results *at that depth*. Distinct breakouts in the Terra Resources Anderson Canyon No. 3-17 well indicate northeast  $S_{Hmax}$  direction, as do the most reliable ASR results from Holditch SFE No. 4-24 core. ASR results from both Wexpro wells show bimodal patterns. Remotely monitored microseismicity from hydraulic fractures give a generally eastward azimuth of hydraulic fracture growth in three wells, but in the Enron S. Hogsback No. 13-8A

well, where breakouts suggest north-trending  $S_{Hmax}$ , a north-trending feature could also be fitted to the signal pattern.

The bimodal patterns of breakouts, core strain, acoustic velocity, and axial point-load strength are difficult to reconcile with simple, uniform regional stress patterns. We hypothesize that results of these tests are scattered partly because sedimentary and structural anisotropy have interfered with detection of stress-related anisotropy. Interpretation of the results of acoustic velocity and point-load methods depends on an evaluation of the origin of microfractures creating anisotropy or accomplishing core strain. If arrays of microfractures existed in the subsurface before coring, then the assumption that microfractures developed at right angles to in situ  $S_{Hmax}$  and conventional interpretations of test results may be misleading. For example, natural microfracture anisotropy may be unrelated to current stress directions, or in the subsurface, microfractures may parallel  $S_{Hmax}$ . According to the latter interpretation, acoustic anisotropy and point-load-fracture directions in Holditch SFE No. 4-24 core would be consistent with east-trending ( $090^\circ$  to  $110^\circ$ ) maximum horizontal stress. This explanation is not as likely to account for bimodal breakout and ASR results because these methods measure a direct response of rock to subsurface conditions.

#### Low Horizontal Stress Anisotropy

Dispersed  $S_{Hmax}$  directions could reflect a low contrast in the magnitude of horizontal stresses. Where nearly isotropic horizontal stresses exist, methods designed to detect stress directions are more likely to record physical heterogeneities or anisotropies that are unrelated to in situ stress. Evidence of low contrasts in horizontal stresses include low velocity anisotropy (~4 percent for some Frontier sandstones) and low values of core strain. Stress test and hydraulic fracture treatment data should be evaluated to help test this hypothesis.

Where horizontal stress contrast is low, natural fractures might control or influence the growth direction of hydraulic fractures, making inferences of stress directions from microseismic monitoring results problematic. Studies where hydraulic fractures have been mined out show



that natural fractures can modify the strike of hydraulically induced fractures (Diamond and Oyler, 1987), especially where horizontal stress contrast is low and natural fractures are planes of weakness (for example, if fractures are open). Open fractures occur in Frontier Formation cores, and in Frontier Formation outcrops near these research wells that may have fracture patterns similar to those that exist in the subsurface, large natural fractures exist. In outcrop, fracture sets having north, east, and northeast strikes are common (Laubach, in press). These are the same directions that are detected using acoustic velocity and strength anisotropy tests of Frontier Formation cores. In the subsurface, such fractures might modify the growth direction of treatment fractures, or become microseismically active (and detectable) following treatments. Even if treatment fractures grew primarily parallel to in situ stress directions, this might account for bimodal northerly and easterly seismic signals detected in some wells.

In addition to data measurement uncertainties (such as improperly oriented core or faulty strain gauges), several geologic factors may in principle contribute to contradictory, or at least variable, stress directions and low horizontal stress contrast. For example, it is possible that in shallow wells near the west side of the Green River Basin, stress-direction measurements are influenced by loads caused by large topographic features such as the mountains of the thrust belt (which presumably would increase east-west compression). It is also plausible that active deformation related to normal fault movement may locally modify stress directions. For example, the hanging-wall block of the Teton normal fault, north of the northern Green River Basin, shows patterns of aseismic creep deformation that are opposite (apparent reverse motion) to the pattern of Quaternary east-west (presumably seismic) extensional slip on the fault (Sylvester and others, 1990). Although evidence of tectonic activity is lower in the Green River Basin than near the Teton Fault, seismicity and young north-striking normal fault scarps do occur along the margins of the Green River Basin (Case, 1986). Finally, the position of the basin relative to stress provinces caused by plate-scale motion may govern the observed stress pattern, as discussed later.

## Stress Provinces

The Green River Basin is in the east-west Cordilleran extensional stress province on Zoback and Zoback's (1989) map of principal stress orientations and stress provinces in the United States (fig. 74). In this province,  $S_{Hmax}$  is predicted to trend north-northwest to north-northeast as a result of northeast- to east-southeast-directed extensional deformation. The attributes that suggest that the Green River Basin belongs in this province include a few north-trending  $S_{Hmax}$  determinations (Zoback and Zoback, 1980, and references therein), north-striking young (Quaternary to Recent) normal fault scarps along the west margin of the basin, sparse earthquake focal mechanisms indicating normal faulting (Case, 1986), and the high regional elevation and high heat flow of part of this area. Our measurements that show north-trending  $S_{Hmax}$  agree with Zoback and Zoback's placement (1980) of the Green River Basin in the Cordilleran stress province (fig. 74), but our east  $S_{Hmax}$  directions are more consistent with stress azimuths typical of the midcontinent compressional stress province, which is east of the Green River Basin. In the midcontinent province, east-northeast to east maximum horizontal stress azimuths are common.

The position of the Green River Basin near the boundary between the Cordilleran extensional province and the midcontinent compressional stress province may be responsible for the scattered and opposed stress directions we recorded. Boundaries between stress provinces may be broad and transitional and characterized by variations in tectonic stress orientation. For example, according to Zoback and Zoback (1989), the boundary between the San Andreas and Cordilleran extensional stress province is about 180 mi (300 km) wide. Along the east boundary of the Cordilleran extensional province, Zoback and Zoback (1989) recognized small, local anomalies of east-west  $S_{Hmax}$  orientation in the area north of Yellowstone. This suggests that the east margin of the Cordilleran stress province may have transitional or inconsistent stress directions. Although the nature of stress province boundaries is uncertain, areas of nearly equal horizontal stress may also exist in the transition zone where dominantly northeast-trending compression gives way to east-directed extension. Our results in

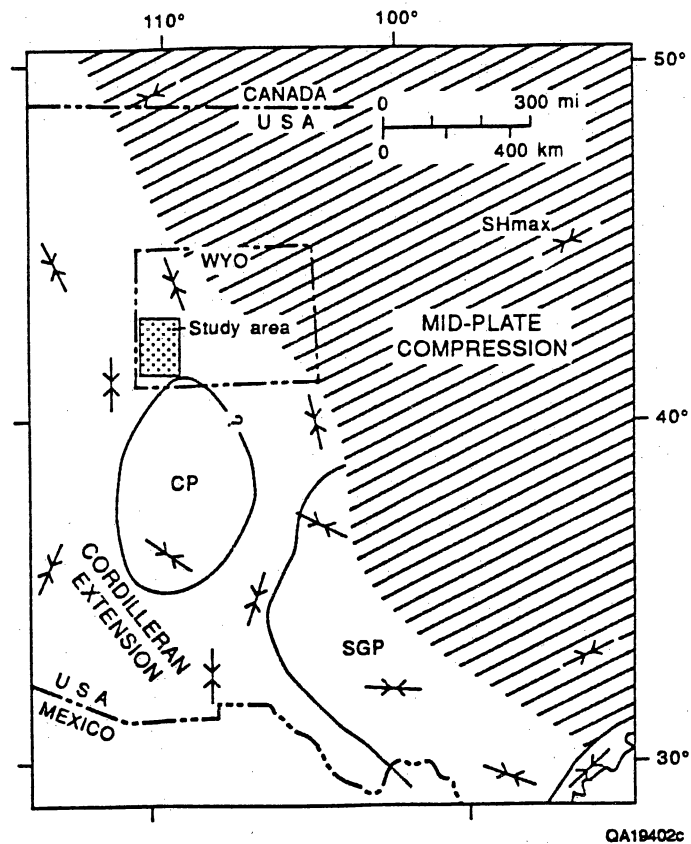


Figure 74. Generalized stress map of the western United States (from Zoback and Zoback, 1989). Inward-pointing arrows show direction of maximum horizontal stress ( $S_{Hmax}$ ). Only those stress provinces adjacent to the study area are labeled: Mid-plate compression, Cordilleran extension; CP = Colorado Plateau. The locations of Wyoming and the study area are indicated.

the Green River Basin are consistent with variable stress directions along this boundary and low contrasts in the magnitudes of horizontal stress.

#### Summary of Stress-Direction Results

Tests in five Frontier Formation wells give highly scattered estimates of maximum compression direction in the Moxa Arch area of the Green River Basin, with estimates for  $S_{Hmax}$  ranging from north to east or northeast. The most reliable wellbore breakout data are consistent with north-trending maximum horizontal stress. We speculate that dispersed results partly reflect the influence of natural macro- and microfractures on stress estimates derived from acoustic velocity, strength anisotropy, and (possibly) core strain recovery experiments, and on the growth direction of hydraulic fractures. These effects are likely exacerbated by low horizontal stress anisotropy; scattered test results possibly are a manifestation of nearly equal horizontal stresses. We hypothesize that spatially variable stress directions (or perhaps low contrasts in horizontal stresses) exist near the margin of the Cordilleran extensional province and the midcontinent compressional province, where the Green River Basin is located.

#### CONCLUSIONS

The main goal of the geologic studies of the Tight Gas Sands program in the Green River Basin, Wyoming, was to document the geologic framework of the Frontier Formation. Insights gained from this multifaceted study increased the understanding of geologic controls on the distribution and behavior of the Frontier tight gas reservoir. Within the Tight Gas Sands program, the geologic information supported the testing and application of new technologies for resource exploitation. Stratigraphic, diagenetic, and structural studies formed the three main areas of geologic investigation that were needed to characterize this tight gas sandstone.

Gas producers directly benefit from this research because the collection and assimilation of geologic information can lead to improved gas recovery and lowered completion costs through

better field-development and well-completion programs in the Frontier Formation and similar tight gas sandstones. The results of petrographic examination of two potential pay intervals in a Frontier well provide an example of the benefit of geologic characterization to an operator. Log-calculated permeability determined by the Geochemical Logging Tool\* (GLT) matched core-measured permeability in one interval but not in the other. By looking at thin sections of the two potential pay zones, we determined that one of the intervals had abundant microporosity but little intergranular primary porosity. Log-derived permeability for this interval was too high because log-derived porosity included abundant microporosity as effective porosity. The other interval had more primary porosity and less microporosity, so the log-derived permeability was correct. On the basis of the petrographic information, the operator was able to recognize pay zones using the GLT log in combination with a resistivity log.

Mapping and core description studies indicate that the main depositional and stratigraphic controls on distribution and quality of Frontier reservoirs are sandstone continuity and detrital clay content. Frontier production trends reflect sandstone distribution and continuity. The Second Frontier was deposited in a fluvial-deltaic system having prominent delta-flank strandplains. Marine shoreface and fluvial channel-fill sandstones are the reservoir facies. On the La Barge Platform, the widespread productivity of the Second Bench can be attributed partly to the remarkable continuity of this marine shoreface sandstone. The First Bench contains numerous discontinuous fluvial channel-fill sandstones, and only those wells penetrating these channels typically have First Bench production. However, First Bench channel-fill sandstones are the primary reservoir facies in the Second Frontier along the south part of the Moxa Arch (Moslow and Tillman, 1986, 1989) where Second Bench upper shoreface sandstone is commonly absent owing to erosional truncation. Fluvial channel-fill sandstones form southeast-trending belts, which are a few miles wide, several tens of feet thick, and separated by interchannel shale and sandy shale. Within the channel belts, clean sandstone occurs as discontinuous lenses as much as 20 ft (6 m) thick that are interlayered and laterally

---

\* The use of firm and brand names in this report is for identification purposes only and does not constitute endorsement by the Bureau of Economic Geology.

gradational with mud-clast-rich shaly sandstone. The marine shoreface facies forms a continuous northeast-thinning sheet of sandstone, 40 to 120 ft (12 to 37 m) thick. Clean sandstone is best developed near the top of the shoreface facies in northeast-oriented trends 5 to 40 ft (1.5 to 12 m) thick. The Fourth and Fifth Benches of the Second Frontier and the Third and Fourth Frontier, which were deposited in mud-dominated coastal plain and marine shoreline systems, contain isolated sandstones that are locally productive.

Detrital clay content exerts a strong influence on the porosity and permeability of Frontier sandstone before diagenetic modification, and detrital clay content is controlled by depositional environment. Most Frontier sandstones along the Moxa Arch were deposited in one of three depositional environments: lower shoreface, upper shoreface, and fluvial channel. Frontier lower shoreface sandstone is characterized by abundant pore-filling detrital clay matrix, which was mixed into the sand by burrowing organisms on the sea floor. In Frontier lower shoreface sandstone, permeabilities are generally low, although porosities may be similar to those in the other sandstone facies. Frontier upper shoreface sandstone was free of clay at the time of deposition because in the shallow-water upper shoreface environment strong currents winnow fine-grained sediment and inhibit burrowing organisms. On the La Barge Platform, the most prolific Frontier reservoirs lie in Second Bench upper shoreface sandstone. Frontier fluvial channel-fill sandstone contains abundant sand- and gravel-sized mud rip-up clasts, which deform into pores and pore throats during compaction. The channel-fill facies typically consist of mud-clast-rich sandstone interlayered, and laterally gradational, with sandstone that is relatively free of mud clasts. Thus, clean sandstone typically occurs as discontinuous lenses within the channel-fill facies. Upper shoreface clean sandstone, on the other hand, consistently occurs at the top of the progradational shoreface sequence and therefore is a more predictable target.

The major causes of porosity loss in Frontier sandstones during burial diagenesis were mechanical and chemical compaction and cementation by calcite, quartz, and authigenic clays. Quartz cement is most abundant in deeply buried fluvial channel-fill sandstones at the south

end of the Moxa Arch and in the Green River Basin. Calcite cement is most abundant in Frontier sandstones deposited in lower shoreface environments. Both upper and lower shoreface sandstones from the Hogsback area at the north end of the Moxa Arch contain significantly more calcite cement than do shoreface sandstones in either the Fontenelle or Church Buttes areas.

Despite extensive diagenetic modification, reservoir quality in the Frontier Formation is best in facies that had the highest porosity and permeability at the time of deposition. Original intergranular porosity has been substantially reduced in these clean sandstones by compaction and precipitation of authigenic cements, but they still retain higher porosity and permeability than do sandstones that have abundant detrital clay matrix. Thus, exploration for Frontier reservoirs should focus on locating clean sandstones deposited in high-energy depositional environments. The reservoir intervals in the wells in this study are mainly in clean, upper shoreface and fluvial channel-fill sandstones.

Nevertheless, reservoir quality in clean sandstones is variable because diagenetic modification is highly variable. Whereas some upper shoreface sandstones have low porosity and permeability because of abundant calcite cement, other sandstones from the same depositional environment contain little calcite and may have relatively high porosity and permeability. Similarly, upper shoreface sandstones having abundant rock fragments have lost more intergranular porosity by mechanical compaction than have quartz-rich upper shoreface sandstones. Some fluvial channel-fill sandstones are extensively cemented by quartz, and others are not. Fibrous illite and MLIS can drastically reduce reservoir permeability in any facies.

The general distribution of quartz cement is predictable because a strong correlation exists between volume of quartz cement and depth. Thus, fluvial channel-fill sandstones at the deeper, south end of the Moxa Arch can be expected to contain a greater volume of quartz cement than can fluvial channel-fill sandstones from the north end. Unfortunately, occurrences of calcite and fibrous illite cannot be predicted on the basis of current knowledge,

and these two cements exert a powerful control on porosity and permeability in Frontier reservoirs. Although the presence of pervasive calcite cement or fibrous illite and MLIS in a particular sandstone bed cannot be predicted, patterns in the distribution of these cements provide general guidelines of where they are most likely to occur. Fibrous illite and MLIS are most abundant in upper shoreface samples from Fontenelle field. Calcite cement is most plentiful in the Hogsback area on the northwest part of the La Barge Platform. Calcite cement commonly is most abundant at the top of clean, well-sorted sandstones, directly below the contact with an overlying muddy sandstone. Once a well has been drilled, zones of intense calcite cementation can be recognized on logs, for example by high resistivity response. Intervals of intense calcite cementation should not be counted as part of the pay in a well.

Fractures are sparse in Frontier Formation core, but this does not necessarily mean that natural fractures are an unimportant reservoir element in these rocks. Open fractures exist in core, and production and fracture treatment results suggest that natural fractures locally play significant roles. Fracture networks in outcrops that likely resemble fractures existing at depth have attributes such as wide spacing and great lateral extent that would tend to make them both effective fluid conduits and difficult to intersect and detect by means of vertical wells.

Outcrop studies show that fractures are in networks where fracture connectivity is locally highly variable and anisotropic. For example, the direction of fracture strike can shift by 90° among adjacent beds. Moreover, fractures commonly are in discrete, irregularly spaced swarms separated laterally by domains that have few fractures, rather than in regularly spaced, orthogonal fracture sets. Average strikes of fracture sets can be predicted from regional tectonic extension directions, so an optimum direction for drilling in flat-lying rocks can be determined. More challenging to predict is fracture orientation in a specific bed, fracture density, and the probability of encountering a dense cluster of fractures with hydraulic fractures or horizontal wells. For predicting open natural fractures, the direction of maximum horizontal stress also needs to be taken into account.



Natural fracture swarms in the Frontier Formation are potential high permeability "sweet spots" that can be included in reservoir models and targeted in exploration. In outcrop, swarms are separated laterally by domains commonly tens or hundreds of meters wide where fractures are markedly less common or not in contact with other fractures. Fluid communication between adjacent swarms, both laterally and vertically, is likely to be poor to nonexistent, resulting in elliptical islands (in plan view) where fracture permeability is high. This view of fracture patterns is in sharp contrast to conventional views in which regional fractures are in regularly spaced, orthogonal arrays. The implication for hydraulic fracturing and horizontal drilling is that good fracture targets can still be missed, even if hydraulic fractures or horizontal wells are correctly oriented in a direction that crosses fracture strike. Methods are needed for detecting fracture swarms and improving predictions of swarm spacing, length, and connectivity.

Reservoir heterogeneities resulting from fractures may be as pronounced as those produced by stratigraphic variations. The drastic differences in fracture-network connectivity and fracture density in otherwise similar upper shoreface sandstones is one type of evidence for this heterogeneity. Another is evidence for clustered fracture patterns that are similar over a range of observation scales (fractal dimension  $D \sim 1.2$ ), showing that fractal concepts are a valid approach to describing fracture distributions in these sandstones. The discontinuous, fractal nature of fracture networks, such as those in Frontier Formation sandstones, should be incorporated in exploration plans and models that simulate flow in these reservoirs. Using production results to diagnose the presence of natural fractures that could ultimately play a significant role in production over the life of a well may not be straightforward. The well tests and production characteristics of variably interconnected fracture networks, over the short term, might mimic the behavior of a reservoir having only matrix permeability, yet the impact of fractures on drainage patterns and stress sensitivity over longer production times could be significant.

Stress-direction indicators suggest north-trending  $S_{Hmax}$  but give inconsistent orientations of  $S_{Hmax}$  in the Frontier wells we studied. Borehole breakouts, coring-induced fractures,

anelastic strain recovery, P-wave velocity anisotropy, and strength anisotropy tests each show large dispersion in inferred maximum horizontal stress direction. Wellbore breakouts and coring-induced fractures, which are generally among the most reliable methods, are poorly expressed. We interpret wellbore breakout data to show north-trending maximum horizontal stress. The scatter of stress directions from these methods we used may indicate that a low contrast in the magnitudes of horizontal stresses exists in the Frontier Formation on the Moxa Arch. This is compatible with the position of the western Green River Basin near a stress province boundary, and with evidence from remote monitoring of hydraulic fracture growth that created fractures propagated to the east-northeast rather than to the north, parallel to inferred maximum horizontal stress (Laubach and others, in press). If this is the case, tensile strength anisotropy, in the form of natural fractures, is likely the main control on hydraulic fracture growth directions in these wells.

#### ACKNOWLEDGMENTS

Funding for this study was provided by the Gas Research Institute under contract number 5082-211-0708, Mark Johnson and Larry R. Brand, Project Managers. The Geologic Survey of Wyoming, through a subcontract under the direction of Rodney H. De Bruin, compiled Frontier production data and provided other data and assistance. Donations of cores, well logs, and other data by Pacific Enterprises, Enron, Wexpro, Texaco, and Mobil form an important part of the data base for this study and are gratefully acknowledged. Nina L. Baghai, Robert L. Buehring, Kyle L. Kirschenmann, Jennifer Kopf, and Glenn A. Klimchuk assisted in various phases of the project. Robert W. Baumgardner, Jr., evaluated borehole breakouts in SFE No. 4-24. Sigrid J. Clift, Karen L. Herrington, and John M. Mendenhall performed SEM analyses. X-ray analyses were performed by David K. Davies and Associates, Inc. (Enron South Hogsback samples), and Andrew R. Scott (all others). Core processing and handling were coordinated by Sigrid J. Clift, Karen L. Herrington, and Robert A. Sanchez, under the supervision of Allan R. Standen, curator of the Bureau of Economic Geology Core Research Center.

We have benefited from discussions about the Frontier Formation with William A. Ambrose, Walter B. Ayers, Jr., Beverly Blakeney-DeJarnett, Robert L. Folk, William E. Galloway, Karen L. Herrington, Robin E. Hill, Randal F. LaFollette, Lee F. Krystinik, John C. Lorenz, Don L. Luffel, Earle F. McBride, Robert A. Morton, and Bradley M. Robinson. We appreciate the helpful review of this report by Raymond A. Levey. Figures in this report were prepared under the direction of Richard L. Dillon, Chief Cartographer. Word processing was done by Susan Lloyd under the direction of Susann V. Doenges, Editor-in-Chief. Lana Dieterich edited the report, and Jamie H. Coggin was designer.

## REFERENCES

- Adler, P. M., 1989, Flow in porous media, *in* The fractal approach to heterogeneous chemistry: New York, John Wiley, p. 341-359.
- Asquith, D. O., 1966, Geology of Late Cretaceous Mesaverde and Paleocene Fort Union oil production, Birch Creek Unit, Sublette County, Wyoming: American Association of Petroleum Geologists Bulletin, v. 50, p. 2176-2184.
- Atkins, J. E., 1989, Porosity and packing of Holocene river, dune and beach sands: The University of Texas at Austin, Master's thesis, 224 p.
- Barton, C. C., and Hsieh, P. A., 1989, Physical and hydrogeologic flow properties of fractures: 28th International Geological Congress, Field Trip Guidebook T385, 36 p.
- Barton, C. C., and Larsen, Eric, 1985, Fractal geometry of two-dimensional fracture networks at Yucca Mountain, southwest Nevada, *in* Fundamentals of rock joints: Bjorkliden, Sweden, Proceedings of the international symposium, p. 77-84.
- Barton, C. C., Larsen, Eric, Page, W. R., and Howard, T. M., 1987, Characterizing fractured rock for fluid-flow, geomechanical, and paleostress modeling: methods and preliminary results from Yucca Mountain, Nevada: U.S. Geological Survey, Open-File Report USGS-OFR-87, 36 p.
- Barton, N. R., 1986, Deformation phenomena in jointed rock: Geotechnique, v. 36, p. 147-167.

Bjorlykke, Knut, Ramm, Mogens, and Saigal, G. C., 1989, Sandstone diagenesis and porosity modification during basin evolution: *Geologische Rundschau*, v. 78, p. 243-268.

Blackstone, D. L., Jr., 1979, Geometry of the Prospect-Darby and La Barge faults at their junction with the La Barge Platform, Lincoln and Sublette Counties, Wyoming: The Geological Survey of Wyoming, Report of Investigations No. 18, 34 p.

Blatt, Harvey, Middleton, G. V., and Murray, R. C., 1972, Origin of sedimentary rocks: Englewood Cliffs, New Jersey, Prentice-Hall, Inc., 634 p.

Burley, S. D., and Kantorowicz, J. D., 1986, Thin section and S.E.M. textural criteria for the recognition of cement-dissolution porosity in sandstones: *Sedimentology*, v. 33, p. 587-604.

Byers, C. W., and Larson, D. W., 1979, Paleoenvironments of Mowry Shale (Lower Cretaceous), western and central Wyoming: *American Association of Petroleum Geologists Bulletin*, v. 63, p. 354-375.

Case, J. C., 1986, Earthquakes and related hazards in Wyoming: The Geological Survey of Wyoming Public Information, Circular No. 26.

Clift, S. J., Laubach, S. E., and Holder, Jon, in press, Strength anisotropy in low-permeability sandstone gas reservoirs: application of the axial point-load test: *Gulf Coast Association of Geological Societies Transactions*, v. 42.

Collins, E. W., Hovorka, S. D., and Laubach, S. E., in press, Fracture systems of the Austin Chalk, North-Central Texas, *in* Schmoker, J. W., ed., *Geological aspects of horizontal drilling: Rocky Mountain Association of Geologists Guidebook*.

- Collins, E. W., Laubach, S. E., and Vendeville, B. C., 1990, Faults and fractures in the Balcones Fault Zone, Austin region, Central Texas: Austin Geological Society, Guidebook 13, 32 p.
- Craddock, J. P., Kopania, A. A., and Wiltchko, D. V., 1988, Interaction between the northern Idaho-Wyoming thrust belt and bounding basement blocks, central western Wyoming: Geological Society of America Memoir 171, p. 333-351.
- Crews, G. C., Barlow, J. A., Jr., and Haun, J. D., 1973, Natural gas resources, Green River Basin, Wyoming, *in* 25th annual field conference, Wyoming Geological Association Guidebook, p. 103-113.
- Curry, W. H., III, 1973, Late Cretaceous and Early Tertiary rocks, southwestern Wyoming, *in* 25th annual field conference, Wyoming Geological Association Guidebook, p. 79-86.
- De Chadenedes, J. F., 1975, Frontier deltas on the western Green River Basin, Wyoming, *in* Bolyard, D. W., ed., Symposium on deep drilling frontiers in the central Rocky Mountains: Rocky Mountain Association of Geologists, p. 149-157.
- DeFord, R. K., Kehle, R. O., and Connolly, E. T., 1976, Geothermal gradient map of North America: American Association of Petroleum Geologists and U.S. Geological Survey, scale 1:5,000,000.
- Delphia, J. G., and Bombolakis, E. G., 1988, Sequential development of a frontal ramp, imbricates, and a major fold in the Kemmerer region of the Wyoming thrust belt: Geological Society of America Special Paper 222, p. 207-222.

Diamond, W. P., and Oyler, D. C., 1987, Effect of hydraulic stimulation on coalbeds and surrounding strata—evidence from underground observations: U.S. Bureau of Mines, Report of Investigations 9083.

Dutton, S. P., 1990, Variations in diagenesis and reservoir quality in the Frontier Formation along the Moxa Arch, Green River Basin, Wyoming (abs.): American Association of Petroleum Geologists Bulletin, v. 74, p. 1321-1322.

\_\_\_\_\_ 1991, Diagenetic controls on reservoir properties of low-permeability sandstone, Frontier Formation, Moxa Arch, southwest Wyoming: The University of Texas at Austin, Bureau of Economic Geology, topical report no. GRI-91/0057 prepared for the Gas Research Institute under contract no. 5082-211-0708, 48 p.

Dutton, S. P., and Diggs, T. N., 1990, History of quartz cementation in the Lower Cretaceous Travis Peak Formation, East Texas: Journal of Sedimentary Petrology, v. 60, p. 191-202.

Dutton, S. P., and Hamlin, H. S., 1991, Geologic controls on reservoir properties of Frontier Formation low-permeability gas reservoirs, Moxa Arch, Wyoming: Society of Petroleum Engineers Joint Rocky Mountain Regional/Low Permeability Reservoirs Symposium Proceedings, SPE Paper 21851, p. 479-488.

\_\_\_\_\_ in press, Interaction of burial history and diagenesis of the Upper Cretaceous Frontier Formation, Moxa Arch, Green River Basin, Wyoming: Wyoming Geological Association Guidebook.

Edman, J. D., and Surdam, R. C., 1984, Influence of overthrusting on maturation of hydrocarbons in Phosphoria Formation, Wyoming-Idaho-Utah Overthrust Belt: American Association of Petroleum Geologists Bulletin, v. 68, p. 1803-1817.

- Engelder, T., 1985, Loading paths to joint propagation during a tectonic cycle: an example from the Appalachian Plateau, U.S.A.: *Journal of Structural Geology*, v. 7, p. 459-476.
- Engelder, T., and Geiser, P., 1980, On the use of regional joint sets as trajectories of paleostress field during development of the Appalachian Plateau, New York: *Journal of Geophysical Research*, v. 85, p. 6319-6341.
- Fix, J. E., Adair, R. G., Mahrer, K. D., Myers, B. C., Swanson, J. G., and Woerpel, J. C., 1990, Development of microseismic methods to determine hydraulic fracture dimensions: Teledyne Geotech Report No. 89-6, final report (GRI-90/0220) prepared for Gas Research Institute, 110 p.
- Folk, R. L., 1974, *Petrology of sedimentary rocks*: Austin, Hemphill Publishing Company, 182 p.
- Friedman, Irving, and O'Neil, J. R., 1977, *Data of geochemistry; compilation of stable isotopic fractionation factors of geochemical interest (6th ed.)*: U.S. Geological Survey Professional Paper 440K, Chapter KK, variously paginated.
- Galloway, W. E., and Cheng, E. S., 1985, Reservoir facies architecture in a microtidal barrier system—Frio Formation, Texas Gulf Coast: The University of Texas at Austin, Bureau of Economic Geology, Report of Investigations No. 144, 36 p.
- Gregory, R. W., and De Bruin, R. H., 1991, Oil and gas fields map of the Greater Green River Basin and Overthrust Belt: The Geological Survey of Wyoming, Map Series 36, scale 1:316,800.
- Haas, M. R., McFall, K. S., and Coates, J.-M., 1988, Site selection for GRI cooperative tight gas field research, volume I: screening of candidate tight gas formations: topical report



no. GRI-89/0018 prepared for the Gas Research Institute under contract no. 5083-211-817, 66 p. plus appendices.

Hamlin, H. S., 1991, Stratigraphy and depositional systems of the Frontier Formation and their controls on reservoir development, Moxa Arch, southwest Wyoming: The University of Texas at Austin, Bureau of Economic Geology, topical report no. GRI-91/0128, prepared for the Gas Research Institute under contract no. 5082-211-0708, 45 p.

Hamlin, H. S., and Buehring, R. L., 1990, Facies-related permeability trends in the Frontier Formation along the Moxa Arch, Green River Basin, Wyoming (abs.): American Association of Petroleum Geologists Bulletin, v. 74, p. 1325.

Hancock, P. L., and Bevan, T. G., 1987, Brittle modes of foreland deformation, *in* Coward, M. P., Dewey, J. F., and Hancock, P. L., eds., Continental extensional tectonics: Geological Society of London Special Publication No. 28, p. 127-137.

Hansen, W. R., 1965, Geology of the Flaming Gorge area, Utah-Colorado-Wyoming: U.S. Geological Survey Professional Paper 490, 196 p.

Heward, A. P., 1981, A review of wave-dominated clastic shoreline deposits: Earth-Science Reviews, v. 17, p. 223-276.

Hodgson, R. A., 1961, Regional study of jointing in Comb Ridge-Navajo Mountain area, Arizona and Utah: American Association of Petroleum Geologists Bulletin, v. 45, p. 1-38.

Houseknecht, D. W., 1987, Assessing the relative importance of compactional processes and cementation to the reduction of porosity in sandstones: American Association of Petroleum Geologists Bulletin, v. 71, p. 633-642.

- Hyman, L. A., Malek, D. J., Admire, C. A., and Walls, J. D., 1991, The effects of microfractures on directional permeability in tight gas sands: Society of Petroleum Engineers/Department of Energy Low-Permeability Reservoir Symposium, SPE Paper 21878, unpaginated.
- Jordan, T. E., 1981, Thrust loads and foreland basin evolution, Cretaceous, western United States: American Association of Petroleum Geologists Bulletin, v. 65, p. 2506-2520.
- Kaiser, W. R., 1984, Predicting reservoir quality and diagenetic history in the Frio Formation (Oligocene) of Texas: American Association of Petroleum Geologists Memoir 37, p. 289-316.
- Kraig, D. H., Wiltschko, D. V., and Spang, J. H., 1987, Interaction of basement uplift and thin-skinned thrusting, Moxa Arch and Western Overthrust Belt, Wyoming: a hypothesis: Geological Society of America, v. 99, p. 654-662.
- Kulander, B. R., Dean, S. L., and Ward, B. J., Jr., 1990, Fractured core analysis: American Association of Petroleum Geologists, Methods in Exploration No. 8, 88 p.
- Ladeira, F. L., and Price, N. J., 1981, Relationship between fracture spacing and bed thickness: Journal of Structural Geology, v. 3, p. 179-183.
- Land, L. S., 1980, The isotopic and trace element geochemistry of dolomite: the state of the art: Society of Economic Paleontologists and Mineralogists Special Publication No. 28, p. 87-110.
- LaPointe, P. R., 1988, A method to characterize fracture density and connectivity through fractal geometry: International Journal of Rock Mechanics and Geomechanics Abstracts, v. 25, p. 421-429.

Laubach, S. E., 1988, Subsurface fractures and their relationship to stress history in East Texas basin sandstone: *Tectonophysics*, v. 156, p. 37-49.

\_\_\_\_\_ 1989a, Paleostress directions from the preferred orientation of closed microfractures (fluid-inclusion planes): *Journal of Structural Geology*, v. 11, p. 603-611.

\_\_\_\_\_ 1989b, Fracture analysis of the Travis Peak Formation, western flank of the Sabine Arch, East Texas: The University of Texas at Austin, Bureau of Economic Geology Report of Investigations No. 185, 55 p.

\_\_\_\_\_ 1991, Fracture patterns in low-permeability-sandstone gas reservoir rocks in the Rocky Mountain region: Society of Petroleum Engineers Joint Rocky Mountain Regional Meeting/Low-Permeability Reservoir Symposium Proceedings, SPE Paper 21877, p. 501-510.

\_\_\_\_\_ in press, Attributes of fracture networks in selected Cretaceous sandstones of the Green River and San Juan Basins, *in* Schmoker, J. W., ed., Geological aspects of horizontal drilling: Rocky Mountain Association of Geologists Guidebook.

Laubach, S. E., Clift, S. J., Hill, R. E., and Fix, J. E., in press, Stress directions in Cretaceous Frontier Formation, Green River Basin, Wyoming: Wyoming Geological Association Guidebook.

Laubach, S. E., Hamlin, H. S., Buehring, Robert, Baumgardner, R. W., Jr., and Monson, E. R., 1990a, Application of borehole-imaging logs to geologic analysis, Cotton Valley Group and Travis Peak Formation, GRI Staged Field Experiment wells, East Texas: The University of Texas at Austin, Bureau of Economic Geology, topical report prepared for Gas Research Institute under contract no. 5082-211-0708, 115 p.

- Laubach, S. E., Hoak, T. E., Dutton, S. P., and Diggs, T. N., 1989, Coevolution of fracture pattern, rock mechanical properties, and diagenesis in a low-permeability gas reservoir sandstone, East Texas (abs.): Geological Society of America, Abstracts with Programs, v. 21, p. 16.
- Laubach, S. E., and Lorenz, J. C., in press, Preliminary assessment of natural fracture patterns in Frontier Formation sandstones, southwestern Wyoming: Wyoming Geological Association Guidebook.
- Laubach, S. E., and Monson, E., 1988, Coring-induced fractures: indicators of hydraulic fracture propagation in a naturally fractured reservoir: Society of Petroleum Engineers Annual Technical Conference and Exhibition Proceedings, SPE Paper 18164, p. 587-596.
- Laubach, S. E., and Tremain, C. M., 1991, Regional coal fracture patterns and coalbed methane development, *in* 32nd U.S. Symposium on Rock Mechanics: The Netherlands, A. A. Balkema, p. 851-861.
- Laubach, S. E., Tremain, C. M., and Ayers, W. B., Jr., 1991b, Coal fracture studies: guides for coalbed methane exploration and development: *Journal of Coal Quality*, v. 10, p. 81-88.
- Laubach, S. E., Tremain, C. M., and Baumgardner, R. W., Jr., 1991a, Fracture swarms in Upper Cretaceous sandstone and coal, northern San Juan Basin, Colorado: potential targets for methane exploration, *in* Ayers, W. B., Jr., Kaiser, W. R., Laubach, S. E., Ambrose, W. A., Baumgardner, R. W., Jr., Scott, A. R., Tyler, Roger, Yeh, Joseph, Hawkins, G. J., Swartz, T. E., Schultz-Ela, D. D., and Zellers, S. D., eds., Geologic and hydrologic controls on the occurrence and producibility of coalbed methane, Fruitland Formation, San Juan Basin: The University of Texas at Austin, Bureau of Economic Geology, topical report prepared for Gas Research Institute under contract no. 5087-214-1544, p. 119-140.

- Law, B. E., 1984, Relationships of source rock, thermal maturity, and overpressuring to gas generation and occurrence in low-permeability Upper Cretaceous and Lower Tertiary rocks, Greater Green River Basin, Wyoming, Colorado, and Utah, *in* Wood, J., Meissner, F. F., and Clayton, J. L., eds., Hydrocarbon source rocks of the greater Rocky Mountain region: Rocky Mountain Association of Geologists, p. 469-490.
- Law, B. E., Spencer, C. W., and Bostick, N. H., 1980, Evaluation of organic matter, subsurface temperature and pressure with regard to gas generation in low-permeability Upper Cretaceous and Lower Tertiary sandstones in Pacific Creek area, Sublette and Sweetwater Counties, Wyoming: *The Mountain Geologist*, v. 17, p. 23-35.
- Law, B. E., Spencer, C. W., Charpentier, R. R., Crovelli, R. A., Mast, R. F., Dolton, G. L., and Wandrey, C. J., 1989, Estimates of gas resources in overpressured low-permeability Cretaceous and Tertiary sandstone reservoirs, Greater Green River Basin, Wyoming, Colorado, and Utah, *in* 40th annual field conference, Wyoming Geological Association Guidebook, p. 39-61.
- Law, E. W., 1983, Petrologic, geochronologic, and isotopic investigation of the diagenesis and hydrocarbon emplacement in the Muddy Sandstone, Powder River Basin: Case Western Reserve University, Ph.D. dissertation, 360 p.
- Law, E. W., Burrows, S. M., Aronson, J. L., and Savin, S. M., 1990, A petrologic, geochronologic and oxygen isotopic study of the diagenesis of the Cretaceous Muddy Sandstone, east flank of the Powder River Basin (abs.): 27th annual meeting program and abstracts, Clay Minerals Society, p. 110.

Long, J. C. S., and Billaux, D. M., 1987, From field data to fracture network modeling: an example incorporating spatial structure: *Water Resources Research*, v. 23, p. 1201-1216.

Long, J. C. S., and Witherspoon, P. A., 1985, The relationship of the degree of interconnection to permeability in fracture networks: *Journal of Geophysical Research*, v. 90, p. 3087-3099.

Lorenz, J. C., and Finley, S. J., 1991, Regional fractures II: fracturing of Mesaverde reservoirs in the Piceance Basin, Colorado: *American Association of Petroleum Geologists Bulletin*, v. 75, p. 1738-1757.

Lorenz, J. C., and Hill, R. H., 1991, Subsurface fracture spacing: comparison of inferences from slant/horizontal core and vertical core in Mesaverde reservoirs: *Society of Petroleum Engineers Joint Rocky Mountain Regional/Low-Permeability Reservoirs Symposium Proceedings*, SPE Paper 21877, p. 705-716.

Lorenz, J. C., Teufel, L. W., and Warpinski, N. R., 1991, Regional fractures I: a mechanism for the formation of regional fractures in flat-lying reservoirs: *American Association of Petroleum Geologists Bulletin*, v. 75, p. 1714-1737.

Love, J. D., and Christiansen, A. C., 1985, *Geologic map of Wyoming*: U.S. Geological Survey Map, 3 sheets, scale 1:500,000.

Luffel, D. L., Herrington, K. L., and Harrison, C. W., 1991, Fibrous illite controls productivity in Frontier gas sands, Moxa Arch, Wyoming: *Society of Petroleum Engineers Joint Rocky Mountain Regional/Low-Permeability Reservoirs Symposium Proceedings*, SPE Paper 21876, p. 695-704.

- Luffel, D. L., Howard, W. E., and Hunt, E. R., 1989, Relationships of permeability, porosity, and overburden stress derived from an extensive core analysis data base in the Travis Peak Formation: Society of Petroleum Engineers Joint Rocky Mountain Regional/Low-Permeability Reservoirs Symposium Proceedings, SPE Paper No. 19008, p. 729-740.
- Matthews, J. L., Emanuel, A. S., and Wobus, R. A., 1989, Fractal methods improve miscible predictions: *Journal of Petroleum Technology*, v. 41, p. 1136-1145.
- McBride, E. F., 1989, Quartz cement in sandstones: a review: *Earth-Sciences Reviews*, v. 26, p. 69-112.
- McDonald, R. E., 1973, Big Piney-La Barge producing complex, Sublette and Lincoln Counties, Wyoming: 25th annual field conference, Wyoming Geological Association Guidebook, p. 57-77.
- McGookey, D. P., 1972, Cretaceous System, in Mallory, W. W., ed., *Geologic atlas of the Rocky Mountain region*: Rocky Mountain Association of Geologists, p. 190-228.
- Merceron, T., and Velde, B., 1991, Application of Cantor's method for fractal analysis of fractures in the Toyoha Mine, Hokkaido, Japan: *Journal of Geophysical Research*, v. 96, p. 16,641-16,650.
- Merewether, E. A., Blackmon, P. D., and Webb, J. C., 1984, The mid-Cretaceous Frontier Formation near the Moxa Arch, southwestern Wyoming: U.S. Geological Survey Professional Paper 1290, 29 p.
- Merewether, E. A., and Cobbin, W. A., 1986, Biostratigraphic units and tectonism in the mid-Cretaceous foreland of Wyoming, Colorado, and adjoining areas, in Peterson, J. A., ed.,

- Paleotectonics and sedimentation in the Rocky Mountain region, United States, part III, middle Rocky Mountains: American Association of Petroleum Geologists Memoir 41, p. 443-467.
- Merewether, E. A., Krystinik, K. B., and Pawlewicz, M. J., 1987, Thermal maturity of hydrocarbon-bearing formations in southwestern Wyoming and northwestern Colorado: U.S. Geological Survey Miscellaneous Investigations Series, Map I-1831.
- Milliken, K. L., and Land, L. S., 1991, Reverse weathering, the carbonate-feldspar system, and porosity evolution during burial of sandstones (abs.): American Association of Petroleum Geologists Bulletin, v. 75, p. 636.
- Molenaar, C. M., and Wilson, B. W., 1990, The Frontier Formation and associated rocks of northeastern Utah and northwestern Colorado: U.S. Geological Survey Bulletin 1787-M, p. M1-M21.
- Monley, L. E., 1971, Petroleum potential of Idaho-Wyoming overthrust belt: American Association of Petroleum Geologists Memoir 15, p. 509-537.
- Moslow, T. F., and Tillman, R. W., 1986, Sedimentary facies and reservoir characteristics of Frontier Formation sandstones, southwestern Wyoming, *in* Spencer, C. W., and Mast, R. F., eds., Geology of tight gas reservoirs: American Association of Petroleum Geologists Studies in Geology No. 24, p. 271-295.
- \_\_\_\_\_ 1989, Characterization, distribution of Frontier Formation reservoir facies of Wyoming fields: Oil and Gas Journal, v. 87, p. 95-104.



- Myers, R. C., 1977, Stratigraphy of the Frontier Formation (Upper Cretaceous), Kemmerer area, Lincoln County, Wyoming: 29th annual field conference, Wyoming Geological Association Guidebook, p. 271-311.
- Pittman, E. D., 1979, Porosity, diagenesis, and productive capability of sandstone reservoirs, *in* Scholle, P. A., and Schluger, P. R., eds., Aspects of diagenesis: Society of Economic Paleontologists and Mineralogists Special Publication No. 26, p. 159-173.
- Plumb, R. A., and Hickman, S. H., 1985, Stress-induced borehole elongation: a comparison between the four-arm dipmeter and the borehole televiewer in the Auburn geothermal well: *Journal of Geophysical Research*, v. 90, p. 5513-5521.
- Power, D. V., Schuster, C. L., Hay, R., and Twombly, J., 1976, Detection of hydraulic fracture orientation in cased wells: *Journal of Petroleum Technology*, v. 28, p. 1116-1124.
- Pryor, W. A., 1973, Permeability-porosity patterns and variations in some Holocene sand bodies: *American Association of Petroleum Geologists Bulletin*, v. 57, p. 162-189.
- Ryder, R. T., 1988, Greater Green River Basin, *in* Sloss, L. L., ed., Sedimentary cover—North American craton, U.S.: Geological Society of America, *The Geology of North America*, v. D-2, p. 154-165.
- Ryer, T. A., 1977, Patterns of Cretaceous shallow-marine sedimentation, Coalville and Rockport areas, Utah: *Geological Society of America Bulletin*, v. 88, p. 177-188.
- Sayers, C. M., 1988, Stress-induced ultrasonic S-wave velocity anisotropy in fractured rock: *Ultrasonics*, v. 26, p. 311-317.

Schmoker, J. W., and Gautier, D. L., 1989, Compaction of basin sediments: modeling based on time-temperature history: *Journal of Geophysical Research*, v. 94, p. 7379-7386.

Schultz, M. S., and Lafollette, R. F., 1989, Effect of drilling and completion methods on Frontier gas production, northern Moxa Arch, southwest Wyoming, *in* 40th annual field conference, Wyoming Geological Association Guidebook, p. 247-254.

Skuce, A. G., Goody, N. P., and Maloney, James, 1992, Passive-roof duplexes under the Rocky Mountain Foreland Basin, Alberta: *American Association of Petroleum Geologists Bulletin*, v. 76, p. 67-80.

Spencer, C. W., 1987, Hydrocarbon generation as a mechanism for overpressuring in Rocky Mountain region: *American Association of Petroleum Geologists Bulletin*, v. 71, p. 368-388.

Stonecipher, S. A., Winn, R. D., Jr., and Bishop, M. G., 1984, Diagenesis of the Frontier Formation, Moxa Arch: a function of sandstone geometry, texture and composition, and fluid flux: *American Association of Petroleum Geologists Memoir 37*, p. 289-316.

Strickland, F. G., and Ren, N. K., 1980, Predicting the in situ stress state for deep wells using differential strain curve analysis: *Society of Petroleum Engineers Unconventional Gas Recovery Symposium*, SPE Paper 8954, p. 251-258.

Sullivan, Raymond, 1980, A stratigraphic evaluation of the Eocene rocks of southwestern Wyoming: *The Geological Survey of Wyoming Report of Investigations No. 20*, 50 p.

Sylvester, A. G., Byrd, J. O. D., and Smith, R. B., 1990, A seismic (?) creep across the Teton Fault, Wyoming, with implications for interseismic strain (abs.): *Geological Society of America Abstracts with Programs*, v. 22, p. 88.

TerraTek, 1989, Consolidated core testing report, Church Butte No. 48, Sweetwater County, Wyoming: Salt Lake City, Utah, TerraTek Geoscience Services, unpaginated.

Teufel, L. W., 1983, Determination of the principal horizontal stress directions from anelastic strain recovery measurements of oriented core: application to the Cotton Valley Formation, East Texas: American Society of Mechanical Engineers Symposium on Geomechanics Proceedings, unpaginated.

Thomaidis, N. D., 1973, Church Buttes arch, Wyoming and Utah, *in* 25th annual field conference, Wyoming Geological Association Guidebook, p. 35-39.

Wach, P. H., 1977, The Moxa Arch, an overthrust model?: Rocky Mountain Thrust Belt, geology and resources, *in* 29th annual field conference, Wyoming Geological Association Guidebook, p. 651-664.

Waples, D. W., 1980, Time and temperature in petroleum formation: application of Lopatin's method to petroleum exploration: American Association of Petroleum Geologists Bulletin, v. 64, p. 916-926.

Warpinski, N., *in press*, Analysis of SFE 4 ASR and CVA data, *in* Peterson, R., ed., GRI Staged Field Experiment No. 4 report: CER Corporation, topical report prepared for the Gas Research Institute.

Weimer, R. J., 1961, Uppermost Cretaceous rocks in central and southern Wyoming, and northwest Colorado: 16th annual field conference guidebook, Wyoming Geological Association, p. 17-28.

- \_\_\_\_\_ 1986, Relationship of unconformities, tectonics, and sea-level changes in the Cretaceous of the western interior, United States, *in* Peterson, J. A., ed., Paleotectonics and sedimentation in the Rocky Mountain region, United States, part III, middle Rocky Mountains: American Association of Petroleum Geologists Memoir 41, p. 397-422.
- Wiltschko, D. V., and Dorr, J. A., 1983, Timing of deformation in overthrust belt and foreland of Idaho, Wyoming, and Utah: American Association of Petroleum Geologists Bulletin, v. 67, p. 1304-1322.
- Wiltschko, D. V., and Eastman, D. B., 1983, Role of basement warps and faults in localizing thrust fault ramps, *in* Hatcher, R. D., Jr., Williams, H., and Zietz, I., eds., Contributions to the tectonics and geophysics of mountain chains: Geological Society of America Memoir 158, p. 177-190.
- Winn, R. D., Jr., and Smithwick, M. E., 1980, Lower Frontier Formation, southwestern Wyoming: depositional controls on sandstone compositions and on diagenesis, *in* 31st annual field conference, Wyoming Geological Association Guidebook, p. 247-254.
- Winn, R. D., Jr., Stonecipher, S. A., and Bishop, M. G., 1984, Sorting and wave abrasion: controls on composition and diagenesis in lower Frontier sandstones, southwestern Wyoming: American Association of Petroleum Geologists Bulletin, v. 68, p. 268-284.
- Zoback, M. L., and Zoback, M. D., 1980, State of stress in the conterminous United States: Journal of Geophysical Research, v. 85, p. 6113-6156.

\_\_\_\_\_ 1989, Tectonic stress field of the continental United States, *in* Pakiser, L. C., and Mooney, W. D., eds., Geophysical framework of the continental United States: Geological Society of America Memoir 172, p. 523-539.